INFORMATION TO USERS

This manuscript has been reproduced from the microfilm master. UMI films the text directly from the original or copy submitted. Thus, some thesis and dissertation copies are in typewriter face, while others may be from any type of computer printer.

The quality of this reproduction is dependent upon the quality of the copy submitted. Broken or indistinct print, colored or poor quality illustrations and photographs, print bleedthrough, substandard margins, and improper alignment can adversely affect reproduction.

In the unlikely event that the author did not send UMI a complete manuscript and there are missing pages, these will be noted. Also, if unauthorized copyright material had to be removed, a note will indicate the deletion.

Oversize materials (e.g., maps, drawings, charts) are reproduced by sectioning the original, beginning at the upper left-hand corner and continuing from left to right in equal sections with small overlaps. Each original is also photographed in one exposure and is included in reduced form at the back of the book.

Photographs included in the original manuscript have been reproduced xerographically in this copy. Higher quality 6" x 9" black and white photographic prints are available for any photographs or illustrations appearing in this copy for an additional charge. Contact UMI directly to order.

UMI

A Bell & Howell Information Company
300 North Zeeb Road, Ann Arbor MI 48106-1346 USA
313/761-4700 800/521-0600

UNIVERSITY OF OKLAHOMA

SCHOOL OF CIVIL ENGINEERING AND

ENVIRONMENTAL SCIENCE

IRON AND SULFUR MICROBIAL PROCESSES APPLIED TO THE BIODEGRADATION OF ORGANIC CONTAMINANTS IN GROUNDWATER

A Dissertation

SUBMITTED TO THE GRADUATE FACULTY

in partial fulfillment of the requirements for the

degree of

Doctor of Philosophy

by

Lonnie G. Kennedy

Norman, Oklahoma

1998

IRON AND SULFUR MICROBIAL PROCESSES APPLIED TO THE BIODEGRADATION OF ORGANIC CONTAMINANTS IN GROUNDWATER

A Dissertation APPROVED FOR THE
SCHOOL OF CIVIL ENGINEERING AND
ENVIRONMENTAL SCIENCE

BY

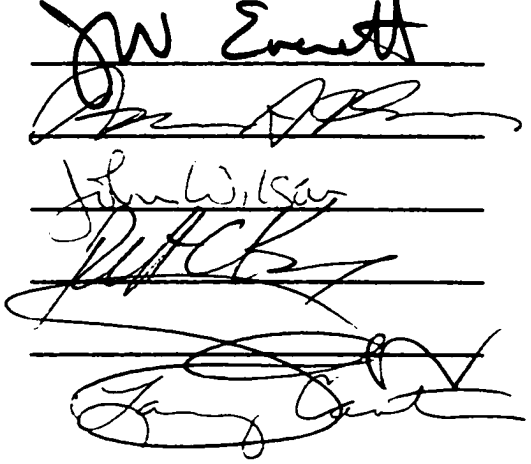

ACKNOWLEDGMENTS

At the conclusion of this work, I consider with deep gratitude the numerous people who have helped me both with technical support and encouragement. First, I would like to thank my wife, Shelly Kennedy, for selflessly taking on the mantel of additional family duties that allowed me the opportunity to pursue this degree. Next, I owe a debt of gratitude to Dr. Jess Everett who, in addition to providing technical guidance, bolstered my resolution many times over the years. Dr. John Wilson was an inspiration to me as he has been to countless others. As a mentor, he provided a wellspring of ideas and patently reviewed my own work with a unique mixture of kindness, patience, and the knowledgeable authority of a master in his field. Dr. Keith Strevett will always be a source of amazement to me. In addition to his own grueling schedule he somehow found time to counsel me and provide sage advise just when I seemed to need it most. I also wish to thank my other committee members, Dr. Larry Canter, Dr. Tom Dewers, and Dr. Robert Knox, for sticking it out with me. You gentlemen were great and I truly appreciate your support.

A host of other experts and collogues helped me in many ways. I wish to thank Glen Ulrich and Dr. Joe Suflita in the microbiology department for their technical advise, which in many ways enabled my own work. Dr. Bill Lyon, at EPA's Robert S. Kerr Research Laboratory, gave me much needed technical support on mineral extractions, timely literature, and aided in data analysis. I

was also very fortunate to be able to work with Dr. Gorm Heron who's own doctorate and ongoing research was groundbreaking in this field.

I had the help of many students at the University of Oklahoma including Kevin Ware, Jeff Canty, and Bob Parsons. Of these, I'd especially like to thank Kevin Ware for helping me run analyses in the late hours of the night for little more than my gratitude. Last, but certainly not least, I wish to thank Joe Grego, our department technician. In addition to providing excellent analytical support, he literally built some of the equipment that was critical for my research.

To all these above my sincere thanks and

a lifetime of gratitude.

This research was funded in part by the NSF EPSCoR Experimental Systemic Initiative: "Automation and Characterization of an Environmental Research Facility" Contract OSR-9553363.

TABLE OF CONTENTS

LIST OF TABLES

LIST OF FIGURES

ABSTRACT

This research emphasizes microbial/mineral interactions associated with Fe^{3+} and SO_4^{2-} reduction. When an organic contaminant is released to the subsurface, some electron acceptor types are limited and a redox sequence can develop where various electron acceptor types are consumed more or less consecutively. Based on thermodynamic considerations, it is thought that this consumption sequence is O_2 > NO_3^- > Fe^{3+} > SO_4^{2-} > methanogenesis. The microbial oxidation of organic contaminants with the concurrent reduction of O_2 and NO_3^- involve aqueous/gas interactions. Conversely, Fe^{3+} and SO_4^{2-} reductions involve aqueous, gas, and solid mineral interactions. With respect to availability, concentrations of Fe^{2+} and SO_4^{2-} are often much greater than O_2 and NO_3^- in an aquifer. This suggests that Fe^{3+} and SO_4^{2-} reduction are important processes in the natural biological degradation of organic contaminants.

Simplified methods are developed to evaluate Fe^{3+}, Fe^{2+}, and S mineral species. These techniques allow an approximation of biologically available Fe^{3+} minerals and permit analysis of Fe^{2+} and reduced S minerals deposited as a result of microbial processes. Methods developed herein were applied to three test sites contaminated with gasoline, landfill leachate, and natural methane gas. At these sites, the effects of Fe^{3+} and SO_4^{2-} reduction could be distinguished based on mineral analysis. Evaluation methods were also developed especially with respect to understanding Fe data.

Fe and S mineral analysis was used in conjunction with a typical natural attenuation study, where only aqueous water analyses are used, at a gasoline

spill site. It was found that most of the measurable expressed capacity was present as either solid mineral Fe^{2+} or reduced S species. Measurable expressed capacity showed that greater than 92% of the original hydrocarbon was destroyed by microbial processes. Methods were developed to incorporate mineral analysis into a natural attenuation study.

Fe and S processes were examined under laboratory conditions in microcosms. Microcosms were developed with two different types of native sands containing varying amounts of natural Fe^{3+} minerals. To some systems, mineral sources of Fe^{3+} and SO_4^{2-} were added in the form of $Fe(OH)_3$ and gypsum ($CaSO_4 \cdot 2H_2O$). Some microcosms were prepared with no mineral amenities other than those found naturally in the native sediments. A synthetic leachate consisting of straight chain fatty acids was added as a carbon source. The major observations were that: 1) simulated leachate organic was removed from all systems at about the same rate (~0.35 mMol C/week); 2) solid Fe^{3+} and SO_4^{2-} sources can serve as electron acceptor sources; 3) SO_4^{2-} reduction resulted in the formation of iron sulfides and H_2S; 4) the ability to form iron sulfide is limited and is apparently a function of Fe^{3+} 5) SO_4^{2-} reduction inhibits methanogenesis; 6) Fe^{3+} reduction only partially inhibits methanogenesis; 7) Fe^{3+} reduction greatly reduces CO_2; 8) natural Fe^{3+} minerals did not inhibit methanogenesis or CO_2; 9) Natural Fe^{3+} minerals were poor short term sources of Fe^{3+}; 10) aqueous Fe^{2+} poorly represents Fe^{3+} reduction processes; and 11) the utilization of native Fe^{3+} minerals and gypsum SO_4^{2-} followed a first order kinetic model.

This research has several potential scientific and engineering applications. Implications for natural attenuation are first discussed. With respect to natural attenuation theory it is concluded that: 1) expressed capacity for Fe^{3+} and SO_4^{2-} reduction is largely found in mineral form; 2) the rate of reduced Fe and S mineral formation is rapid and these minerals probably precipitate close to the area where microbial activity occurred; 3) although large amounts of mineral Fe^{3+} may be present in aquifer material the kinetics of utilization may be slow; and 4) the probable electron acceptor utilization sequence is O_2 > NO_3^- > SO_4^{2-} > methanogenesis with Fe^{3+} reduction occurring in a wide redox range from SO_4^{2-} through methanogenesis. Secondly, this research suggests that a landfill leachate treatment system based on solid Fe^{3+} and/or SO_4^{2-} microbial reduction might be feasible. A batch or continuous flow reactor system using Fe^{3+} and SO_4^{2-} could rapidly degrade landfill leachate with little green house gas emissions. Using such a system, the leachate and most respiratory gases could largely be converted to a solid or mineral form. Finally, recommendations are made to incorporate these findings into bioreactive mass transport models to more accurately simulate intrinsic biodegradation processes. It is suggested that; 1) bioreactive models be developed that include Fe^{3+} reduction simultaneously with SO_4^{2-} and methanogenesis, 2) simulate the precipitation of reduced Fe and S minerals, and 3) incorporate methanogenesis in a manner that is independent of inorganic electron acceptor stoichiometry. Finally, the results of this research indicate that in some cases organic degradation is controlled by fermentation processes rather that respiration. This observation

suggests that in some cases simplified predictive models might be appropriate where electron acceptor reactions are not simulated.

1. INTRODUCTION

1.1. Statement of Problem

Along with supplies of fresh surface water, ground water has generally been increasingly relied upon to meet our needs. From 1950 to 1990, ground water consumption in the United States increased 200% to about 80 billion gallons per day (Fetter, 1994) while the population grew by only 65% (US Census Bureau, 1998). Increasing dependence on ground water is likely to continue in response to population and industrial growth, demographics, and political resistance towards public works projects that dam or divert surface waters.

While population, agricultural, and industrial growth place new demands on ground water supplies, these same forces contribute to ground water pollution. Shallow aquifers are very vulnerable to pollution. Contamination by industrial or municipal wastes, agricultural operations, petroleum operations, or others may lead to dramatic changes in ground water composition and make it useless for drinking or irrigation. Contaminant sources are numerous and stem from industrialization, urbanization, and other direct or indirect human activities.

It is estimated that there are between 300,000 and 400,000 sites where ground water has been contaminated, as defined by various state and federal government regulations (National Research Council, 1994). Russel et al. (1991) estimated the total national costs of cleaning up contaminated ground water to be between $480 billion to $1 trillion with a "best guess" estimate of $750 billion over

the next 30 years. With 90 million households in the nation, this represents a cost of $8,000 per household.

Historically, the rate at which contaminated sites were discovered far exceeded the evolution of cleanup technologies (McCarty, 1990). The nation had little experience with ground water cleanup when the Comprehensive Environmental Response and Compensation Liability Act (CERCLA) was passed in 1980. There was, at the same time, tremendous political and public pressure to remediate contaminated sites. Consequently, the ground water cleanup efforts of the 1980s could be summarized as series of large, relatively uncontrolled experiments using existing technology to see if they were capable of overcoming natural physical and chemical factors that retain contaminants in the subsurface. Several studies raised troubling questions about whether existing technologies were capable of solving this large and costly problem. Performance evaluations of early pump-and-treat based systems found that while they may remove significant amounts of contaminant mass and prevent contaminants from spreading, they generally failed to reach cleanup goals (EPA, 1989 and 1992).

The inability of traditional remediation systems to achieve cleanup goals can be summarized in terms of both technological and regulatory barriers. First, from a technological perspective, subsurface soil and aquifer cleanup is encumbered by numerous physical/chemical factors including contaminant adsorption/desorption onto soil particles, aquifer anisotropy, density flow, chemical interactions, and many others. In recognition of these limitations, there has been an increasing emphasis in the last decade on developing new

technologies, such as surfactant flooding or in-situ bioremediation, that could potentially enhance treatment efficiency and reduce restoration costs.

Secondly, it can be argued that strict adherence to regulatory limits on ground water cleanup goals, in some cases, made attainment practically unachievable. Initially, cleanup policies relied on the assumption that restoring contaminated ground water was technically straightforward. This problem was exacerbated by the fact that promulgation of new environmental laws necessitated the rapid development of state and federal regulatory staff who were well intentioned but largely inexperienced. These new regulators were very cautious and administrative laws and regulatory enforcement tended to be very conservative. Consequently, throughout the 1980's and much of the 1990's, regulators enforcing Resource Conservation and Recovery Act (RCRA), CERCLA, and state level equivalents established strict numerical concentration goals for cleanup. Such ground water cleanup goals or "action levels" were often set to drinking water maximum contaminant level (MCL) standards. In some cases, action levels for soil were even established using drinking water MCL criteria. When establishing action levels, government regulators rarely considered whether technology was capable of meeting the cleanup goal. Additionally, cleanup goals were, in large part, independent of individual site characteristics that might make such cleanup physically impossible or unnecessary based on human or environmental risk or resource preservation needs.

Technological limitations coupled with conservative drinking water-based MCLs, meant that treatment might be required for decades or even centuries, in some cases, with ever increasing costs. At many remediation sites it was observed that contaminant concentrations decreased rapidly when treatment started, but then leveled off and decreased much more slowly than the designers originally predicted (National Research Council, 1994)(e.g., as shown in Figure 1). Overall treatment time can be long when contaminant removal becomes progressively less effective, driving up treatment costs. This situation is exacerbated when conservative action level standards are enforced, making attainment even more unrealizable.

In the 1990's there has been increasing attention focused on resolving the two major problems of subsurface remediation (technological limitations, and restrictive non-site specific action levels) on the part of both the potentially responsible parties (PRPs) and regulators. Recently, cleanup standards have been increasingly based on site-specific conditions by adopting risk based corrective action (RBCA) limits. It has also been recognized that soil/aquifer systems often possess properties that facilitate natural intrinsic cleanup. RBCA and natural attenuation largely developed independently; however, both are interrelated. Unlike earlier regulatory practices, treatment standards based on either RBCA or natural attenuation are developed on a site-by-site examination of data. Individual contaminant levels are negotiated with regulators based on levels deemed safe for human exposure and other environmental concerns rather than on broad-brush guidelines applied universally to all sites.

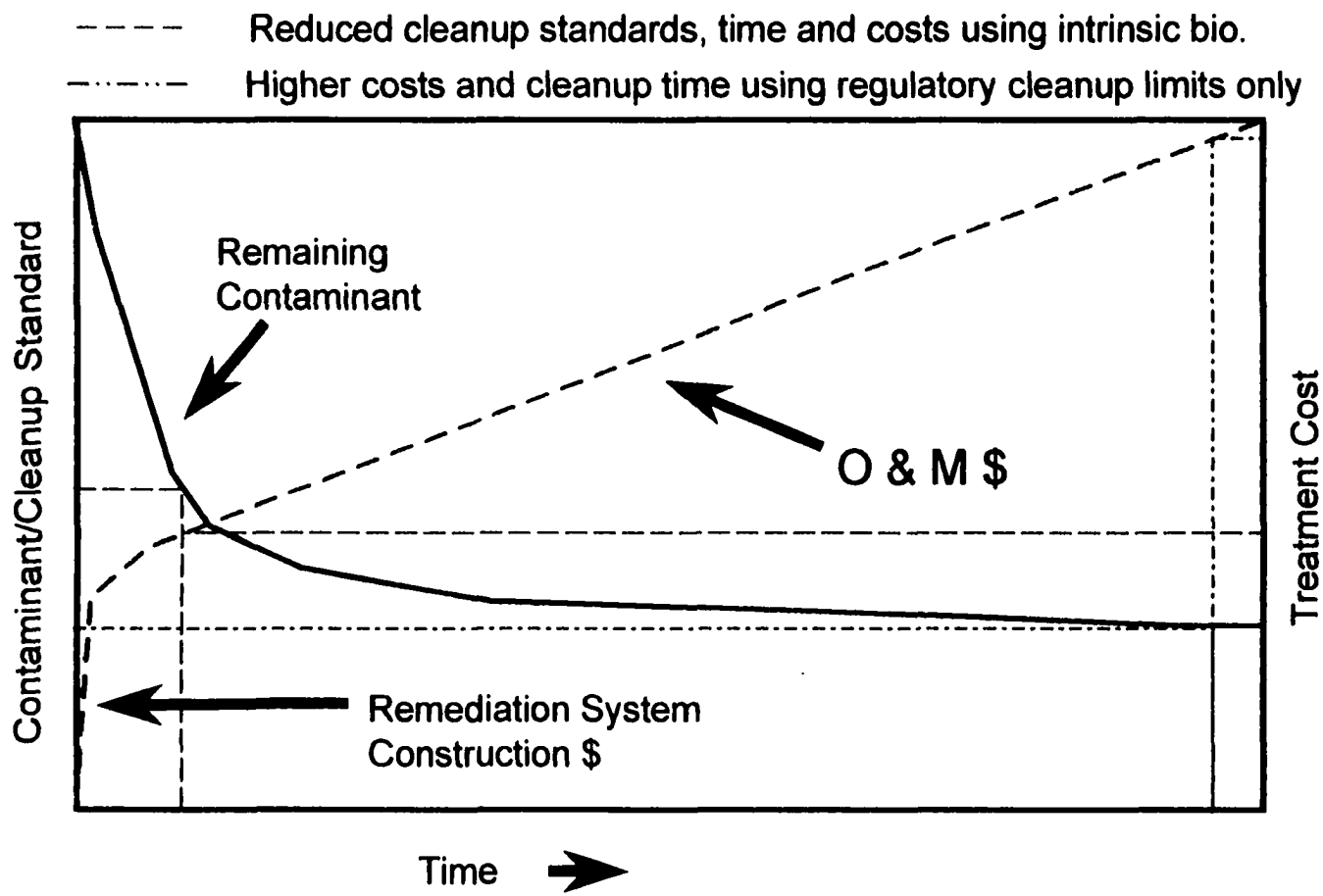

Figure 1. Theoretical economic impact on remediation costs using natural attenuation or RBCA to decrease target cleanup levels.

Both RBCA and natural attenuation can be coupled and mutually benefit from an intrinsic bioremediation analysis. Fundamentally, RBCA seeks to examine individual site characteristics to determine the relative threat that the contaminant poses to human health and the environment (ASTM, 1995). In practical terms, RBCA often results in a relaxation of cleanup standards. Raising the cleanup standard can result in a significant reduction in treatment time or possibly eliminate the need for engineered cleanup altogether (Figure 1). In a RBCA analysis, contaminant effects on human health are often predicted based on modeled assumptions of exposure that depend on contaminant loading. Thus, reduced contaminant loading can equate to decreased exposure and allow for relaxation of treatment requirements. Such a reduction of contaminant loading could be predicted by a natural attenuation study, which would depend in large part upon an in-situ bioremediation analysis to demonstrate contaminant destruction through microbial processes.

Natural attenuation is the reduction of contaminant concentrations by inherent aquifer processes (Wiedemeier et al., 1997 and ASTM, 1996). Based on a natural attenuation study one can negotiate raising an action level by demonstrating that a certain residual level of contaminant can be remediated by intrinsic processes. Again, raising the action level can result in the reduction of treatment time or the elimination of cleanup requirements. Elements facilitating the natural degradation of organic contaminants can include 1) intrinsic bioremediation, 2) advection/dispersion, 3) adsorption, 4) volatilization, and 5) abiotic chemical reactions. Of the natural attenuation processes, intrinsic

bioremediation is usually the most significant destructive mechanism of organic contaminants in an aquifer. *Intrinsic bioremediation* is the degradation of organic contaminants in soil or ground water by indigenous bacteria through natural (non-engineered) processes. Natural attenuation can be though of both as a "passive remediation technology" as well as a predictive risk based closure technique.

Intrinsic bioremediation hinges on biodegradation by various indigenous subsurface bacterial groups generically classified according to electron acceptor type, including O_2, NO_3^-, Mn^{4+}, Fe^{3+}, and SO_4^{2-} reducing bacteria and methane producers. Of these groups, less is known about the practical operation of Mn^{4+}, Fe^{3+}, and SO_4^{2-} reducing bacteria in part because their respiratory processes invariably involve mineral and aqueous interactions that are difficult to examine by ground water monitoring alone. As discussed below, a cursory assessment of electron acceptor abundance in the subsurface would suggest that Fe^{3+} and SO_4^{2-} reduction are dominant microbial processes. It follows that research into Fe^{3+} and SO_4^{2-} reduction processes may contribute greatly to an overall understanding of both RBCA and natural attenuation. Further, such research may suggest ways to augment Fe^{3+} and SO_4^{2-} reduction in engineered remediation systems.

1.2. Purpose

This research focuses on Fe^{3+} and SO_4^{2-} reducing bacterial and mineral processes in aquifers contaminated with hydrocarbon fuel and landfill leachate. This document:

- Reviews intrinsic bioremediation processes with emphasis on Fe^{3+}, and SO_4^{2-} reducing bacteria;
- Describes methods developed to examine oxidized and reduced Fe and S minerals in field studies;
- Examines the distribution of Fe and S minerals at several organic contaminated sites;
- Suggests ways to implement Fe and S mineral analysis into intrinsic bioremediation assessment protocols;
- Examines Fe and S processes in microcosms under controlled laboratory conditions;
- Investigates the potential for engineered treatment systems using solid Fe^{3+} and SO_4^{2-} supplementation;
- Suggests methods to integrate Fe and S reduction processes with reaction-path ground water modeling.

The goals outlined above were achieved by combining literature research with field investigations and laboratory experimentation. Field investigations of Fe and S mineral distribution were primarily conducted at a gasoline fuel contaminated site; however, work was also conducted at a landfill and at an unusual site where the soil was flooded with methane gas from a natural gas well blowout. Here, the research emphasized observing the distribution of oxidized Fe^{3+} and reduced Fe and S minerals in situations where the soil/aquifer was contaminated.

Laboratory work could be divided into two phases, method development, and microcosm analysis. First, during method development, tests were conducted to create and evaluate Fe and S mineral extraction techniques required for this research. Second, the effects of amending native soils with Fe^{3+} and SO_4^{2-} minerals on synthetic leachate degradation were examined through microcosm experimentation. This microcosm research examined Fe^{3+} and SO_4^{2-} reduction under controlled conditions by observing changes in aqueous, solid, and gaseous phases. Microcosm analysis is used for:

- Exploring the possibility of engineered remediation systems based on supplementation of Fe^{3+} and SO_4^{2-} minerals, and
- Better defining Fe and S microbial/mineral interactions that occur naturally under aquifer conditions.

Chapter 2 describes the environmental problems associated with landfills and hydrocarbon fuels. Intrinsic bioremediation, redox zone development, and electron acceptor origin and occurrence are described in Chapter 3. In Chapter 4, Fe and S mineral extraction methods are developed and used at three different contaminated sites. Data evaluation techniques are also described in this chapter. Chapter 5 applies Fe and S mineral analysis to a natural attenuation study at a gasoline contaminated site. Chapter 6 presents the results of microcosm analysis, emphasizing Fe and S microbial processes, to degrade a synthetic landfill leachate. Chapter 7 summarizes all research work. In that chapter, research conclusions are examined for application to natural attenuation and for active remediation system design based on Fe^{3+} and SO_4^{2-} reduction.

Research results are also examined for conceptual application to new reaction pathway mass-transport computer models.

1.3. Introduction Summary

Ground water generally is recognized as a critical resource that is increasingly relied upon as an essential resource. Remediation of contaminated ground water is often technologically limited by many factors inherent to both the contaminant and subsurface properties. Technological limitations, combined with conservative action levels based on non-site specific standards can greatly increase treatment time and costs. These problems are potentially ameliorated through the implementation of RBCA and natural attenuation. Intrinsic bioremediation is an integral part of both RBCA and natural attenuation. Fe^{3+} and SO_4^{2-} reducing bacteria are believed to play an important, and possibly, dominant roles in natural attenuation and are the focus of this research.

2. BACKGROUND

2.1. Literature Search

This research is multidisciplinary and includes elements of microbiology, geology, geochemistry, mineralogy, hydrogeology, and environmental science. As a result, a variety of research materials were needed. Pertinent literature on all of those areas was reviewed, but special attention was placed on material related to Fe and S bacterial/mineral studies. Emphasis was placed on recent periodicals, though older research was also reviewed for background development. Several new textbooks, including Stumm and Morgan (1996), Chapelle (1992), and Enrlich (1995), were valuable resources because they synthesized the research results from numerous, often interdisciplinary resources. Many on-line data resources were found by searching the World Wide Web. Finally, much information was gained by discussions with colleges actively engaged in Fe and S bacterial research including Dr. John Wilson, Dr. Gorm Heron, Dr. Bill Lyon, and Mr. Glenn Urlich.

2.2. Review of Environmental Problem

This chapter presents an overview of the environmental problems associated with hydrocarbons and landfills. For landfills, the discussion is split to separately address issues related to leachate and gas. The physical/chemical characteristics of some associated contaminants are described. A summary is

presented of the historical development of the environmental problems related to landfills and petroleum hydrocarbons. This chapter also reviews engineering controls that have been applied to the petroleum industry and landfills to provide environmental control. It is observed that many of these engineering controls cure some environmental problems but often create others.

2.2.1. Municipal Landfills

According to recent U.S. EPA figures, about 180 million tons of municipal waste are produced each year in the U.S. Without source reduction, the EPA estimates that U.S. citizens will generate approximately 216 million tons of municipal waste in the year 2000. Waste volumes are growing even faster than our population. The U.S. now produces about four pounds per person per day of municipal solid waste, up from about 3.5 pounds per person per day in 1960, and projected to be about 4.4 pounds per person per day in the year 2000 (USEPA, 1990). There are approximately 3,000 municipal solid waste landfills in use in the United States alone (Goldstein, 1997) and many closed landfills. Landfills present environmental concerns principally in the form of liquid leachate and gaseous emissions, problems that dominate the environmental engineering control systems required in modern municipal landfills.

Landfill Leachate

Until the 1900s, solid waste was dumped directly on the land (McBean et al., 1995). Until the 1950s, municipal refuse disposal consisted of careless

dumping; open-pit dumping and burning was standard practice. During the 1950s, there was a general recognition of the adverse health and environmental effects of open dumping. Landfill pits were generally covered with a minimum of soil and surface vegetation was encouraged. Concern for the environmental impacts of landfills culminated in the passage of the Solid Waste Disposal Act of 1965. This act largely provided resources for research and development to improve solid waste management and provide for the promulgation of regulatory guidelines. Landfills are currently regulated under the Resource Conservation and Recovery Act (RCRA). As passed in mid 1976, RCRA included a section on solid waste management under Subtitle D, part 40, subpart 257. EPA published draft guidelines for municipal solid waste management in 1978 and expanded those guidelines in 1984 and 1988. The final RCRA Subtitle D regulations, promulgated in October 1991 required: daily cover; the installation of liners and leachate collection systems; gas and ground water monitoring; final cover; closure and financial surety. Among other things, these regulations had the benefit of minimizing leachate impacts on ground water; however, new problems were created, including the need to treat collected quantities of landfill leachate. Promulgation of these regulations forced the closure of many unlined landfills often operated by smaller cities and towns; however, many of these older, closed landfills still release leachate to soil/ground water.

Leachate may be defined as liquid that has percolated through solid waste and extracted or dissolved portions of that waste. The generation of leachate is typically modeled through a mass balance approach (EPA, 1977 and 1984).

Sources of water into the landfill include moisture in the waste, rainwater infiltration, ground water flux, and moisture in the cover material. Water loss can be from microbial respiration, evaporation, and by leachate leaving from the bottom of the landfill. In general, leachate quantity is a direct function of the amount of external water entering the landfill. Vertical advective leachate movement can occur only after sufficient fluid is available to overcome the residual saturation of the host matrix (waste pile or soil). Once leachate reaches an aquifer its movement is generally in the direction of ground water flow and subject to typical solute transport effects including advection, dispersion, ion exchange, sorption, and others.

Municipal waste landfill leachates are high strength and have been compared to industrial waste leachate with respect to toxic characteristics (Brown and Donnelly, 1988). Fresh leachate contains high concentrations of organic compounds (1,500 – 20,000 mg/L organic carbon); between 1,000 – 10,000 mg/L alkalinity ($CaCO_3$); less than 3,000 mg/L major dissolved ions such as Ca, Mg, K, Na Cl, SO_4^{2-}, and Fe; less than 40 mg/L NO_3^-; and smaller amounts of heavy metals including Pb, Cu, Ni, Cr, Zn, Cd, Hg, Ba, Ag, As, Cn, and Fl (Tchobanoglous et al., 1993). The organic fraction can be comprised of dozens of compounds (Robertson et al., 1974). However, more than 90% of the organic content is comprised of simple straight chain fatty acids ranging from 2 to 6 carbon atoms in length (acetic to caporic) as shown on Tables 1 and 2 (Baedecker and Back, 1979; Hoeks and Borst, 1982; Kjeldsen and Christensen, 1994). Of the remaining organic constituents, those commonly found in leachate

Table 1. Fresh leachate organic composition.

Table 2. Average organic acid composition in fresh leachate.

of regulatory concern include benzene, tetrachloroethylene, trichloroethylene, trichloroethane, vinyl chloride and others (Kmet and McGinley, 1982; and Ground Water Quality Standards, 1988). The actual leachate composition found at a landfill will depend upon waste composition and conditions within the landfill such as temperature, moisture content, moisture routing, depth of fill, stage of decomposition, ability of intermediate soil layers to remove contaminates, and quality of water entering the landfill (Ehrig, 1989).

Leachate is often subject to a microbially induced transformation within the landfill that dictates its characteristics as a waste or contaminant. This maturation process is though to occur in five, more or less sequential phases (Tchobanoglous et al., 1993). Phase 1 is an *initial adjustment* phase where labile organics are consumed aerobically. Phase 2 is termed the *transition phase*. During this phase, the leachate is anoxic and may be degraded by NO_3^- and SO_4^{2-} reducing bacteria. During Phase 3, the *acid phase*, higher molecular mass organic compounds (e.g., lipids, polysaccharides, proteins, and nucleic acids) are fermented by bacteria to simpler organic acids typified by acetic acid (CH_3COOH). These organic acids, plus generated CO_2, can decrease leachate pH to 5 or lower which may solublize heavy metals. In Phase 4, the *methane fermentation* phase, a second group of microorganisms convert acetic acid and hydrogen gas to CH_4 and CO_2. During this time, pH may rise to the circum-neutral range facilitating the precipitation of heavy metals. Finally, Phase 5, the *maturation phase*, occurs after the readily available labile organic material is

consumed. Essentially, the residual recalcitrant organic compounds are degraded at a much slower rate with much less gas generation.

Typically, Phases 1 and 2 are thought to be of short duration. Phases 3 and 4 are typically assumed to last about 5 years after waste emplacement; however, Phase 5 can last many decades (Belevi and Baccini, 1992; Tchobanoglous et al., 1993). These phases often overlap because fresh waste can be added to a landfill over many decades. The availability of adequate moisture is a strong controlling factor in organic conversion that can greatly impede organic degradation and gas production rates (Gurljala and Suflita, 1993).

It is thought that leachate will eventually migrate from a landfill facility, to the broader environment years or decades after placement of the waste in the facility even with the application of best available land disposal technology (Federal Register, 1981). EPA again emphasized that landfills will inevitably leak, saying "A liner is a barrier technology that prevents or greatly restricts migration of liquids into the ground. No liner, however, can keep all liquids out of the ground for all time. Eventually liners will either degrade, tear, or crack and will allow liquids to migrate out of the unit," (Federal Register, 1982).

Landfill Gas

In 1996, new standards and emission guidelines were implemented under Section 111 of the Clean Air Act. These rules were promulgated based on the determination that municipal solid waste landfills cause, or contribute significantly to, air pollution that may reasonably be anticipated to endanger public health or

welfare. The intended effect of the standards and guidelines was to require certain municipal solid waste landfills to control emissions to the level achievable by the best demonstrated system of continuous emission reduction, considering costs, nonair quality health, and environmental and energy impacts (Federal Register, 1996).

As already mentioned, gaseous emissions from landfills are largely the product of microbial processes. Table 3 shows typical landfill gas composition (Ham, 1979). The primary constituents are CH_4 and CO_2, which comprise roughly 47% each. Non-organic compounds include mostly nitrogen (3.7%) with smaller amounts of oxygen, hydrogen, hydrogen sulfide, and carbon dioxide. Non-methane organic compounds (NMOC) constitute about 0.3% and are comprised mostly of alkane gases up to C12 with occasionally high concentrations of benzene and toluene (0.03 – 615 mg/m^3) (Rettenberger, 1987). These constituents include volatile organic compounds (VOC), hazardous air pollutants (HAPs), and odorous compounds.

Landfill gases have various environmental and human health impacts. VOC emissions contribute to ozone formation, which can result in adverse effects to human health and vegetation (Federal Register, 1996). Ozone can penetrate into different regions of the respiratory tract and be absorbed through the respiratory system. The health effects of exposure to HAPs can include cancer, respiratory irritation, and damage to the nervous system. Although landfill gases

Table 3. Average landfill gas composition

contain organic chemicals that may be toxic, these gases are usually vented directly into the ambient air where they can move downwind exposing people who live nearby. Field evidence suggests an increased incidence of human health problems, including respiratory, skin, narcotic and mood disorders, in landfill workers and residents living near landfills. These symptoms are thought to be from vapors, fumes or particulate matter emanating from landfills (Hertzman et al., 1987). A correlation between increased risk of cancer and human proximity to landfills has also been found and attributed to landfill gas emissions (Goldberg et al., 1995).

Methane, and to a lesser extent CO_2 emissions, contribute to global climate change. Augenstein (1992) estimated that over the next 10 years, U.S. landfill emissions would add about 1% to the total annual increase of greenhouse gases in the earth's atmosphere. This infers that in localized areas of poor air quality, landfill emissions could represent an even more significant problem. A cost analysis suggests that landfill methane abatement is one of the most cost-effective measures for reducing greenhouse emissions (Augenstein, 1992).

Methane buildup can result in fires or explosions if it accumulates in structures on or off the landfill site. Methane gas concentrations in excess of 5% by weight are explosive. Landfill gas (CO_2 and/or CH_4) can be an asphyxiant in enclosed areas. These gases can displace oxygen in the soil root-zone and kill vegetation, which may be needed to protect final landfill cover from erosion. Finally, CO_2 buildup within the landfill contributes to acidic conditions that can encourage heavy metals dissolution (Tchobanoglous et al., 1993).

The mechanics of gas movement through refuse and soil is extremely complex. The gas will tend to migrate from the landfill on a path through the refuse and surrounding soils that offers the least resistance or highest permeability. The rate of migration is strongly influenced by weather conditions: when barometric pressure is falling, gas will tend to be forced out of the landfill into the surrounding soil formations (Metcalfe, 1982). As pressure rises, gas may be retained within the landfill for a time. Impermeable layers such as clay or frozen ground can cause landfill gas to migrate laterally. An impermeable landfill cap may have the similar effect of forcing gas to move laterally into areas surrounding the landfill.

Landfill gas is generally thought of as a being formed within the waste pile proper. However, because it is a byproduct of microbial respiration, it can be generated some distance from the landfill by the biodegradation of an organic-rich leachate plume. This increases the risks associated with landfill gas especially with respect to explosive methane buildup. Elevated concentrations of methane have been documented down-gradient of landfills (Murray et al., 1981 and Lyngkilde and Christensen, 1992).

2.2.2. Hydrocarbon Fuel

Currently, the United States consumes approximately 17 billion barrels of crude oil per year (DOE, 1997 and 1994). Hydrocarbon contaminants enter the soil/ground water during crude production, and transportation, refining, and distribution operations. Because of wide-spread hydrocarbon use, the incidence

of petroleum related subsurface contamination is very high. For example, it is estimated that there are over 2 million under ground storatge tanks (UST) systems alone at over 700,000 facilities nationwide and between 295,000 to 400,000 of these sites have released fuel (EPA, 1993; Russel et al., 1991; and OTA, 1989).

The environmental control of hydrocarbons is regulated under many state and federal statutes. Pipeline facilities (including gathering lines) are regulated under the Natural Gas Pipeline Safety Act of 1968 and the Hazardous Liquid Pipeline Act of 1979, or state laws comparable to these Acts. 40 CFR Parts 280 and 281 regulate USTs under authority of the Hazardous and Solid Waste Amendments (HSWA) of 1984, which ultimately produced RCRA, Subtitle I. Subtitle I, provides for the development and implementation of a comprehensive regulatory program for "underground storage tanks" containing "regulated substances" and releases of these substances to the environment. "Regulated substances" are substances defined as hazardous under the Comprehensive Environmental Response, Compensation, and Liability Act of 1980 (CERCLA), except hazardous wastes regulated under Subtitle C of RCRA, and petroleum. Many hydrocarbon-based petrochemicals are, however, considered hazardous wastes by definition or characteristic.

Gasoline is a complex chemical mixture containing more than 1,000 substances. Specific composition of fuel is related to crude type and refining; however, the major chemical groups in gasoline include roughly 15% n-paraffins, 30% iso-paraffins, 12% cycloparaffins, 35% aromatics, and 8% olefins

(Hamilton, 1995 and Johnson et al., 1990). Of the fuel components, alkylbenzenes including benzene, toluene, xylene, and ethylbenzene (BTEX) are typically regulated due to concerns about human health effects. BTEX compounds are generally assumed to constitute between 5 to 15% of the total hydrocarbon mass (Newell et al., 1996). Most fuel components are largely immiscible with water and tend to partition to the soil when released (Kennedy and Hutchins, 1993). Due to variations in compound solubility, the aromatic hydrocarbons, and in particular, BTEX, constitute by far the greatest mass of compounds that partition from fuels into ground water (Cline et al., 1991).

Mehlman (1992) examined the evidence from 29 human epidemiological studies and concluded that exposure to gasoline significantly increased tumors of the kidney, liver, and other tissues. There are several known toxic substances in gasoline, some of which are confirmed human carcinogens including lead and benzene. Other aromatics and some toxic olefins also have regulated environmental concentrations.

2.3. Environmental Engineering Controls

2.3.1. Landfill Leachate

Landfill leachate is an unwanted product of waste storage. Preventative engineering controls largely center on minimizing leachate generation by reducing liquids entering the landfill. Barring this, produced leachate is ideally kept from escaping the landfill through the utilization of a liner/leachate collection system. A modern landfill liner consists of 1) a protective soil layer, 2) collection

pipes in sand or a geonet for leachate collection, 3) a synthetic membrane, and 4) compacted clay (Tchnobanoglous et al., 1993). A number of alternatives have been used to manage collected leachate including 1) leachate recycling, 2) evaporation, 3) discharge to municipal wastewater collection systems by sewer or tank truck, and 4) treatment followed by disposal. In many cases, onsite pretreatment is required before leachate can be discharged to the sewer and in other instances, sewers may not be available. Onsite leachate treatment systems are usually biological and similar to those used in wastewater treatment. Such systems include activated sludge, sequencing batch reactors, aerated stabilization basins, fixed film processes, and anaerobic lagoons/contactors (Tchnobanoglous et al., 1993). High chemical oxygen demand (COD) leachate favors anaerobic treatment because of the expense of aerobic treatment.

As discussed above, liners were not installed in old landfills, allowing leachate to easily escape. Furthermore, leaks can occur even where liner/leachate collection systems are employed. In many cases, escaped leachate has been left to naturally attenuate in the soil/aquifer, although remediation systems have been installed in some landfills, especially those classified as CERCLA sites. Potential technologies which could be used to control the spread of a leachate plume include 1) various pump-and-treat systems, 2) barrier walls, 3) reactive walls, 4) in-situ bioremediation, and others.

2.3.2. Landfill Gas

Although methane has potential economic value as a fuel source, in general, modern landfills are operated on a principle of permanent waste containment. Consequently, landfill gases are generally viewed as an undesirable product of waste storage. As a preventative measure, limiting moisture in the landfill could inhibit gas generation by retarding microbial respiration (Beeman and Suflita, 1990). The clay cap installed upon completion of a landfill for excluding moisture infiltration and restricting leachate and gas generation will, at the same time, tend to facilitate the buildup of landfill gas.

Gas control systems are installed to 1) prevent the buildup of gases in the landfill or cover, 2) recover gas for energy purposes, 3) control air emissions, and 4) prevent off-site subsurface migration. Passive vents and active gas pumping systems are used to control landfill gas migration. Passive systems rely on natural pressure and convection mechanisms to vent the landfill gas to the atmosphere. Gas venting pipes, installed within the landfill and vented to the atmosphere, have been used to allow gas from interior regions of the landfill to escape. These natural vents may be equipped with flares to burn off the gas in order to prevent odor problems.

In areas where there is a significant risk of methane accumulating in buildings, passive systems are not considered reliable enough to be the sole means of protection and active systems are used. Active gas collection systems remove the landfill gas under a vacuum from the landfill or the surrounding soil formation, with the gas being literally pumped out of the ground using a blower.

These systems may provide migration control or recover methane for energy recovery purposes. In this case, gas is routed to a gas burning electrical generator.

When the primary purpose is migration control, recovery wells, or trenches can be constructed near the perimeter of the landfill. Depending on site conditions, the vent wells may be placed in the waste or in the soil formation immediately adjacent to the landfill.

2.3.3. Hydrocarbon Fuels

The past seventy years constitute the automobile age in the United States. During this time, as many as one million filling stations, each with a life expectancy of about fifteen years, were built. When mass-produced, gasoline-powered automobiles became available about 1909, the only gasoline distribution stations around were general stores using barrels for storage and buckets as dispensers. A fill up was a messy and dangerous task. Invention followed need, however, and in the early 1910's, the introduction of pumps to dispense gasoline allowed the burial of storage tanks underground (Wesolowski and Le Grand, 1996). Though the USTs system eliminated the potential for explosion and reduced human exposure, this engineering control created the new problem of undetected soil and ground water pollution by leaking fuel.

Through RCRA Subtitle I, EPA mandates detection, correction, and prevention of leaks in existing tanks, and provides standards for installation of new tanks. To reduce fuel leaks, new regulations call for enhanced performance

standards for new tanks, leak detection, devices for overfill protection and other engineering or management controls designed to prevent fuel leaks.

On the opposite end of the hydrocarbon delivery system, petroleum pipelines were built in the United States in an ad hoc manner to connect newly discovered oil fields to refineries or storage terminals. Therefore, the construction of petroleum pipelines largely mirrors oil field development, with most being built in the 1920's through 1960's. In addition to being old, these pipelines were not originally built with modern environmental concerns in mind. Pipe was simply painted or coated with tar to inhibit external corrosion. Finally, low oil prices in recent years, and dwindling domestic oil production, have placed an added economic burden on oil transporters. Consequently, pipeline maintenance is often marginal, further increasing the likelihood of a leak occurring. Most of these pipelines are buried below the surface and are in remote areas so that when a leak occurs, hundreds or thousands of barrels of product can be lost before detection and repair. Chemical inhibitors are added for internal corrosion control and impressed current or catholic protection is used to reduce external corrosion, but pipeline failures are still very common. The author has examined pipelines for several major oil companies and found dozens of significant spills occurred per year in systems of just a few hundred miles in length. This situation poses a very significant and ongoing threat to ground water supplies over wide geographic regions.

So many techniques have been developed to treat aquifers contaminated with hydrocarbons that they cannot be covered here. Free-phase (floating)

product is generally recovered by some form of direct pumping (Testa and Winegardner, 1991). Hydrocarbons sorbed onto shallow soil can be land farmed, placed in compost or static piles, or incinerated (Sims et al., 1986; and LaGrega et al., 1994). For deeper contaminated vadose zone soils, vacuum extraction or bioventing is commonly used (Pedersen and Curtis, 1991). Contaminated ground water is often pumped to the surface then treated using many different processes including air sparging, carbon sorption, chemical oxidation, biological treatment and many others (LaGrega et al., 1994). As discussed below, many remediation processes have been developed to promote in-situ bioremediation of hydrocarbon contaminated aquifers. In-situ bioremediation can directly degrade the contaminants in all three media phases.

2.3.4. In-Situ Bioremediation Systems

In-situ bioremediation is the treatment of contaminants in the soil/aquifer system by stimulating soil bacteria. Such technology is applicable to landfill leachate and hydrocarbon contaminants. Conceptually, in-situ bioremediation has several potential advantages:

- Soil bacteria may degrade both dissolved and sorbed organics so that treatment time may not be limited by desorption kinetics;
- The biological end products are usually nonhazardous and include biomass, organic daughter products, and various inorganic respiratory products (e.g. CO_2, N_2, and etc..);

- There is sometimes less human exposure;
- In some cases it has the lower-cost;
- Contaminant transfer from one media to another during treatment (e.g., volatilization of VOCs from water to air during air stripping) is minimized; and
- Depending upon the design, treated ground water can remain in the aquifer thus preserving the natural resource.

Most in-situ bioremediation systems are designed to increase the concentration of electron acceptors and, possibly, nutrients such as nitrate and phosphate, etc. It is assumed that such additions stimulate microbial growth and catabolism, facilitating the degradation of organic contaminants that are used as a carbon substrate. The contaminant is ultimately converted to other organic compounds, CO_2 gas, or biomass (bacterial cells).

Most in-situ bioremediation systems have utilized aerobic processes. The addition of oxygen to facilitate organic degradation is established and well understood in wastewater engineering. This treatment type has been in use for greater than 40 years in the United States (Tchobanoglous and Burton, 1991). Many of the principles of wastewater engineering were initially applied to subsurface remediation. For some systems, produced ground water is oxygenated by sparging then injected back into the impacted portions of the aquifer (LaGrega et al., 1994). Oxygen can also be added by direct air injection to the subsurface through sparging or bioventing (Norris et al., 1993). Finally,

oxygen can be added by direct chemical supplementation by adding calcium or magnesium peroxide (Odencrantz et al., 1996 and Bianchi-Mosquera et al., 1994) or hydrogen peroxide (Huling and Bledsoe, 1990; Hinchee et al., 1991; and Aggarwal et al., 1991).

Aerobic substrate utilization rates are generally acknowledged to be high (McCarty, 1971); however, there are problems when O_2 is applied to subsurface remediation:

- Oxygen solubility is generally low in water (typically $\leq$ 8 mg/L at surface conditions) which limits mass transfer and can slow microbial processes;
- The rate of aerobic bacterial growth and yield coefficient is high (McCarty, 1971) often causing microbial slime buildup and fouling of remedial system equipment; and
- Some oxygen will be consumed by abiotic oxidation of reduced inorganic cations (Fe^{2+}, Mn^{3+}, HS^-) which may be especially prevalent in contaminated, reduced aquifers (Kennedy and Hutchins, 1992 and Canfield et al., 1993).

Less work has been done with anaerobic in-situ bioremediation though, in theory, the addition of alternative electron acceptors (NO_3^-, SO_4^{2-}, or Fe^{3+}) could also enhance organic contaminant removal. The addition of NO_3^- for ground water remediation has been tested (Hutchins et al., 1991 and 1996; and Kennedy and Hutchins, 1992). Though nitrate is very soluble, its concentration in drinking water is restricted by regulation in the U.S. to only 10-mg/L maximum

contaminant level (MCL), potentially inhibiting its utility as an amendment. In contrast, SO_4^{2-} has a non-enforceable, suggested maximum contaminant level (SMCL) of 250 mg/L with an MCL of 400 mg/L. Oxidized Fe^{3+} is largely insoluble in water, however, an SMCL for iron of 0.3 mg/L does exist.

Theoretically, bioremediation technologies using Fe^{3+} and SO_4^{2-} have the potential to operate in quite reduced aquifer redox conditions, unlike O_2 or NO_3^- based treatment systems. Additionally, as discussed below, inexpensive sources for naturally occurring Fe^{3+} and SO_4^{2-} minerals are available making their use economically possible on a commercial basis. These facts encourage research into the development of Fe^{3+} and SO_4^{2-} based remediation like that performed here.

2.4. Review Summary

Before the promulgation of landfill regulations, municipal waste was often dumped in open unlined pits and/or burned. Landfills were open systems and little thought was given to ground water contamination. Though there was little actual planning, leachate was treated as though the landfill was a large septic leachfield. At this time, the native soils were viewed as a natural treatment/filtration system. Although not defined as such, natural attenuation processes were relied upon as the only method of treatment. Conversely, a philosophy of complete containment was adopted with the promulgation of the 1991 RCRA Subtitle D regulations. Principally, landfills are sealed by liners above and below. Whereas this engineering approach resolves some problems

it creates others, at least in the short term, including the generation of high strength leachate and high concentrations of off-gases. Even lined landfills can still leak and there are many older landfills which were never lined and continue to pose a potential threat to ground water.

Hydrocarbon products are ubiquitous in our society. Leaks occur at every stage of production, transportation, refinement, and marketing, causing widespread ground water contamination. To minimize explosion hazards and maximize land usage, many petroleum and fuel transportation and storage facilities are built underground; however, this engineering control increases the chance of petroleum being released undetected to the ground water.

Microbial based treatment technologies exist for both leachate and hydrocarbons. These have emphasized aerobic processes, though some experimentation has occurred with nitrate reducing bacteria. It is theoretically possible that engineered treatment systems could be developed utilizing Fe^{3+} and SO_4^{2-} reducing bacteria. Such systems could be used to accelerate contaminant degradation or provide other benefits such as the inhibition of green house gases. Fe and S based treatment systems have the potential advantages of:

- Operating at the prevailing low redox conditions often found in an organic contaminated aquifer;
- Having the ability to be used in high concentrations unlike O_2 and NO_3^-; and

- Being present in inexpensive naturally occurring mineral deposits.

3. INTRINSIC BIOREMEDIATION BACKGROUND

This chapter initially reviews the concepts behind redox development in organic rich subsurface systems. Possible sources for electron acceptors are described. Thermodynamic considerations of common redox reactions are examined including reactions involving solid phase Fe and S based electron acceptors. Observations are also made with respect to electron acceptor abundance in the environment. Special emphasis is given to the geomicrobiology of Fe and S reactions. Finally, examples are also shown of existing intrinsic bioremediation studies focusing on the apparent relationship between Fe^{3+} and SO_4^{2-} reduction and methanogenesis.

3.1. Microbial Environment

In simplest terms, the subsurface environment is comprised of multiple components, including water (with dissolved ions); organic matter (including biomass), gases, and minerals. In the absence of significant microbial processes, aquifer geochemistry can be remarkably stable with significant changes often measured in terms of decades or even centuries for regional flow systems. Alternatively, under certain conditions, bacteria play a pivotal role and dramatically alter the subsurface environment in short periods measured in days. Such rapid changes can occur when labile organic contaminants are released to

a soil/aquifer system causing a rapid increase in microbial growth and respiration.

Soil bacteria can play a central role in determining an aquifer's mineral, organic, dissolved ion, and gaseous contents. Under certain conditions, soil bacteria catalyze mass transfer between these phases (Figure 2). When an organic is introduced to the subsurface, bacterial processes facilitate a very complex sequence of events. Chemoheterotrophic bacteria oxidize organic carbon through the complimentary reduction of various dissolved and solid electron acceptors. New organic substances are also created (e.g., biomass or fermentation products) while some carbon is converted to inorganic CO_2. Gases, such as O_2, H_2, CO_2, H_2S, CH_4 and N_2, can be both generated and/or removed. The geochemical system is also forced out of equilibrium, causing some minerals to dissolve while others are precipitated. This entire process occurs in a complex ecosystem where numerous microbial types interact with each other as well as with their surrounding inorganic environment.

Geochemical equilibrium studies have shown the importance of microbial processes on a regional scale (Thorstenson et al., 1979; Plummer, 1977; and Plummer et al., 1990). For example, Plummer et al. (1990) suggested that bacteria oxidized naturally occurring organics in the Madison aquifer of Wyoming and Montana. In that study, variations in water chemistry caused by microbial activity could be attributed to the dissolution of mineral gypsum (CaSO4•2H2O),

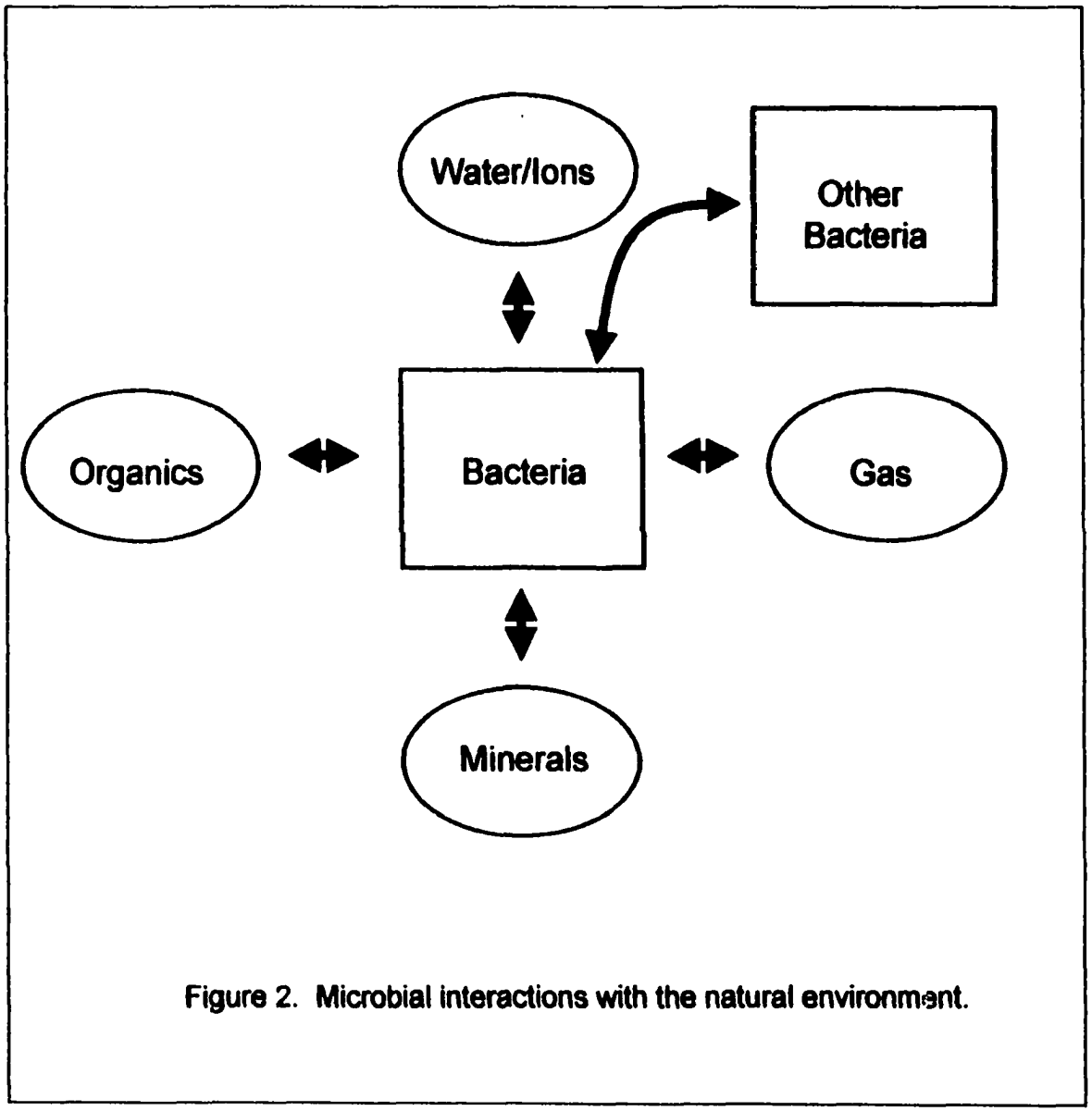

Figure 2. Microbial interactions with the natural environment.

dolomite ($Ca \bullet Mg(CO_3)$), and goethite (FeOOH) with the concurrent precipitation of pyrite (FeS_2) and calcite ($CaCO_3$). Microbial activity was associated with organic consumption; biomass production; gas production (H_2S and CO_2); and mineral dissolution and precipitation, which contributed significantly to changes in overall water chemistry. Evaluated on a regional scale, these microbially produced changes occur slowly because organic carbon is limited, keeping bacterial growth/reproduction minimal. However, many of these same changes can occur very rapidly on a local scale if labile organic contaminants are released to shallow soil/aquifers through pollution.

3.2. Bioremediation Processes/Redox Zone Development

Considerable information as been amassed in support of intrinsic bioremediation of many organic contaminants in the subsurface. With respect to fuels, bacteria capable of degrading hydrocarbons are ubiquitous in soils (Litchfield and Clark, 1973; and Ridgeway et al., 1990). Microbial degradation of organic substrates is accomplished through a complex series of enzymatically-mitigated fermentative and respiratory pathways, which ultimately can be described in terms of simple redox processes. Here, energy is generated by heterotrophic bacteria and used to make ATP by oxidizing an organic substrate. This redox reaction requires the complimentary reduction of an electron acceptor compound. For example, aerobic oxidation can be represented as:

(1) $CH_2O + O_2 \rightarrow CO_2 + H_2O$

Here, carbon (C^0) is oxidized to C^{4+} by transferring $4e^-$ to oxygen, which is reduced. Often it is necessary for complex organics to be fermented to create smaller carbon compounds, which may also be activated through the ultimate insertion of a carboxyl group (Gaudy and Gaudy, 1988). In some cases, a single bacterial strain is capable of accomplishing both fermentation and respiratory oxidation. However, many complex interspecies relationships occur between bacterial groups and one or more groups may accomplish fermentation while oxidation is done by others. Energy can be released as a result of some fermentation reactions; however, in many cases, a required fermentation step results in a loss of ATP energy. Respiratory oxidation, through the TCA cycle, usually results in considerable conservation of ATP forming energy.

In addition to oxygen, indigenous soil bacteria have the ability to oxidize organics using other electron acceptors. Alternative electron acceptors include nitrate (NO_3^-), manganese (Mn^{4+}), sulfate (SO_4^{2-}), and iron (Fe^{3+}) (Barbaro et al., 1992; Beller et al., 1992; Lovley and Phiilips, 1986 and 1987; Lovley, 1990; and Hutchins et al. 1991 and 1992).

Electron acceptors are often limited in the subsurface. If a sufficiently large hydrocarbon spill occurs, carbon mass may greatly exceed electron acceptor supply and a redox series may develop as certain electron acceptor types are preferentially used (Berner, 1980; Norris et al., 1994; and Stumm and Morgan, 1996). Common convention holds that the order of utilization is O_2 > NO_3^- > Mn^{4+} > Fe^{3+} > SO_4^{2-} > methanogenesis. Overall, this represents a redox change (pe) ranging from approximately +15 to −10. However, as discussed

below, and observed in this research, mineral Fe^{3+} reduction may occur over a wide redox range through methanogenesis.

For complete mineralization, an organic is oxidized to CO_2. In this case, organic removal is stoichiometrically balanced against a given mass of electron acceptor. A certain fraction of organic, however, may be biotransformed to intermediate organic products that are not fully oxidized. Additionally, some substrate can be converted to biomass through anabolic processes with little or no oxidation. Therefore, the observed organic consumption is usually greater than that predicted from mass of electron acceptor consumed based on stoichiometry.

Given the exceptions above, reactions involving O_2, NO_3^-, Mn^{4+}, Fe^{3+}, and SO_4^{2-} are often written in terms of redox processes involving an organic balanced with a specified mass of inorganic electron acceptors. However, this is not true with respect to methanogenesis. Acetoclastic methanogenesis involves the simultaneous oxidation and reduction of the organic compound (acetate) as:

(2) $CH_3COOH \rightarrow CH_4 + CO_2$

Chemoautotrophic bacteria as can also generate methane as:

(3) $CO_2 + 4H_2 \rightarrow CH_4 + 2H_2O$

In Equation 2, the electron donor and acceptor is the organic substrate. For Equation 3, the reactants are both inorganic, CO_2 and H_2 gas, so an organic

substrate is not directly oxidized. H_2 can, however, be generated through organic substrate fermentation. In general, methanogenesis occurs in the relative absence of inorganic electron acceptors.

The electron acceptor redox succession is believed to be thermodynamically related (Berner, 1980 and Stumm and Morgan, 1996). The amount of free energy (ΔG) that can be generated for each of these oxidation/reduction reactions decreases for each successive electron acceptor couple. The bacterial type capable of deriving the most energy per unit organic oxidized/electron acceptor reduced has a natural advantage over other types and may dominate the local environment (McCarty, 1971). When an electron donor is in abundance, a lower energy yielding electron acceptor is utilized only if the electron acceptors of higher energy levels have been substantially depleted. This situation infers the secession of microbial species with changing redox conditions.

Evidence of redox sequence development has been observed in the field at various contaminated sites. In landfills, redox development was noted by Nicholson et al. (1983); Lyngkilde, and Christensen, (1992); and Bjerg et al. (1995). Numerous examples of redox zone development associated with hydrocarbon fuel spills are reported by Wiedemeier et al. (1995 and 1997). Successively lower redox zones are thought to develop concentrically towards the center of the organic plume (Figure 3). Oxygen is depleted around the outer edge of a plume followed by NO_3^-, ~Fe^{3+}, and SO_4^{2-} consumption. In the center of the plume, methanogenic processes may dominate. The observed distribution

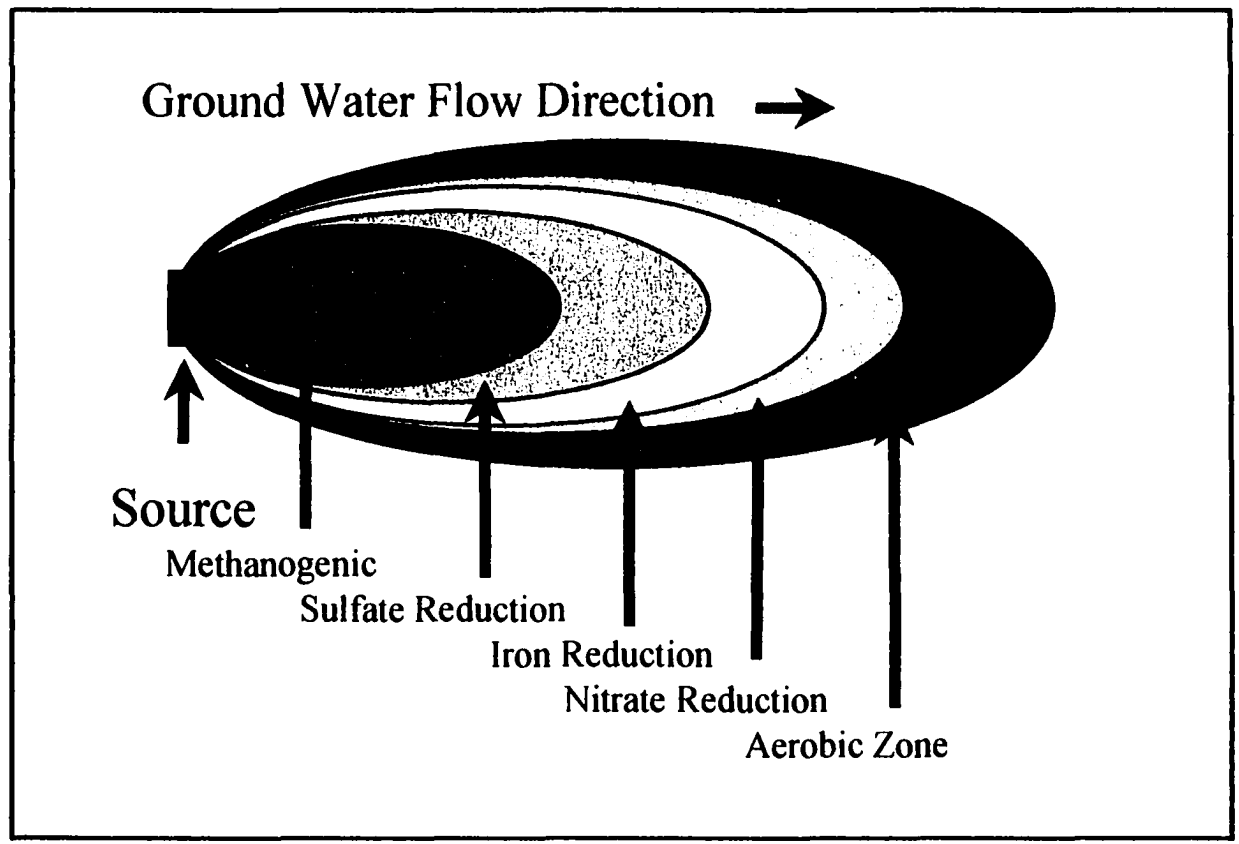

Figure 3. Conceptual redox zone development based on classical electron utilization sequence.

of redox areas is generally similar for landfill leachate and hydrocarbon plumes. Based on the literature studies referenced above, however, there are some notable exceptions. Due to the composition of municipal waste, landfill leachate can contain many dissolved ions, including significant amounts of Fe^{2+} and SO_4^{2-}, which are redox zone indicators. In some cases, SO_4^{2-} concentrations in ground water may increase next to a landfill from the addition of SO_4^{2-} bearing leachate even though SO_4^{2-} reduction may be occurring. Conversely, elevated concentrations of dissolved Fe in landfill leachate may locally give the appearance of Fe^{3+} reduction where none occurs. In contrast, fuel hydrocarbon rarely contains significant inorganic constituents, which simplifies redox analysis.

3.3. Electron Acceptor Occurrence In the Subsurface

Though each aquifer is unique, certain generalities can be made concerning natural electron acceptor abundance. All electron acceptors are involved in microbial cycling where elements are alternatively oxidized or reduced. In relation to general subsurface abundance, however, the development of the oxidized forms is only discussed here by type. Additionally, although Mn^{4+} is an electron acceptor it is usually not examined in natural attenuation studies and is not considered here.

3.3.1. Oxygen

The equilibrium concentration of oxygen in pure water is a function of the concentration in the surrounding atmosphere, as described by Henry's Law:

(4) $$N_g = N_w * \frac{P_g}{H} * (1 - \frac{P_g}{H})^{-1}$$

Where:

N_g = Moles gas in solution at equilibrium

N_w = Moles of water per liter

H = Henry's law constant for gas (atm/mole fraction)

P_g = Percent gas (oxygen) at prevailing condition

Using Equation 4 the dissolved oxygen content for surface water is calculated to be 9.76 mg/L assuming 20 C°, 1 atm, N_w = 55.6 moles/L, and H = $4.01X10^4$ atm/mole given an atmospheric O_2 concentration of 22%. The oxygen concentration in the vadose zone soil gas is, however, much lower. Soil oxygen content is depleted by aerobic bacteria and plant root respiration. Additionally, air exchange with the soil is greatly inhibited both by the solid matrix and soil water content. Under dry conditions there is limited gas exchange between the soil and atmosphere through soil macropores (fissures and cracks) and micropores (intergranular porosity). With increasing moisture, first micropores then macropores become blocked with water and oxygen exchange becomes increasingly restricted. Consequently, concentrations of oxygen in the shallow soil (<120 cm) typically range from 15% when dry to 5% when wet (Brady, 1990).

Under typical soil conditions, non-contaminated ground water would be expected to have between 6.6 mg/L to as little as 2.2 mg/l dissolved O_2. Obviously, even lower concentrations of oxygen can occur with increasing depth,

soil moisture, and soil organic content. This range is consistent with the average 5.0-mg/L background O_2 found at several fuel-contaminated sites by Wiedemeier et al. (1995).

3.3.2. Nitrate

Nitrate salts are extremely soluble in water (e.g. 1.8 g/cm^3 water for NH_4NO_3 (Weast et al., 1987)), so that the solubility limit is unlikely to be exceeded in ground water; however, concentrations of NO_3^- are typically low. The drinking water standard is 10 mg/L (NO_3^-) which is usually not exceeded in normal ground water, though higher concentrations can be found especially in agricultural regions where nitrogen based fertilizers are applied. There are no common mineral sources of NO_3^-. Small amounts of nitrogen oxides come by combustion of fossil fuels and oxidation of atmospheric nitrogen from lightning; however, naturally occurring nitrate is predominantly generated by microbial processes (nitrogen fixation and nitrification) (Pierzynski et al., 1994). Wiedemeier et al. (1995) found average NO_3^- concentrations of 23 mg/L for non-hydrocarbon fuel contaminated water at several air force bases.

3.3.3. Iron

Iron is the fourth most abundant element in the earth's crust and, in the broadest sense, all sediments are likely to be iron bearing (Pettijohn, 1975). As discussed further below, Fe is largely insoluble at normal pH and exists, for all

practical purposes, as a solid mineral phase. Iron mineral content may exceed 80% in biogenically produced iron ore sediments. In more typical sediments, iron minerals average 4.56% in graywacke (feldspar rich) sand to 0.34% in quartz arenites, and 6% in shale sediments (Pettijohn, 1975). Based on this research and the author's experience, Fe^{3+} in sandy sediments is generally in the range of 1%. As discussed below, only a fraction of this (typically 0.01% or 100 mg/Kg) is available for immediate bacterial reduction.

Recent studies have indicated active chemolithotrophic bacterial populations obtain energy through reactions with igneous basalt at depths of 1,500 meters below the surface (Kerr, 1997). In general, however, simple iron minerals (hydroxides, oxides, sulfides, etc.) in shallow sedimentary rock is of greatest interest to natural attenuation. Originally these simple iron minerals were formed from the weathering and diagenesis of primary (parent) Fe-bearing igneous/metamorphic minerals, the more common of which include hematite, ilmenite, and Fe-bearing silicates including amphiboles, pyroxenes, olivine, and biotite (Chesterman and Lowe, 1987).

There are numerous common Fe^{2+} and Fe^{3+} sedimentary minerals as shown in Table 4. More than one species can be present in the same sediment, depending on sedimentary and post depositional (diagenetic) conditions. Although these minerals can exist as crystalline or amorphous particles, the oxides are often present as coatings on silicates. Simple Fe^{3+} rusts are more rare because they are unstable and tend to develop into more crystalline forms,

Table 4. Major iron minerals with valence and chemical composition

such as hematite or goethite over time and with heat and pressure (Huang and Schnitzer, 1987). The occurrence of Fe^{3+} minerals is probably greatest in shallow sediments where the concentration of oxygen is highest.

Oxidized Fe^{3+} can be incorporated during sedimentation or develop authigenically (formed in place after deposition) by the precipitation of dissolved Fe in ground water. Iron cycling is relatively straightforward. Under alkaline to neutral conditions, Fe^{2+} is inherently unstable in the presence of O_2 and is oxidized spontaneously to Fe^{3+} so microorganisms have little chance to extract energy from the oxidation process (Atlas and Bartha, 1993). Under acidic conditions, Fe^{2+} oxidation is used as the foundation for energy generation by chemolithotrophic acidophilic bacteria.

3.3.4. Sulfate

SO_4^{2-} can be generated by both biotic and abiotic means. Sources for reduced forms of S include elemental sulfur (S^o), hydrogen sulfide (H_2S), polysulfides, and various metal sulfides of which the iron sulfides shown in Table 4 are the most common. A combination of autoxidation and microbial sulfur oxidation of iron sulfide minerals produces large amounts of acidic water or acid mine drainage (Evangelou and Zhang, 1995; and Fortin et al., 1994 and 1996). At a neutral pH, oxidation by atmospheric oxygen occurs spontaneously and quite rapidly, but below pH 4.5, autoxidation slows drastically and acidophilic bacteria are responsible for continued oxidation. Reduced S forms are also oxidized by many bacterial species at the normal pH ranges typically found in

ground water (Atlas, 1993). Reduced S can also oxidize abiotically to SO_4^{2-} by the reduction of NO_3^- and possibly by Fe^{3+} (Postma et al., 1991; and Jorgensen, 1990).

Sulfate occurs in certain igneous-rock minerals of the feldspathoid group, but the most extensive and important occurrences are in evaporite sediments (Hem, 1985). As shown in Table 5, there are thirteen common minerals containing SO_4^{2-} found in evaporitic deposits which can be sources for dissolved SO_4^{2-} in ground water (Hardie, 1991). Of these, gypsum ($CaSO_4 \cdot 2H_2O$) and anhydrite ($CaSO_4$) are very common in some areas, where evaporite deposits can be hundreds of feet thick. As a practical matter, because gypsum and anhydrite are highly soluble, ground water is rarely saturated with them unless mineral forms are present in quantity. The concentration of SO_4^{2-} in ground water is dictated by mass action principally controlled by Ca. In pure water, the total solubility for gypsum can be calculated by summing the amount of the mineral present in both ionic and complexed form. The solubility product for gypsum is:

(5) $$(\gamma_{Ca2+} * m_{Ca2+})*(\gamma_{SO4} * m_{SO4}) = 10^{-4.6}$$

and the stability constant for complexed gypsum is:

(6) $$\frac{[CaSO4^o]}{[Ca][SO_4]} = 10^{2.31}$$

Table 5. Naturally occurring sulfate salt minerals in evaporite

For low ionic strength solutions, Equations 5 and 6 would yield SO_4^{2-} concentrations of approximately 1,400 mg/L at equilibrium (Hem, 1985). Increased Ca^{2+} content will reduce SO_4^{2-} concentrations, and accordingly, carbonate-type ground water in gypsiferous aquifers actually contain lower SO_4^{2-} concentrations, often only several hundred mg/L. Conversely, up to 299,000 mg/L SO_4^{2-} has been measured in some unusual Ca^{2+} deficient brines (Hem, 1985). High SO_4^{2-} concentrations, however, make ground water of poor quality and limited use. The SO_4^{2-} content in a good quality aquifer is usually much lower than the solubility limit. An average of 39 mg/L SO_4^{2-} was found by Wiedemeier et al. (1995) in nonfuel contaminated ground water from several U.S. air force bases.

3.3.5. Comparison of Electron Acceptor Abundance by Type

It is instructive to compare the amount of organic that could potentially be oxidized for each electron acceptor type in an aquifer with typical electron acceptor properties. To complete this analysis, a hypothetical aquifer is assumed to have 30% liquid filled porosity (300 L/m^3) and have a bulk density of 1,876 Kg/m^3. Electron acceptors are assigned concentrations based on the discussion above, as shown on Table 6. The following half reactions are observed:

(7) Oxygen $O_2 + 4H^+ + 4e^- \rightarrow 2H_2O$

Table 6. "Average" electron acceptor concentrations and calculated equivalent electron capacity

(8) Nitrate $NO^{3-} + 6H^+ + 5e^- \rightarrow \frac{1}{2}N_2 + 3H_2O$

(9) Sulfate $SO_4^{2-} + 10H^+ + 8e^- \rightarrow H_2S + 4H_2O$

(10) Iron $Fe^{3+} + e^- \rightarrow Fe^{2+}$

Table 6 shows the calculated electron equivalent mass that could be accepted by each type. As shown, electron acceptance potential is lowest for O_2 and NO_3^- but becomes higher for SO_4^{2-} and Fe^{3+}, respectively. As discussed above, concentrations of SO_4^{2-} and Fe^{3+} can be quite variable. Although concentrations can be lower than those used here they are often much higher. O_2 and NO_3^- concentrations, however, will usually not vary much from those used. This simple comparison illustrates that the amount of organic that could potentially be degraded by SO_4^{2-} and Fe^{3+} reduction may be much greater than the amount possible by O_2 or NO_3^-. It suggests that SO_4^{2-} and Fe^{3+} reduction processes may play a significant role in the biodegradation of organic contaminants.

3.4. Iron Microbial Geochemical Processes

Fe^{3+} is very insoluble in the near neutral pH conditions usually found in ground water. For example, Whittemore and Langmuir (1975) found ground water in equilibrium with Fe-oxyhydroxides to have log iron activity products (IAP) ranging from –36 to –43. Usually, little dissolved Fe^{3+} is found, although considerable solid phase Fe^{3+} may be present for bacterial use. Iron mineral

forms, in ascending order of crystallinity (decreasing lattice disorder and specific surface area) include ferrihydrite rust ($Fe(OH)_3$), lepidocrocite and akageneite (γ- & β-FeOOH), goethite (α FeOOH), and hematite α-(Fe_2O_3) (Heron et al., 1994[a]).

As discussed above, sediments and sedimentary rocks commonly contain about 1% by weight Fe minerals or 10,000 mg/Kg. Assuming this iron is Fe^{3+} and extending the mass calculations developed in the preceding section, this quantity of iron would equate to approximately 336,000 mMol/m^3 electron acceptance capacity. Assuming chemical redox balance, this mass of Fe^{3+} would be sufficient to oxidize 9,333-mMol/m^3 toluene or approximately 1 L toluene/m^3. With such great oxidizing potential, it is apparent that 1) only a fraction of the total Fe^{3+} is ordinarily utilized and/or 2) the kinetic rate for Fe^{3+} utilization is slow. It is, however, generally observed that only a portion of the total iron present in a given subsurface system, the *biologically available* Fe^{3+} fraction, is susceptible to direct enzymatic reduction at any one time.

The ability of bacteria to enzymatically reduce Fe^{3+} is dependent on many factors including:

- Variations in free energy for various iron forms.
- Available or reactive Fe^{3+} mineral specific surface area; and
- Reaction time or kinetics.

Based on free energy calculations, dissolved or chelated iron is thought to be more biologically reactive than solid forms Ehrlich (1996). Additionally, there is a tendency for decreasing thermodynamic (ΔG) energy available for the bacterium with increasing Fe^{3+} mineral crystallinity. Figure 4 shows the free

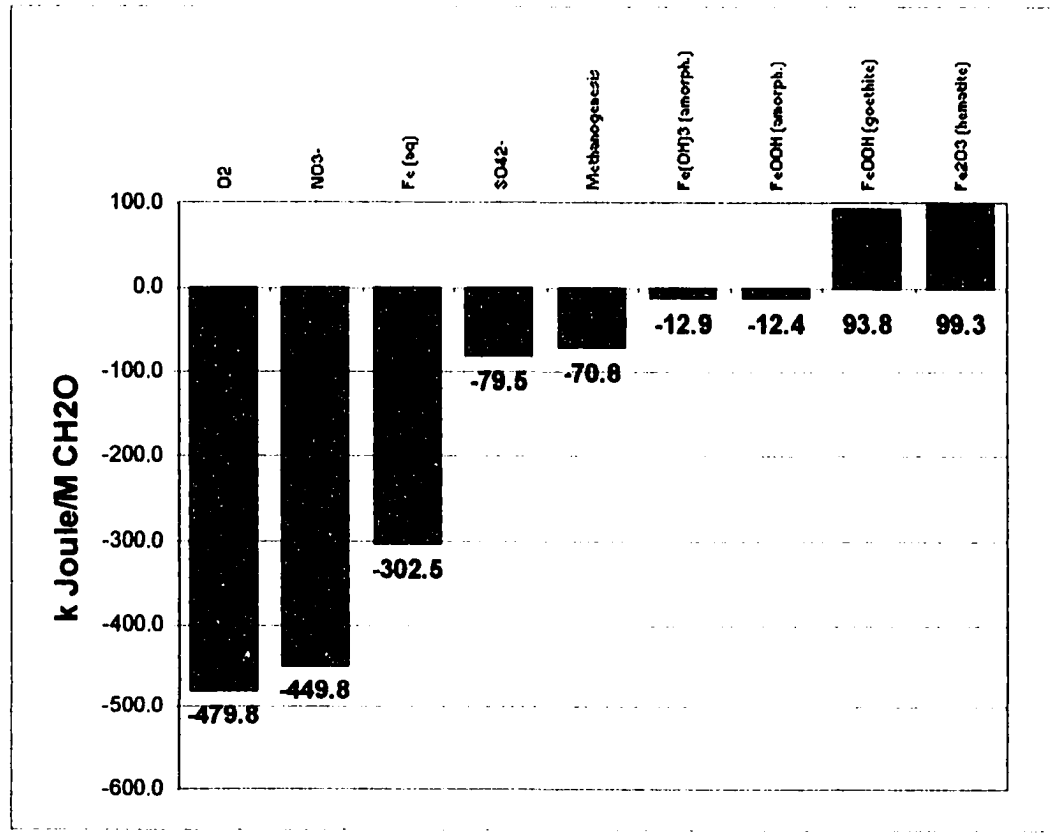

Figure 4. Calculated Gibbs free energy for common redox reactions with CH_2O including various common forms of Fe^{3+}.

energy calculations for a generalized organic (CH_2O) at standard conditions assuming reduction of various electron acceptors including several common Fe^{3+} mineral forms (modified after Lyon, 1995). Recall that a negative ΔG value indicates an exothermic (energy releasing) reaction favorable for the formation of microbial ATP. As discussed above, the order of diminishing thermodynamic benefit is O_2 then NO_3^- (-479.8 and –449.8 kJ/Mole CH_2O respectively). The energy yield for dissolved Fe^{3+} is quite high (-302.5 kJ/Mole CH_2O); however, Fe^{3+} is poorly soluble and usually does not exist in large amounts at normal pH ranges in an aquifer. Organic oxidation coupled with sulfate reduction or methanogenesis would produce -79.5 and -70.8 kJ/Mole CH_2O, respectively. Reactions involving solid Fe are thermodynamically poor compared to other redox reactions and have decreasing energy benefits with respect to increasing crystalline structure. These reactions range from -12.9 kJ/Mole CH_2O for amorphous $Fe(OH)_3$ to +99.3 kJ/Mole CH_2O for Fe_2O_3. Note that Berner (1980) reported –114 kJ/Mole CH_2O for $Fe(OH)_3$ so there appears to be some controversy, presumably regarding thermodynamic constants at standard conditions. In any case, based on thermodynamic evidence, it appears that Fe^{3+} reduction could theoretically occur across a wide redox range, beginning after NO_3^- and extending beyond methanogenesis.

Munch and Ottow (1980 and 1983) observed decreasing bacterial Fe^{3+} utilization with increasing mineral crystalline structure and observed that direct, physical contact with the mineral was necessary. In general, there is a relationship between increasing specific surface area and decreasing Fe mineral

crystalline structure. Taking these facts together, it is not surprising that Roden and Zachara (1996) found a relationship between increased Fe^{3+} mineral specific surface area and increased microbial utilization. The requirement for intimate microbial contact further suggests that only the outer layer or surfacial portion of the total Fe^{3+} mineral mass, to which the bacterium have access, can be immediately utilized.

The kinetics of microbial Fe^{3+} reduction are discussed in more detail below; however, evidence of active Fe^{3+} reduction has been found at contaminated sites that are many years or even decades old (Wiedemeier, 1997). This suggests that the rate of Fe^{3+} mineral utilization is slow and/or much time is required for bacteria to enzymatically attack more recalcitrant iron forms.

Based on thermodynamic estimates and specific surface area it appears that crystalline Fe^{3+} minerals are resistive to microbial reduction. Indeed, according to free energy calculations, at standard conditions, bacteria should not be able to reduce goethite and hematite at all. However, evidence of microbial reduction of these crystalline forms has been observed in many laboratory studies (Lovley, 1987). Further, direct evidence of crystalline Fe^{3+} microbial attack has been observed in the field both by the author and by others (Heron and Christensen, 1995 and Hiebert and Bennett, 1992). For example, scanning electron microscopy was performed on sediment samples taken from the gasoline fuel contaminated site described in Chapter 5 (Figure 5a and 5b). These images show complete removal of the hematite coating on some quartz sand grains in the contaminated portion of the plume compared to sediment in

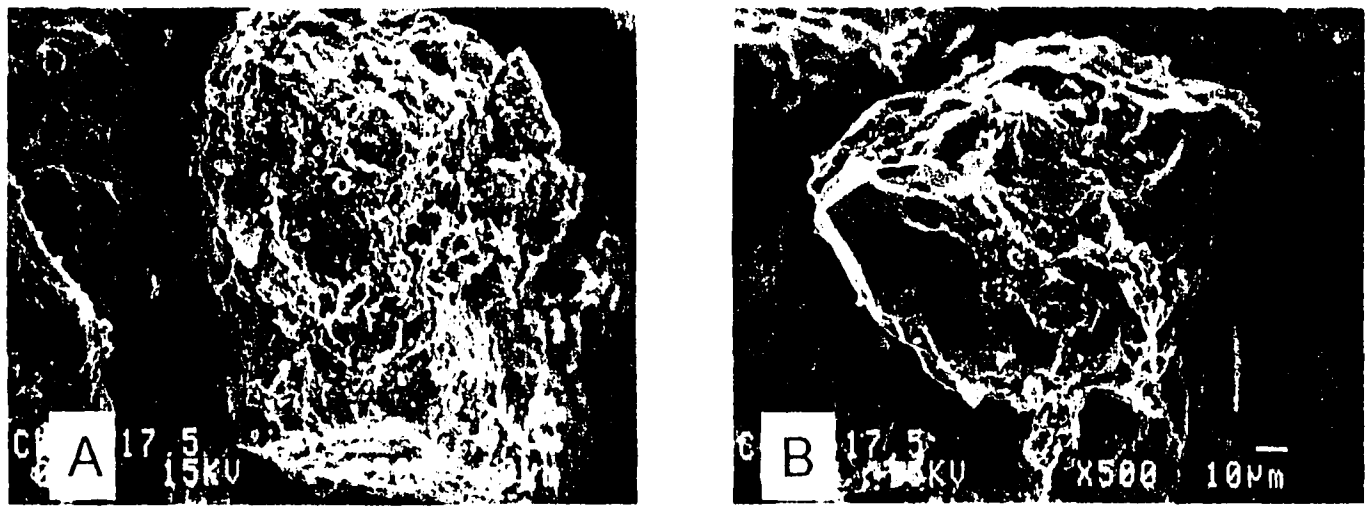

Figure 5. SEM images showing a) sand grain in non-contaminated area with iron oxide (hematite) mineral coating and b) sand grain in contaminated area with iron oxide removed and quartz corroded.

noncontaminated areas (Figure 5 a and 5 b). Heron et al. (1994) has observed similar pitting. On Figure 5b, note that not only is the hematite coating removed but also a portion of the silica quartz grain was apparently etched. Bennett (1991) and Hiebert and Bennett (1992) observed silica corrosion in sands contaminated with crude oil. This phenomenon was thought to be caused by organic chelators produced through microbial fermentation that greatly increased silica solubility.

It has been suggested that not all Fe^{3+} reducing bacteria gain energy in the process. For instance, Ghiorse (1988) and Lovley (1991) propose that a number of bacteria reduce ferric iron merely to dispose of excess reducing power via secondary respiratory pathways without generating energy, or that the iron reduction that was observed for these organisms was part of their iron assimilation process. Additionally, energy might be obtained during the reduction of mineral Fe^{3+} should the reaction be coupled with other respiratory or fermentative processes needed to meet the full energy demand (Ehrlich, 1996).

Finally, it is also possible that recalcitrant Fe^{3+} might be solublized via chelation to an aqueous form with thermodynamically favorable properties. Fe solubility can be strongly controlled by chelation increasing stable aqueous concentrations to very high levels. Hering and Stumm (1990) found that hematite dissolution in the presence of protons only was very slow; however, the dissolution process was accelerated many times in the presence of an organic ligand (oxalate). Chelating agents could be directly produced by bacterium. Alternatively, and of importance to natural attenuation, is the possibility that the

organic contaminant, or its fermentative products, could serve as a chelating compound. Landfill leachate is an example of this possibility. Many common organic acids, including humic and fulvic acids, have chelating properties accelerating mineral corrosion (Huang, 1986). Weis et al., (1989) found landfill leachate shared many similarities to soil humic material while Knox and Jones (1979) noted metal (Cr) complexation in leachate samples from four landfills. Such chelating agents in leachate could help account for the relatively high concentrations of aqueous Fe (usually Fe^{2+}) sometimes observed below landfills. Similarly, organic chelating compounds could also be formed during petroleum hydrocarbon fermentation. Organic acids (e.g. keto- and hydroxy-acid anions) formed through microbial fermentation of hydrocarbons are thought to be responsible for increased mineral solubility and reaction kinetics found at the crude oil spill site examined by Bennett (1991) and Hiebert and Bennett (1992). Although recalcitrant crystalline Fe^{3+} minerals are still resistive to solubilization via chelation, this process provides a mechanism for microbial energy conservation via indirect enzymatic reduction, even for stubborn forms.

Due to mass action constraints, evidence of Fe^{3+} reduction is poorly represented by aqueous analyses alone. Direct enzymatic reduction of Fe^{3+} minerals may produce a certain amount of dissolved Fe^{2+} as:

$$(11) \quad CH_2O + 4Fe^{3+}_{(s)} + 2H_2O \rightarrow 4Fe^{2+}_{(aq)} + HCO_3^- + 5H^+$$

There is, however, a strong tendency for produced Fe^{2+} to precipitate as several mineral forms, e.g., reacting with:

- Sulfides to form iron sulfides (FeS or FeS_2);
- Carbonate to form siderite ($FeCO_3$);
- Other Fe oxides/hydroxides to form magnetite (Fe_3O_4);
- Phosphates to create vivianite ($Fe_3(PO_4)_2 \cdot 8H_2O$)); and others.

These biogenic minerals have been observed in field and laboratory studies where Fe^{3+} reduction occurred (Lovley et al., 1993; Baedecker et al., 1992; and Postma, 1981 and 1982). Geochemical equilibrium conditions constrain both the oxidized and reduced states of Fe to a mineral form. As a result, aqueous Fe (usually Fe^{2+}) may indicate that Fe^{3+} reduction is occurring, but is probably a poor indicator of microbially available Fe^{3+} and also inadequately measures the magnitude of reductive microbial activity represented by produced Fe^{2+}. This observation suggests that solid mineral analysis is a necessity in intrinsic bioremediation studies where Fe^{3+} reduction is suspected.

As discussed previously, based on thermodynamics, the generally accepted redox sequence is $O_2 > NO_3^- > Fe^{3+} > SO_4^{2-}$ > methanogenesis. It is observed that SO_4^{2-} reduction often occurs in the presence of mineral Fe^{3+} (Lovely et al., 1991). SO_4^{2-} reduction may occur largely to the exclusion of, or possibly concurrent with, enzymatic Fe^{3+} mineral reduction. It could also be assumed that the bioavailable Fe^{3+} fraction was consumed thereby allowing SO_4^{2-} reduction in the presence of residual, biologically recalcitrant Fe^{3+}. Other explanations are also possible, singularly or in combination.

One potential explanation for SO_4^{2-} reduction in the presence of Fe^{3+} is based on thermodynamics. The electron acceptor utilization sequence is

typically calculated using a ΔG^o based on aqueous Fe^{3+}. This results in a computed heat of reaction for Fe^{3+} that is greater than that of SO_4^{2-}. However, as pointed out by Ehrlich (1996) and Lyon (1995), the heat of formation (ΔG^o) values for solid iron are high, resulting in thermodynamic calculations where SO_4^{2-} reduction is more energetic than that of Fe^{3+}. Further, thermodynamic benefits decrease with increasing crystallinity. This infers that Fe^{3+} reduction could happen over a wide redox range with some occurring before, during, or possibly after SO_4^{2-} reduction, depending on Fe^{3+} mineral species. In this case, biologically available Fe^{3+} is present as different mineral species that are consumed across a wide redox range due to variations in ΔG^o potential.

A second rationale for SO_4^{2-} reduction in the presence of Fe^{3+} is based on kinetic limitations. Fe^{3+} reducing organisms may slowly reduce crystalline Fe^{3+} forms, such as goethite and hematite, in systems that are otherwise dominated by sulfate reduction or even methanogenesis, as proposed by Lovley (1987). In this case, bioavailable Fe^{3+} is present but slowly used, permitting competitive SO_4^{2-} consumption, more or less independent of thermodynamic constraints.

Finally, Fe^{3+} and SO_4^{2-} reduction may occur simultaneously due to physical aquifer properties. Because Fe^{3+} is a solid, unlike the other electron acceptors, its distribution is fixed in the aquifer matrix. This inhibits mixing and may favor the creation of microenvironments where direct enzymatic Fe^{3+} and SO_4^{2-} reduction occur in close proximity, as suggested by Canfield et al. (1988).

Nonenzymatic reduction of Fe^{3+} can occur. Fe^{3+} oxide minerals are stable in the absence of oxygen but reduce in the presence of a strong reducing agent.

As discussed in detail below, HS- produced by sulfate reducing bacteria can reduce Fe^{3+}. According to Ghiorse (1988), certain microbial organic metabolites can also act as a reductant for Fe^{3+} including formate (formic acid), which is produced by a number of bacteria. Reduction of Fe^{3+} by formic acid can be written as:

(12) $2Fe^{3+} + HCOOH \rightarrow 2Fe^{2+} + 2H^{+} + CO_2$

Fe^{3+} reduction, from reactions like Equation 12, are not the result of direct enzymatic processes, but may be considered an indirect form of organic oxidation via Fe^{3+} reduction. This type of reaction is favored by acid pH.

3.5. Sulfur Microbial Geochemical Processes

In many ways, microbial geochemical processes for S are considerably more complex than for Fe. Though not discussed in detail here, numerous oxidative states are possible for S species ranging from 2^- to 8^+ and many complex intermediates (including thiosulfate and polysulfides) are formed during cycling (Jorgensen, 1990). For simplification, this discussion is directed towards major S processes and end member species that are important with respect to natural attenuation.

A general equation for sulfate reduction can be written as:

(13) $CH_2O + \frac{1}{2} SO_4^{2-} \rightarrow HCO_3^- + \frac{1}{2} HS^-_{(aq)} + \frac{1}{2} H^+$

Equation 13 assumes complete reduction of SO_4^{2-}; however, only partial reduction to an intermediate oxidation state may occur to form S^o, for example as:

(14) $CH_2O + 2/3\ SO_4^{2-} \rightarrow 2/3\ S^o + HCO_3^- + 1/3\ OH^- + 1/3\ H_2O$

Additionally, S^o can be used directly as an electron acceptor for the enzymatic oxidation of organic material as:

(15) $CH_2O + 2H_2O + 2S^o \rightarrow HCO_3^- + 2H_2S + H^+$

Although SO_4^{2-} is typically thought of as a dissolved ion, as discussed above, many SO_4^{2-} based salt minerals exist. In theory, the direct microbial reduction of such a mineral, could occur similar to the reduction of Fe^{3+} minerals. Assuming the reduction of gypsum, coupled with carbonate deposition, one can write:

(16) $CH_2O + ½\ CaSO_4 \cdot 2H_2O \rightarrow ½\ H_2S + ½\ CaCO_3(s) + ½\ HCO_3^- + ½\ H^+ + 2H_2O$

The calculated free energy at standard conditions for Equations 13 through 16 is shown on Figure 6. It is interesting to note that the partial reduction of SO_4^{2-} to S^o should result in nearly the same energy yield as complete reduction of SO_4^{2-} to H_2S. Therefore, S^o generation may be a common reaction when SO_4^{2-} is abundant because complete reduction to H_2S is not needed. As expected, the further reduction of S^o to H_2S produces less energy per unit

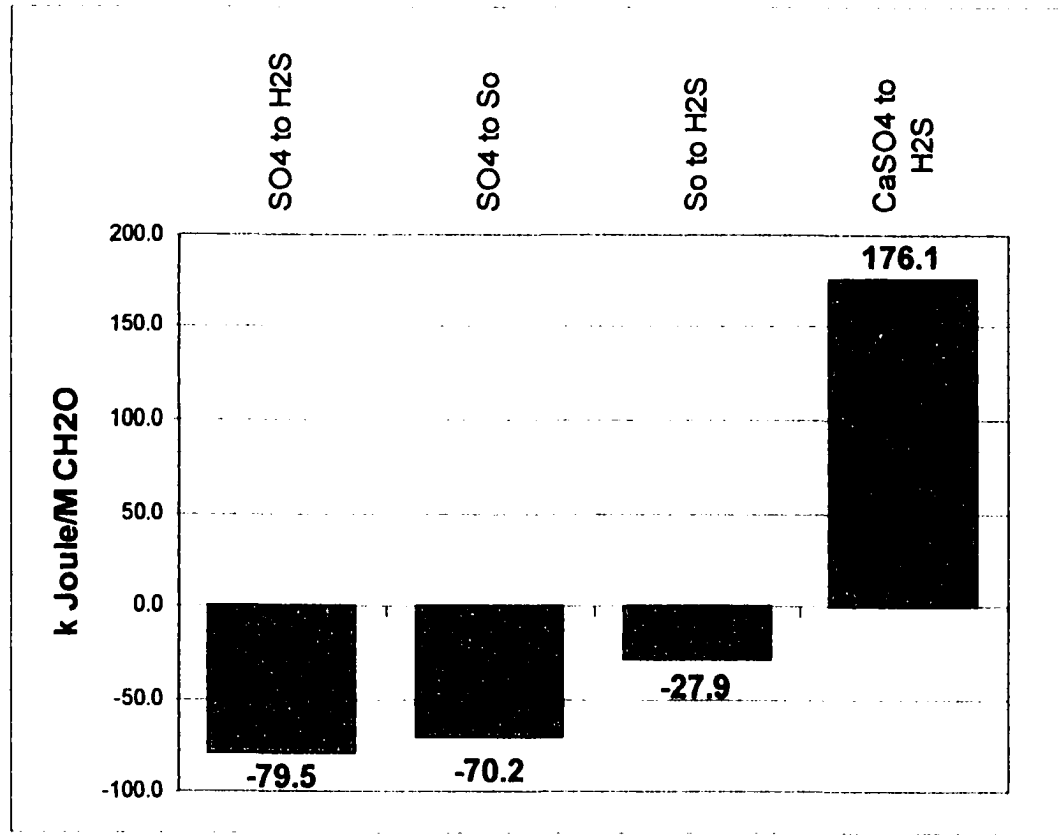

Fiugre 6. Calculated Gibbs free energy for oxidized S reduction.

organic oxidized than full SO_4^{2-} reduction to H_2S or partial reduction to S^o. Finally, direct reduction of mineral $CaSO_4^{2-} \cdot 2H_2O$ by Equation 16 is thermodynamically unfavorable. Therefore, it is likely that SO_4^{2-} reducing bacteria do not directly reduce gypsum. This does not present a significant impediment to gypsum utilization due to its reasonably high solubility and fast reaction rates. In the presence of SO_4^{2-} minerals like gypsum, aqueous SO_4^{2-} is probably resupplied by mineral dissolution as it is reduced by microbial activity.

As part of a natural attenuation study, the detection of aqueous HS^- as a quantitative indicator of SO_4^{2-} reduction is usually not feasible. This is due in part because Fe^{3+} minerals are a chemical sink for HS^-, reducing aqueous concentrations as shown by Appello and Postma (1994):

(17) $2FeOOH_{(s)} + 3HS^- \rightarrow 2FeS_{(s)} + S^o + H_2O + 3OH^-$

Here, Fe^{3+} is reduced abiotically to Fe^{2+} with the simultaneous oxidation of S^{2-} to S^o. This reaction demonstrates partial S cycling because 1/3 of the reduced HS^- is oxidized to S^o that could be reused as an electron acceptor by heterotrophic bacteria. In tests performed by Pyzik and Sommer (1981), S^o accounted for 86% of the oxidized product from Equation 17 with thiosulfate ($S_2O_3^{2-}$) comprising the balance. Jorgensen (1990) found that thiosulfate was used as an electron acceptor by heterotrophic bacteria and converted back to HS-; however, there is a potential dissproportunation to form SO_4^{2-} and HS^- as:

(18) $S_2O_3^{2-} + H_2O \rightarrow SO_4^{2-} + HS^- + H^+$

As is apparent from Equation 18, the formation of thiosulfate could ultimately cycle SO_4^{2-}. Jorgensen (1990) also suggests that thiosulfate could fully oxidize by reaction with Fe^{3+} minerals, however the degree to which this occurs is subject to question in the author's opinion.

Equation 17 represents non-enzymatic reduction of Fe^{3+} by HS^- during SO_4^{2-} reduction, which is well-documented (Lovely et al., 1991). Precipitated iron monosulfide mineral forms include amorphous iron sulfide, mackinawite ($Fe_{0.995-1.023}S$), greigite (Fe_3S_4), and pyrrhotite ($FeS_{1.1}$). These minerals are also known as acid volatile sulfides (AVS) because, in contrast with pyrite (FeS_2) and S^o, they readily dissolve in hydrochloric acid.

The rate of AVS formation is rapid and has been described by Pyzik and Sommer (1981) as:

(19) $d(FeS)/dt = k\ S_t(H^+)A_{FeOOH}$

Where:

$d(FeS)/dt$ = rate of AVS formation

k = rate constant 82 ± 18 ($L^2/(m^2 \cdot min)$)

S_t = Molar sulfide concentration (mol/L)

H^+ = Hydrogen ion activity

A_{FeOOH} = Surface area of goethite (m^2/L)

FeS formation is largely controlled by available Fe^{3+} mineral specific surface area. Initially high FeS formation is due to large unreduced Fe^{3+} surface area. According to Pyzik and Sommer (1981), successive AVS formation proceeds only after the surface Fe^{3+} mineral layer dissolves to expose additional surface area.

It is possible to form AVS by direct reaction with Fe^{2+} as:

(20) $Fe^{2+} + HS^- \rightarrow FeS$

This reaction does not involve oxidation/reduction. Therefore, Fe^{3+} is not reduced and S^o is not formed.

Even under sulfidic conditions, AVS is a transient form in many environments. Monosulfides combine with elemental sulfur to form pyrite (Appello and Postma,1994) according to:

(21) $FeS\ (s) + S^o \rightarrow FeS_2$

This second step involves the simultaneous oxidation and reduction of S so that S^{2-} and S^o produce $2S^-$. This reaction occurs spontaneously and abiotically. Therefore, there is potential competition for S^o which could be used either as an electron acceptor by bacteria or chemically bound as FeS_2. It should also be noted that the direct formation of FeS_2 by H_2S was reported by Drobner et al. (1990) as:

(22) $FeS + H_2S \rightarrow FeS_2 + H_2$

Most research and literature references for FeS_2 formation assume the reaction expressed in Equation 21. Drobner et al., (1990) used an incubation temperature of 100 °C to produce FeS_2 by direct H_2S reaction so the importance of this reaction is unclear at typical aquifer temperatures. The reaction expressed in Equation 22 could be an important source of H_2 for chemolithotrophic bacteria in the deep subsurface.

In the presence of oxygen AVS can be oxidized as:

(23) $FeS + 2.25O_2 + 2.5H_2O \rightarrow Fe(OH)_3 + 2H^+ + SO_4^{2-}$

This reaction may be microbially mediated as in the case of acid mine drainage (Tuttle et al. 1969 and Evangelou and Zhang, 1995). It should be noted that the rate of AVS oxidation is inhibited even with oxygen and aqueous Fe^{3+} in the presence of aqueous Fe^{2+} (Moses and Herman, 1989), a fact that could increase mineral stability in a contaminated aquifer.

AVS is reactive, both by oxidation and by reduction/oxidation to form FeS_2. Therefore, it is reasonable to assume that the presence of AVS is a general indicator of recent sulfate reduction. In marine sediments, AVS is found to disappear with time (depth) as it transforms to pyrite (Appelo and Postma, 1994). Environments rich in AVS relative to FeS_2 may indicate recent or on-going biological processes.

The rapid deposition of iron sulfide minerals has been noted in many natural organic rich environments, such as marine or lake sediments (Morse et

al., 1987; Howarth and Jorgensen, 1984 and Howarth, 1979). Increases in iron sulfide mineral content have been documented in aquifers contaminated with organic rich landfill leachate (Heron, 1994; and Heron et al., 1994[a], 1994[b]) but much less work exists on iron sulfide mineral deposition in hydrocarbon contaminated aquifers.

Although SO_4^{2-} is usually a dissolved ion in an aquifer, the reduced product of microbial respiration (HS^-) often precipitates as an iron sulfide. In an aquifer, evidence of SO_4^{2-} reduction can be inferred by its aqueous depletion. However, the respiratory products of SO_4^{2-} reduction (HS^-) may largely be preserved in mineral form (AVS or FeS_2) which can only be quantified by mineral analysis.

3.6. Examples of Natural Attenuation Fuel Sites

Research was conducted to find examples of good natural attenuation studies. To qualify, the natural attenuation study must have evaluated O_2, NO_3^-, Fe, SO_4^{2-}, and methanogenesis. Additionally, the hydrocarbon plume must have been fully delineated and could not intersect any natural or artificial barrier that prevented the full expression of redox zone development. These studies were conducted following the protocol of Wiedemeier et al. (1997) so all analytes were measured as aqueous phase from water samples taken from monitoring wells.

Natural attenuation studies are increasingly used in environmental feasibility studies as a potentially cost effective alternative to active engineered treatment. The Air Force Center for Environmental Excellence (AFCEE) has

employed such studies as part of their investigative protocol at several air bases. These AFCEE studies were conducted in cooperation with EPA's Robert S. Kerr Research Laboratory (National Environmental Risk Management Laboratory) as research sites. Five sites were found that met the search criteria including:

- Patrick Air Force Base (Wiedemeier et al., 1997);
- Hill Air Force Base (Wiedemeier et al., 1997 and Parsons Engineering Science, Inc., 1994);
- George Air Force (International Technologies, 1996);
- Elmendorf Air Force Base Hanger 10 Site, (Parsons Engineering Science, Inc., 1995[a]);
- Elmendorf Air Force Base Site ST-41, Anchorage, Alaska, (Parsons Engineering Science, Inc., 1995[b]);

These natural attenuation sites are shown on Figures 7 through 11. Concentration contours were available for each analyte for each site listed above. For evaluation purposes, only the boundary areas for dissolved contamination (total BTEX), aqueous Fe^{2+} production, SO_4^{2-} depletion, and CH_4 production are shown; these are combined on a single map for each site. This presentation provides an overview of those observed redox zones based on aqueous data. The contaminant boundary was defined as total BTEX >1 mg/L. SO_4^{2-} reduction was determined as the region where concentrations of SO_4^{2-} first demonstrated depletion below background. The boundary for methanogenesis

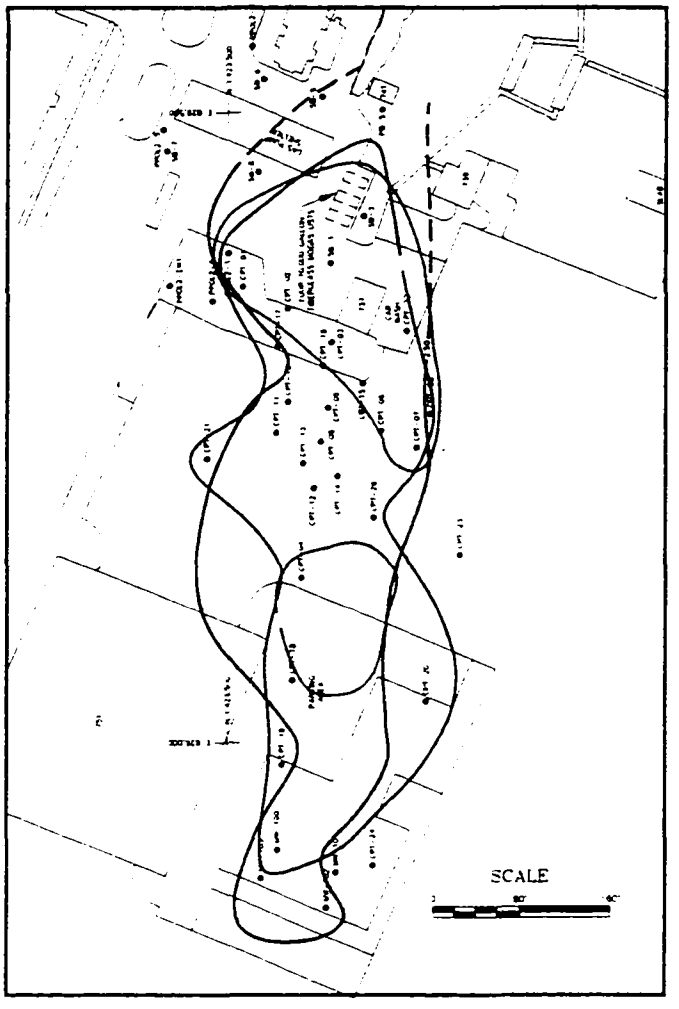

Figure 7. Redox zones for Patrick, AFB.

BTEX > 1 mg/L

Fe > 0.5 mg/L

SO4 (inconclusive)

CH4 > 2.5 mg/L

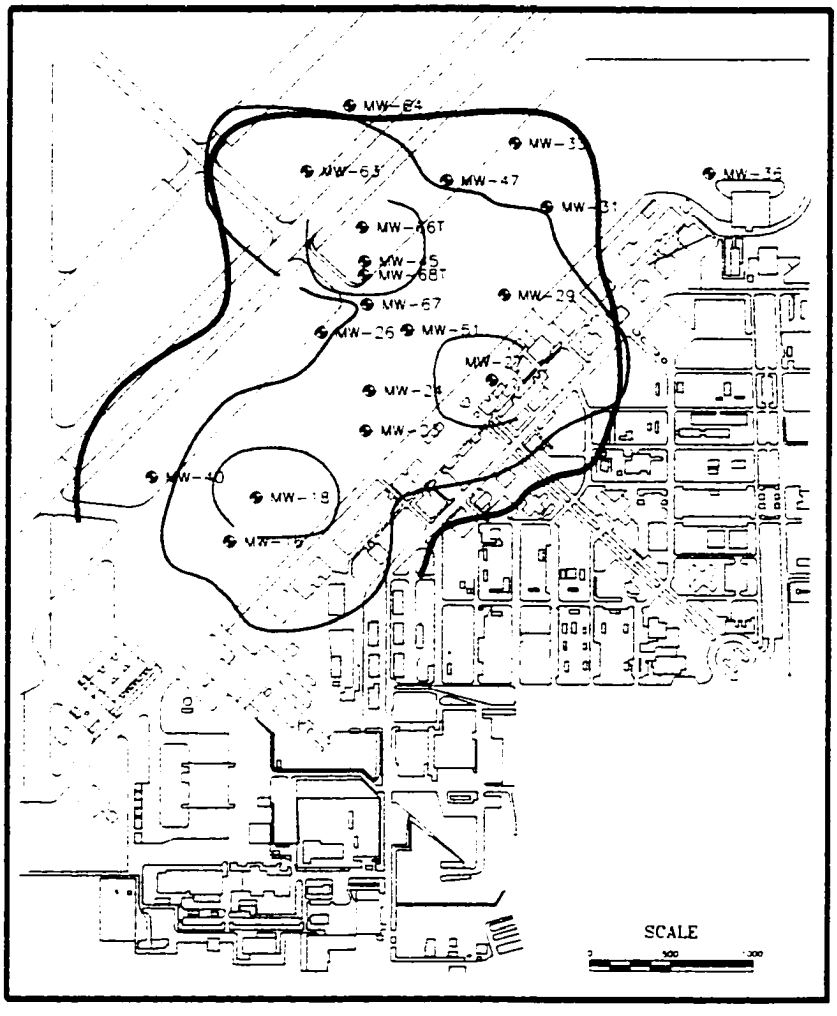

Figure 8. Redox zones for George AFB.

BTEX > 1 mg/L Fe > 0.2 mg/L

SO4 < 300 mg/L CH4 (no data)

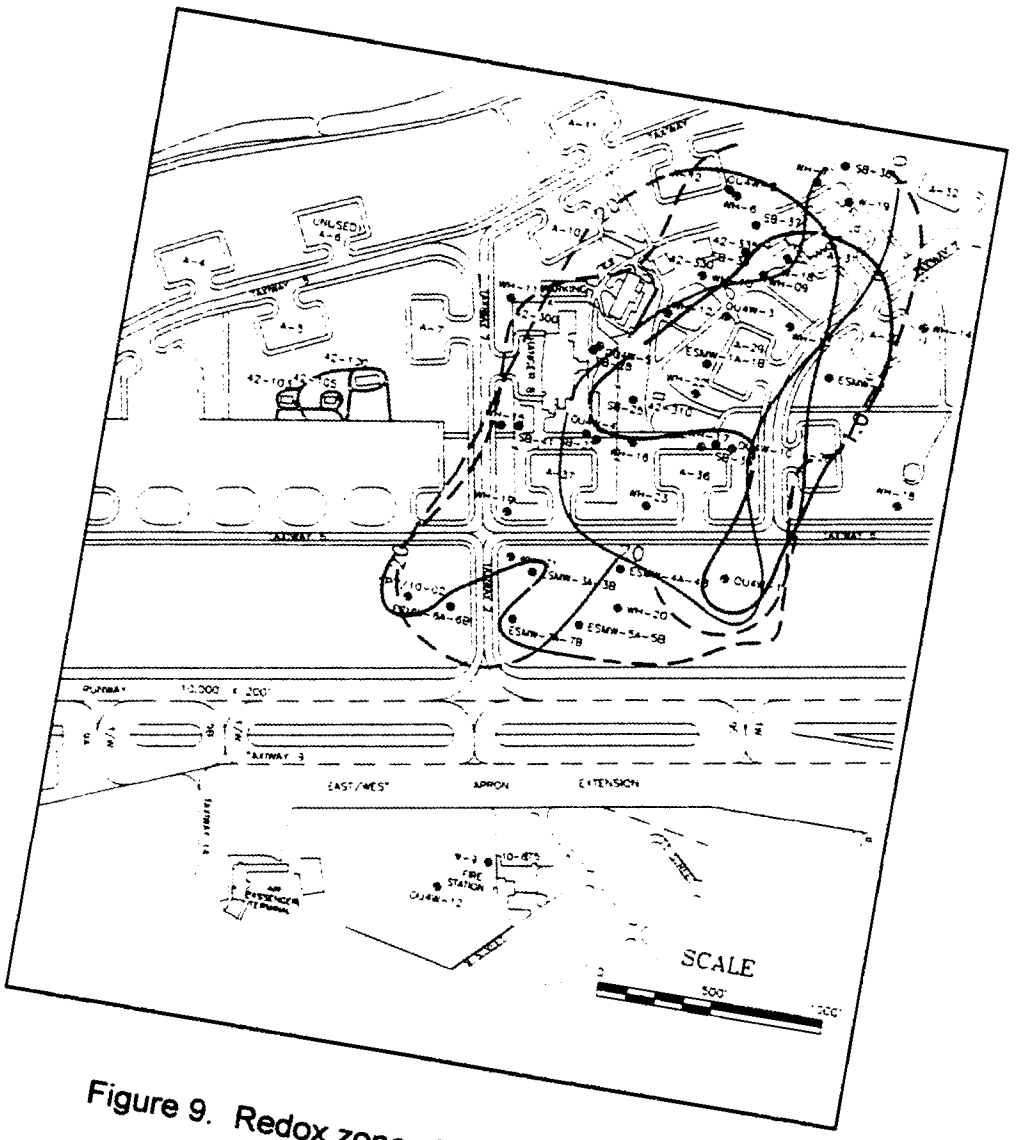

Figure 9. Redox zones for Elmendorf AFB.

— BTEX > 1 mg/L

— SO4 < 20 mg/L

— Fe > 0.1 mg/L

— CH4 > 1.0 mg/L

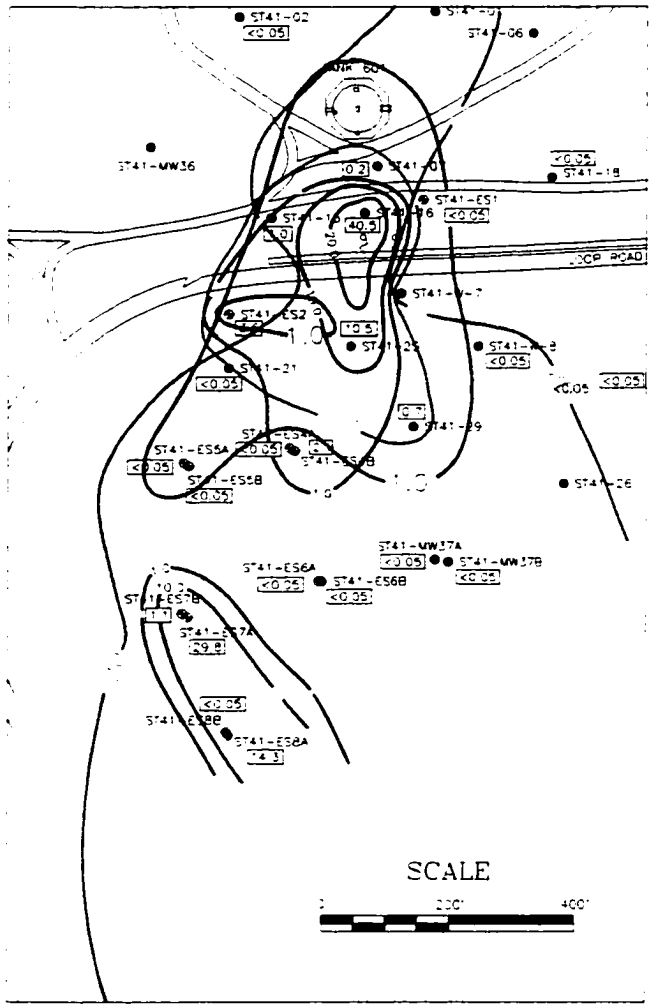

Figure 10. Redox zones for Elmendorf AFB site ST-41.

BTEX > 1 mg/L

Fe > 0.1 mg/L

SO4 < 20 mg/L

CH4 > 1.0 mg/L

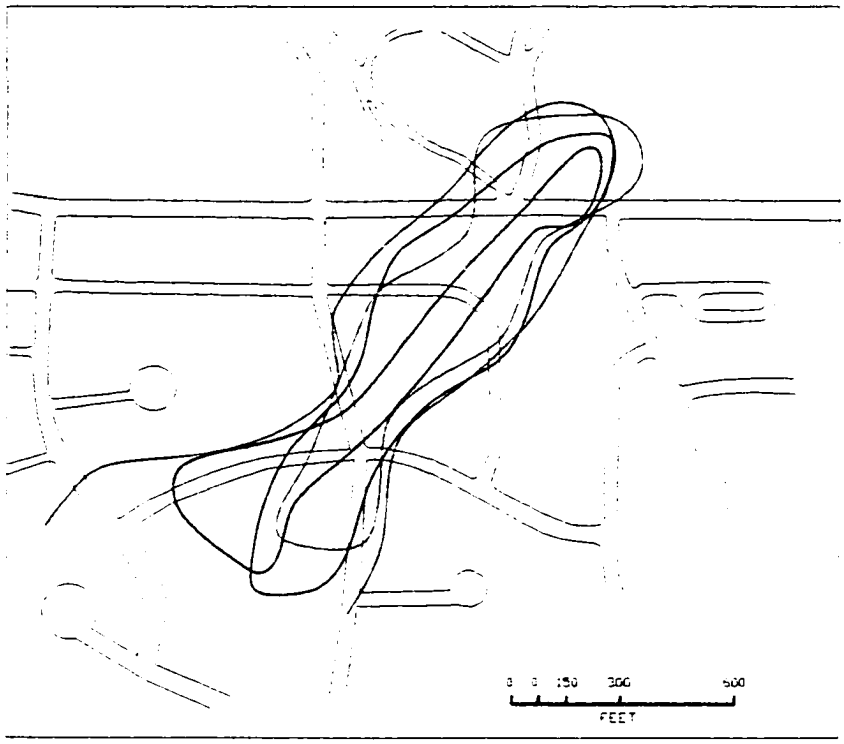

Figure 11. Redox zones for Hill AFB.

BTEX > 1 mg/L

Fe > 0.1 mg/L

SO4 < 80 mg/L

CH4 > 1.0 mg/L

and Fe^{2+} were each defined as the areas where increases in those analytes were observed above their respective background values.

After examining all of the natural attenuation sites the following general observations are made:

- The region of SO_4^{2-} depletion is generally larger than the region of aqueous Fe^{2+} and CH_4;
- Aqueous Fe^{2+} and CH_4 often occur together;
- In no case does aqueous Fe^{2+} extend beyond the contaminant plume suggesting fairly rapid Fe^{2+} mineral precipitation;
- Except in the case of Patrick AFB, aqueous Fe^{2+} forms are found only in areas where SO_4^{2-} is greatly depleted.

Patrick AFB is an unusual case. At that site, there is no evidence of SO_4^{2-} reduction, but there is aqueous Fe^{2+} and CH_4 inferring Fe^{3+} reduction and methanogenesis. The area of Fe^{2+} is wholly contained within the region of elevated CH_4 so competitive exclusion of SO_4^{2-} reducing bacteria by Fe^{3+} seems unlikely. Based on field data it seems likely that well screens have been constructed across two zones. One is a zone containing contaminants and little sulfate and the other has sulfate but little contaminant. The resulting mixture of waters gives the appearance of Fe^{3+} reduction and methanogenesis to the exclusion of SO_4^{2-} reduction where none occurs.

This data shows that there is field evidence that Fe^{3+} reduction occurs concurrent with methanogenesis as is suggested by free energy analysis.

Further, there is no evidence that Fe^{3+} reduction occurs before or inhibits SO_4^{2-} reduction. However, these contaminated sites are old and more labile forms of Fe^{3+}, which may have competitively excluded SO_4^{2-} reduction, could have been consumed in the past leaving no aqueous evidence at the time of sampling. Fe^{3+} reduction may occur concurrent with SO_4^{2-} reduction, but there is no indication of that process because produced Fe^{2+} would probably precipitate as an iron sulfide mineral where SO_4^{2-} reduction is significant.

3.7. Intrinsic Bioremediation Summary

Many organic constituents of either leachate or petroleum can be destroyed through natural microbial processes in the subsurface. Soil bacteria have the ability to respire several common electron acceptor types including O_2, NO_3^-, Fe^{3+}, and SO_4^{2-}. It is generally assumed that the order of utilization is O_2 > NO_3^- > Fe^{3+} > SO_4^{2-} > methanogenesis based on thermodynamic analysis showing lower energy generation for each successive redox couple. This sequence may be correct for aqueous Fe^{3+}, which is rare at normal pH. There is much less thermodynamic benefit for solid Fe^{3+}. Therefore, Fe^{3+} reduction may occur across a broad redox range, possibly concurrent with SO_4^{2-} reduction and methanogenesis when mineral forms are considered. Evidence from natural attenuation studies supports the concept that Fe^{3+} reduction occurs concurrent with methanogenesis. Based on free energy analysis, bacteria can obtain energy using aqueous SO_4^{2-} and solid S^o but probably not using more complex mineral SO_4^{2-} forms, such as gypsum.

In the subsurface, the order of abundance (electron acceptor capacity), the common electron acceptors can be shown to be Fe^{3+} >> SO_4^{2-} > NO_3^- > O_2, which is largely the opposite of the accepted microbial utilization sequence. Acetoclastic methanogenesis is functionally independent of electron acceptor mass. This suggests that methanogenic and Fe^{3+} and SO_4^{2-} reducing bacteria, while thermodynamically constrained, may never the less play a dominant role in intrinsic bioremediation.

Both the oxidized and reduced forms of Fe are usually found as solid minerals, so ground water analysis alone may not adequately reflect Fe^{3+} reduction. Additionally, much respiratory HS^- from SO_4^{2-} reduction can also be trapped in mineral form as AVS, S^o or FeS_2. Therefore, examining solid Fe and S minerals at sites contaminated with organic pollutants could be of benefit in natural attenuation studies and compliment aqueous ground water analyses. Based on the available literature, such analysis is theoretically sound. Inclusion of a mineral study could improve estimates of expressed and assimilative capacity and provide other insights supporting intrinsic bioremediation.

4. MINERAL FE AND S ANALYSIS METHODS

4.1. Objective of Methods Development

Based on electron acceptor abundance, Fe^{3+} and SO_4^{2-} reduction by bacteria may play a dominant role in intrinsic bioremediation of some organic contaminants in the subsurface. Both Fe^{3+} and SO_4^{2-} reduction processes involve mineral phases and may not be properly understood by evaluating only ground water concentrations. Fe and S mineral analyses should be incorporated in natural attenuation studies; however, inherent problems with sample collection and analysis have probably discouraged such efforts.

Whereas routine methods are available for aqueous Fe and S analysis, much of the present research hinges on the ability to measure these species in mineral phase. After a careful review of the problem, it was determined that methods were needed to determine the following mineral types:

- Bioavailable Fe^{3+};
- Biologically produced Fe^{2+};
- Bulk Fe^{2+} and Fe^{3+};
- Acid volatile sulfides (iron sulfide, mackinawite, etc.);
- Cr reducible sulfides (FeS_2 and S^o)

As discussed below, methods for extracting some of these analytes had previously been developed; however, many of those techniques were labor intensive and generally impractical for extensive use. Therefore, an emphasis

was placed on developing methods that could be practically applied, for this research and others. Additionally, techniques were needed that minimized sediment oxygen exposure so that samples could be obtained from the field for Fe and S analysis. This chapter will:

- Discuss field sampling techniques;
- Describe mineral Fe and S extraction methods; and
- Review the results of extraction tests performed using synthetic minerals under laboratory conditions.

This chapter also reviews the results of these test methods when applied to three separate field study sites. Finally, methods of data analysis for the Fe^{3+}/Fe^{2+} system are examined.

4.2. Field Sample Collection and Preservation

Many reduced Fe^{2+} and iron monosulfide minerals will oxidize, so exposure to air should be minimized. Field portable gloveboxes or bags, while potentially minimizing air contact, are not practical for general applications. Alternative methods described here are recommended.

Sediment samples can be obtained utilizing common drilling methods including a continuously coring hollow stem auger equipped with a split spoon sampler or Shelby tube or by using a geocore/hydropunch drilling unit. In poorly consolidated, heaving sands excellent sediment recovery (>90%) has been achieved using a hollow stem auger equipped with a clam-shell fitted auger head (Leach et al., 1988). These drilling methods permit samples to be collected and

maintained in plastic core sleeves. Alternatively, core samples can be transferred to storage bottles in the field. N_2 preservation is possible in either case.

Anoxic conditions can be maintained by placing sediments in a N_2 gas atmosphere. A portable nitrogen gassing station can be built for use in the field similar to that shown on Figure 12(a). This gassing station permits multiple samples to be nitrogen purged at once. For safety, the regulator should be set for a delivery pressure of no more than 10 psi.

If plastic core sleeves are used, an intact core can be retrieved from the field. Using this technique, entire cores can be taken to the laboratory for further processing in an anaerobic glovebox. Sample integrity is maintained and virtually the entire core can be collected; however, additional laboratory sample preparation and equipment (e.g., anaerobic glovebox) is needed. Upon collection, loose sediment in the core must be stabilized to prevent loss and mixing. A porous material such as nylon mesh or cloth can be packed into the ends of the core and large rubber stoppers can be inserted and taped into place in the ends of the core sleeve. The ends of the core should be purged by piercing the stopper with a N_2 gas and vent needle. The core is then loaded into a PVC collection tube as shown on Figure 12(b). After core insertion, this tube may be tightly sealed using a plumbers test plug (compression j-plug). The collection tube includes two butyl rubber stoppers installed through the side of the collection tube and secured with plastic tape. These stoppers permit N_2 to be injected in one end of the tube while gas is vented out of the other end with a

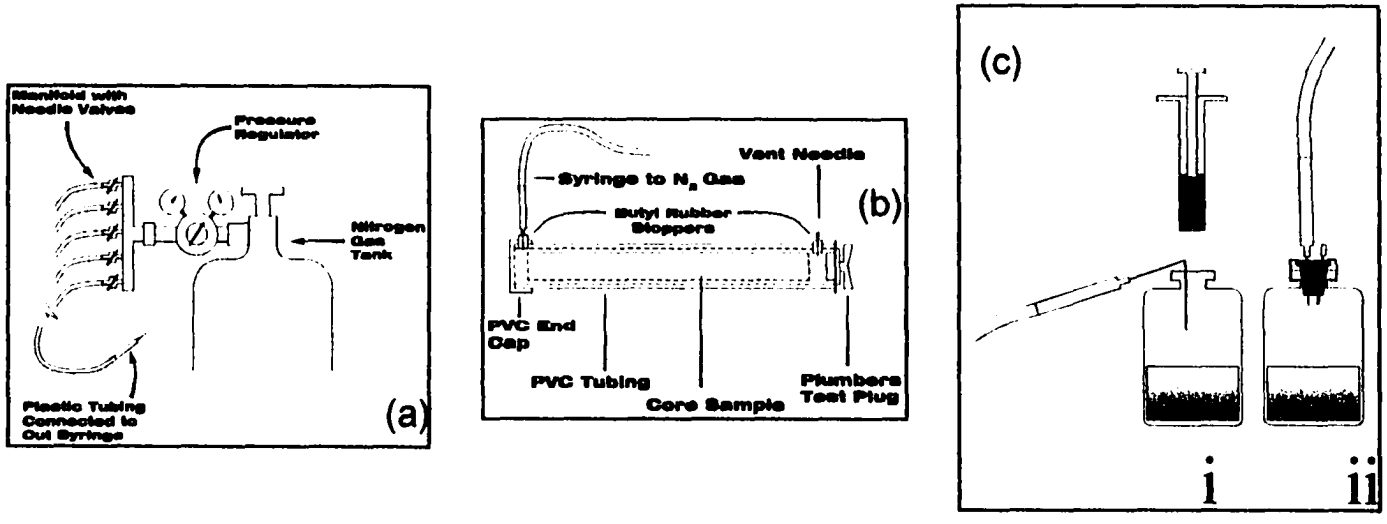

Figure 12. (a) field gassing station, (b) core storage device, and (c) field N_2 bottle purge technique.

disposable syringe needle. After purging, the vent needle should be removed first so that positive gas pressure is maintained in the sample tube. Tube pressure should be bled off with a vent needle before opening.

Alternatively, sediment samples can be transferred to storage bottles in the field. Compared to collecting an entire core, this technique is simpler, faster, and requires less specialized equipment, however, core integrity is not maintained and a smaller amount of sample is collected. Here, the tip of a 5 cc plastic syringe is cut to create a disposable piston-coring tool. This tool can be used to subsample a sediment core and inject it directly into a 160 ml N_2 purged serum bottle (Figure 12(c)i. The serum bottle can be stoppered, sealed using an aluminum crimp, and purged again with N_2 as shown on Figure 12(c)ii. As above, after purging the vent needle should be withdrawn first followed by the purge needle to form positive atmospheric pressure in each storage bottle. All sediment samples should be refrigerated while awaiting analysis.

4.3. Mild Acid Extraction Iron Analysis

4.3.1. Method Background

Fe minerals of interest are generally either so finely particulate or poorly crystalline that identification by direct X-ray diffraction is difficult (Jenne, 1977). Consequently, various chemical extractions are used for mineral speciation; however, many of these demonstrate inconsistent selectivity (Robinson, 1984). Similarly, chemical extraction scenarios have been adapted to try to quantify biologically available Fe^{3+} and biogenically produced Fe^{2+} iron minerals in

sediments. Therefore, in addition to the requirement for a certain level of mineralogical speciation, for an intrinsic bioremediation study there is an additional requirement that the analyses relate to minerals associated with biological processes.

Microbial/mineral interactions tend to be surface phenomena. The Fe^{3+} reduced is on the outer exposed portion of the sediment grain (Figure 13). Alternatively, precipitated Fe^{2+} is deposited either on sediment surfaces or as discrete particulates. The chemical extraction procedures employ a weak extractant that dissolves only a small fraction of the total iron present in the sediment. The goal of the mild acid extraction is to distinguish small quantities of those microbially important iron forms from a much larger bulk mass of iron inherently present in abundance in many sediments. As described below, many techniques have been proposed for this purpose. All of these are semiquantitative due to the nonspecific nature of the extraction process.

Many iron extractants have been proposed, including 0.5N HCl, 0.2 M ammonium oxalate, dithionite-citrate-bicarbonate, and 0.008 M Ti(III) - 0.05 M EDTA, as summarized by Heron et al. (1994[b]). For biologically available Fe^{3+}, Lovley and Phillips (1987) recommend a one-hour extraction employing 0.5 N HCl and hydroxylamine hydrochloride. Protocol for a 24 hour extraction using 0.5 N HCl is being developed by the USEPA (Lyon and Glass, 1997[a] and 1997[b]; Lyon et al., 1997). For reactive biogenically produced Fe^{2+} species, Heron et al. (1994), used an extraction time of 24 hours, also using 0.5

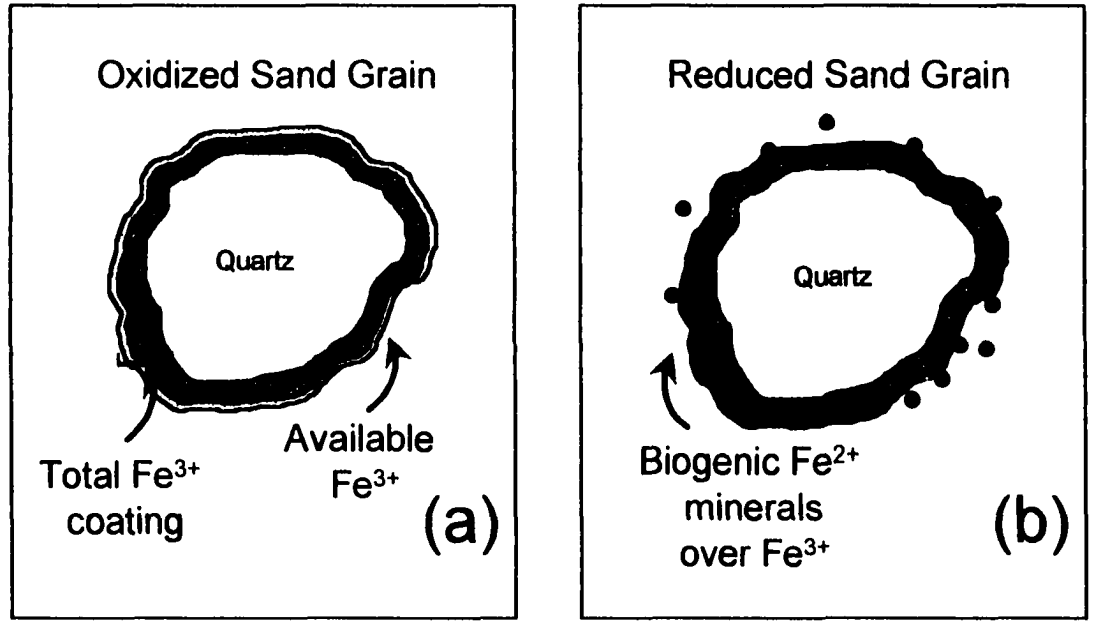

Figure 13. Conceptual sediment (a) non-reduced with oxidized F^{3+} coating and (b) sediment from a contaminated area with Fe^{2+} coating and particulates.

N HCl. In light of its predominance in the literature and ease of use, 0.5 N HCl is used here.

4.3.2. Laboratory Testing and Discussion

Methods

An experiment was designed to evaluate the time dependent extraction potential of 0.5 N HCl for varying concentrations of different iron mineral species. Objectives included:

- Determining if extraction rates are concentration dependent, and
- Observing variations in extraction rates between selected mineral end-point species.

The reactive Fe^{2+} and Fe^{3+} species selected included monosulfide (FeS) and ferrihydrite $Fe(OH)_3$, respectively. Relatively non-reactive Fe^{3+} forms included hematite (Fe_2O_3), goethite (Fe(OOH)), and crystalline magnetite (Fe_2O_3).

$Fe(OH)_3$ and Fe(OOH) were prepared by respectively adjusting the pH of 0.4 N FeCl solution to 7 and 11 with 4N NaOH as described by Roden and Zachara (1996). The $Fe(OH)_3$ solution was washed immediately upon neutralization, however, the Fe(OOH) solution was permitted to react for 3 days before washing. Iron jells were then dried for approximately 2 days at 60 C°, crushed, and sieved (100 μm). Fe_2O_3 and FeS were purchased (Alpha Aesar).

Crystalline magnetite was obtained from magnetic separation of river alluvium sediment from the Canadian River, near Norman, Oklahoma. Except for magnetite, the iron content for each mineral was determined by digestion in 6N HCl. Magnetite was dissolved in hot 12 N HCl.

A Hach DR2010 spectrophotometer was used for Fe^{2+} and Fe total analysis, respectively, using 1,10 Phenanthroline and 3-(2-pyridyl)-5, 6-bis(4-phenlsulfonic acid)-1,2,4-triazine, monosodium salt (Ferrozine) (Hach, 1992; Komadel and Stuki, 1988; and Stookey, 1970). Using these methods, Fe^{2+} could be measured from 0 to 3.00 mg/L and Fe total from 0 to 1.300 mg/L. Although spectrophotometric methods are used here, direct ion-chromatographic analysis of Fe^{3+} and Fe^{2+} is also possible (Moses et al., 1988).

For each test extraction, 500 ml of 0.5 N HCl was prepared using reagent grade 12 N HCl and n-pure water. Varying amounts of iron minerals were added so that upon complete dissolution, the theoretical concentration of Fe would be 250, 500, 1000, 1500, or 2,000 mg/L for each test conducted. These solutions were covered and gently mixed with a stir bar at room temperature. Periodically, 3-ml samples were withdrawn using a plastic syringe, filtered (0.45 μm), and analyzed for Fe content.

Results and Discussion

Extraction test results are presented as the fraction of iron recovered (Ct/Co) where Ct is the measured iron mass and Co is the total amount added for extraction (Figure 14). For all iron species, varying Co did not change the extraction rate significantly. Approximately 85 to 90% of the easily extractable

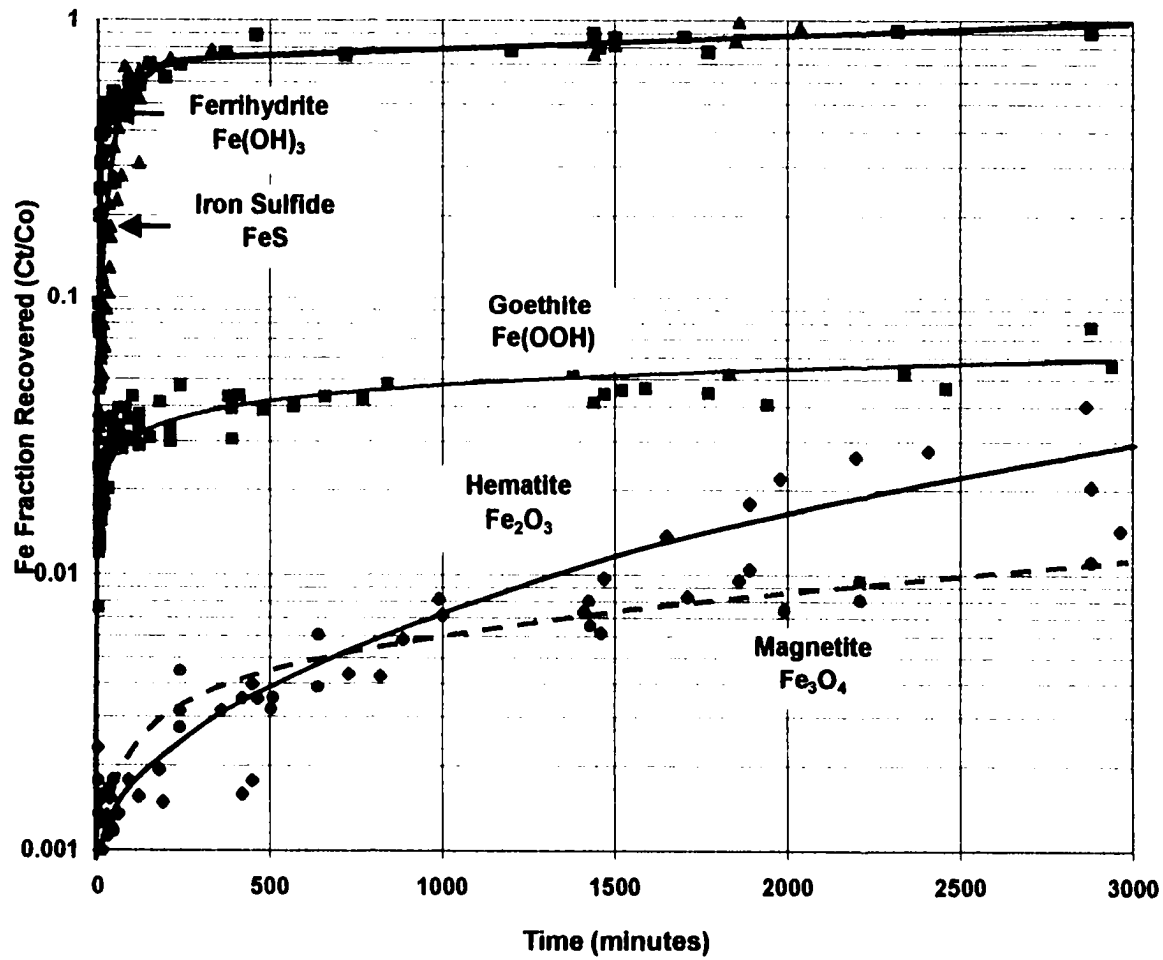

Figure 14. Extraction tests with 0.5 N HCl using various iron minerals showing percent extraction per unit time.

Fe^{2+} and Fe^{3+} species (FeS and $Fe(OH)_3$) were extracted in 24 hours with the remainder recovered in 48 hours. Of the poorly extractable iron forms, the rate of extraction was Fe(OOH) > Fe2O3 > Fe3O4. Significantly, Fe2O3 and crystalline Fe3O4, common iron forms in mature sediments, had average maximum recoverable concentrations of less than 3%. Approximately 6% of Fe(OOH) was extracted. Similar dissolution tests using 0.5 N HCl were conducted by Sidhu et al., 1981, who performed experimentation on the isomorphic varieties of Fe(OOH) for periods up to 100 hours. There is reasonable correlation with respect to extraction rates for minerals common to both studies.

These results indicate that reactive iron species are extracted in 24 to 48 hours of exposure to 0.5N HCl. Crystalline Fe^{3+} species (principally hematite, goethite, and magnetite), which usually comprise much of the background bulk iron species, are poorly extracted. This suggests that a reaction time between 24 to 48 hours should maximize the measurement of reactive, biologically important, iron species while minimizing the contribution of bulk iron typically found in sediments from primary deposition or abiotic diagenesis. Although the percent extraction for crystalline species is small, some sediments can contain very high concentrations of these minerals so high total iron recovery might occur.

It should be noted that synthetic and/or crushed iron forms used in any extraction testing may or may not behave like natural mineral samples for several reasons. The iron forms used for extraction were powdered; however, natural iron minerals often exist as high specific surface area mineral coatings or as ultra fine particulate crystals, which could extract more rapidly. Alternatively, natural iron

minerals may experience diagenic processes for hundreds or even millions of years and could exist in highly stable crystalline forms that could be resistant to extraction. Accordingly, freshly deposited, acid extractable, biogenic Fe^{2+} species appear to be highly reactive; however, over time there may be a tendency towards crystallization that could slow the extraction rate. Finally, FeS_2, though indirectly produced by biogenic activity, is not extracted by 0.5 N HCl (Heron et al., 1994).

Biogenically produced siderite ($FeCO_3$) and magnetite (Fe_3O_4) were not tested here. A high proportion of these iron species (between 73 to 100%), however, were apparently extracted using 0.5N HCl for 48 hours on fresh sediment from Fe^{3+} reducing microcosms as discussed in Chapter 6. Fifty percent recovery of abiotically produced crystalline mineral $FeCO_3$ is reported by Heron (1994), for 0.5 N HCl extractions conducted over 24 hours.

4.3.3. Mild Acid Iron Mineral Extraction Method Description

The suggested method for mild acid extraction of bioreactive Fe^{3+} and biogenic, HCl extractable Fe^{2+} minerals is as follows. Approximately 0.6 to 0.8 g of sediment is placed inside 25 ml serum tubes, which are N_2 purged using a gassing station and stoppered. After all samples are prepared, they are uncorked and 15 ml 0.5 N HCl is added. Each tube is resealed and gently shaken for 48 hours. Each tube is then centrifuged to remove suspended solids and a portion of the extractant analyzed for total Fe and Fe^{2+} spectrophotometrically, as described above. Results are converted to dry weight

per unit soil mass. Sediment moisture content is determined by drying ~10 g wet sediment from each sample interval for approximately 48 hr at 95 C°. Concentrations of Fe^{3+} can be determined by subtracting the Fe^{2+} values from Fe total.

A specially designed rotary shaker was developed for use with 25-ml serum tubes (Figure 15). The rotary shaker provides a swirling motion that works well for the Fe and S extractions described here. The shaker consists of a lightweight wooden or metal rack that can hold up to 100 serum tubes. Individual receptacles are cut at a diameter approximately 3 mm larger than the diameter of the serum tube, to allow free motion. The tube rack is mounted on an ordinary household box fan with plastic blades. All but a portion of one fan blade is trimmed off, shifting the rotational center off-axis. This modification produces a circular vibration in the horizontal plane during operation. Attaching a voltage regulator to the power supply allows shaker speed control. Commercially available rotary, wrist action, or reciprocating bed shakers may be adapted for use.

4.4. Strong Acid Fe Extraction and Extended Sulfide Analysis

4.4.1. Method Background

Crouzet et al. (1994); Wicks (1989); Rice et al. (1993); and Herlihy (1987) have all described extended sulfide extraction techniques. Chemically, these techniques are based on the ability of Cr(II) to extract FeS_2, S^o, and AVS; acetone to extract S^o; and HCl to extract AVS. By subtraction, concentrations of

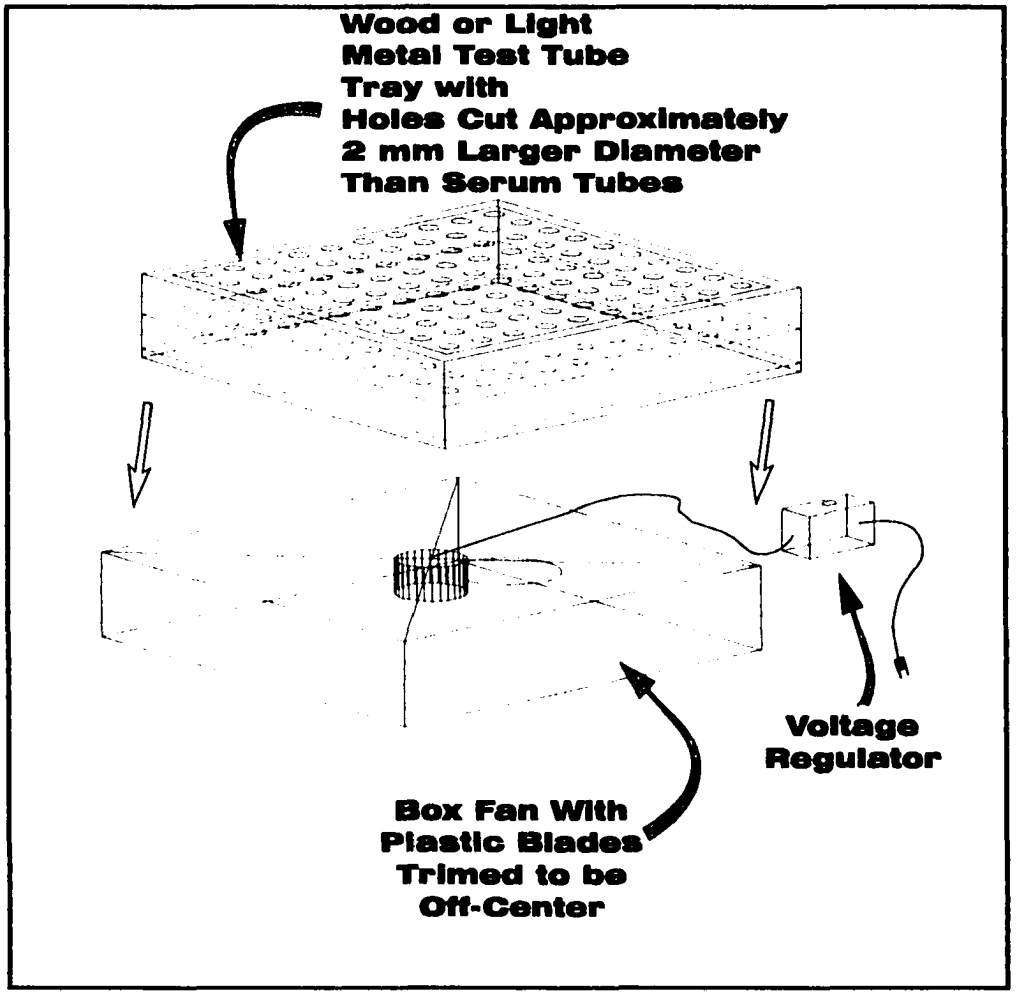

Figure 15. Schematic of rotary shaker used in mineral extractions.

FeS_2, S^o, and AVS are then determined. Here, the technique is simplified using only HCl for AVS analysis followed by a Cr(II) attack on the same sediment sample to determine S^o and FeS_2 (Canfield et al.,1986), which are referred to here as chromium extractable sulfides (CrES). As discussed below, this same sample preparation can also be used to determine strong acid (6 N HCl) extractable Fe^{3+} and Fe^{2+}.

Whereas complete mineral S speciation may be required for some purposes, for natural attenuation studies the division of S into AVS and CrES is adequate. AVS is used as a general indicator of recent sulfate reduction. High CrES concentrations, particularly in the absence of AVS, suggests older microbial activity. Total Fe sulfide (AVS + CrES) can be used for expressed capacity mass determinations.

Sulfide extraction described by earlier workers (Crouzet et al., 1994; Wicks, 1989; Rice et al., 1993; and Herlihy, 1987) used a retort converter technique. That process is slower than the one described here and requires specialized equipment. The method developed here is based on a well-tested, closed vessel method developed by Ulrich et al. (1997). Samples are prepared in an anaerobic glove box using 160 ml serum bottles to determine only the Cr(II) extraction step for a total sulfide value. The technique described below has the following advantages:

- It is much quicker and has been used to process up to 45 samples per day;
- Equipment setup is easy;

- Bulk Fe^{2+} and Fe^{3+}, and AVS and CrES can all be determined with a single sample aliquot using one extraction process.

4.4.2. Method Description

Reagent Preparation

To prevent H_2S oxidation during extraction, all aqueous reagent solutions are deoxygenated by bringing to boil (near boil for acids) for 20 minutes while sparging with N_2 in a boiling flask to maintain a N_2 atmosphere. While hot, the liquid can be immediately transferred using an electric pipetter to nitrogen purged 160 ml serum bottles, sealed with butyl rubber stoppers, and secured with aluminum seals. A gassing station is used to inject N_2 into each sealed serum bottle to obtain a positive pressure of approximately 15 psi. Using this technique, quantities of 10% zinc acetate $Zn(CH_3COO)_2 \bullet 2H_2O$, 6 and 12 N reagent grade HCl, and a supply of deoxygenated deionized water are produced using nano-pure water. Solutions prepared in this manner remain anoxic for long periods of time. During use, solutions are withdrawn via syringe and pressure maintained in the storage bottles by injection of N_2.

A 1N solution of Cr^{3+} is produced similar to Canfield et al. (1986) as follows. A large (1 L) aspirator bottle is filled with zinc chips, which are immersed in 0.5 N HCl for approximately 15 minutes. This acid is drained and the procedure repeated again until the zinc has a shiny, silver finish. A large diameter syringe is inserted into the base of the zinc chips and connected to a gassing station to provide N_2 sparging and headspace. A 1N Cr (III) chloride hexahydrate ($CrCl_3 \bullet 6H_2O$) solution is added to near the top of the zinc chips.

After ~15 minutes the green colored Cr^{3+} solution changes to a blue color indicating that the solution is reduced to Cr^{2+}. Approximately 100 ml fluid is transferred under a nitrogen head using an electric pipetter to 160 ml nitrogen purged serum bottles, which are sealed with butyl rubber stoppers and secured with aluminum seals. Excess pressure may build inside the storage bottles over time so additional N_2 is not added to the headspace and some gas may, in fact, need to be bled after a few days. The Cr^{3+} solution produced in this manner can remain in a reduced form for at least three months.

Sample Preparation

For each sample, approximately 0.8 to 1 g sediment is placed in weighed 25-ml nitrogen purged, serum tubes. Nitrogen is supplied to each tube continuously during sediment transfer through a six-inch long syringe attached to polyvinyl hose connected to a nitrogen gassing station. The actual sediment weight is then determined for each sample. A small diameter rubber o-ring (approximately 3-mm dia.) is placed around a smaller 4-ml test tube approximately 1 cm from the top. The serum tubes are reopened, and the smaller 4-ml test tube is placed inside each larger serum tube while maintaining an anoxic head by continuously flooding with N_2 (Figure 16). Using a syringe, 2.5 ml of zinc acetate solution is extracted from a sealed serum bottle and placed into the 4-ml test tube. The serum tube is then sealed with a butyl rubber stopper and secured with an aluminum seal. Using a syringe, approximately 8-ml nitrogen gas is withdrawn from the headspace of the sealed test tube to create a slight vacuum. Using a syringe, 3 ml of 6N HCl is withdrawn from a sealed

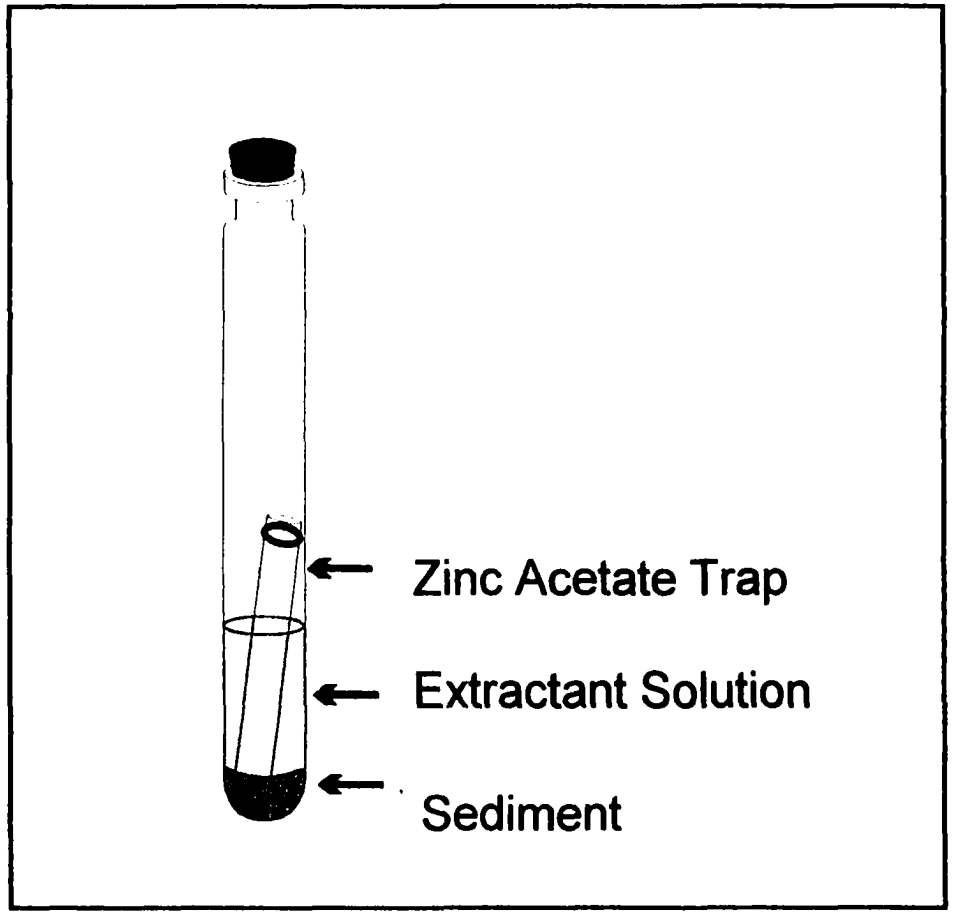

Figure 16. Schematic of closed system AVS and CrES extraction.

serum bottle. This acid is carefully injected through the stopper against the inner wall of the serum tube so that it immerses the sediment without entering the 4-ml tube containing the acetate solution. The tube is then placed in a rotary shaker for 3 days. The shaker rotates the tubes sufficiently to provide good mixing without spilling the acetate solution.

For this first step, the 6N HCl acid 1) dissolves many Fe^{3+} and Fe^{2+} minerals, and 2) eludes H_2S, from AVS minerals, which is subsequently trapped in the Zn acetate solution as ZnS. Following the extraction period, the serum tubes are unsealed but kept under a constant nitrogen gas flow. The Zn acetate traps are removed and analyzed for sulfide spectrophotometrically using the methylene blue technique (Eaton et al., 1995). Five milliliters deoxygenated deionized water is added to the 6N HCl/sediment solution. Each tube is restoppered, vigorously shaken by hand, then centrifuged to settle suspended solids. Again, the tubes are unsealed but kept under nitrogen flow. Samples of the extractant are withdrawn and evaluated for total Fe and Fe^{2+} spectrophotometrically, as above.

To begin the second extraction, most of the HCl solution is carefully decanted from the serum tubes, under a N_2 atmosphere, and discarded. A fresh Zn acetate trap is inserted into the seal tube. The steps involved in the first extraction are repeated, using 2.5 ml 1N Cr^{3+} and 1 ml 12 N HCl instead of 6 N HCl. Again, the serum tubes are placed in the rotary shaker for 3 days. Sulfide, from pyrite (FeS_2) and S^o (CrES), are eluted during this extraction and trapped in Zn acetate. At the end of this time, the serum tubes are unsealed and the Zn

acetate traps analyzed for sulfide, as above. Solid phase Fe and S data are typically presented on a dry weight basis.

4.4.3. Laboratory Testing and Discussion

Tests were performed to verify the efficacy of the method used here. Test samples were made using a crushed glass matrix mixed with 0.5% FeS and FeS_2 and 1% Fe_2O_3 (Alpha Aesar) in quadruplicate lots. Using the methods described above, the average recoveries were FeS = 99.6%, FeS_2 = 105.4%, and Fe_2O_3 = 100.0%. These tests also showed that negligible FeS_2 was extracted during the initial HCl phase.

As above, it should be noted that synthetic and/or crushed minerals used in extraction testing may or may not extract like natural sediment samples. However, some natural sediment samples, from the test sites, were originally bright red from abundant Fe^{3+} minerals, but at the conclusion of the HCl acid extraction phase they were usually completely white or very light gray, indicating near complete Fe removal. After this extraction, residual iron may remain in some sediments, which may only be extracted by heating the sample. Complete Fe removal, however, is probably not necessary for the analyses, as discussed below. Rice et al. (1993) warns that during the acid extraction phase some eluded H_2S may become oxidized by Fe^{3+} minerals to create S^o. Therefore, measured AVS may be under-reported in some conditions. In the author's experience, the Cr solution maintains a bluish color throughout the second extraction process; indicating sufficient quantity of the reagent was used.

4.5. Field Examples of Fe and S extraction

The Fe and S mineral extraction methods described above were tested on three separate contaminated locations 1) a hydrocarbon fuel spill site, 2) a methane gas contaminated site, and 3) a landfill leachate contaminated site. The objectives of these tests were to demonstrate the efficacy of the extraction methods and to develop a better understanding of data analysis, especially with respect to Fe. Multiple core holes were drilled at each location, however, only representative analyses are shown below.

4.5.1. Site Descriptions

The following discussion is intended to give a general understanding of site geology and contaminant characteristics. Although each of the study sites was unique, all three were located in Oklahoma.

Site A: Fuel Contaminated Aquifer

A complete description of this study area is described below in Chapter 5. Briefly, the site is an abandoned gas station located in Oklahoma City, Oklahoma with a fuel leak that occurred >15 years ago. In addition to 16 ground water monitoring wells, five core holes were drilled at this site for mineral analyses along the ground water flow-path, to a depth of 7.62 m (25 ft) (Figure 17). Of those, two representative core holes (A-1 and A-2) are discussed here. Figure

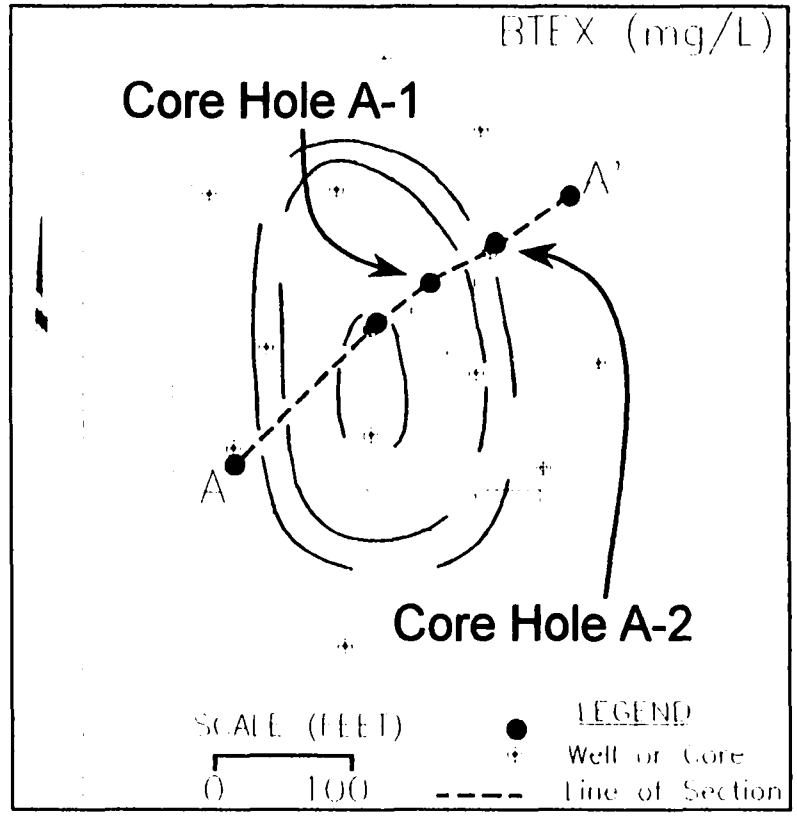

Figure 17. Fuel contamination site map showing total dissolved BTEX and locations of Core Holes A-1 and A-2.

17 shows the measured total concentration of benzene, toluene, ethylbenzene, and xylene (BTEX) in ground water. Depth to ground water is approximately 4.7 m (15 ft) below the surface. The aquifer consists mostly of red, fine grained, very poorly cemented Permian aged sandstone belonging to the Garber Group. The deep red color is indicative of high concentrations of hematite found in this unit, often above 1% by weight (Parkhurst et al., 1993)

Site B: Natural Gas Contaminated Aquifer

Site B is an unusual study area found in western Oklahoma near the town of Elk City. Due to a casing failure, a deep, high pressure, natural gas well blew out under ground in the mid 1980's. Natural gas (principally methane) has seeped to the surface through fissures, inundating localized areas of soil near the well head. This site has been thoroughly studied by Parsons (1998). A non-contaminated, background core hole (B-1) and a methane contaminated core hole (B-2) are shown for comparison in this paper. Soil gas samples from core hole B-2 contained 42% methane. The native soil is a red, fine-grained silt loam with high iron (hematite) content.

Site C: Landfill Leachate Contaminated Aquifer

This site is also described in more detail in Chapter 5. It is an unlined, closed municipal landfill south of the City of Norman, Oklahoma. This area was first used for disposal in the early 1920's and was closed in 1985 (Robertson et al., 1974 and Tohme, 1994). The sediment is river alluvium consisting mostly of fine to coarse sand with thin layers of clay. The water table is approximately

0.6 m (2 ft) below the surface. Six core holes have been drilled and evaluated at this site, each to a depth of approximately 10.7 m (35 feet). Two core holes, C-1 and C-2, are discussed (Figure 18).

4.5.2. Mineral Iron Reduction Evaluation

Figure 19 shows iron concentration data from the 0.5 N and 6 N acid extractions from Site A, core hole A-1. Iron mineral data are typically calculated on a mass/mass basis (e.g., mg/Kg). As expected, much more Fe is extracted using the strong acid, which has been found for all sediment samples analyzed. For this sample set the strong acid extracted more than 10 times the weak acid extraction amount. Data presented on a mass basis is needed for calculation purposes to properly estimate available or expressed capacity for Fe^{3+} reduction in natural attenuation studies (Kennedy et al., 1998).

Observing the ratio of Fe^{2+} to total Fe can aid in identifying zones of significant Fe^{3+} reduction. Figure 20 shows core hole A-1 data evaluated in terms of percent Fe^{2+} for both the strong and weak acid extraction. For the 0.5 N HCl extraction, the fraction of Fe^{2+} to total Fe increases to approximately 90% below the water table indicating probable Fe^{3+} reduction occurred in that area. Alternatively, the Fe^{2+} ratio averaged only 7.5% (not exceeding 15%) for the same interval when 6 N HCl acid was used. Overall, only a small fraction of the bulk iron in this system is in the Fe^{2+} form.

The Fe^{2+} to Fe total ratios for both the weak and strong acid extractions may help define areas where Fe^{3+} reduction has occurred. Exposure to weak acid typically

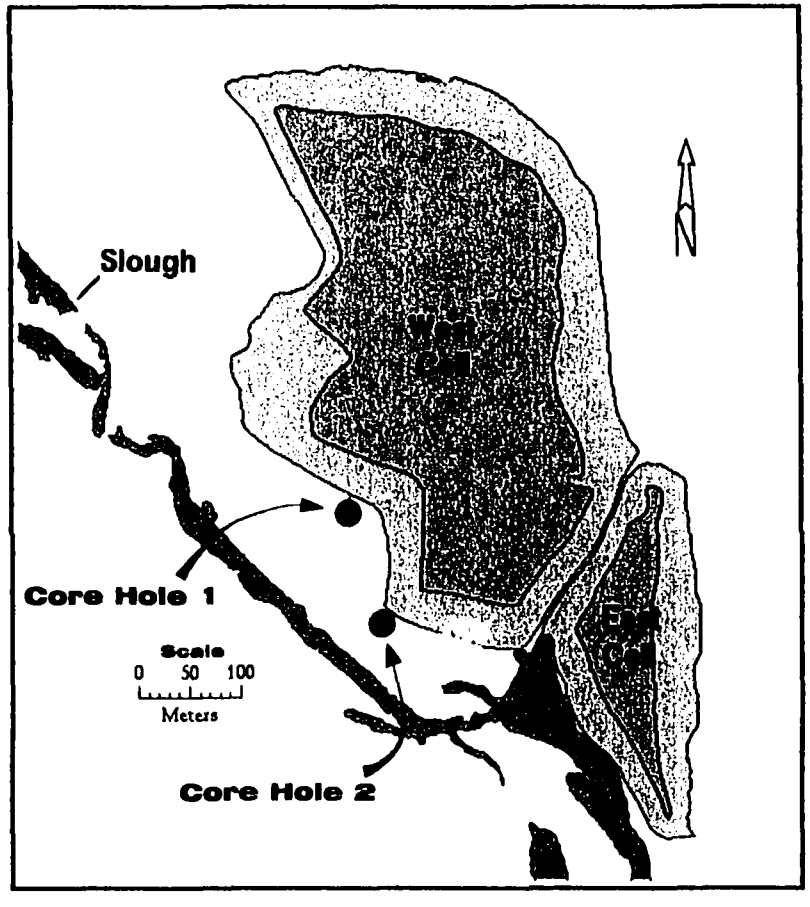

Figure 18. Landfill example site map showing sampling points.

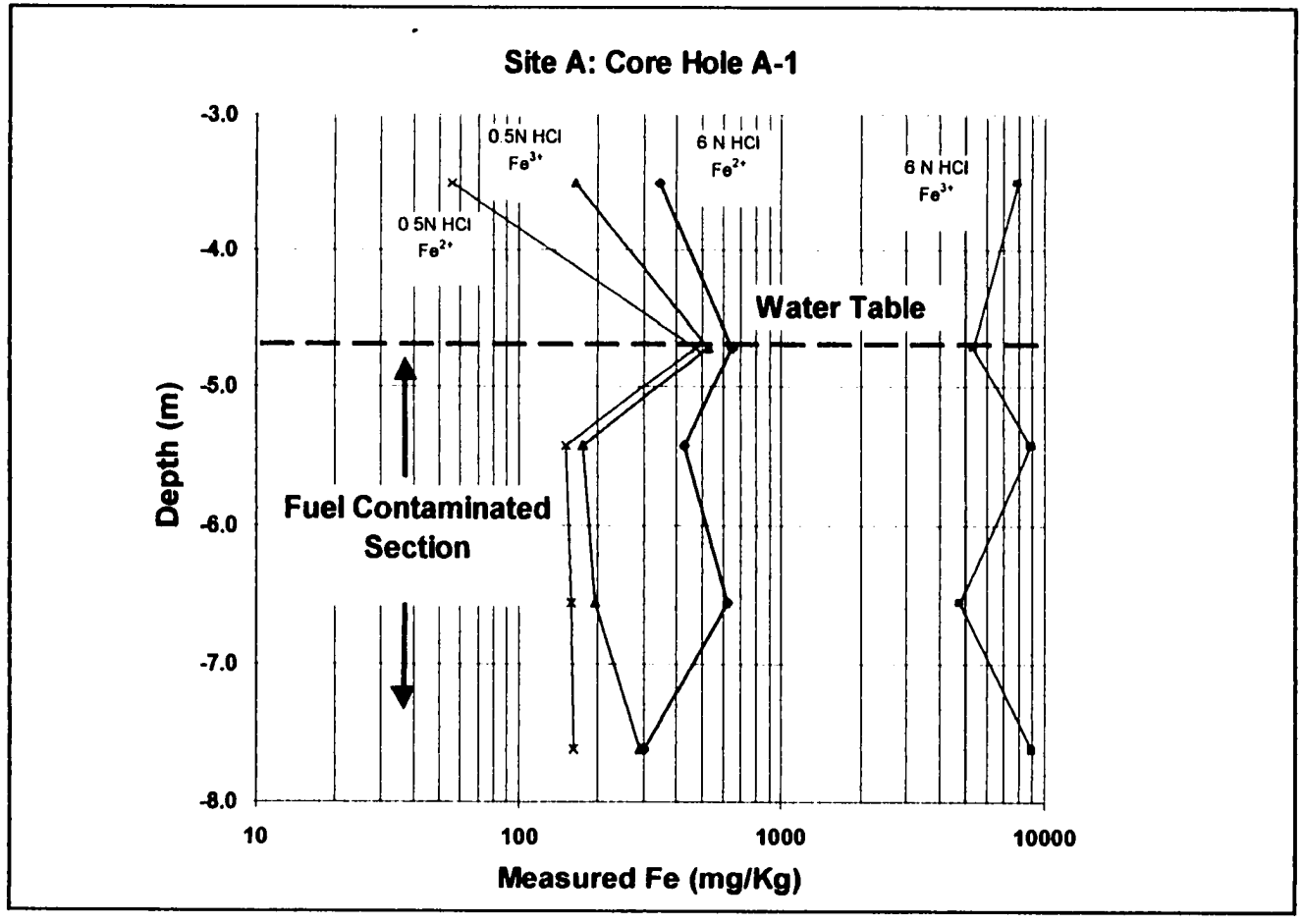

Figure 19. Site A, core hole A-1, iron mass/mass data in mg/Kg from 0.5 N and 6N HCl extractions.

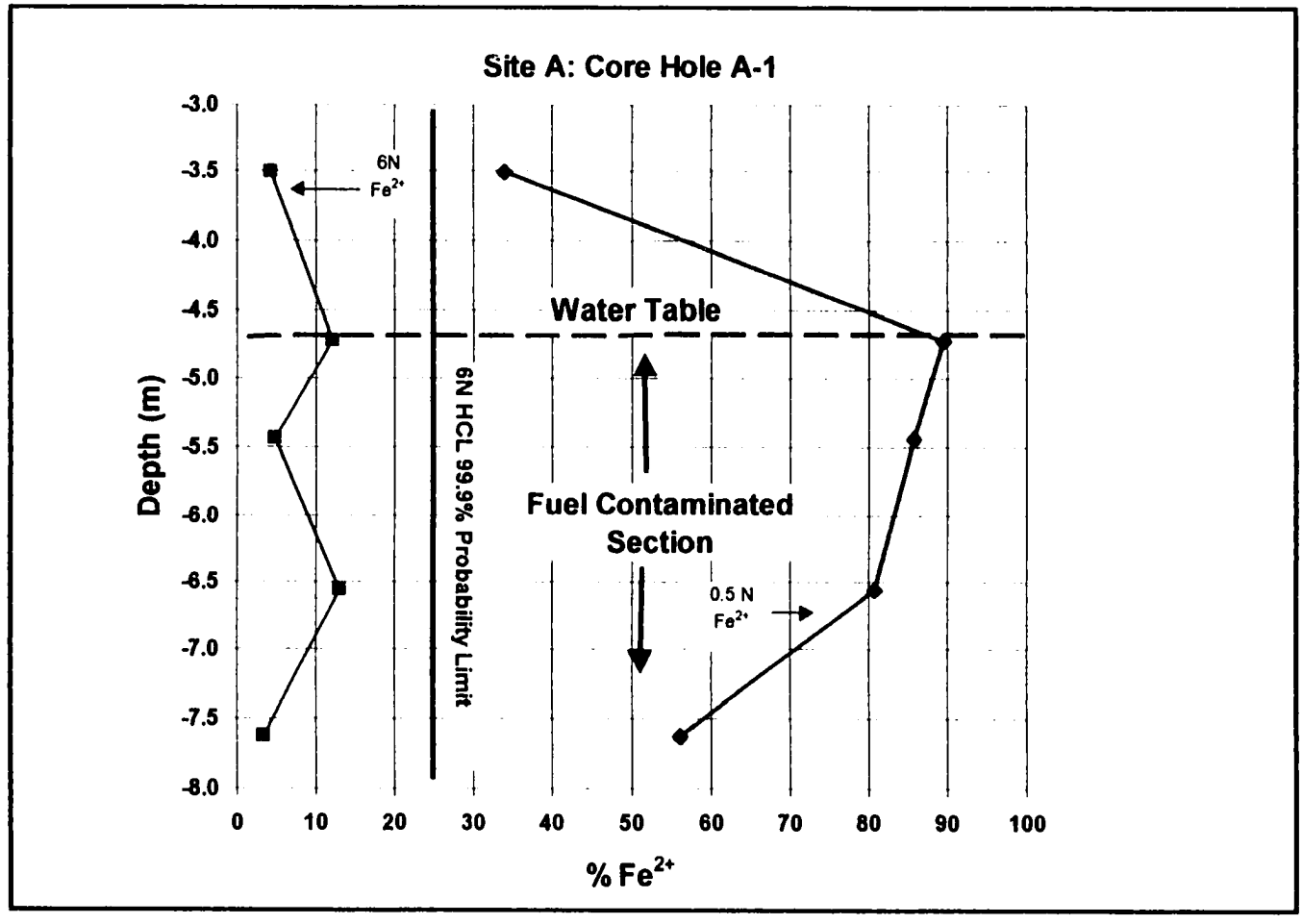

Figure 20. Site A, core hole A-1, near fuel source: percent Fe^{2+} per total Fe recovered by 0.5 N HCl and 6 N HCl extractions.

extracts only a small portion of the total iron present in a sediment sample. For these study sites, the 0.5 N HCl extracted between 5 to 10% of the total amount of Fe when compared to the amount extracted with 6 N HCl. Weak acid extracts a small part of exposed iron surfaces and poorly crystalline iron particles. Alternatively, the 6 N HCl extraction removes much greater amounts of iron including all of the 0.5 N extractable fraction and much of the background bulk iron mass. During microbial reduction, some of the original Fe^{3+} mass is used to form new Fe^{2+} minerals. These biological processes often alter only a small amount of the total iron so there is little change in the overall Fe^{2+} to total Fe ratio over time as expressed by the 6N HCl extraction. However, newly formed Fe^{2+} minerals are not evenly distributed in the total iron matrix. Rather, they are deposited almost exclusively as surface coatings or poorly crystalline particulates, which are preferentially dissolved by the weak 0.5 N HCl acid extraction. Therefore, where microbial iron reduction has occurred, the Fe^{2+} ratio will tend to be high for the 0.5 N HCl compared to that for the 6 N HCl extraction. Conversely, where Fe^{3+} reduction has not significantly occurred there is little difference between the Fe^{2+} ratio when comparing the weak and strong acid extractions.

Comparing strong and weak acid extraction Fe^{2+} ratios is appropriate only where the 0.5 N extracted iron is a relatively small fraction of that extracted by 6 N HCl. When this is not the case, relating the 0.5 N and 6 N HCl Fe^{2+} ratios may be inconclusive or at worst, highly conservative. Where possible it is advisable to examine Fe^{2+} ratios from non-contaminated portions of the aquifer to aid in

establishing background conditions. Note that obtaining such sediment samples from different geographic areas of an aquifer is not necessarily ideal because true background conditions may not be represented due to spatial heterogeneity in mineralogical composition inherent in any aquifer.

A statistical approach is proposed for using the 6 N HCl acid data to establish a relevant threshold limit for the 0.5 N HCl acid Fe^{2+} to total iron ratio. The 99.9% probability limit is determined using the percent Fe^{2+} to total iron data from the 6 N HCl extraction as:

(24) $$\hat{x}_p = \bar{x} + Z_p * s$$

Where:

$\hat{x}_p$ = 99.9% percentile of the 6N HCl Fe^{2+} %

$\bar{x}$ = 6 N HCl %Fe^{2+} sample average

Z_p = 99.9% percentile of the standard normal distribution; and

s = Sample standard deviation

The 99.9% percentile establishes a limit value which a sample could only be expected to exceed by random chance 1:1,000 times. Significant iron reduction has occurred where Fe^{2+} ratio values from the 0.5 N HCl extraction exceed the calculated statistical threshold. Subsequent interpretation is still required, however, to discriminate Fe^{3+} reduction from naturally occurring soil organics versus reduction brought on as a result of organic contamination.

Applying the test to the data shown in Figure 20 indicates that the 0.5 and 6 N HCl extractions produce statistically different results.

The statistical analysis proposed here is based on the assumption that the data are normally distributed. This type of analysis is desirable because the determined upper probability limit is dependent upon both the sample deviation and sample size. Based on the W goodness-of-fit test (Gilbert, 1987), all of the 6 N Fe^{2+} ratio data sets in this study were from normally distributed populations. However, because those data are expressed in terms of percent, the system is finite (bounded between 0 and 100) and cannot be considered truly normal. In this case, however, the degree of error presented by truncating the extreme ends of the normal density function, or bell curve, is insignificant, especially if only the upper half of the curve is considered, as is done here. Nonparametric analyses may be considered for use, but such evaluations tend to limit calculated percentiles to only the range of the observed data set which, in this case, leads to a much less conservative estimation of a significant threshold limit.

The relevance of these analytical and evaluation techniques can be seen from additional field site examples. Core hole A-2 is down-gradient from core A-1 in a less contaminated area. In shallow sediments, the 0.5 N Fe^{2+} ratio roughly tracks the 6 N Fe^{2+} ratio and many points are below the 99.9% 6 N HCl Fe^{2+} probability limit (Figure 21). Below a tightly cemented sandstone, in the contaminated portion of the aquifer, the 0.5 N Fe^{2+} percent increases up to 85%, well beyond the calculated probability limit. For Site B, core hole B-1 was a background soil sample with no methane. For that sample location, there is little

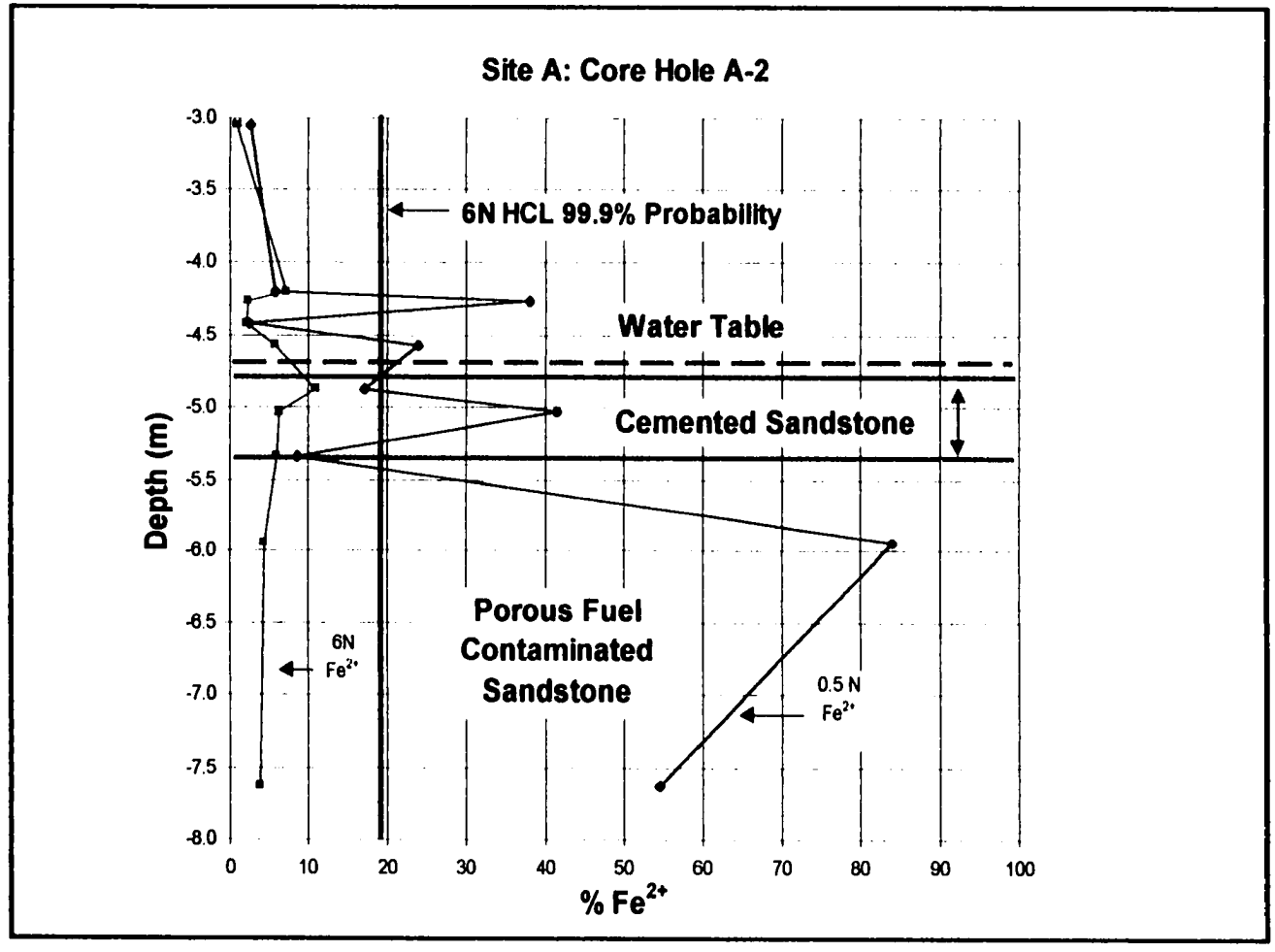

Figure 21. Site A, core hole A-2, edge of fuel plume: percent Fe^{2+} per total Fe recovered by 0.5 N and 6 N HCl extractions.

difference between the 0.5 N and 6 N Fe^{2+} ratios (Figure 22). Here, the 0.5 N data are generally below the 6 N HCl Fe^{2+} probability limit. For Site B, at a methane contaminated core hole (B-2) most of the 0.5 N HCl ratio data are well above the probability limit (Figure 23). Finally, for the landfill site (Site C), core hole C-1 shows highly elevated 0.5 N HCl Fe^{2+} ratios across almost the entire thickness of the aquifer (Figure 24) in an area known to have been contaminated with landfill leachate for many years.

In overview, field data from the 0.5 N HCl extraction in contaminated areas commonly spike in the range of 80% < Fe^{2+}% < 100%. This high ratio suggests that the 48 hr 0.5 N HCl extraction technique used here recovered biogenically produced Fe^{2+} mineral species without overly extracting the bulk matrix iron largely comprised of Fe^{3+} species. Over extraction would have reduced the 0.5 N HCl Fe^{2+} ratio because, based on 6 N HCl extractions, the bulk sediment iron contained a much higher percentage of Fe^{3+}. Secondly, those high 0.5 N HCl Fe^{2+} ratios reflect the amount of Fe^{3+} that was biologically reduced to Fe^{2+} over many years. Because there is little residual 0.5 N HCl Fe^{3+} observed in those areas it is suggested that the 48 hour extraction procedure approximates the biologically available Fe^{3+} fraction.

4.5.3. Mineral Sulfide Evaluation

Areas of sulfate reduction were found at all three study sites; however, Site C, core hole C-2, is used as a representative example. For this core, 28 sediment samples were analyzed across the aquifer thickness (Figure 25). Two

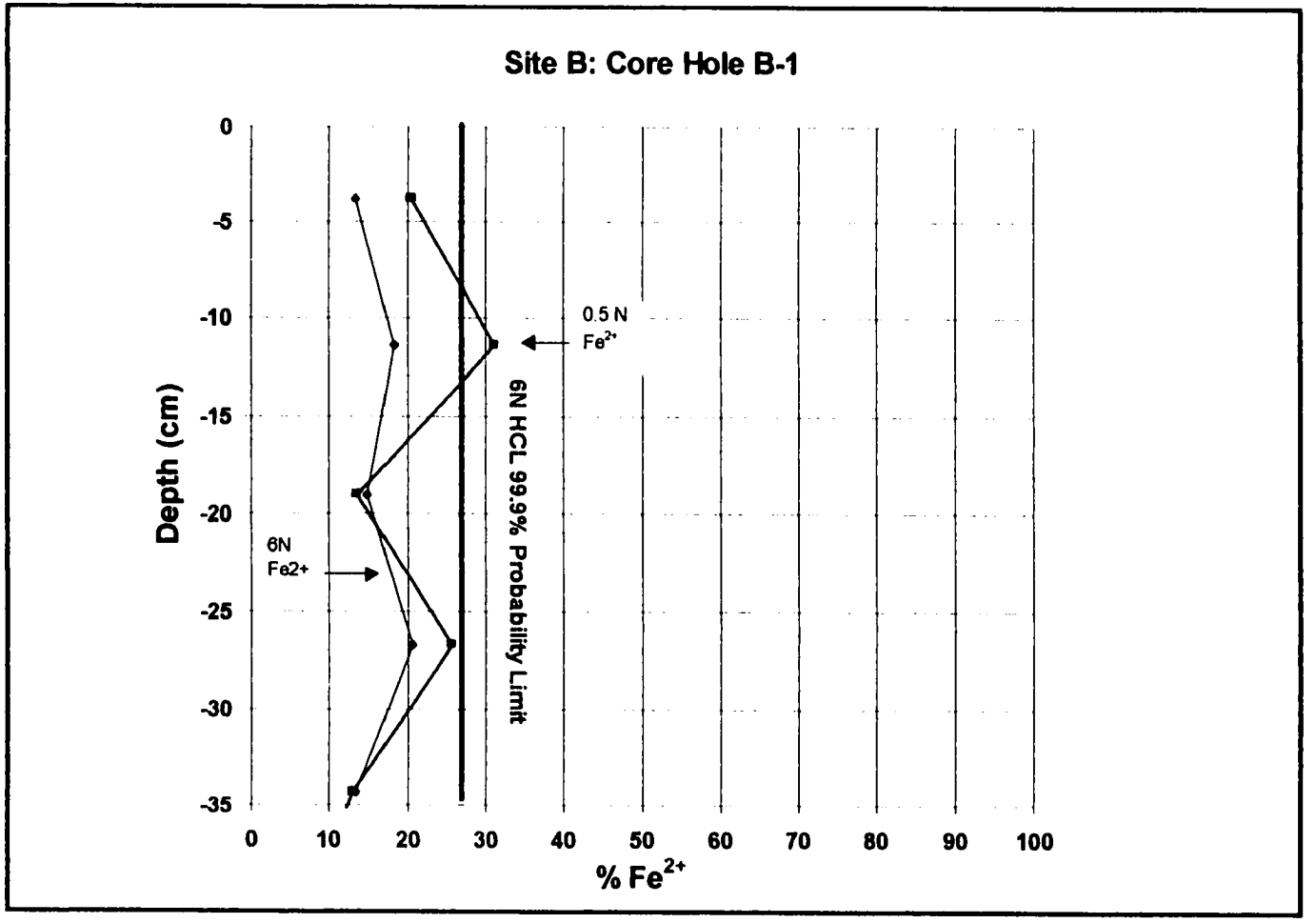

Figure 22. Site B, core hole B-1, background soil: percent Fe^{2+} per total Fe recovered by 0.5 N HCl and 6 N HCl extractions.

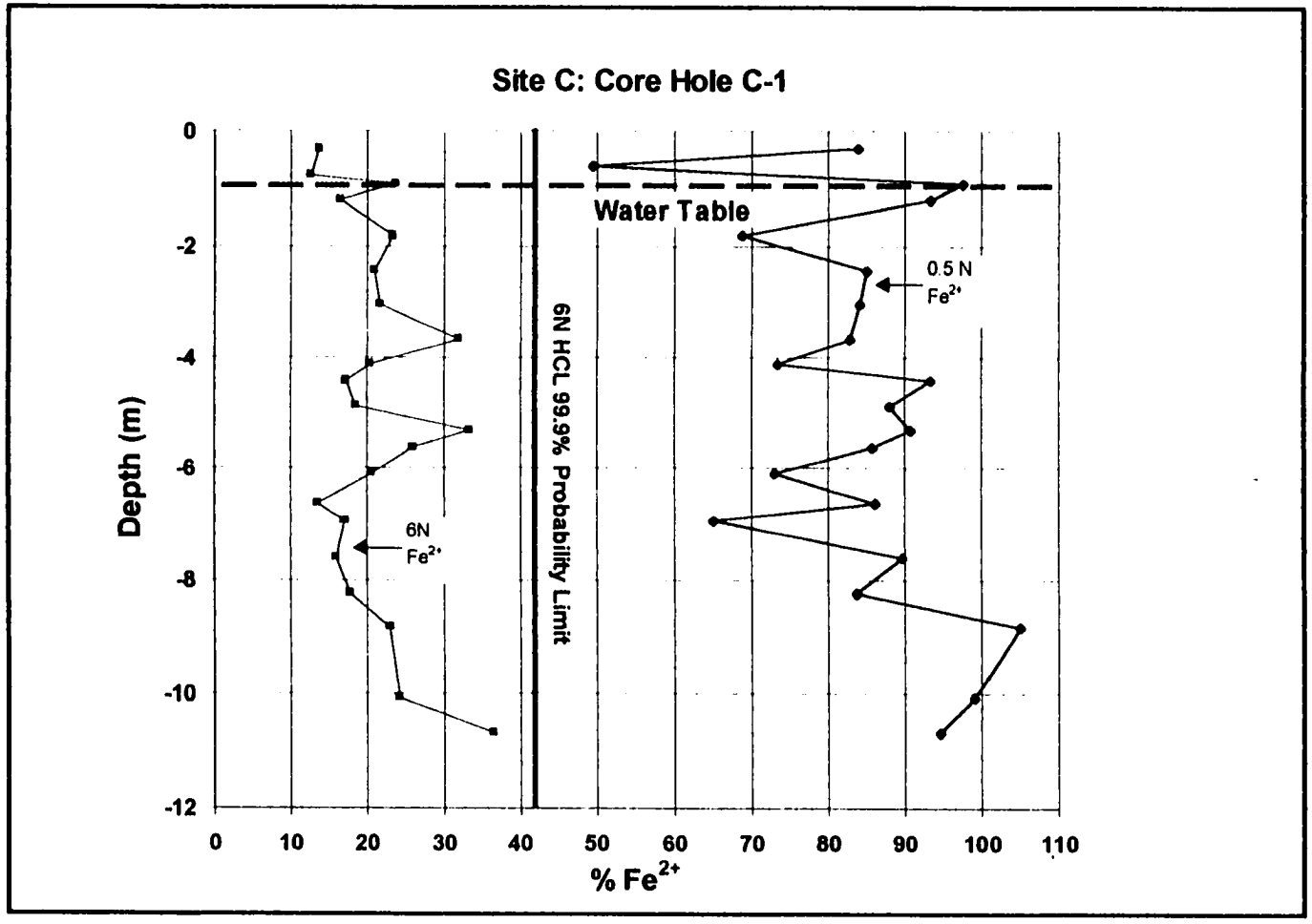

Figure 23. Site C, core hole C-1, landfill leachate site: percent Fe^{2+} per total Fe recovered by 0.5 N HCl and 6 N HCl extractions.

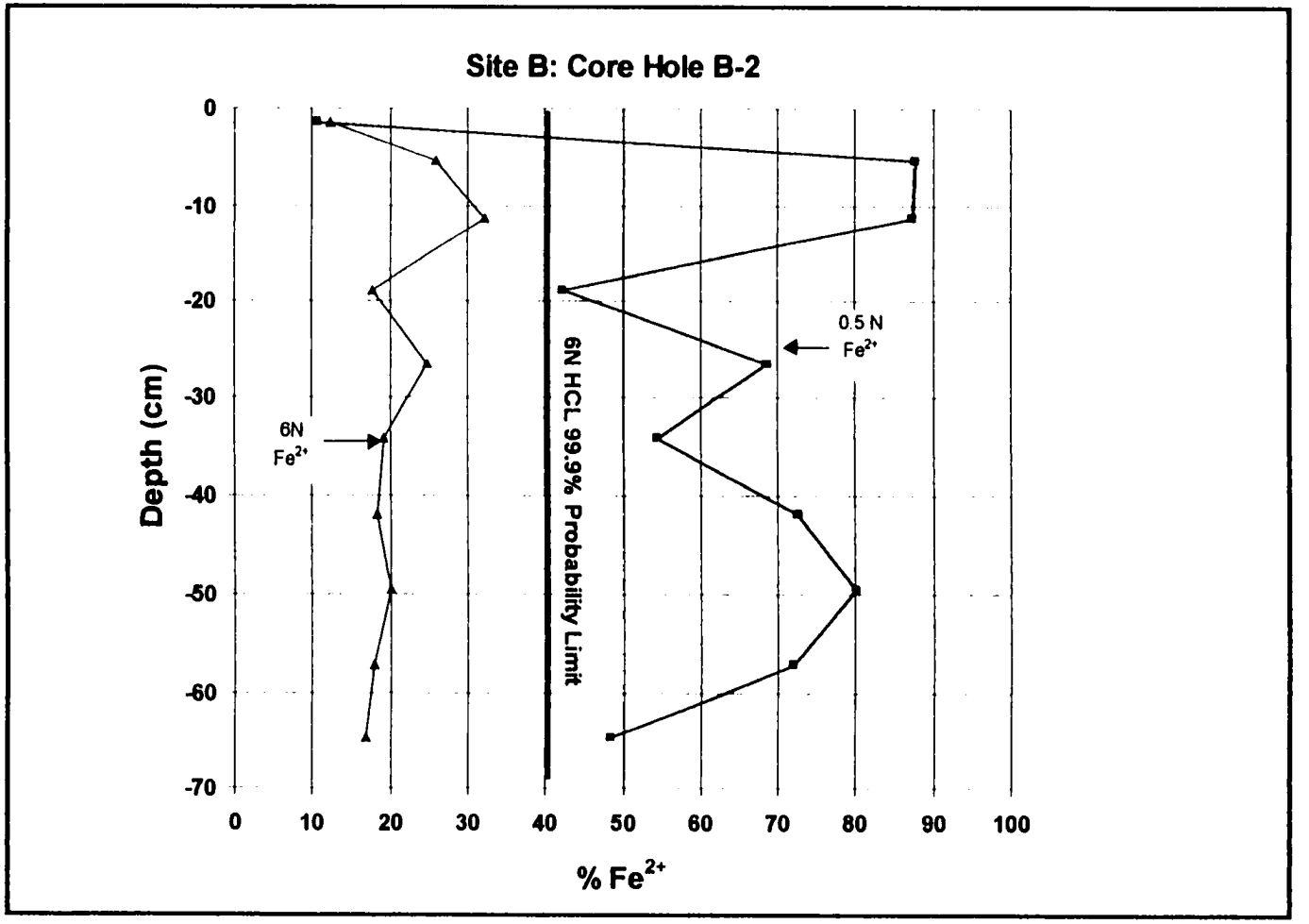

Figure 24. Site B, core hole B-2, methane enriched soil: percent Fe^{2+} per total Fe recovered by 0.5 N HCl and 6 N HCl extractions.

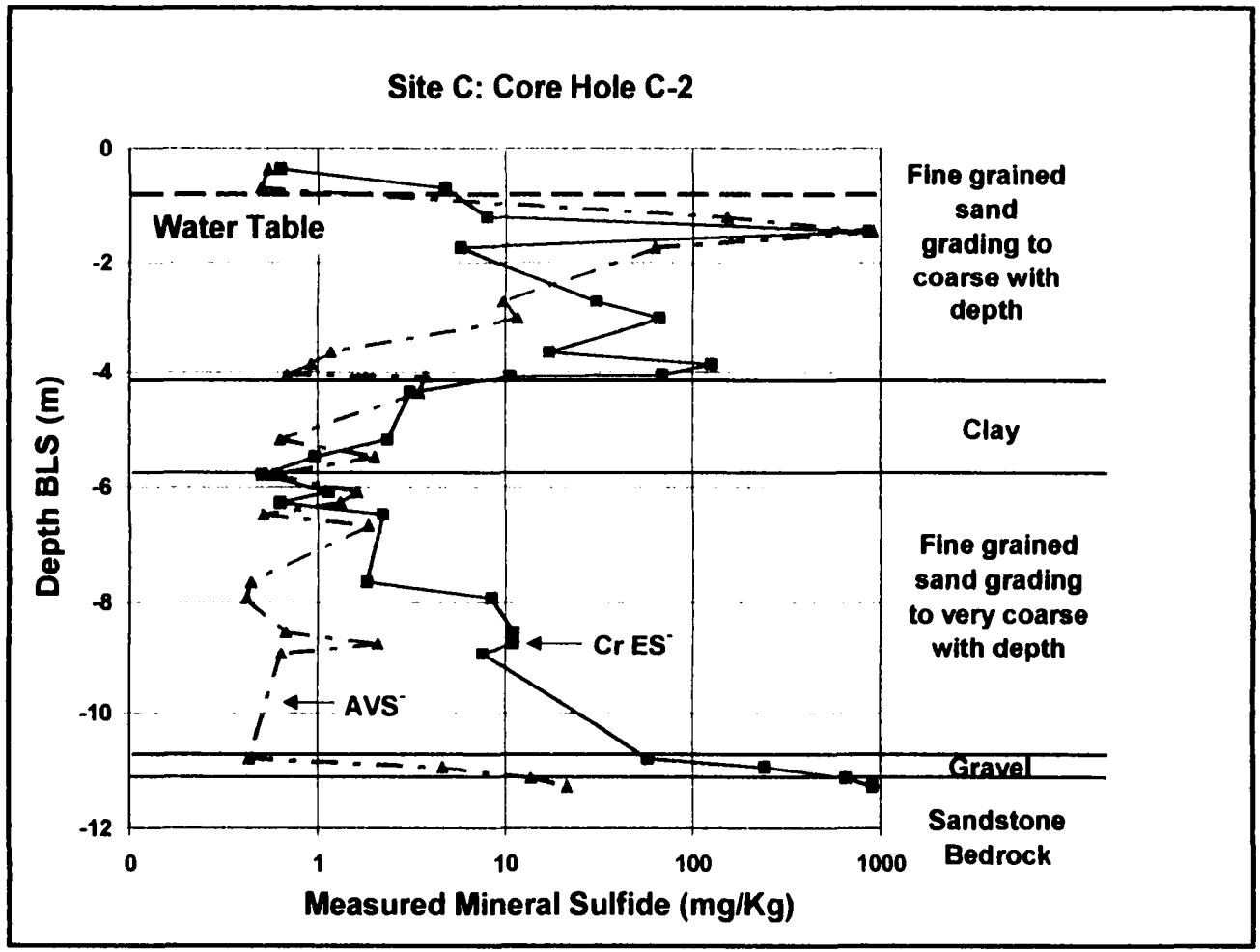

Figure 25. Site C, core hold C-2, landfill leachate site: mass concentration data for AVS and CrES (mg/Kg)

fluvial depositional sequences are recognized at this core site, denoted by two coarsening-downward sediment grain size sequences. Fine grained sand grades to coarse sand across the first 4.3 m (15 ft) of section. A clay zone lies between 4.3 to 5.8 m (15 to 19 ft). Below that, fine sand grades to gravel just above bedrock at 11 m (36 ft).

As shown, the technique presented here can discern independent trends for AVS and CrES using actual sediments. Both AVS and CrES concentrations are low (< 1 mg/Kg) above the water table. Concentrations of both AVS and CrES peak below the water table. Deeper in the aquifer, AVS decreases to background levels, except through the basal gravel zone, where concentrations increase again. CrES levels remain high above the clay zone but drop to background in the clay. Below the clay layer, CrES levels increase again, reaching a peak in the gravel layer.

The pattern of AVS suggests recent SO_4^{2-} reduction just below the water table and at the base of the aquifer. The pattern of CrES infers past geologic control of SO_4^{2-} reduction and/or organic contaminant migration. High levels of CrES above the clay zone may have been caused by preferential leachate migration in porous sand across the top of the clay layer. Little SO_4^{2-} reduction occurred in the clay layer; however, below that zone CrES levels increased correlative to aquifer grain size. Increased grain size usually equates to increased permeability, which probably enhanced advective mass transport of SO_4^{2-} and/or organic leachate. That condition undoubtedly promoted SO_4^{2-} reduction, which caused increased CrES mineral deposition over time.

4.6. Fe and S Extraction and Field Examples of Conclusions

Due to geochemical constraints, many of the microbial processes associated with natural attenuation involving Fe and S are expressed in mineral form. Although SO_4^{2-} is usually aqueous, its reduction often results in the deposition of AVS or CrES solids. Little Fe^{3+} is aqueous at normal pH and much produced Fe^{2+} precipitates in mineral form. Therefore, it is logical that natural attenuation studies should include mineral Fe and S analysis to determine expressed and assimilative capacity, as demonstrated in Chapter 5. Difficulties in mineral sample collection and analyses have probably inhibited routine mineral Fe and S evaluation and simplified methods were needed.

The methods presented to collect and preserve sediment samples for subsequent Fe and S mineral analysis are practical and effective. Relatively intact sediment cores can be preserved for subsequent processing in a laboratory. However, grab samples can be more easily preserved in the field by transferal to serum bottles. These bottles can be sealed and purged with nitrogen to prevent further exposure to oxygen.

Laboratory testing with pure mineral forms using 0.5 N HCl, suggests substantial extraction of some reactive iron forms occurs between 24 to 48 hours without extracting a large percent of the more crystalline Fe minerals that commonly constitute much of the bulk iron mass in sediments. Due to the nonspecific nature of the extraction process, and many other factors, a chemical determination of the biologically available Fe^{3+} or biogenically produced Fe^{2+}

minerals is largely subjective. However, Fe^{3+} minerals that are prone to microbial reduction are more easily extracted by weak acid attack. Additionally, certain precipitated Fe^{2+} minerals can also be extracted with some degree of specificity with regard to background Fe mineralogy.

Identifying areas where Fe^{3+} reduction occurred can be difficult when examining mass concentration data, such as mg/Kg, although data presented in that form is often important for an intrinsic bioremediation study. Evaluating the ratio of Fe^{2+} to Fe total can aid in identifying areas where significant Fe^{3+} reduction occurred. Tests on actual samples commonly showed Fe^{2+} to total Fe ratios less than 50% in noncontaminated areas but between 80 to 100% in contaminated areas.

Data from field tests suggests that the extraction technique used on these sediments recovered the biogenically produced, HCl extractable, Fe^{2+} mineral species without overly extracting background iron, which is largely comprised of Fe^{3+} species. Had the extraction time been too long, lower 0.5 N HCl Fe^{2+} to total Fe ratios would be expected, reflecting unwanted dissolution of background Fe^{3+}. The fact that the Fe^{2+} ratio approaches 100% in these contaminated areas also suggest that the 0.5 N extraction procedure described here is a reasonable approximation of the biologically available Fe^{3+} fraction.

Comparing the Fe^{2+} to Fe total ratios between the 6 N HCl and 0.5 N HCl extractions may aid in differentiating zones where Fe^{3+} reduction has occurred. Microbial Fe^{3+} reduction often only converts a small amount of the total Fe present in a sediment to Fe^{2+}. In non-contaminated areas the Fe^{2+} to Fe total

ratios are approximately the same for both the strong and weak acid extractions for the same sediment. However, in contaminated areas, where Fe^{3+} reduction has occurred, the Fe^{2+} ratios increase for weak acid extractions but remain about the same for the strong acid. Therefore, 6 N HCl extraction data can be used to develop a statistical probability limit. This limit could serve as a benchmark to evaluate the significance of 0.5 N HCl Fe^{2+} ratio data. Interpretation is still required, however, to discriminate between Fe^{3+} reduction from naturally occurring organics versus that occurring as a result of organic contamination. Also, this comparative technique may not work in Fe limited sediments where the amount of Fe total extracted using 6N and 0.5 HCl are similar. Background conditions could also be established by comparing weak acid extraction values from contaminated and noncontaminated areas; however, spatial variability may make such analyses difficult.

The extended sulfide analysis method proposed here is simplified in that it only quantifies AVS and CrES; however, for most natural attenuation studies this level of discretion is adequate. The room temperature, closed system method of sulfide trapping is greatly simplified over previous methods and permits many samples to be prepared for evaluated per day. The resulting AVS data is used as a general indicator of recent SO_4^{2-} reduction whereas high CrES concentrations suggests older microbial activity. AVS plus CrES yields a total Fe sulfide mass number that can be used to determine expressed capacity in natural attenuation studies.

The simple techniques presented here make mineral Fe and S analysis feasible for common use. It is hoped that such methods or subsequent improvements thereof, will eventually be considered routinely for natural attenuation studies. This is demonstrated in the next chapter.

5. APPLICATION TO EVALUATE NATURAL ATTENUATION

5.1. Application Objectives

An investigation was conducted of the natural attenuation (bioremediation) potential in a gasoline-contaminated aquifer. Typically, only aqueous O_2, NO_3^-, Fe^{2+}, and SO_4^{2-} are examined in investigations of this type; however, this study also considered mineral iron and sulfide as sampled in five core holes along a longitudinal transect of the fuel plume. These samples were subjected to sequential extractions using 6N HCl and 1 N Cr^{2+} to determine the mineral content of Fe^{2+}, Fe^{3+}, FeS, and FeS_2. A 0.5 N HCl solution was used to estimate available Fe^{3+} and biogenically produced authigenic Fe^{2+} minerals.

As a remediation option, natural attenuation (intrinsic bioremediation) can be thought of as making an informed decision to allow organic contaminant cleanup to occur through natural subsurface processes. This treatment alternative is gaining acceptance. Biodegradation of contaminants by naturally occurring soil bacteria is the most important destructive mechanism of natural attenuation. To assess biodegradation potential, many natural attenuation studies focus on quantifying electron acceptors or respiratory products that are used to:

- Determine which microbiological redox processes are or have been active;

- Evaluate the mass of hydrocarbons that has been destroyed for a specific redox condition (*expressed capacity*); and
- Estimate the future ability of an aquifer system to degrade hydrocarbons through specific redox processes (*assimilative capacity*).

Protocols for natural attenuation assessment are being developed (Wiedemeier et al., 1997; ASTM, 1996). Additionally, natural attenuation can be applied in Risk Based Corrective Action (RBCA) studies to develop relaxed alternative cleanup standards (ASTM 1995). As typically practiced, these protocols place heavy emphasis on quantifying aqueous phase electron acceptors, including Fe and S species; however, microbially mitigated redox reactions involving Fe and S often involve solid/aqueous interactions which may not be assessed adequately if data are obtained only from water analyses. This chapter is used to:

- Examine Fe and S minerals at a hydrocarbon fuel contaminated aquifer; and
- Suggest ways that a study of this type could be used to evaluate natural attenuation as part of a risk-based approach to site closure.

5.2. Site Description

The study area is in southeastern Oklahoma City. A gasoline service station with underground fuel storage tanks was located on this property but was

removed about 10 years ago. The shallow aquifer is in the Permian Garber Formation, an important drinking water aquifer. The Garber Formation is a fine-grained, poorly cemented, thick-bedded sandstone with intermittent lenses of siltstone and shale. Quartz sand constitutes the bulk of the matrix; however, large amounts of hematite (Fe_2O_3) are present, giving the sediment a bright red or reddish brown color. Parkhurst et al. (1993) reported up to 20% hematite by weight in this formation, though values of 1 to 6% are common.

5.3. Methods

5.3.1. General Methods

Sixteen ground water monitoring wells have been installed on the property since 1994. The current research effort included drilling five core holes along the center of the dissolved hydrocarbon plume parallel to the ground water flow direction (CH-1 through CH-5) (Figures 26 and 27). Each boring was fully cored from surface to a total depth of 7.62 m (25 ft) using a hollow stem auger and evaluated for gross lithology using a binocular microscope.

Dissolved oxygen was measured in-situ for all existing monitoring wells using a YSI 600 dissolved oxygen probe. At the time of this study, ground water was evaluated for benzene, toluene, ethylbenzene, and xylene (BTEX), total petroleum hydrocarbons (TPH), and dissolved NO_3^- and SO_4^{2-} using EPA Methods 8020, 8015, 353.1 and 375.4, respectively (SW-846, 1990). Sediment samples were collected by hand bailing from each core hole near the water table

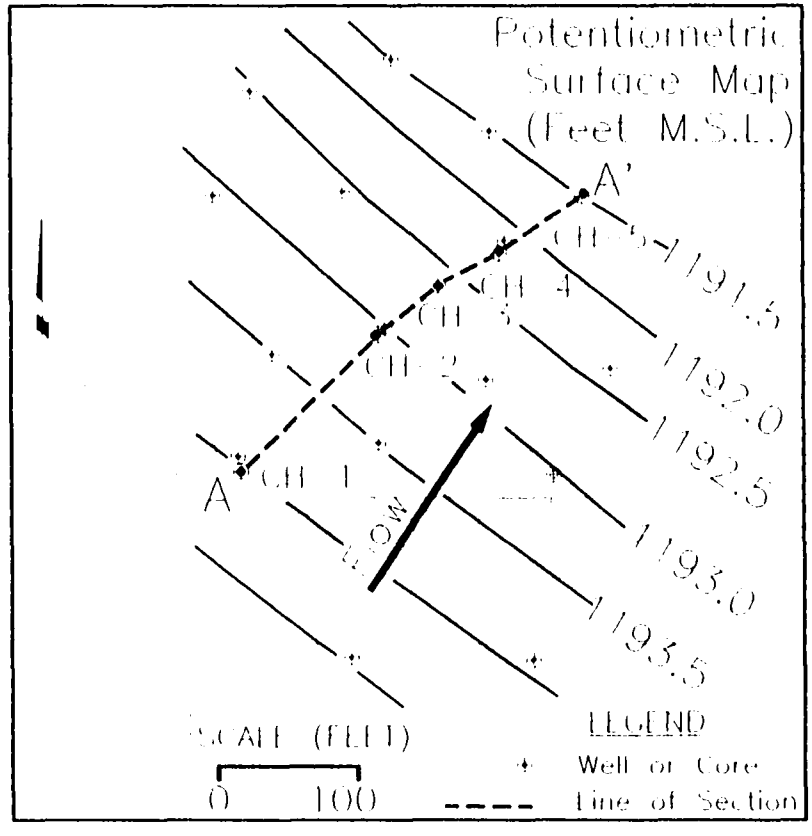

Figure 26. Water table surface map showing ground water flow towards the northeast.

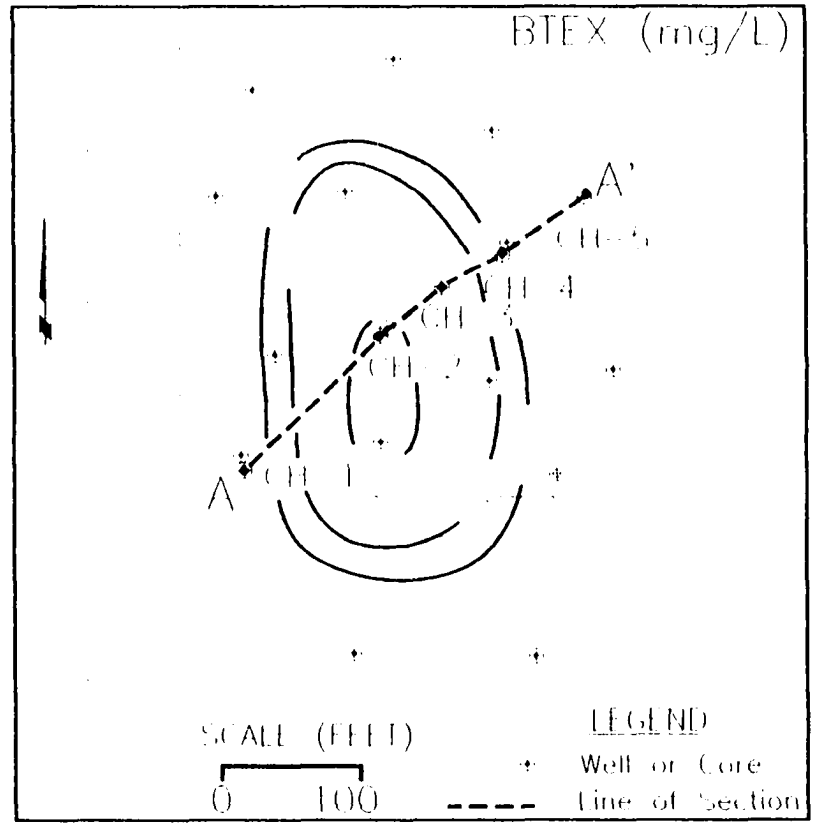

Figure 27. Total dissolved BTEX in ground water in mg/L.

and at the bottom of the boring and evaluated for BTEX and TPH by EPA Methods 8020 and 8015 (SW-846, 1990).

Water samples were collected from the monitoring wells and core holes for Fe^{2+}, Fe^{3+}, and HS^- analyses. These ions are unstable and must be measured as quickly as possible so these water samples were filtered and analyzed in the laboratory only a few hours after collection. Fe^{2+} and total Fe were determined with a HACH DR2100 spectrophotometer using 1,10 Phenanthroline and 3-(2-pyridyl)-5, 6-bis (4-phenlsulfonic acid)-1,2,4-triazine, monosodium salt (FerroZine) (Stookey, 1970; Eaton et al., 1995). Sulfide (S^{2-}) was also evaluated spectrophotometrically using the methylene blue technique (Eaton et al., 1995).

5.4. Mineral Sample Collection and Analysis

Twenty-eight sediment samples were collected from the core holes for Fe and S mineral analysis in or just above the Garber sandstone. These samples were preserved under N_2 in the field and analyzed for AVS, CrES, 6N HCl bulk Fe^{2+} and Fe^{3+}, and 0.5 N HCl readily extractable "bioavailable" Fe^{3+} and "biogenically produced" Fe^{2+} using the methods described in Chapter 4.

5.5. Results and Analyses

5.5.1. Hydrocarbon Distribution

The spill source was the underground tanks and lines once located near CH-2. Tanks and contaminated soils had been removed prior to this investigation. At the time of sampling, the released fuel at this site was in a dissolved phase; there was no significant amount of hydrocarbons detected in any soil sample. The dissolved phase BTEX plume is shown on Figure 27. Along the core holes, concentrations of BTEX are highest at CH-2 (10.6 mg/L), near the source area, and decrease to nondetectable levels between CH-4 and CH-5.

5.5.2. Site Geology

Sediment lithology was determined by core examination along the line of section A to A'. Unconsolidated creek alluvium extended from the surface to approximately 4 m deep. This unit consisted of reddish brown clayey silt and silty clays with thin lenses of reddish brown clayey gravel near the base of the section. The bedrock (Garber Formation) has a 1.22 m (4 foot) siltstone lens at CH-1 and a well cemented sandstone lens at CH-4 and CH-5 (Figure 28). Elsewhere, the bedrock consists of red, fine grained, very poorly cemented sandstone. The water table is in the Garber Formation at approximately 4.57 m (15 feet) below the surface. Ground water flow is towards the northeast.

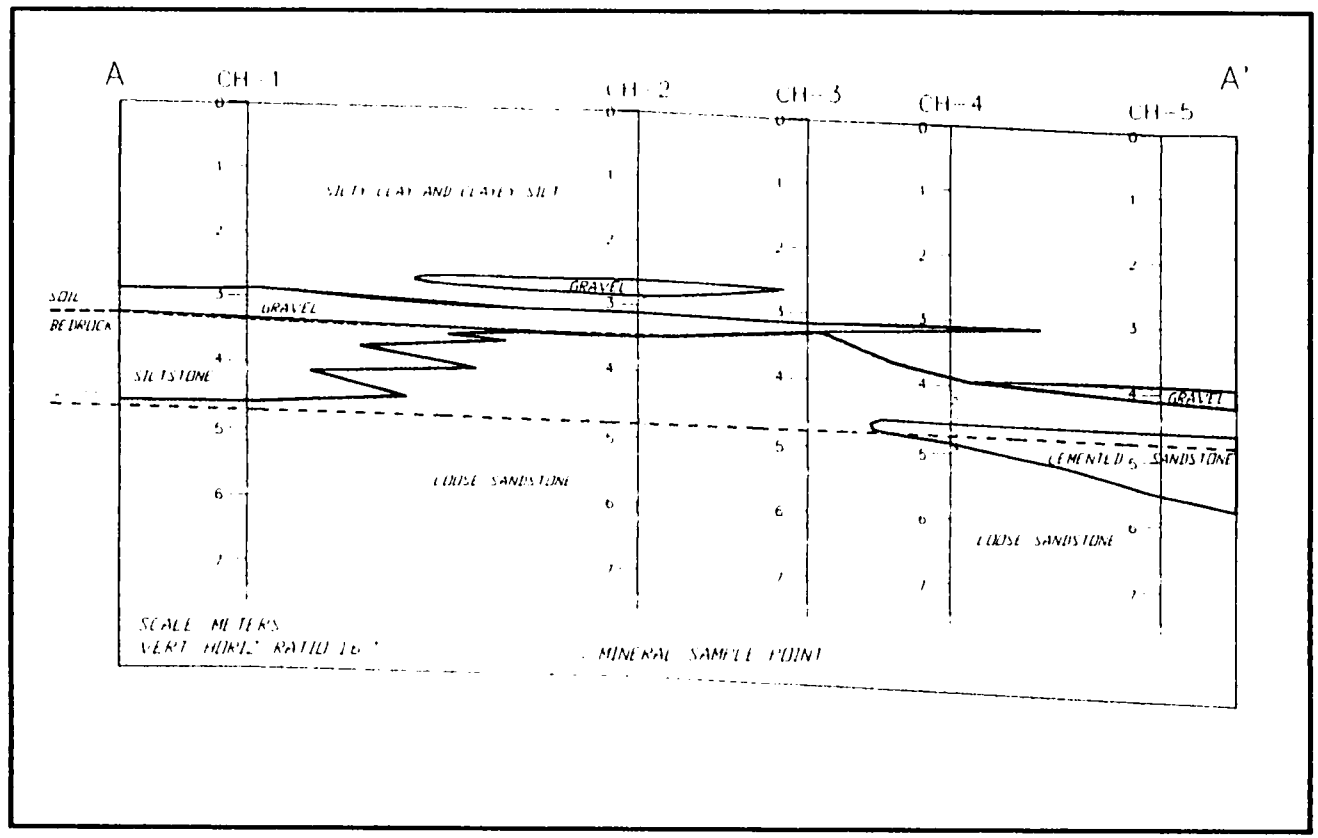

Figure 28. Structural cross-section from A to A' showing site lithology.

5.5.3. Dissolved Phase Intrinsic Bioremediation Indicators

Dissolved O_2, NO_3^-, and SO_4^{2-} concentrations show good evidence that intrinsic bioremediation processes have been active. The background concentrations of dissolved O_2 (~5 ppm) and NO_3^- (~6 ppm) are reduced to ~0.2 ppm and <0.05 respectively in the hydrocarbon plume (Figures 29 and 30). Similarly, background sulfate (~14 ppm) is reduced to <5.0 ppm (Figure 31). Although Fe^{3+} and SO_4^{2-} reduction is evident at this site, only small concentrations of dissolved Fe^{2+} (< 0.08 mg/L), Fe^{3+} (< 0.02 mg/L), and S^- (< 0.023 mg/L) were found.

5.5.4. 6N HCl Extractable Iron

Total mineral Fe^{3+}, from the 6N HCl extraction, shows that iron is a large fraction of the sediment, up to 1.3% (13,000 mg/Kg) by dry weight, which is consistent with concentrations found in the Garber formation by Parkhurst et al. (1993). Less than 10% of the total Fe extracted with 6N HCl was Fe^{2+}. The distribution of total 6N extractable Fe^{2+} and Fe^{3+} shows no discernible pattern and probably represents heterogeneity from primary sedimentation and other mostly nonbiological diagenetic processes (Figure 32 and 33). Because the strong 6N HCl extracts all of the biological and most of the background Fe^{3+} and

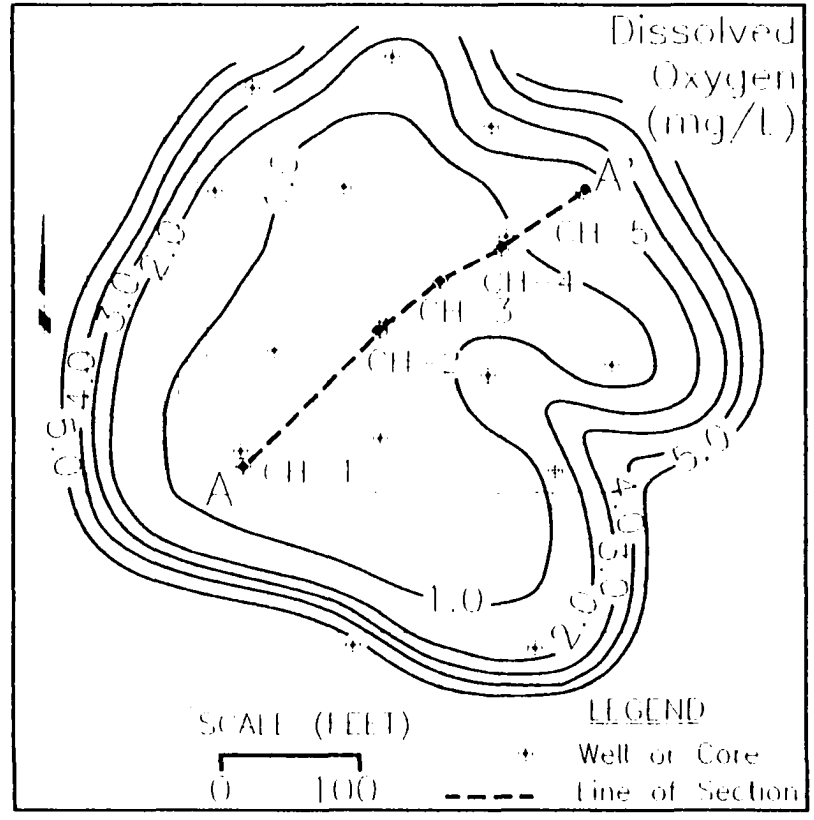

Figure 29. Total dissolved oxygen in ground water.

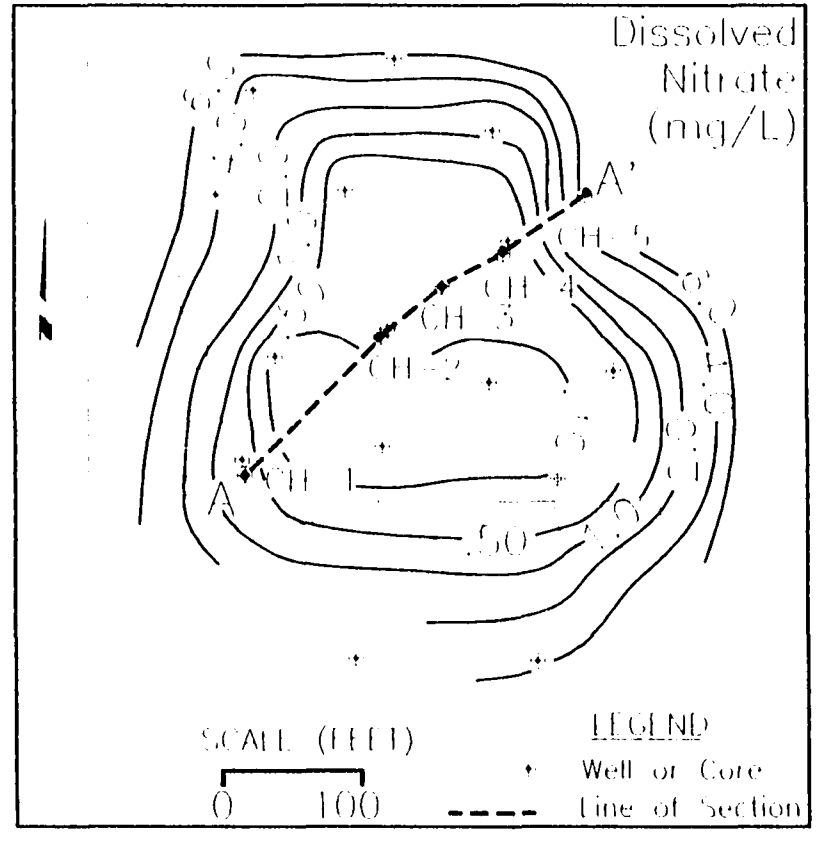

Figure 30. Total dissolved nitrate in ground water in mg/L.

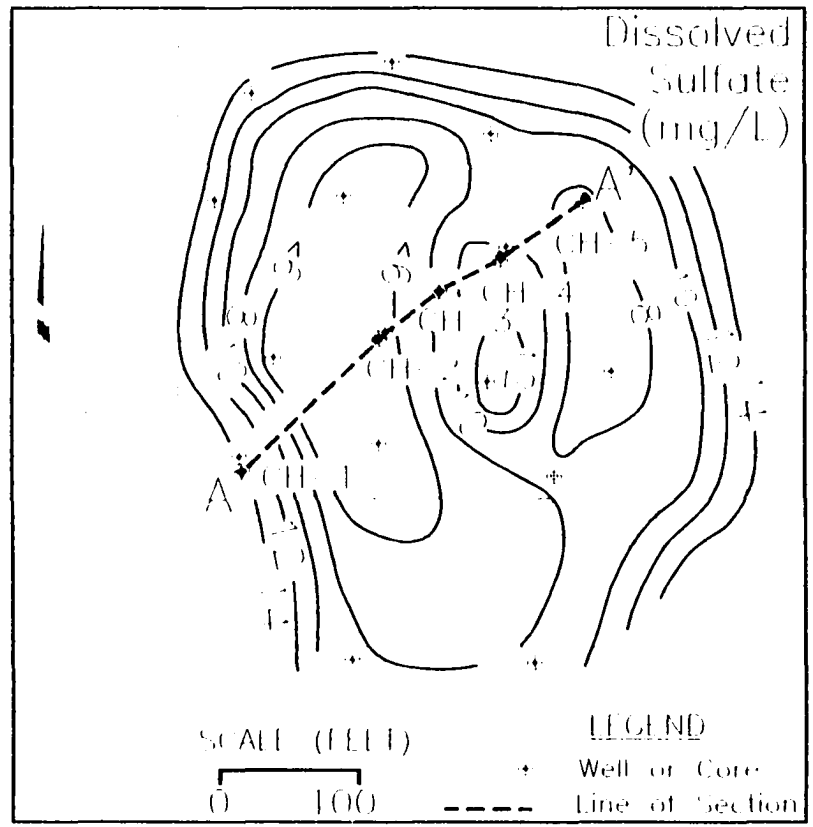

Figure 31. Total dissolved sulfate in ground water in mg/L.

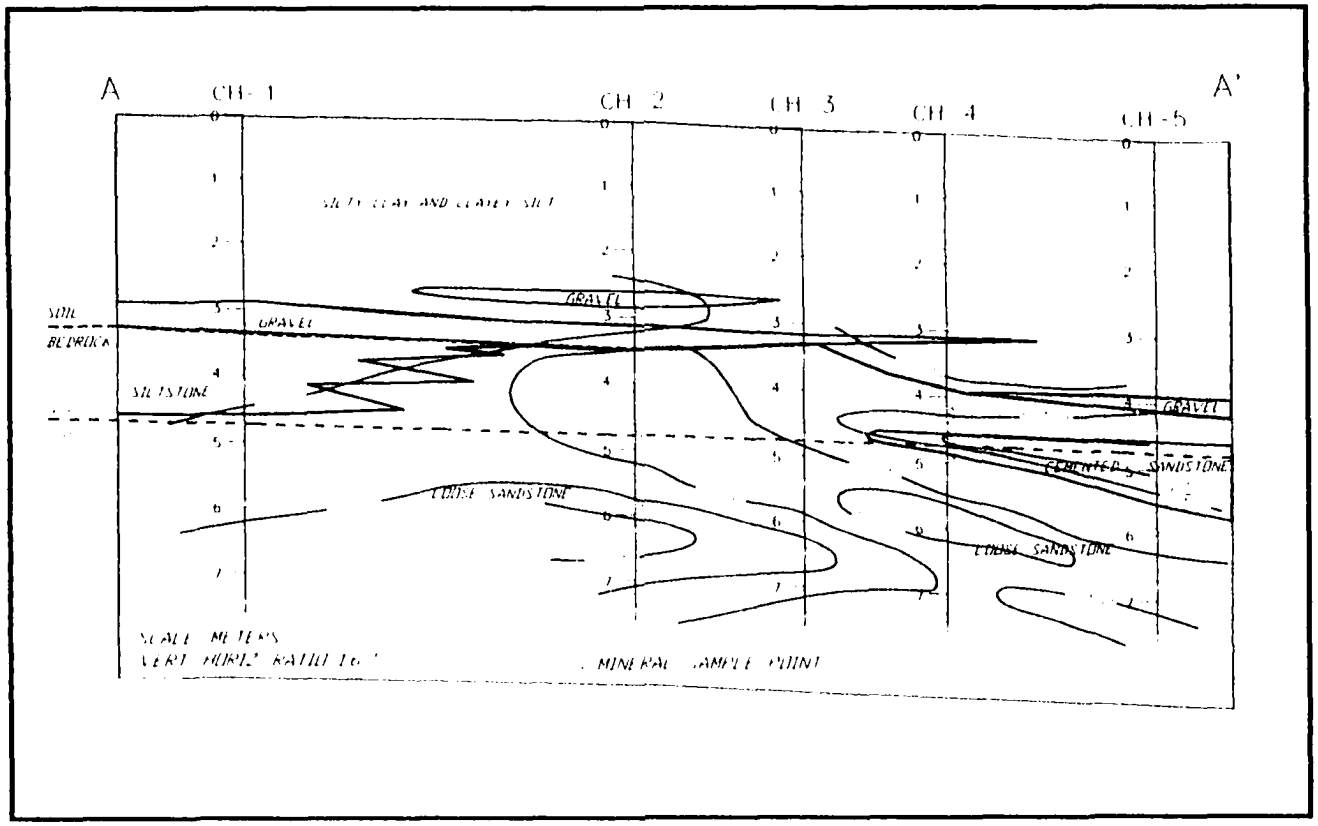

Figure 32. Cross-section A to A' showing distribution of total mineral Fe^{3+} in % or 10,000 mg/Kg units from 6N HCl extraction.

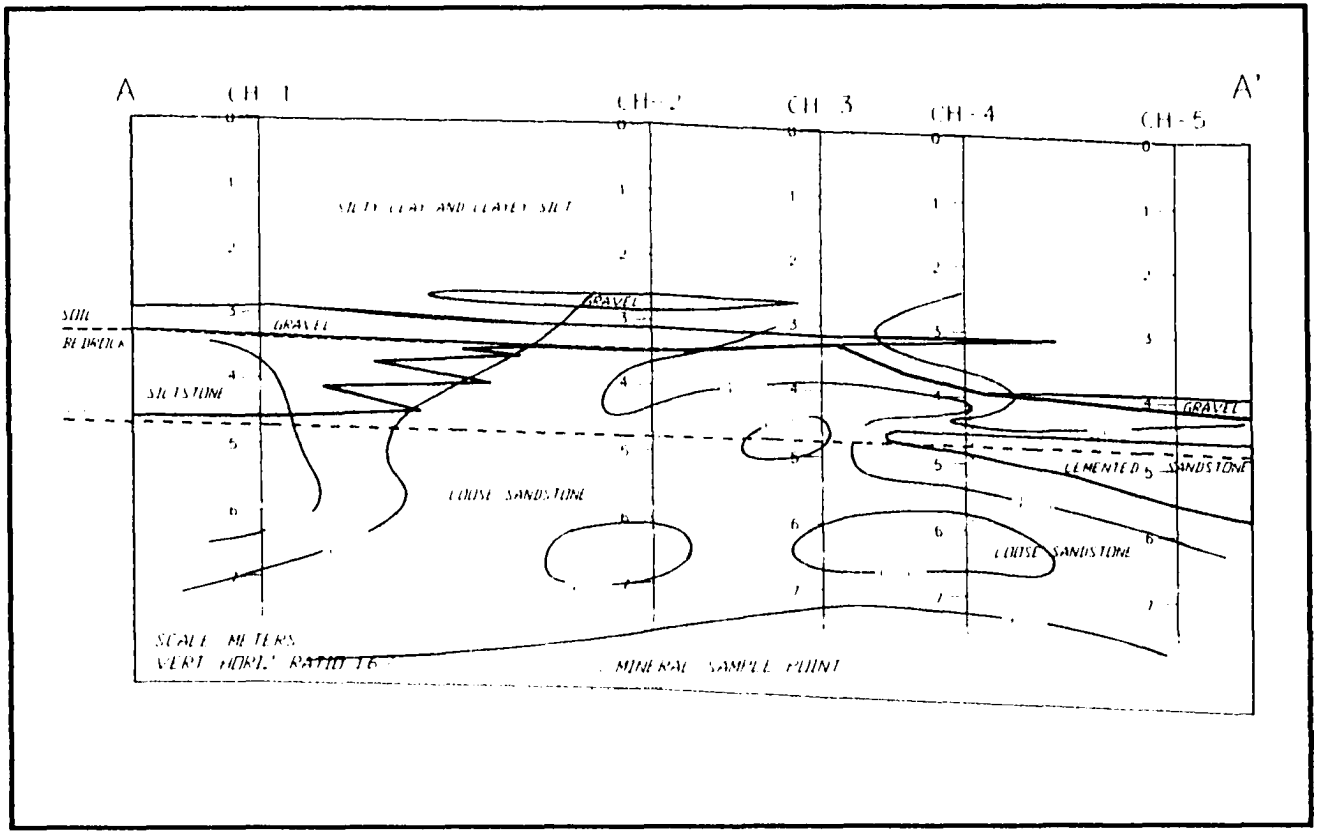

Figure 33. Cross-section A to A' showing distribution of total mineral Fe^{2+} in mg/Kg from 6 N HCl extraction.

Fe^{2+}, it fails to isolate the small iron fraction involved in microbiological oxidation/reduction reactions alone.

5.5.5. 0.5 N Extractable Iron

The total Fe extracted by 0.5 N HCl also shows a nonuniform distribution, which may be caused by depositional or nonbiological processes (Figure 34). In contrast, the 0.5 N HCl extraction shows a marked increase in Fe^{2+} towards the most contaminated portion of the aquifer, with the highest concentrations around CH-3 (Figure 35). Measured Fe^{2+} ranges from 25 mg/Kg away from the contaminated area to, over 150 mg/Kg near the source. As shown below, some of this Fe^{2+} is associated with acid volatile sulfide deposition and may have been produced from either enzymatic or indirect abiotic reduction (reaction with HS^-) processes. The majority of the Fe^{2+}, however, is in areas where no AVS is present and, therefore, appears to be from direct enzymatic reduction. Most of the produced Fe^{2+} is not associated with iron sulfides, inferring that siderite or other Fe^{2+} minerals are the dominant forms.

The distribution of the 0.5 N HCl extractable Fe^{3+} is largely the inverse of the Fe^{2+} fraction (Figure 36). Concentrations of this Fe^{3+} in non-contaminated areas are >200 mg/Kg, but largely absent in the most contaminated portions of the aquifer. This observation suggests that subjecting this sediment to 0.5 N HCl for 48 hours is a reasonable for approximating the biologically available Fe^{3+} fraction.

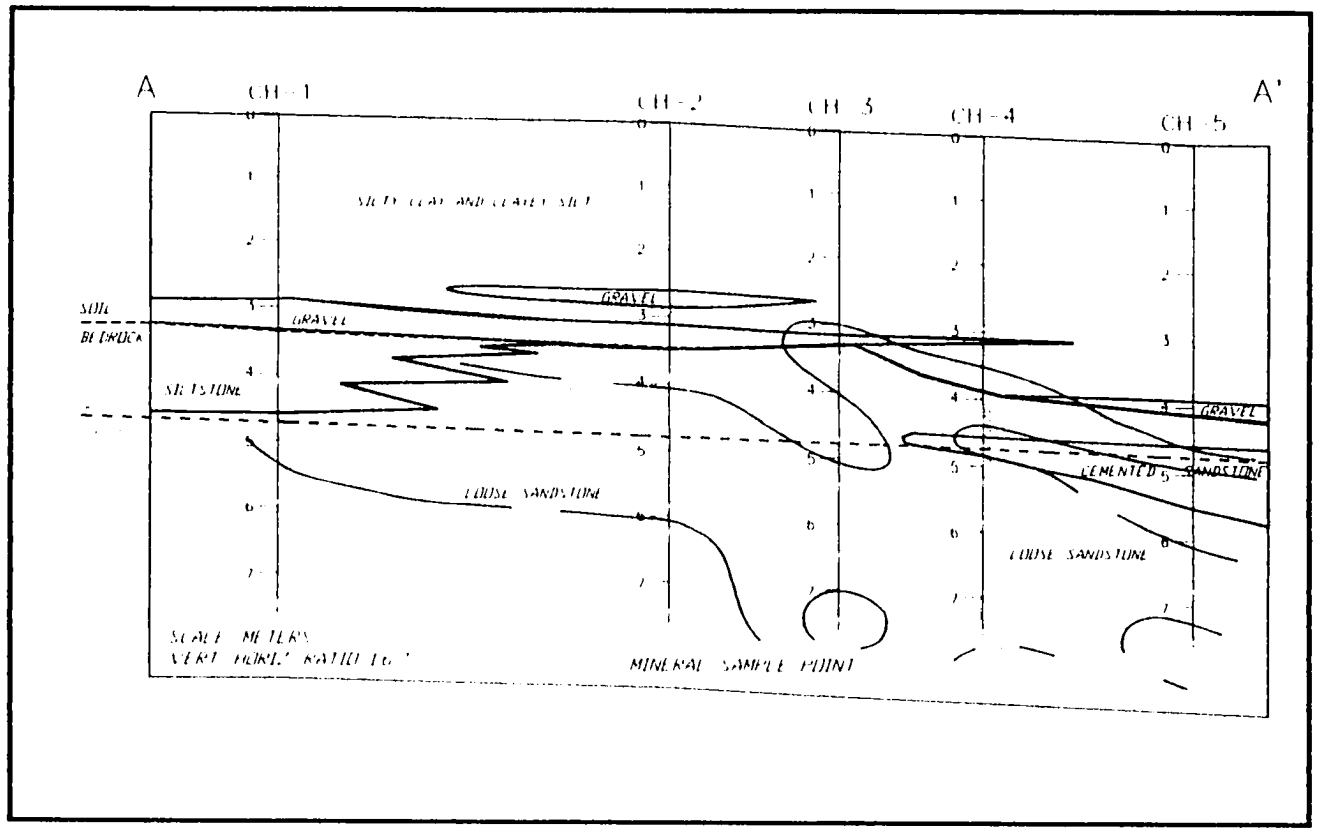

Figure 34. Cross-section A to A' showing distribution of 0.5 N HCl total Fe in mg/Kg.

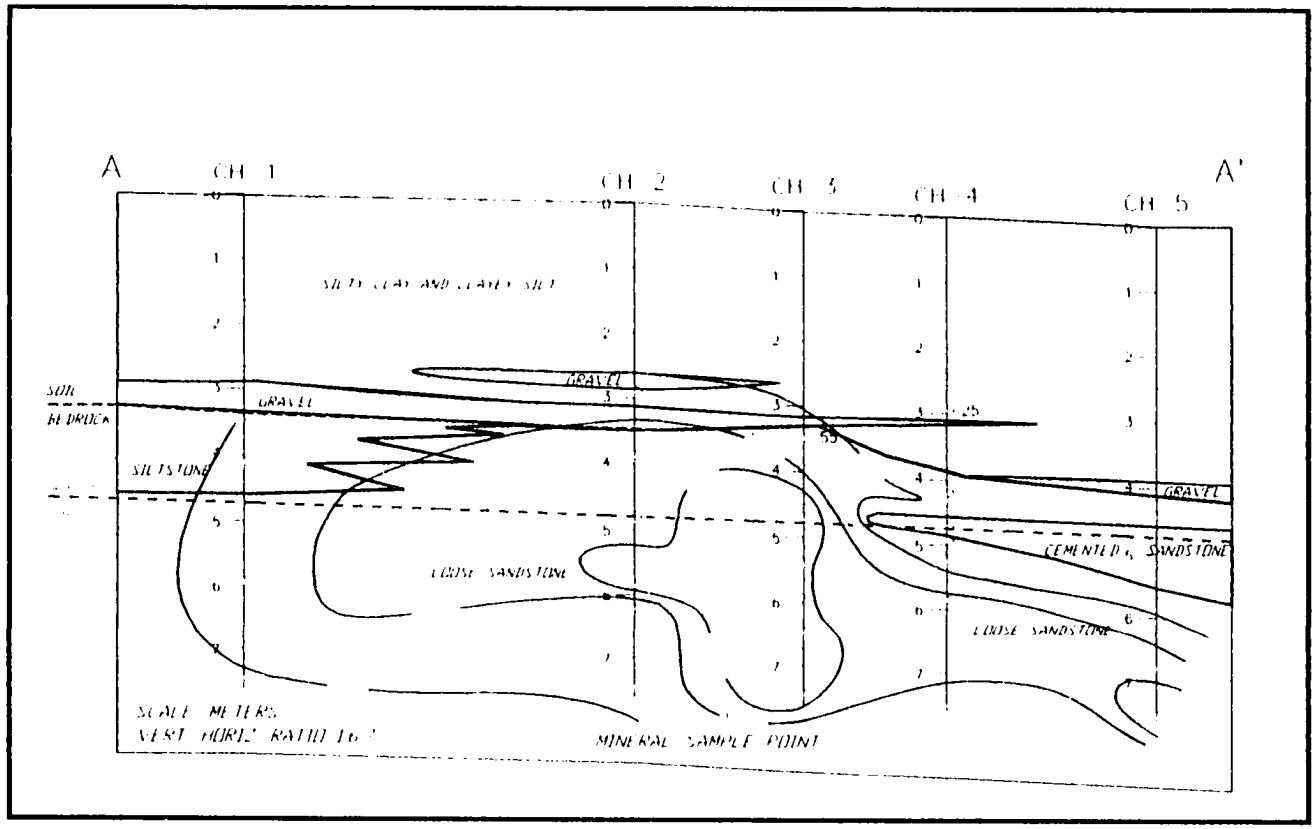

Figure 35. Cross-section A to A' showing distribution of 0.5 N HCl Fe^{2+} in mg/Kg.

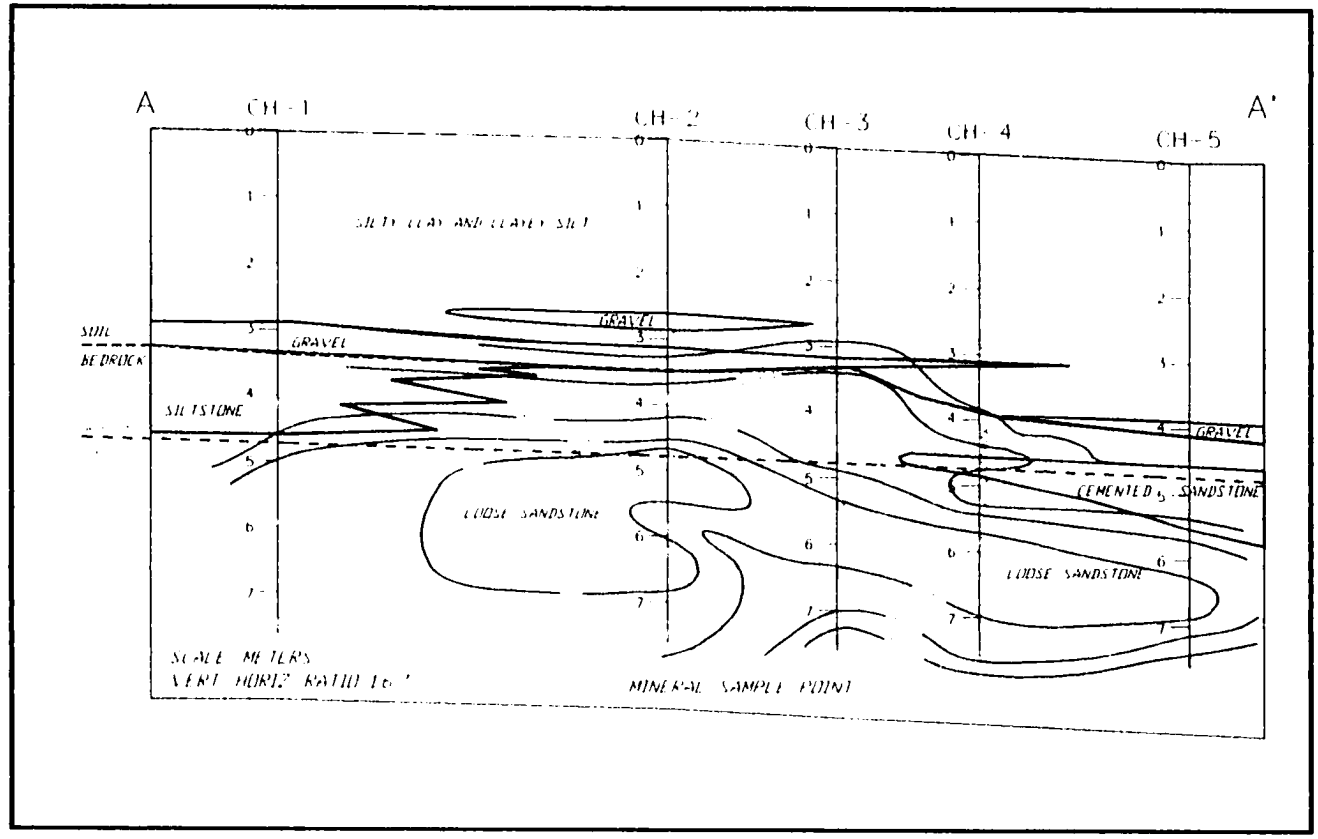

Figure 36. Cross-section A to A' showing distribution of 0.5 N HCl Fe^{3+} in mg/Kg.

5.5.6. Mineral Sulfide Analyses

The distributions of acid volatile sulfides (AVS) and chromium extractable sulfides (CrES) are shown on Figures 37 and 38. Marked increases in both AVS and CrES are found near the center of the hydrocarbon plume, mostly at CH-2 with lesser amounts at CH-3. This observation correlates with the depletion of dissolved SO_4^{2-}, which also indicates that SO_4^{2-} reduction is still operative. The fact that little dissolved HS^- was found in the ground water infers that mineral iron sulfides precipitated near the site of SO_4^{2-} reduction with little transport of HS^- from the site of origin. The presence of AVS suggests SO_4^{2-} reduction was ongoing or recently operative.

5.6. Summary of Redox Zone Development

Aqueous analyses show that O_2 and NO_3^- reductive processes dominate at the most upgradient, leading edge of the plume at (CH-1). Based on mineral sulfide data, SO_4^{2-} reduction occurred at CH-2 and to a lesser degree at CH-3. Inspection of 0.5 N HCl extraction data indicates that Fe^{3+} reduction mostly occurred at CH-3, but also occurs at CH-4 and CH-5. Water analyses alone give no indication that Fe^{3+} reduction took place at all in this system because aqueous Fe^{2+} is very low. Mineral analyses were helpful in establishing microbial redox patterns at this site.

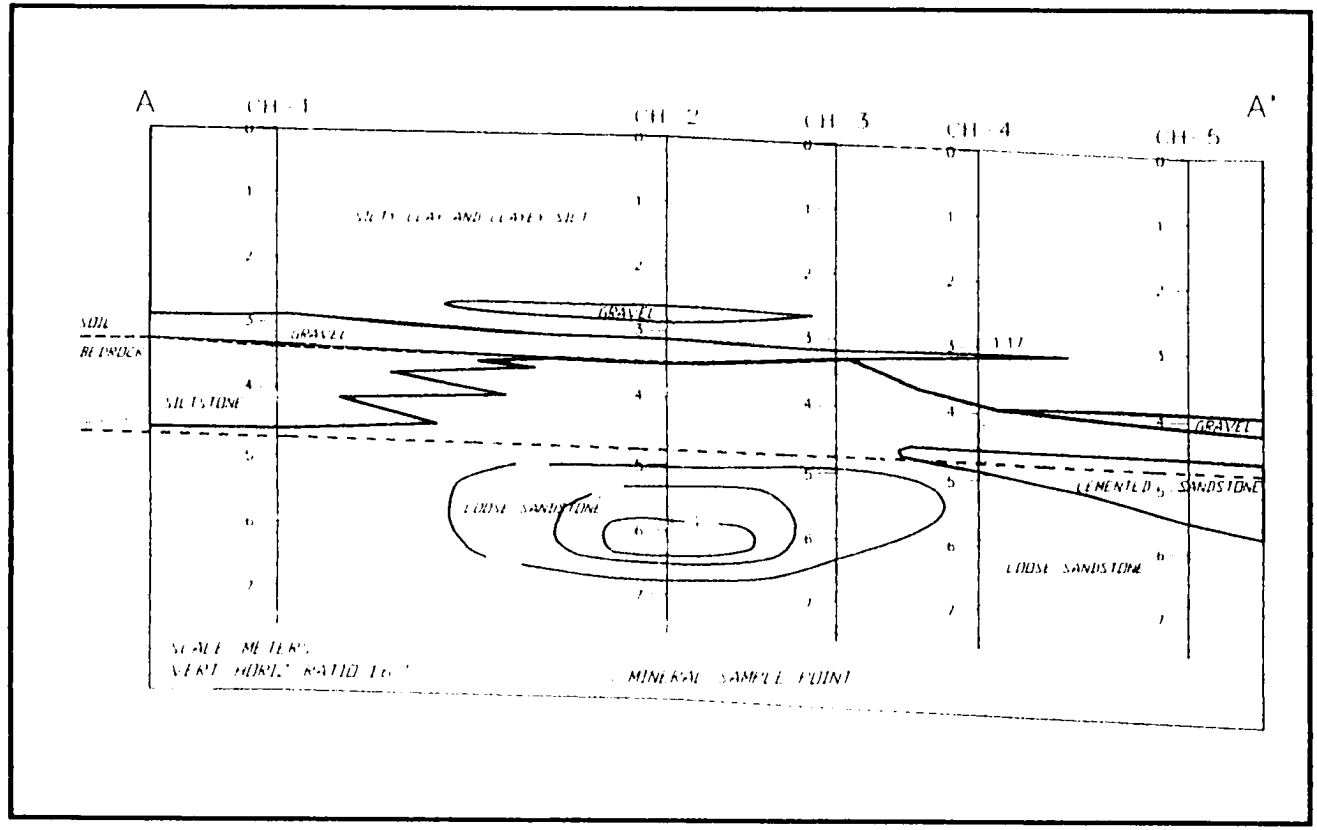

Figure 37. Cross-section A to A' showing distribution of AVS in mg/Kg.

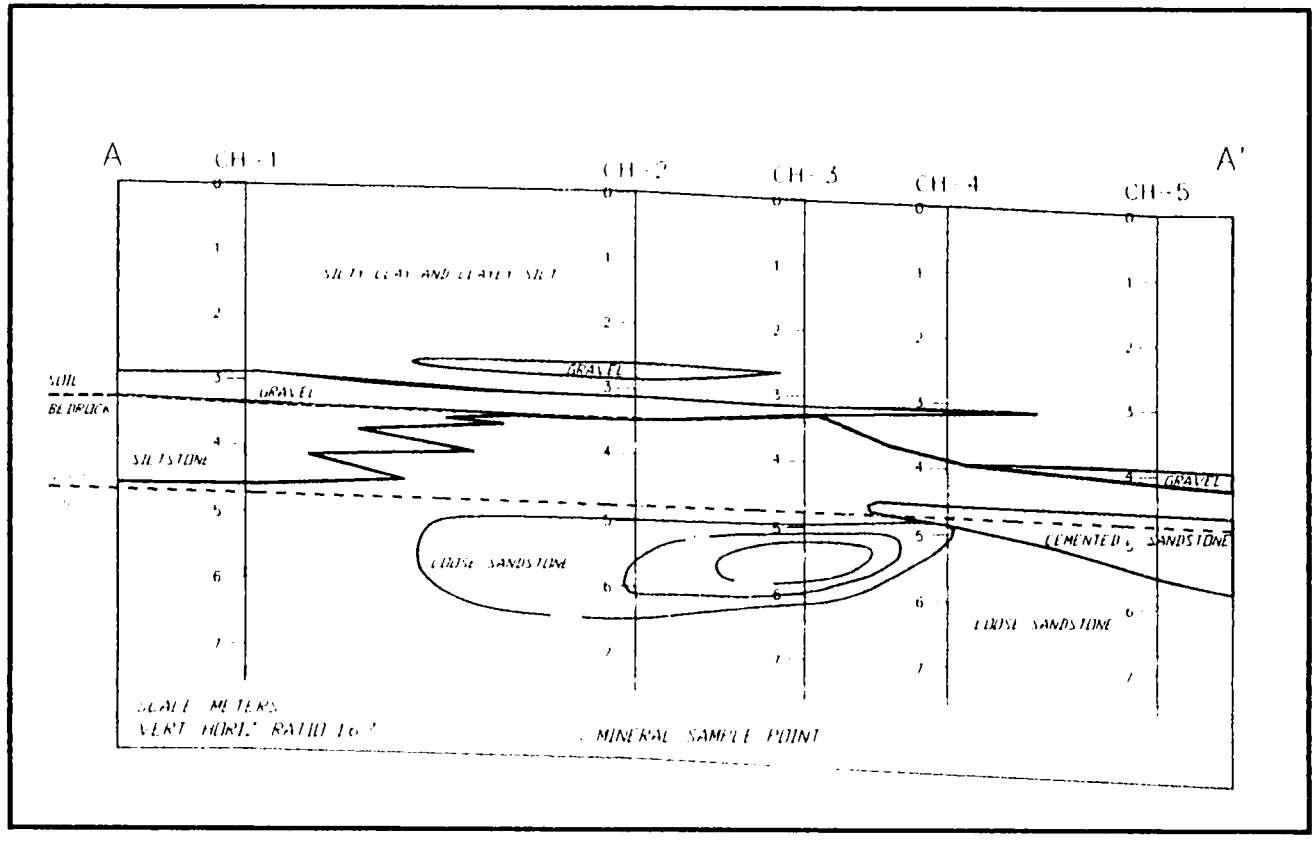

Figure 38. Cross-section A to A' showing distribution of CrES in mg/Kg.

5.7. Natural Attenuation Application

Quantifying both the solid and aqueous electron acceptor/respiratory product distribution can permit an enhanced assessment of natural attenuation. As will be shown here, inclusion of Fe and S mineral data may be used to improve estimates of expressed and assimilative capacity. Further, the spatial distribution of reduced Fe and S minerals may delineate historical intrinsic bioremediation processes.

One goal in intrinsic bioremediation is to demonstrate the degree to which organic contaminants have been degraded in the past. In a closed system, the moles of oxidized organic can be equated to the moles of reduced electron acceptors. In an open aquifer system, however, this approach is less accurate because many of the reduced products of biological respiration are transient. This is especially true of O_2 and NO_3^- reduction, for which the respiratory products are gases (CO_2 and N_2) and water, which may be transient and cannot be easily distinguished from other sources. In contrast, SO_4^{2-} and Fe^{3+} reductive processes often result in the generation of reduced insoluble mineral species that are primarily trapped in the aquifer system near the point of formation. Reduced mineral species may better represent cumulative microbial reduction and incorporate effects of advective and/or diffusive fluxes through the aquifer. For both dissolved and solid electron acceptor analyses, this approach is conservative because it does not consider biotransformation of fuel contaminants into cell mass or other metabolic products.

As developed here, both assimilative and expressed capacity are described in terms of hydrocarbon mass required to balance a specified amount of electron acceptor according to chemical stoichiometry. The "average" hydrocarbon composition used here was based on toluene (C_7H_8). Toluene, is a seven carbon compound (C7) and represents a reasonable average carbon form considering both the C5 to C12 range typically quantified in total petroleum hydrocarbon and the C6 to C8 composition for BTEX. The electron acceptor stoichiometry used is:

Oxygen:

(25) $C_7H_8 + 9O_2 \rightarrow 7CO_2 + 4H_2O$

Nitrate Reduction:

(26) $C_7H_8 + 7.2NO_3^- + 7.2H^+ \rightarrow 7CO_2 + 3.6N_2 + 7.6H_2O$

Iron Reduction (Hematite)

(27) $C_7H_8 + 18Fe_2O_3 + 72H^+ \rightarrow 36Fe^{2+}\ 7CO_2 + 40H_2O$

Sulfate Reduction:

(28) $C_7H_8 + 4.5SO_4^{-2} + 9H^+ \rightarrow 4.5H_2S + 7CO_2 + 4H_2O$

The mass of reduced and oxidized acceptors and the residual hydrocarbon mass were calculated for a volume of aquifer material surrounding one square meter about each core hole. The measured concentrations for each dissolved phase constituent are assumed to represent an average value across

the exposed section of the saturated aquifer interval. As such, the calculated mass of dissolved phase O_2, NO_3^- and dissolved hydrocarbons were based on 1.52 m (5 ft) of saturated aquifer material; a thickness equivalent to the length of saturated monitoring well screen. The measured concentration of total petroleum hydrocarbons is greater than total BTEX and, to be conservative, was used for fuel mass calculations.

Fe and S mineral distributions are vertically and horizontally variable. For solid constituents, the average mineral concentrations were determined by graphical integration across the cored bedrock interval, disregarding the well-cemented sandstone layer in CH-4 and CH-5. The well-cemented sandstone layer was excluded because its low permeability impedes hydrocarbon solute transport. A theoretical unit of aquifer material is thus defined over a one meter surface area at each core hole through a specified thickness, with a matrix density of 1,876 Kg/m^3 and porosity of 30% resulting in 300 L of ground water per cubic meter.

To calculate expressed capacity for dissolved phase O_2 and NO_3^- the net change in electron acceptor concentration for each hole was first calculated by subtracting measured concentrations at each core hole from background concentrations (5 mg/L O_2 and 31 mg/L NO_3^-). Mass of hydrocarbons destroyed (expressed capacity) at each core hole was calculated as:

$$(29) \quad EC_L = \Delta C_L * H * \varphi * k$$

Where:

EC_L = Expressed capacity for aqueous electron acceptors in mg/m^2 toluene equivalent

ΔC_L = Change in concentration from background at core hole location

H = Interval thickness (1.52 m)

φ = Porosity used to calculate interval water volume converted to L/m^3 (30%), and

k = Factor to convert mg electron acceptor consumed to mg hydrocarbons, as toluene, destroyed (k = 0.319 for O_2 and 0.206 for NO_3^-).

The variable k is determined as:

(30) $k = HC_{fw}/EA_{fw} * MR$

Where:

HC_{fw} = Hydrocarbon formula weight

EA_{fw} = Electron acceptor or respiratory product formula weight, and

MR = Molar ratio of hydrocarbons to electron acceptor or reducted product (e.g. 1/9 for O_2 as per equations 25 to 28).

For SO_4^{2-} and Fe^{3+}, expressed capacity was calculated based on solid mineral extraction data. The average concentration of total mineral sulfide and Fe^{2+} was calculated across the defined bedrock interval by graphical interpolation. To be conservative, 80 mg/Kg Fe^{2+} and 1 mg/Kg S^{2-} was considered background. Therefore, only Fe^{2+} concentrations greater than 80 mg/Kg were used in mass calculations. Expressed capacity was then calculated as:

(31) $EC_s = \Delta C_s * H * P_b * k$

Where:

EC_s = Expressed capacity for solid electron acceptors in mg/M^2 toluene equivalent

ΔC_s = Average concentration of reduced electron acceptor across interval above background

P_b = Bulk density of rock (1,876 Kg/M^3)

H = Solid phase electron acceptor thickness as described above, and

k = Conversion factor for reduced electron acceptors calculated as above (k = 0.639 for S^- and 0.046 for Fe^{2+})

A similar logic was used to calculate the assimilative capacity of the aquifer. The approach calculates the amount of hydrocarbon that could be oxidized based on the remaining amount of electron acceptor. Electron acceptor mass was determined as the measured amount of electron acceptor minus the *threshold concentration* of the electron acceptor, below which bacteria apparently cannot use it. For example, the measured concentration of oxygen at CH-2 is 0.21 mg/L and sulfate reduction is occurring at CH-2. Therefore, 0.21 mg/L O_2 is assumed to be the minimum threshold concentration and no oxygen is available for reduction at this core hole location. The *available electron acceptor mass* (C_a) is equal to the measured value minus the threshold concentration. This approach was applied to O_2, NO_3^-, and SO_4^{2-}, which were assigned residual concentrations of 0.21, 0.26, and 5.0 mg/L, respectively. All of the 0.5 N HCl extractable Fe^{3+} is considered available. For dissolved O_2, NO_3^-, and SO_4^{2-}, the assimilative capacity was calculated using Equation 29, substituting C_a for ΔC_L. The assimilative capacity of Fe^{3+} was determined using Equation 31 substituting C_a for C_s.

A summary of the expressed capacity is shown in Table 7 and Figure 39. Most of the measurable expressed capacity occurred as SO_4^{2-} and Fe^{3+}. This is

Table 7. Summary of expressed capacity as toluene equivalent consumed per square meter area along transect A to A'.

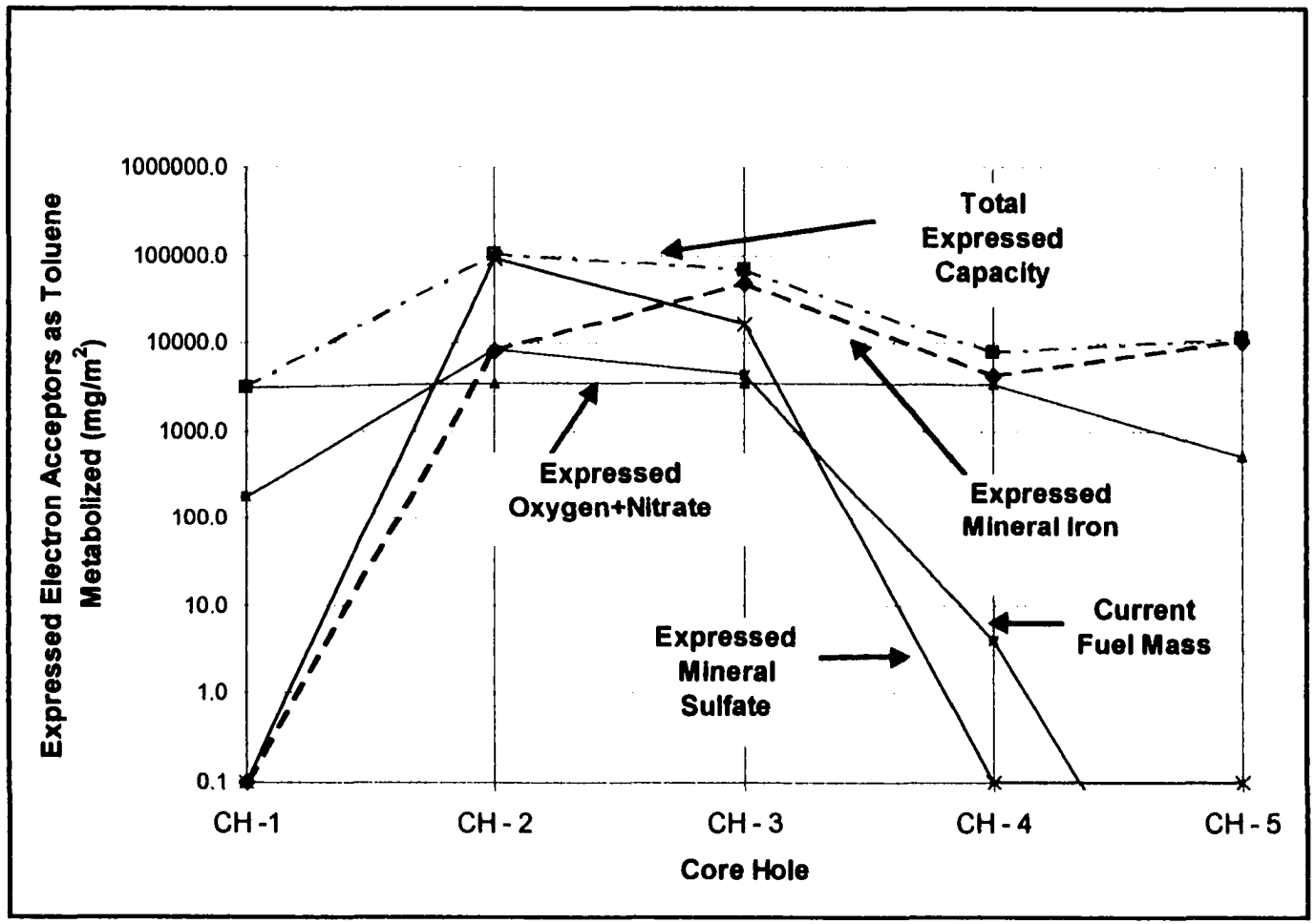

Figure 39. Calculated expressed capacity as toluene metabolized across line of section.

to be expected because the respiratory products of O_2 and NO_3^- reduction are transient in the subsurface, whereas the products of SO_4^{2-} and Fe^{3+} reduction tend to precipitate as solids that can be directly measured. Thus, the method described here will underestimate expressed and assimilative capacity associated with O_2 and NO_3^-.

With the incorporation of mineral data, expressed capacity can be determined more accurately and used to generate an index of overall biodegradation efficiency. The total amount of fuel spilled at this site is unknown; however, a portion of the original hydrocarbon mass can be estimated by adding the current hydrocarbon mass with the known destroyed hydrocarbon mass calculated from expressed capacity. An index of expressed capacity (ECI) can then be determined as:

(32) $ECI = EC/(HC + EC) * 100$

Where:

EC = Expressed assimilative capacity mass

HC = Current hydrocarbon mass

Applying Equation 32 to the study site shows that over 90% of the electron acceptor demand originally present in the spill has been expressed, suggesting that biodegradation processes have been highly effective at this site.

The distribution of 0.5 N Fe species documents that reductive processes occurred at CH-4 and CH-5, so there is expressed capacity though no

hydrocarbons were identified in that area at the time of the investigation. This indicates that the plume attained maximum size sometime in the past and is currently receding. This idea is consistent with computer modeling results that predict that the plume would have extended beyond its current position if intrinsic bioremediation were not occurring at this site.

As shown in Table 8, the assimilative capacity of the aquifer exceeds residual hydrocarbon demand though it is somewhat limited in the center of the plume at CH-2 and CH-3. In that area, the Fe^{3+} contributes the bulk of the assimilative capacity. This technique only considers a static system and ignores the effects of ground water flow-through. Additional electron acceptor capacity could be demonstrated in the up gradient portion of the hydrocarbon plume by including the contribution of soluble electron acceptor flux from ground water through-flow over time. As a result, the true effects of O_2, NO_3^-, and SO_4^{2-} on assimilative capacity are underestimated in some areas of the plume.

5.8. Application Conclusions

In many cases, natural attenuation assessment can be improved by including an evaluation of Fe and S minerals with aqueous water analyses. Incorporating Fe and S mineral analyses provide a better understanding of *in-situ* biodegradation processes and give a more complete assessment of expressed and assimilative capacity. The extraction techniques described above make such mineral analyses practical enough to be included in a typical site assessment program.

Table 8. Summary of assimilative capacity expressed as oxidizable toluene per square meter along transect A to A'.

The extended sulfide extraction technique is simple to use and results in estimates of acid volatile sulfide (AVS) and chromium reducible sulfides (CrES) as well as values approximating the bulk Fe^{2+} and total Fe content of the sediment. The ability to distinguish between sulfide mineral species can be important because the presence of AVS may indicate recent or ongoing SO_4^{2-} reduction.

The 0.5 N HCl acid extraction is recommended for discerning both the available Fe^{3+} and biogenically produced Fe^{2+} mineral species. Using this technique showed an increase in Fe^{2+} with a complimentary decrease in Fe^{3+} towards the most contaminated areas at this site. The distribution of 0.5 N Fe species inferred that reductive processes occurred as far down gradient as CH-5, though there was no measured hydrocarbons or aqueous Fe^{2+} in that area at the time of sampling. This suggests that the plume attained maximum size sometime in the past and is currently receding. This type of observation could further support natural attenuation as an option to engineered remediation at other sites where mineral Fe and S analysis are conducted.

The bacterial byproducts of SO_4^{2-} and Fe^{3+} reduction tend to precipitate as solids that can be directly measured. Therefore, Fe and S mineral analyses can facilitate good estimates of expressed capacity for Fe^{3+} and SO_4^{2-} reduction. In conjunction with aqueous electron acceptor analyses, such data can be used to demonstrate the effectiveness of intrinsic bioremediation processes.

This is the first study that documents the relative importance of Fe and S mineral analysis to intrinsic bioremediation assessment. The concepts presented here should aid in demonstrating the efficacy of intrinsic bioremediation at fuel contaminated sites and may provide valuable data for RBCA assessments.

6. IRON AND SULFUR MICROCOSM EXPERIMENTATION

6.1. Purpose

As described in Chapter 2, there are approximately 3,000 municipal solid waste landfills in use in the United States alone (Goldstein, 1997) and many closed landfills. Some of these landfills, particularly the older, unlined ones, have released leachate to soil/ground water. Though microbial O_2 and NO_3^- respiration are thermodynamically favorable, naturally occurring concentrations of O_2 and NO_3^- are usually low in ground water. The addition of oxygen to facilitate organic degradation is well established in wastewater engineering and has also had application to subsurface remediation, e.g. air sparging or bioventing (Norris et al., 1993; and Horan, 1990). In theory, the addition of alternative electron acceptors (NO_3^-, SO_4^{2-}, or Fe^{3+}) could also enhance organic contaminant removal.

In contrast to O_2 and NO_3^-, comparatively large amounts of solid Fe^{3+} and dissolved SO_4^{2-} can occur naturally, suggesting a dominant role in intrinsic bioremediation in some cases. Both Fe^{3+} and SO_4^{2-} are found in solid mineral forms (natural or synthetic) which could, in theory, be provided as amendments to stimulate in-situ bioremediation of organic contaminants in an engineered treatment system. Beeman and Suflita (1990) and Suflita et al. (1992) suggest that gypsum wallboard from demolition debris incorporated in landfill waste serves as a source of usable SO_4^{2-}. Therefore, the possibility exists to use construction debris in an engineered leachate treatment system.

Four potential types of engineered systems using Fe^{3+} and gypsum are envisioned. Application could be in the form of a reactive wall or flow-through trench similar to the funnel and gate system proposed by Starr and Cherry (1994) and those currently being researched for chlorinated hydrocarbons and Cr(VI) abatement (Puls, 1997). For shallow ground water aquifers, a trench could be excavated across the path of an organic plume and back-filled with porous media amended with Fe^{3+} and/or SO_4^{2-} rich material. For deeper aquifers, a series of closely spaced borings could be used. Similarly, Fe^{3+} and/or SO_4^{2-} could be added to interceptor trench/barrier wall designs already used to passively control landfill gas migration (Tchobanoglous et. al., 1993). These minerals could also be incorporated in either landfill waste, liners, or drainage layers (Kennedy and Everett, 1996). Finally, mineral Fe^{3+} and/or SO_4^{2-} could be employed as the basis for an ex-situ anaerobic reactor system. Sources of solid Fe^{3+} and SO_4^{2-} could potentially come from synthetic or naturally occurring mineral forms that were evaluated in this study.

The interaction of landfill leachate with sediment and the development of redox zones has been observed in field studies (Heron and Christensen, 1995; Bjerg et al., 1995). Laboratory column studies examining leachate or lactate and native sediments have also been conducted (Furrer et al., 1996; Hoeks and Borst, 1981; and Kjeldsen and Christensen, 1984). Albrechtsen et al. (1994) and Gurljala and Suflita (1993) conducted microcosm studies showing that leachate degradation occurs from Fe^{3+} and SO_4^{2-} reduction.

This study is unique in that it examines the relative effects of adding solid Fe^{3+} or SO_4^{2-} minerals compared to nonamended systems. It also tracks aqueous, gaseous, and solid reactants and products. This research was predominantly concerned with:

- Testing the hypothesis that the addition of mineral Fe^{3+} and SO_4^{2-} can potentially be of benefit in controlling problems associated with landfill leachate, and
- Using these experimental results to enhance the overall understanding of Fe and S microbial/mineral interactions, which may occur naturally, or by design, near landfills.

To address these goals a microcosm experiment was developed. As described below, a series of microcosms were constructed with two different oxidized sediment types. Some microcosms were amended with mineral sources of Fe^{3+} and SO_4^{2-}. A synthetic leachate was used as a source of carbon.

6.2. Methods

6.2.1. Microcosm Construction

Two different native sediments were used as microcosm media; Quaternary alluvial sand (Qal) from the South Canadian River and sand from the Permian aged Garber-Wellington (Pgw) sandstone formation. Both sands were obtained from surface exposures near the City of Norman, Oklahoma. Many landfills have been constructed in these sediment types in Oklahoma and Kansas. The closed Norman Municipal Landfill was constructed on the South Canadian River alluvium. This landfill site has been designated as a USGS

Toxic Substances Site and continues to be the focus of intensive interdisciplinary study by many scientists associated with the USGS, USEPA, and several universities. The Qal sand used for this study was collected in the river valley near this landfill; the Pgw sandstone was obtained from a surface outcrop approximately 8 miles north of Norman.

Both Qal and Pgw sediments are fine to very fine grained. The Qal sand is unconsolidated and contains 1,300 mg/Kg total iron minerals (1,100 mg/Kg Fe^{3+} and 200 mg/Kg Fe^{2+}) based on the 6 N HCl extraction described in Chapter 4. This moderate amount of iron gives this sediment a light pink color. The Pgw sand was originally very poorly consolidated and was easily disaggregated by crushing. The Pgw sand contains 5,300 mg/Kg total iron consisting of 4,700 mg/Kg Fe^{3+} and 600 mg/Kg Fe^{2+}. This higher iron content gives this sediment a bright red color. A mild acid (0.5 N HCl) extraction, as described in Chapter 4, obtained 247 mg/Kg total Fe of which 85 mg/Kg was Fe^{2+} from the Qal sand and 230 mg/Kg Fe total of which 34.6 mg/Kg was Fe^{2+} from the Pgw sand. These sediments were dried at room temperature for approximately two weeks prior to use and sieved to remove any large particles.

In addition to any native iron mineral species naturally present in the sediment, sources of solid SO_4^{2-} and Fe^{3+} were added to some microcosms. Sulfate was added as reagent grade gypsum ($CaSO_4 \bullet 2H_20$). Iron (III) was added as $Fe(OH)_3$ prepared by adjusting the pH of a 0.4 N FeCl solution to pH 7 with 4N NaOH as described by Roden and Zachara (1996). The resulting iron

jell was repeatedly washed then dried for approximately 3 days at 60 C^{o}, crushed, and sieved (100 μm).

A synthetic leachate solution was developed by averaging the major organic species found to comprise landfill leachates described by Baedecker and Back (1979); Hoeks and Borst (1982); and Kjeldsen and Christensen (1994) as shown on Table 1. A 2,000 mg/L total non purgable organic carbon (NPOC) solution was made comprised of 29% acetic, 12% propionic, 29% butyric, 12% valeric, and 18% caproic acid by carbon mass. These fatty acids (stench acids) range from two to five carbon atoms respectively. The following pH buffers and nutrients were added (in grams/liter): 0085 KH_2PO_4, 0.218 K_2HPO_4, 0.334 $Na_2HPO_4 \bullet 7H_2O$, 0.250 $NaHCO_3$, 0.050 NaCl, 0.075 $CaCl_2$, 0.400 NH_4Cl, 0.050 $MgCl \bullet 6H_2O$, 0.020 $MgSO_4 \bullet 7H_2O$, and 0.020 yeast extract. Also added was 10 ml/L of a micronutrient solution consisting of (in grams/liter): 0.286 H_3BO_4, 0.500 $MnCl \bullet 4H_2O$, 0.040 $CuSO_4 \bullet 5H_2O$, 0.021 $ZnSO_4 \bullet 7H_2O$, 0.041 $CoCl_2 \bullet 6H_2O$, 0.020 $NiCl_2 \bullet 6H_2O$, and 0.800 $Fe(NH_4)_2 \bullet (SO_4)_2 \bullet 6H_2O$. This solution was prepared anoxically by first boiling n-pure H_2O for 45 minutes while sparging with N_2. This solution was anoxically sealed and transferred to an anaerobic glovebox containing a N_2 atmosphere.

Bacterial seed was obtained by collecting sediment from the capillary fringe area, approximately 0.6 m below the surface, near the contaminated toe of the closed Norman Landfill. As described above, field studies showed increased solid mineral Fe^{2+} and iron sulfides (~FeS and FeS_2) at the collection depth, indicating the presence of iron and sulfate reducing bacteria. This native sand

crossed a transition zone that was visually faint pink, indicating possible Fe^{3+} reduction (gleying), grading to a light gray color with a slight H_2S odor, indicating a zone of SO_4^{2-} reduction. This sediment was placed in an anaerobic glovebox shortly after collection and used within two days.

To assure that methanogenic, SO_4^{2-} and Fe^{3+} reducing bacteria were present, an initial set of microcosms was prepared. This set used only Qal sand (100 g dry weight per microcosm) amended with either 0.424 g $Fe(OH)^{3+}$ or 0.114 g $CaSO_4 \bullet 2H_2O$. Serum bottles (160 ml volume) were filled with sediment and placed in an anaerobic glove box (N_2 atmosphere), for 24 hours prior to use. To each microcosm, 22 ml synthetic leachate and 5 g of natural bacterial seed sediment were added and thoroughly mixed. Each microcosm was sealed using butyl rubber stoppers and crimped. These microcosms were monitored for six weeks, using the techniques described below, to verify SO_4^{2-} and Fe^{3+} reduction as well as methanogenesis. At that time, sediment from the SO_4^{2-} and Fe^{3+} added microcosms was mixed in equal parts and transferred (5 g) as seed material for the primary microcosm set discussed in this paper.

The primary microcosm set used 85 g of Pgw or 100 g Qal sediment per microcosm. The amount of leachate to be added was sufficient to just cover the top of the sediment in each bottle. The variation in sediment mass between Qal and Pgw microcosms was needed so that equal volumes (equal carbon mass) of leachate solution could be added to microcosms of each sand type, necessitated by porosity differences between the two sediments. The following microcosm types were prepared:

1) Qal + 0.310 g $CaSO_4 \bullet 2H_2O$;

2) Qal + 1.5 g $Fe(OH)_3$;

3) Qal with no added mineral electron acceptors;

4) Pgw + 0.310 g $CaSO_4 \bullet 2H_2O$;

5) Pgw with no added mineral electron acceptors; and

6) Qal and Pgw killed controls as described below.

The amount of Fe and S minerals added provided sufficient oxidative capacity to oxidize 95% of the added organic carbon. This calculation excludes assimilative (anabolic) carbon utilization.

These microcosm sets can be used to compare natural, nonamended sediment processes with sediment amended with Fe^{3+} and SO_4^{2-} minerals. Natural Qal sediment, Qal with added gypsum, and Qal with added $Fe(OH)_3$ are referred to respectively as Qal Nat., Qal+SO_4^{2-}, and Qal+Fe^{3+}. Similarly, unamended and gypsum added Pgw microcosms are referred to as Pgw Nat. and Pgw+SO_4^{2-}.

As with the seed microcosms, mineral mixtures were added to dry sand, then all microcosms were placed in an anaerobic glove box (N_2 atmosphere), for 24 hours. To each microcosm, 22-ml synthetic leachate was added along with a 5 g mixture of sand from the bacterial seed microcosms. All microcosms were incubated in the dark at 23 C^o.

6.2.2. Analytical Methods

For each sampling event, microbially important headspace gases, dissolved organics, dissolved ions, and mineral species were measured. Samples were generally measured in triplicate lots by sacrificing three microcosms of each type per sampling event; however, some samples were only measured in duplicate lots.

Headspace Gas: The gas phases of interest include CO_2, H_2S, and CH_4. These were measured from microcosm headspace gas by direct injection using an HP gas chromatograph with thermal conductivity/flame ionizing detector.

Sulfate Analysis: Before sampling, the sediment in a serum bottle was initially homogenized by mixing under an N_2 atmosphere. Between 3 to 4 g sediment was extracted and placed inside N_2 purged serum bottles to which between 25 and 75 ml deoxygenated deionized water was added. These bottles were sealed, shaken for two hours to solublize gypsum, filtered through a 0.45 μm filter, and analyzed for SO_4 using a Dionex ion chromatograph with a conductivity detector. This procedure results in a measurement of total SO_4^{2-} originating from both aqueous and solid gypsum sources within the microcosm.

0.5 N HCl Fe Extraction: Approximate biologically available mineral Fe^{3+} and certain biogenically produced Fe^{2+} minerals were quantified using mild acid extraction as described in Chapter 4.

Strong Acid Iron Extraction and Mineral Sulfide Analysis: AVS and CrES minerals and bulk Fe^{2+} and Fe total were extracted using analysis techniques described in Chapter 4.

Aqueous NPOC, Fe^{2+}, Fe total, and S^-

Following the procedures above, the remaining water and sediment in each microcosm was tared. To increase fluid volume, 50 ml deoxygenated, deionized water was added to each while maintaining an N_2 atmosphere. These bottles were shaken for fifteen minutes on a shaker table then filtered through a 0.45 μm filter. Aliquots of liquid were acidified to pH<3 to preserve dissolved Fe^{2+}/Fe ratios until spectrophotometrically analyzed as above. Dissolved S^- was not preserved but was immediately analyzed spectrophotometrically. The remaining unpreserved sample was evaluated for non-purgable organic carbon (NPOC) using an Astro 2100 TOC analyzer.

6.3. Killed Controls

The goal of this research is to examine differences between natural microcosm systems and those amended with Fe^{3+} and SO_4^{2-} minerals. In this respect, the natural (unamended) microcosms serve as live controls for this experiment. A limited number of killed controls, however, were prepared by adding 0.400 g HgCl to the added synthetic leachate followed by autoclaving the sealed bottles for 30 minutes. These controls included both Qal and Pgw sands

with mixtures of both $Fe(OH)_3$ and $CaSO_4 \bullet 2H_2O$ as above. These microcosms were evaluated during the 4th, 5th, and 12th weeks. Compared to the initial conditions there were no apparent changes in NPOC, headspace gases, SO_4^{2-}, or solid or aqueous Fe or S concentrations. This indicates that NPOC was not lost through abiotic processes and redox processes did not occur abiotically.

6.4. Results

Data shown in this section represent average values for each sampling event. Because multiple microcosm results are shown on each graph, error bars are omitted for clarity. Analytes for each microcosm are graphed individually with standard deviation error bars generated from the analysis of duplicate or triplicate analyses for each sample point in Appendix I.

Note that succeeding graphs show experimental results in terms of total moles generated per microcosm. Data presentation in that manner provides the most direct and accurate correlation between different microcosm groups; however, for most engineering discussions it is customary to use concentration units. Therefore, where appropriate a complimentary graph scale has been provided that expresses aqueous data in concentration units of mg/L. For analytes typically expressed in terms of mass/soil mass, a complimentary graph scale is provided in milligrams. Divide the Pgw system data by .85 g to convert the results of those microcosm sets to a mg/100 g equivalent sediment basis. As discussed above, the Qal system was based on 100 g sediment so a direct reading in terms of mg/100 g is possible for those analyses.

6.4.1. Organic Removal Rates

Figure 40 shows organic carbon (NPOC) utilization through the experiment. Overall, NPOC consumption was similar for all microcosm systems, averaging 0.35 mMol C/week, after acclimation. Organic consumption appears to follow a zero order model for the substrate concentrations observed. Variations in the final organic carbon consumed at the end of 12 weeks can be attributed to variations in growth/acclimation lag time between the systems. Short term growth rates were highest for both of the natural systems, with 1.8 mMol C/week for the Qal Nat. system during weeks 4 to 6 and 1.0 mMol C/week for the Pgw Nat. system during weeks 7 to 9. Although the Qal Nat. system experienced the fastest short-term growth, little carbon consumption occurred during weeks 6 to 10. For all microcosms it is assumed that more labile, shorter carbon chain leachate organics were initially consumed, as found by Hoeks and Borst (1982). Possibly, the period of low consumption in the Qal Nat. system was an acclimation period required to assimilate remaining longer-chain organic carbon compounds. For the other microcosms, the process of enzymatic adaptation and organic consumption appears to have occurred at a more measured pace.

As discussed below, substrate utilization can be attributed to several microbial processes. Methanogenesis dominated the natural, nonamended systems, with some Fe^{3+} reduction of native iron minerals possible. Significant

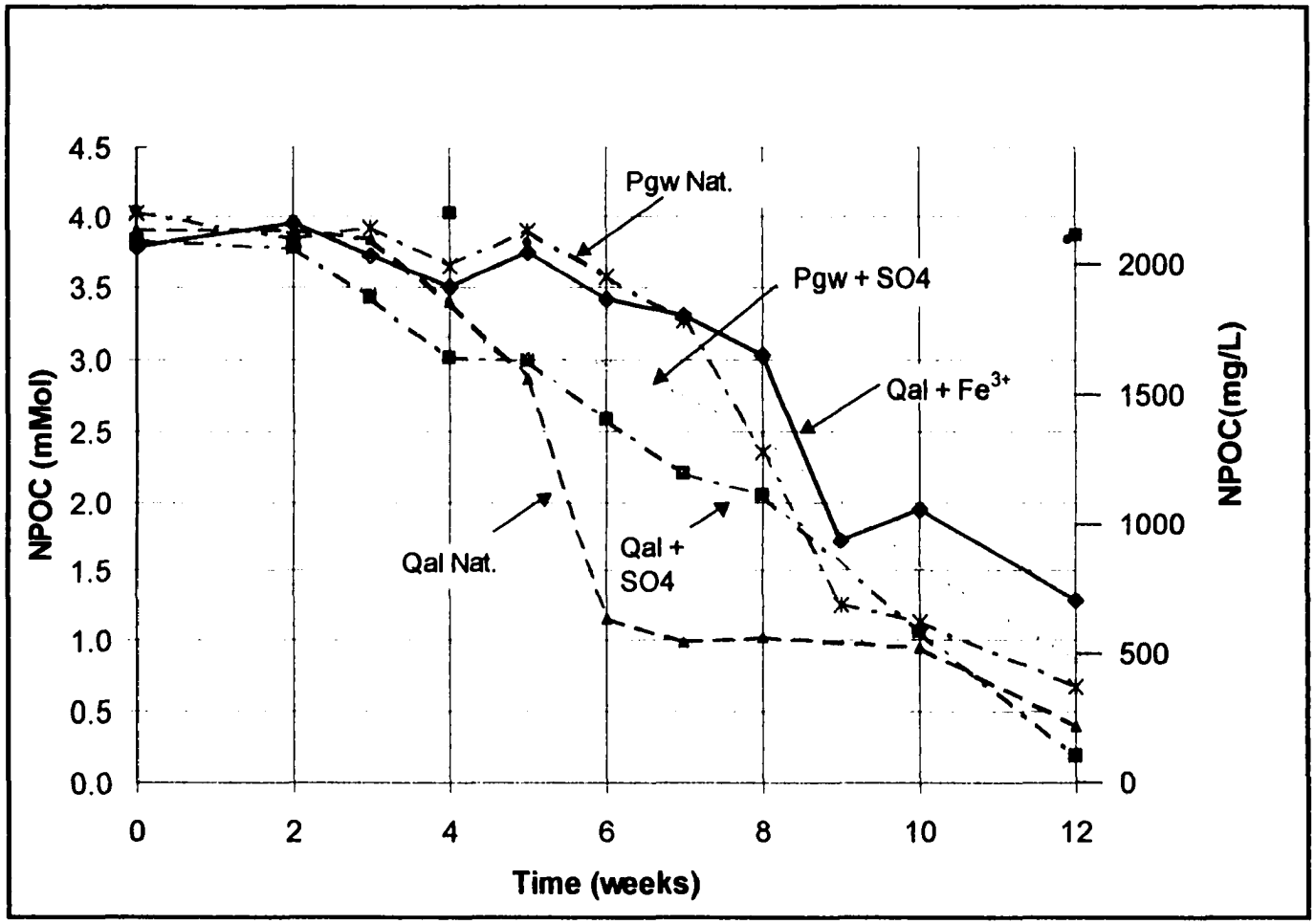

Figure 40. Organic carbon consumption by microcosm system. ■ = Qal killed control; ● = Pgw killed control

Fe^{3+} and SO_4^{2+} reduction is demonstrated in the respective mineral amended systems with varying degrees of methanogenesis.

In overview, biodegradation of leachate can be viewed as a process consisting of:

- Fermentation of complex organics to simpler organics;
- Oxidation through a respiratory pathway (e.g., TCA cycle) if inorganic electron acceptors are available or
- Further fermentation of acetate to CH_4 and CO_2 if inorganic electron acceptors are not available.

The addition of solid Fe^{3+} or SO_4^{2-} minerals does not appear to enhance the rate of organic substrate consumption although reduction of those electron acceptors occurred. This suggests that initial fermentation is relatively slow (rate limiting) compared to respiration or methanogenesis, for the conditions of this experiment.

6.4.2. Headspace Gas

Methane was produced in all active microcosm systems (Figure 41). Methane production can occur as acetoclastic methanogenesis:

(33) $CH_3COOH \rightarrow CH_4 + CO_2$

or chemoautotrophic methanogenesis:

(34) $CO_2 + 4H_2 \rightarrow CH_4 + 2H_2O$

In the non-amended microcosms the final ratio of mMol NPOC consumed to CH_4 produced is approximately 1:0.56 inferring acetoclastic methanogenesis dominated with little ancillary chemoautotrophic methanogenesis. Methanogenesis accounted for between 32 and 49% of the degraded NPOC when gypsum $SO_4^{2-}$was added, 76% when Fe^{3+} was added, and accounted for approximately 98% in native sand where no solid mineral electron acceptors were added. The addition of SO_4^{2-} greatly inhibited methanogenesis. The addition of synthetic solid Fe^{3+} did not inhibit CH_4 production to the extent that added SO_4^{2-} did. The native Fe^{3+} minerals in these sediments do not inhibit methanogenesis appreciably.

Generated headspace CO_2 is shown on Figure 42. With the exception of the Qal+Fe^{3+} system, the rate of headspace CO_2 generation is remarkably similar for all systems, approximately 0.1 mMol/week. As discussed below, CO_2 is generated in the Qal+Fe^{3+} system by the second week at a concentration similar to the other microcosms but drops to very low levels thereafter.

6.4.3. Sulfate System

Sulfate consumption for the Qal+SO_4^{2-} and Pgw+SO_4^{2-} systems are shown on Figure 43. Approximately 75% of the added SO_4^{2-} (~1.3 mMol/microcosm)

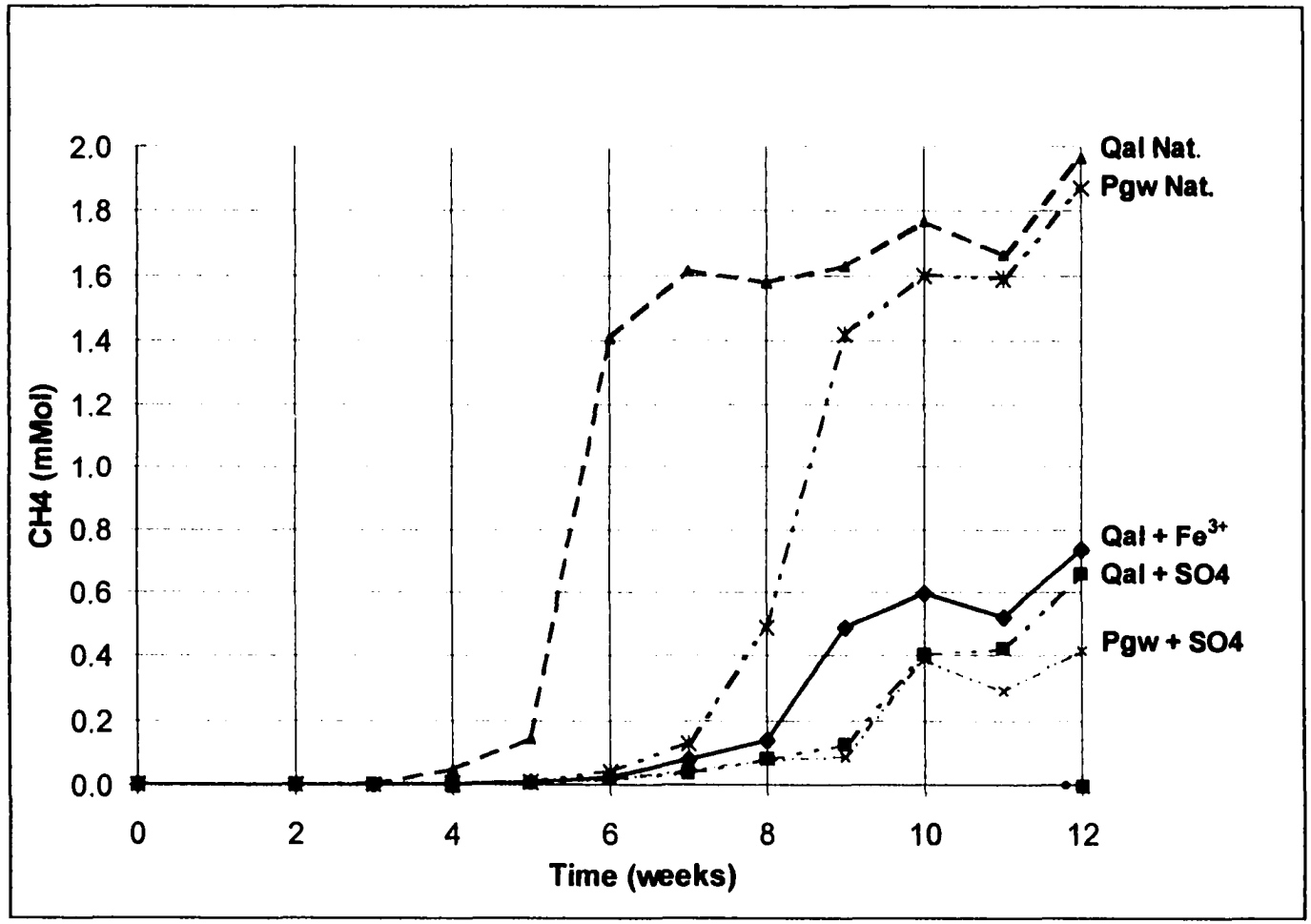

Figure 41. Headspace CH_4 gas production by microcosm system. ■ = Qal killed control; ● = Pgw killed control

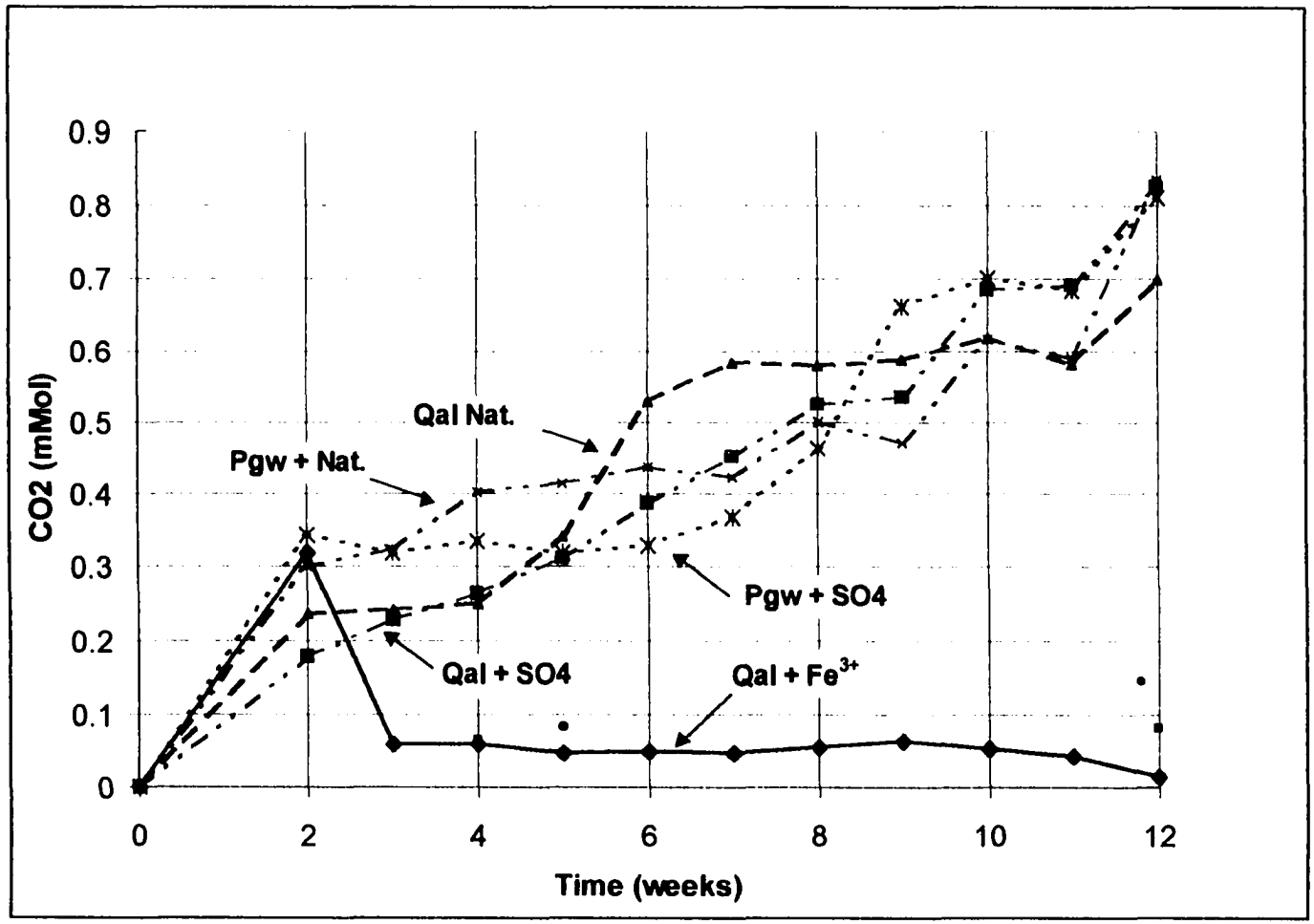

Figure 42. Headspace CO_2 gas production by microcosm system. ■ = Qal killed control; ● = Pgw killed control

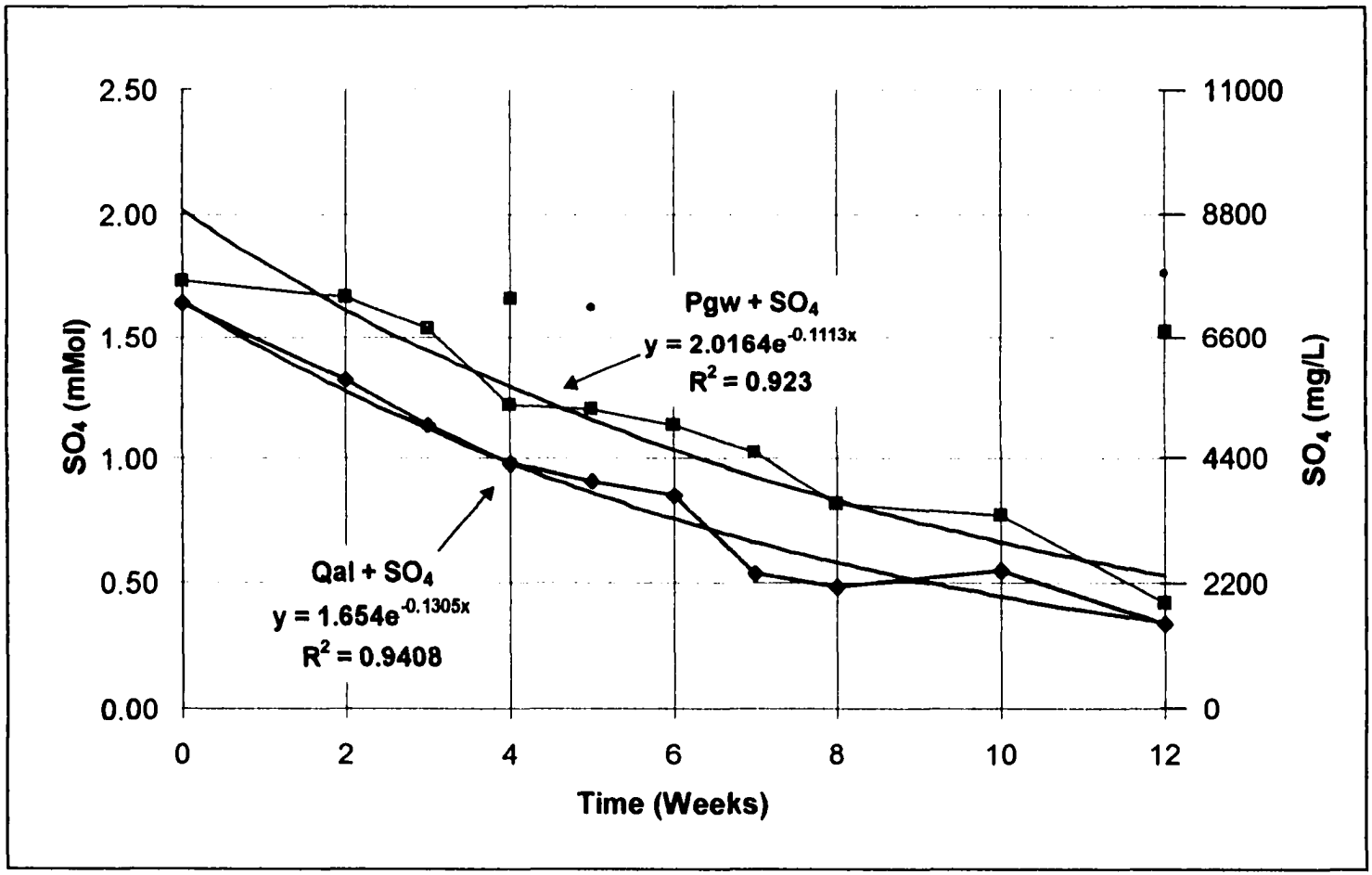

Figure 43. SO_4^{2-} consumption for Qal and Pgw systems. ■ = Qal killed control; ● = Pgw killed control

was consumed during the experiment. Kinetics appear to follow a first order model with an average SO_4^{2-} utilization rate of k = 0.12 $week^{-1}$.

The solubility limit for gypsum, in pure water, for this system is 0.31 mMol SO_4^{2-} per microcosm (Weast et al., 1986); well below the 1.74 mMol SO_4^{2-} added to each microcosm. Therefore, solid gypsum was, at least initially, present. The reduction of SO_4^{2-} from mineral gypsum was probably controlled by dissolution kinetics and mass action. Dissolved SO_4^{2-} may initially have been at aqueous equilibrium. It is likely that bacteria primarily used the aqueous form of SO_4^{2-} rather than the mineral form directly, based on thermodynamic considerations. As aqueous SO_4^{2-} was removed from solution via microbial processes, additional gypsum dissolved.

Significant methanogenesis occurred after week eight even though > 0.50 mMol SO_4^{2-} remained. Methanogenesis appears to have become progressively more competitive as the mass rate of gypsum SO_4^{2-} consumption/dissolution decreased to < 0.09 mMol/week after weeks 5 and 7 for the Qal+SO_4^{2-} and Pgw+SO_4^{2-} systems, respectively. Most of the sulfate reduction is thought to have occurred as:

(35) $CH_3COOH + SO_4^{2-} + H^+ \rightarrow 2CO_2 + HS^- + 2H_2O$

However, partial reduction of SO_4^{2-} to S^o is also possible as:

(36) $CH_3COOH + 4/3\ SO_4^{2-} + 8/3\ H^+ \rightarrow 4/3\ S^o + CO_2 + 10/3\ H_2O$

The resulting HS^- species were distributed across several phases in each system. No significant aqueous (< 0.05 mg/L) HS^- was measured; however, much reduced sulfur was found as gaseous H_2S and in mineral sulfides. Approximately 40% of the SO_4^{2-} consumed could not be accounted for by analysis in either the Qal or Pgw systems. Also, by stoichiometry, combining the CH_4 produced plus the quantity of SO_4^{2-} consumed should have resulted in the consumption of at least 21% more organic carbon than can be accounted for. Some of this SO_4^{2-} discrepancy could be the product of cumulative analytical error from this rather complex system. However, this mass balance error could be addressed if:

- Some of the SO_4^{2-} was not fully reduced, producing, for example polysulfides or organosulfies, that are not be fully extracted as CrES (Fossing and Jorgensen, 1989); and
- Some SO_4^{2-} may have undergone assimilative reduction or conversion to organosulfides or organic bound storage granules, which are not extracted by the techniques used here (Canfield et al., 1986).

With respect to the second possibility listed above, several studies have noted the inclusion of various forms of S as granules within the cellular membrane of bacteria, including the various forms of AVS and FeS_2 (Williams, 1990; Mann et. al, 1990; and Farina et. al, 1990). Because these S forms are completely encased within organic material, they may not be fully extractable with the methods employed here.

A summary of recovered sulfide species for the Qal and Pgw systems are shown on Figures 44 and 45, respectively. The recovered sulfides in the Qal system were distributed as 46% H_2S, 38% AVS, and 15% CrES. For the Pgw system, recovered sulfides were distributed as 34% H_2S, 58% AVS and 8% CrES. The Pgw sand contains more total iron than the Qal media does. Therefore, slightly more sulfide was trapped as a recoverable solid phase in the Pgw system (0.56 mMol or 66%) compared to the Qal system (0.39 mMol or 53%). However, produced H_2S did not vary significantly between the Qal (0.34 mMol) and Pgw (0.29 mMol) systems.

It is logical that iron sulfide formation is finite even with an abundance of H_2S. It is proposed that Fe^{3+} reaction sites are limiting with excess H_2S, causing AVS formation to approach an upper limit. Although several equations are possible, the following, simple, two-parameter equation is suggested to describe total sulfide formation:

$$(37) \quad S_t = \frac{M_{max} * t}{K_m + t}$$

Where:

S_t = Mass of solid sulfides (AVS + CrES) formed in units of S mass per mass soil

M_{max} = S_t mass soil capacity (mass S/mass soil)

K_m = Half mass accumulation constant (t)

t = time

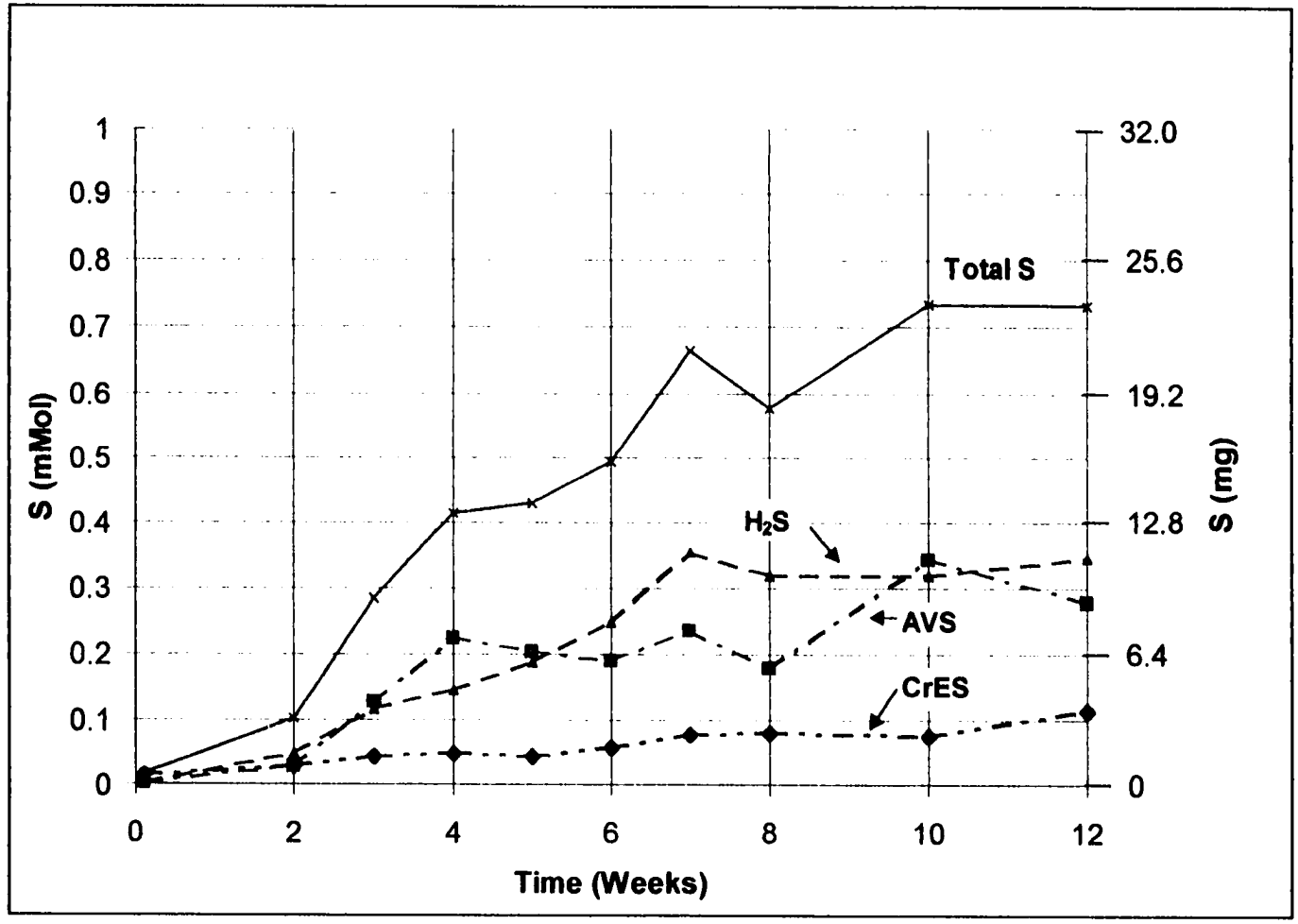

Figure 44. Recovered sulfides by species for Qal+SO_4^{2-} system.

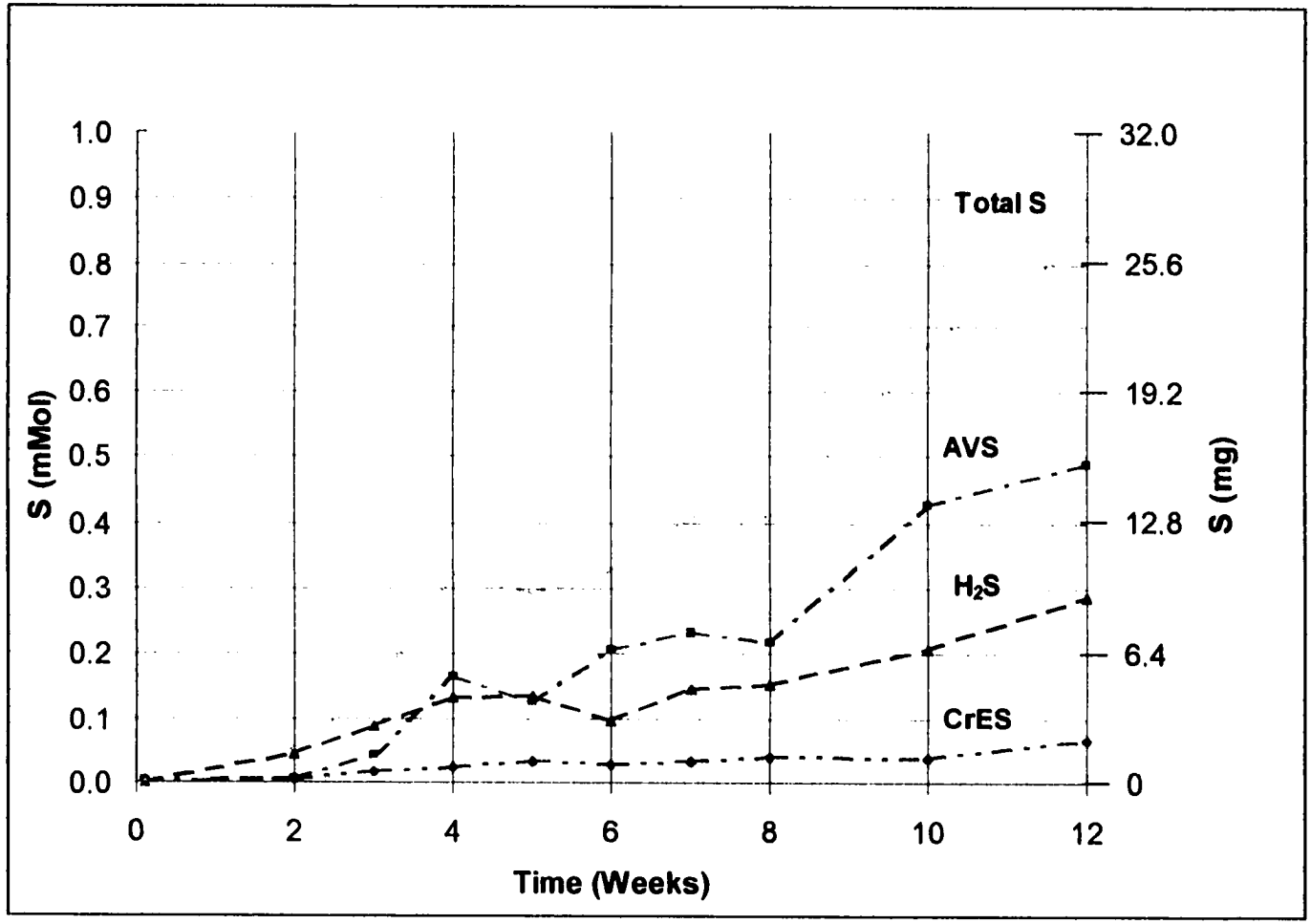

Figure 45. Recovered sulfides by species for Pgw+SO_4^{2-} system.

For this equation, M_{max} is the maximum mass of solid reduced S that can form for a given sediment when H_2S is in excess. K_m is half the time necessary to generate M_{max}. It is stressed that this Equation 37 is empirical and that the quality and quantity of data from this study is insufficient to categorically define the optimum equation. Equation 37 can be linearized as:

$$(38) \quad \frac{1}{S_t} = \frac{K_m}{M_{max}} * \frac{1}{t} + \frac{1}{M_{max}}$$

Here, the y-axis intercept is the reciprocal of M_{max} and K_m can be determined by dividing the slope of the resulting best-fit line by M_{max}. Measured S_t (AVS+CrES) is transformed and plotted in the linearized form as shown on Figures 46 and 47. Equation 38 is limited to late data because plotting the reciprocals of S_t and t for very early data results in large, highly variable transformed values. This places extreme weight on the first few data points in the series, which are the most inaccurate. Therefore, the first data point has been eliminated from the analysis for both Figures 46 and 47. For the Pgw system, the calculated M_{max} = 1.1 mMol and K_m = 12.6 weeks, but for the Qal system M_{max} = 0.6 mMol and K_m = 7 weeks. Measured S_t for the Qal and Pgw systems are plotted against Equation 37 using calculated M_{max} and K_m values derived from Equation 38 (Figures 48 and 49). Nonlinear regression analysis using the computer program SigmaPlot (1997) produced similar results; M_{max} = 0.92, K_m = 10.5 for the Pgw system and M_{max} = 0.6 and K_m = 5.4 for the Qal

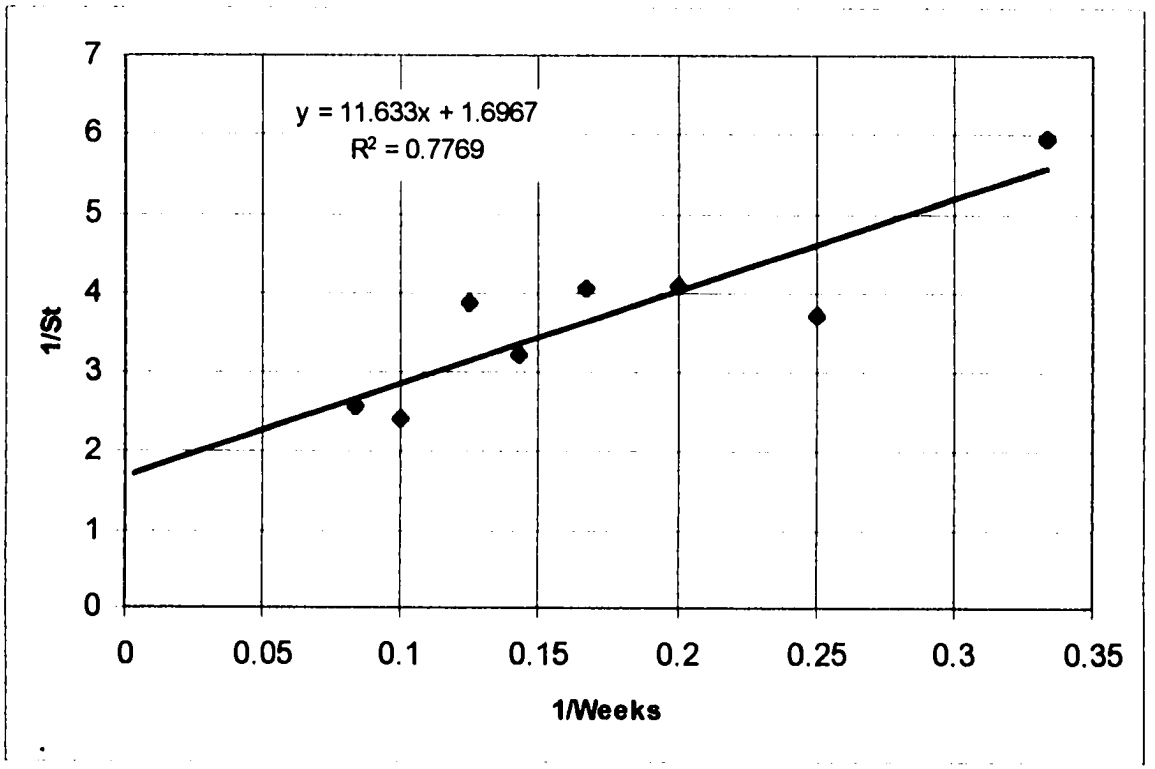

Figure 46. S_t in linear form for the Qal + SO_4 system. Regression analysis variables refer to graph axis.

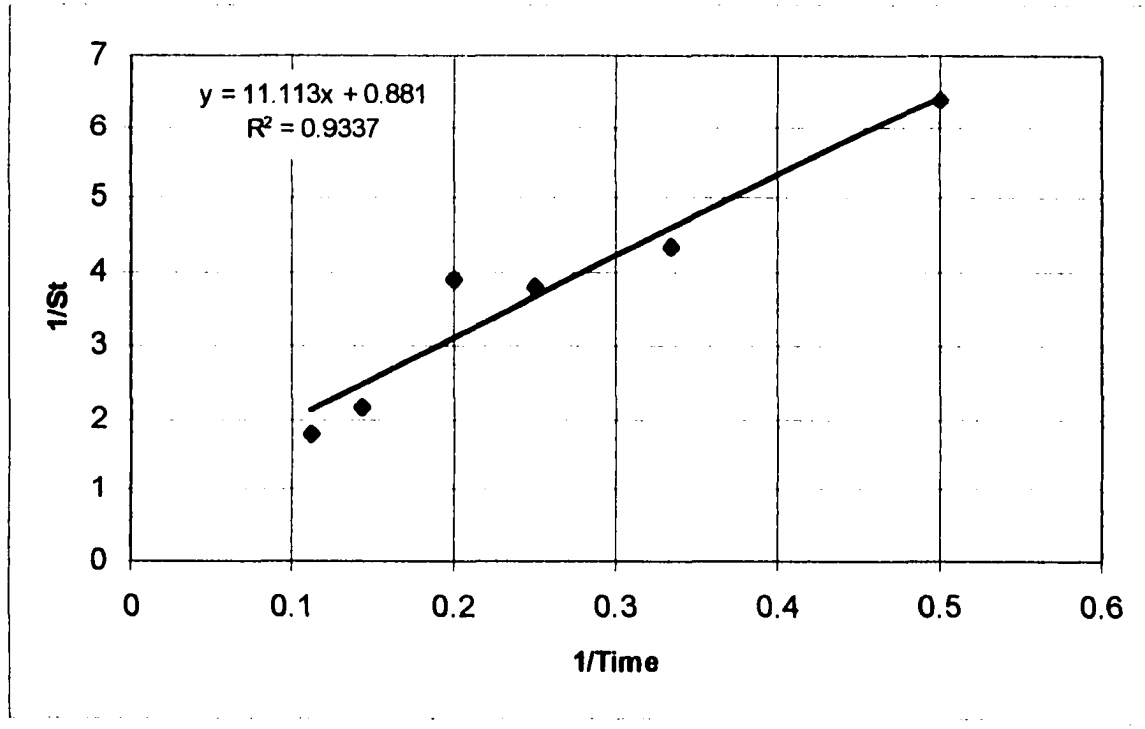

Figure 47. S_t in linear form for the Pgw + SO_4 system. Regression analysis variables refer to graph axis.

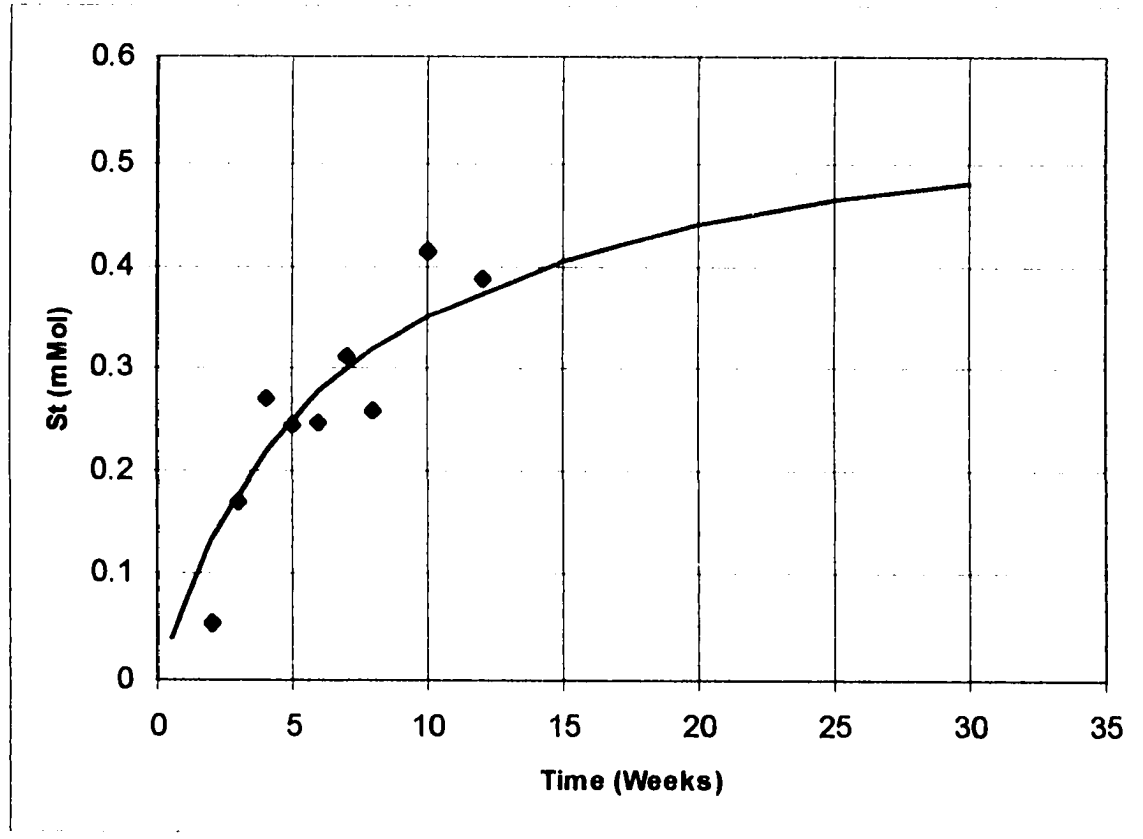

Figure 48. S_t produced for the Qal+SO_4^{2-} system. Line printed past data to demonstrate equation form.

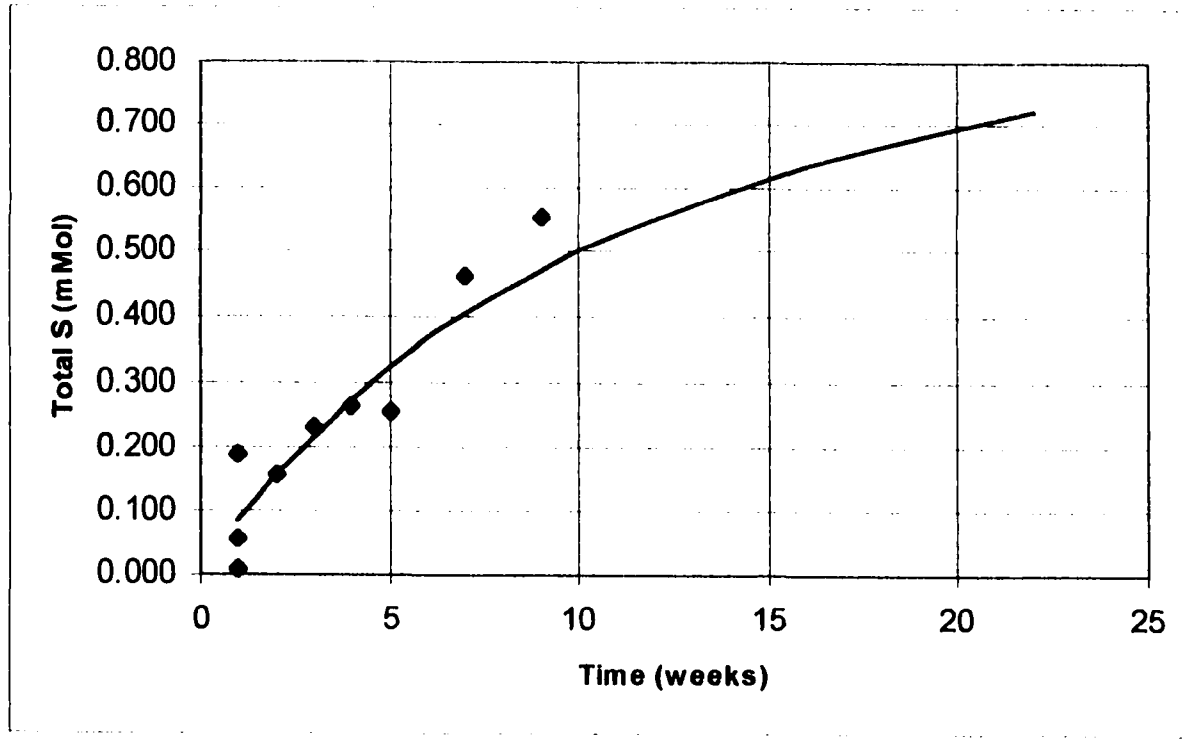

Figure 49. S_t produced for the Qal+SO_4^{2-} system. Line printed past data to demonstrate equation form.

microcosms. Both nonlinear analyses had calculated R^2 values greater than 0.96 (Appendix I).

According to this model, between two to four times more AVS can form in the Pgw system than in the Qal system, probably due to the greater amount of Fe^{3+} solids (reactive surface area) present in the Pgw sand. Half of the possible AVS mass is formed in only six weeks for the Qal system, but between 10 to 12 weeks is required for the Pgw system. At the conclusion of the experiment, 0.55 mMol S_t was formed in the Pgw system. This measured S_t plus the 0.29 mMol H_2S equals 0.84 mMol which is less than the calculated M_{max}, inferring that all H_2S could react with the solid media for this system. For the Qal system, however, the captured S_t at the end of the test (0.55 mMol) plus the headspace H_2S (0.34mMol) requires an M_{max} of approximately 0.9 mMol, which is greater than the M_{max} available. Therefore, it appears that residual H_2S cannot be fully captured by the Qal sand.

The rate of AVS formation can be described by differentiating Equation 37 resulting in:

$$(39) \quad \frac{dS_t}{dt} = \frac{M_{max} * K_m}{(K_m + t)^2}$$

Equation 39 describes a system where the rate of AVS formation approaches a constant rate M_{max}/Km (mass/time) when $t \rightarrow 0$ but approaches 0 as $t \rightarrow \infty$. Graphs of dS_t/dt for the Pgw and Qal systems show the rate of AVS formation decreasing quickly for the Qal sand relative to Pgw (Figure 50).

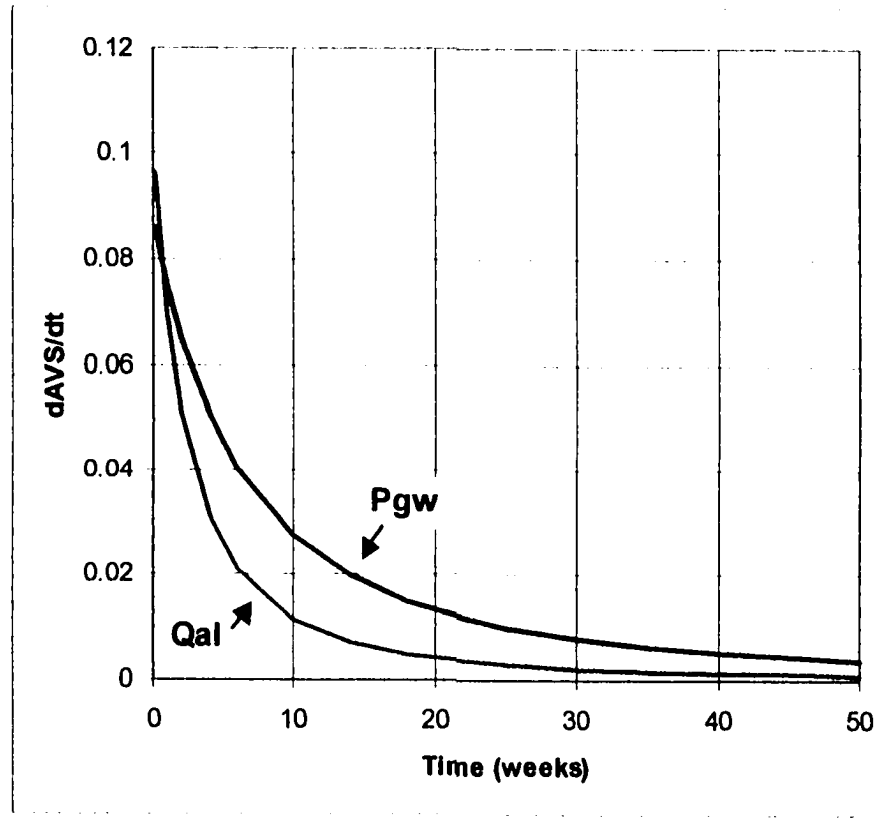

Figure 50. Predicted rate of S_t formation for the Pgw and Qal+SO_4^{2-} systems.

In this experiment, the formation of CrES was found to be zero order according to:

(40) $CrES = k_{CrES}*t + b$

Where:

k_{CrES} = zero order rate constant (mass/time)

b = initial CrES concentration (mass)

t = time

It was found that $k_{CrES} = 0.008$ and $k_{CrES} = 0.005$ S^- mMol/week for the Qal and Pgw systems, respectively (Figure 51). The rate of CrES formation is constant, even early in the microcosm experiment when AVS concentrations were quite low. CrES formation is faster in the Qal system than in the Pgw system. This suggests that FeS_2 formation may be favored if Fe^{3+} is limited. At the conclusion of the experiment, more AVS is formed in the Pgw system than in the Qal system with ratios of AVS to CrES of 7:1 and 2.6:1, respectively.

Assuming 1) conditions remained stable (SO_4^{2-} reduction continued to produce HS^- to excess) and 2) AVS is converted to CrES similar to Equation 40 at the measured rate, then:

(41) $AVS = S_t - CrES$

Note that according to Equations 17 and 21, only half of the formed AVS could ever be converted to FeS_2 because such a system is S^o limited. Therefore,

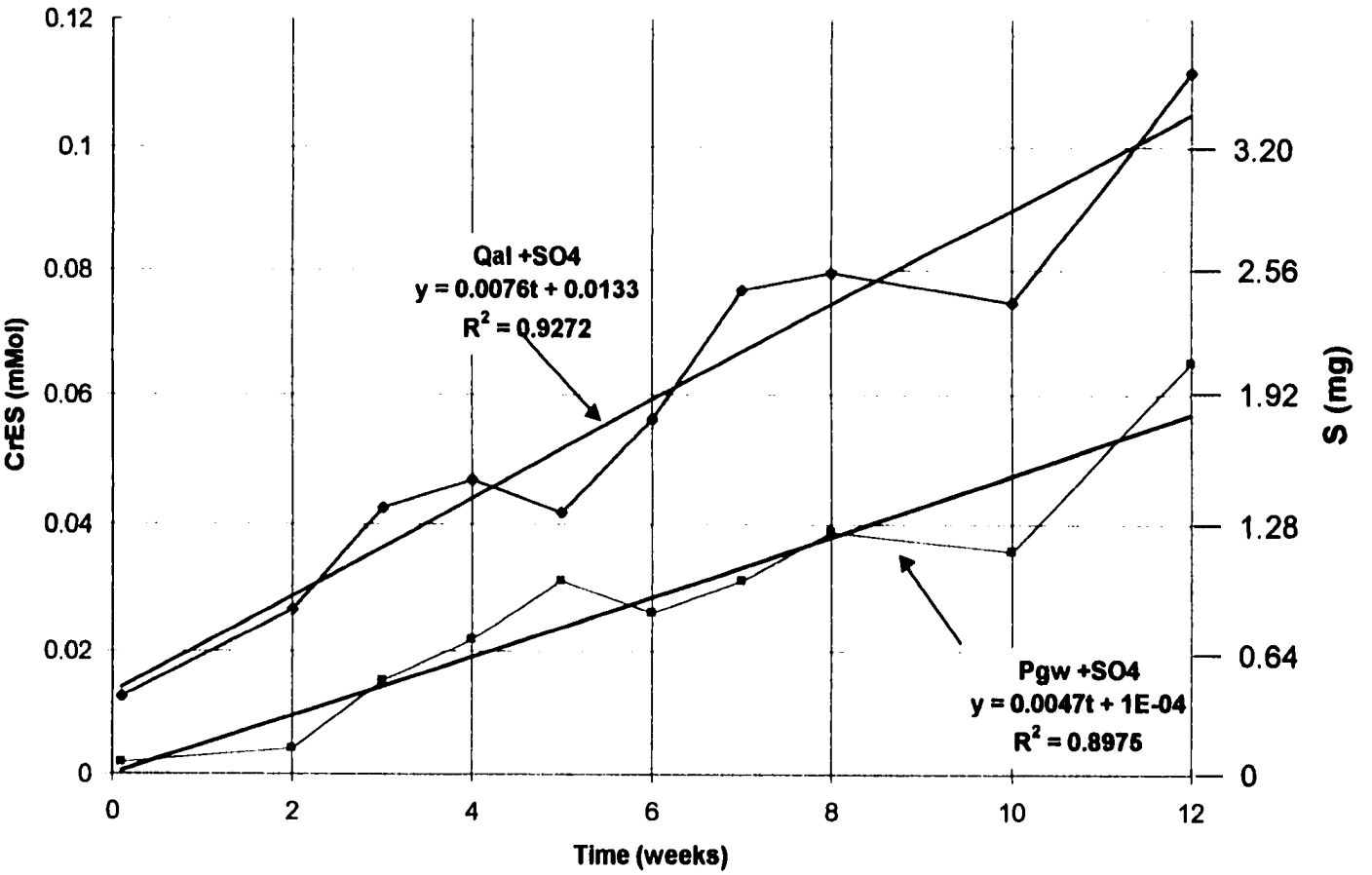

Figure 51. Measured CrES for the Qal + SO4 and Pgw + SO4 systems. Regression analysis variables refer to graph axes.

an additional source of S° is required for all AVS to be converted to FeS_2. Supplemental S° could be provided from the partial reduction of SO_4^{2-} according to Equation 14. Placing Equations 37 and 40 into Equation 41 yields:

$$(42) \qquad AVS = \frac{M_{max} * t}{K_m + t} - k_{CrES} * t$$

Equation 41 is valid provided CrES and AVS formation continue according to the identified models and estimated rate, an assumption that may not be true should AVS become limiting. Predicted S_t, AVS, and CrES are shown on Figures 52 and 53 for the Qal and Pgw systems. These figures show the theoretical increase in measured AVS concentrations, until the rate of AVS formation equals the rate of CrES formation, with progressive AVS decline after that time. The time Figure 52. Predicted m St, AVS, and CrES in the Qal+SO_4^{2-} at which measured AVS stops increasing for a steady state system can be determined by setting Equation 39 to k_{CrES} and solving for t as:

$$(43) \qquad t_x = \sqrt{\frac{M_{max} * K_m}{K_{CrES}}} - K_m$$

Where:

t_x = time of maximum measured AVS concentration.

Given $10 \leq K_m \leq 13$ and $0.9 \leq M_{max} \leq 1.1$ for the Pgw system, t_x ranges between 32 to 40 weeks. For the Qal system tx ≅ 15 weeks given K_m=6 and

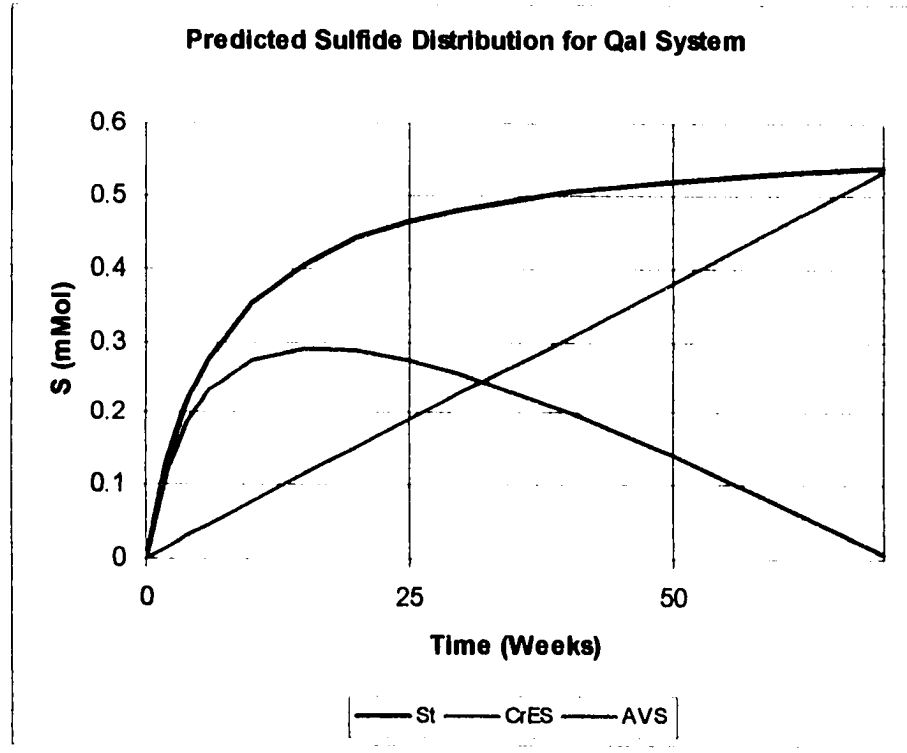

Figure 52. Predicted measured S_t, AVS, and CrES in the Qal+SO_4^{2-} system.

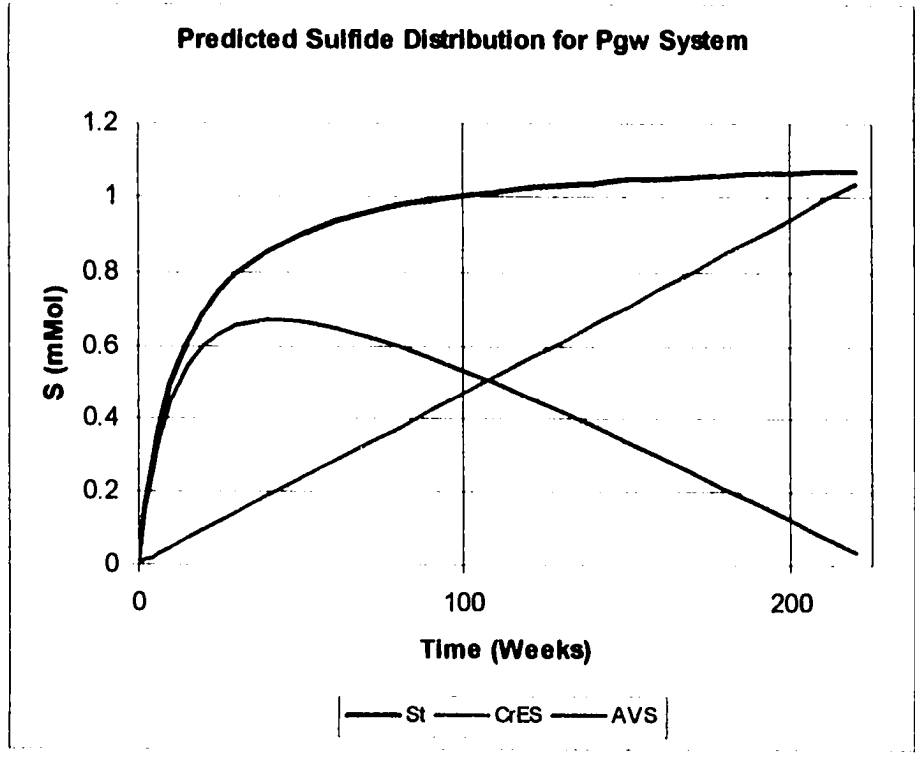

Figure 53. Predicted measured S_t, AVS, and CrES in the Pgw + SO_4^{2-} system.

M_{max} = 0.6. Similarly, the theoretical time (t_{max}) to convert all AVS to CrES could be approximated as:

$$(44) \quad t_{max} = \frac{M_{max}}{K_{CrES}} - K_m$$

For the Pgw system, t_{max} ranges from 3.3 to 3.9 years, whereas t_{max} for the Qal system is estimated to be 1.3 years. This evaluation infers AVS might remain longer in a system rich in Fe^{3+}, which has been generally observed at the contaminated sites investigated here. Core samples taken from the closed Norman landfill, near where the Qal sand was collected, show a predominance of CrES relative to AVS (Figure 25). Conversely, the fuel spill site was in a Permian sand similar to the Pgw sand. There the system was apparently dominated by AVS relative to CrES (Figures 37 and 38). Obviously, exposure time to HS^- for these two examples will have an effect on AVS/CrES ratios so this observation must be taken with caution.

6.4.4. Iron System

The 0.5 N HCl extractable solid Fe^{2+} for all active microcosms is shown on Figure 54. In terms of Fe^{2+} produced, Qal+Fe^{3+}>Pgw+SO_4^{2-}>Qal+SO_4^{2-}>Pgw Nat.>Qal Nat. As discussed below, all systems show possible evidence of enzymatic Fe^{3+} reduction. The suggested chemical reaction is:

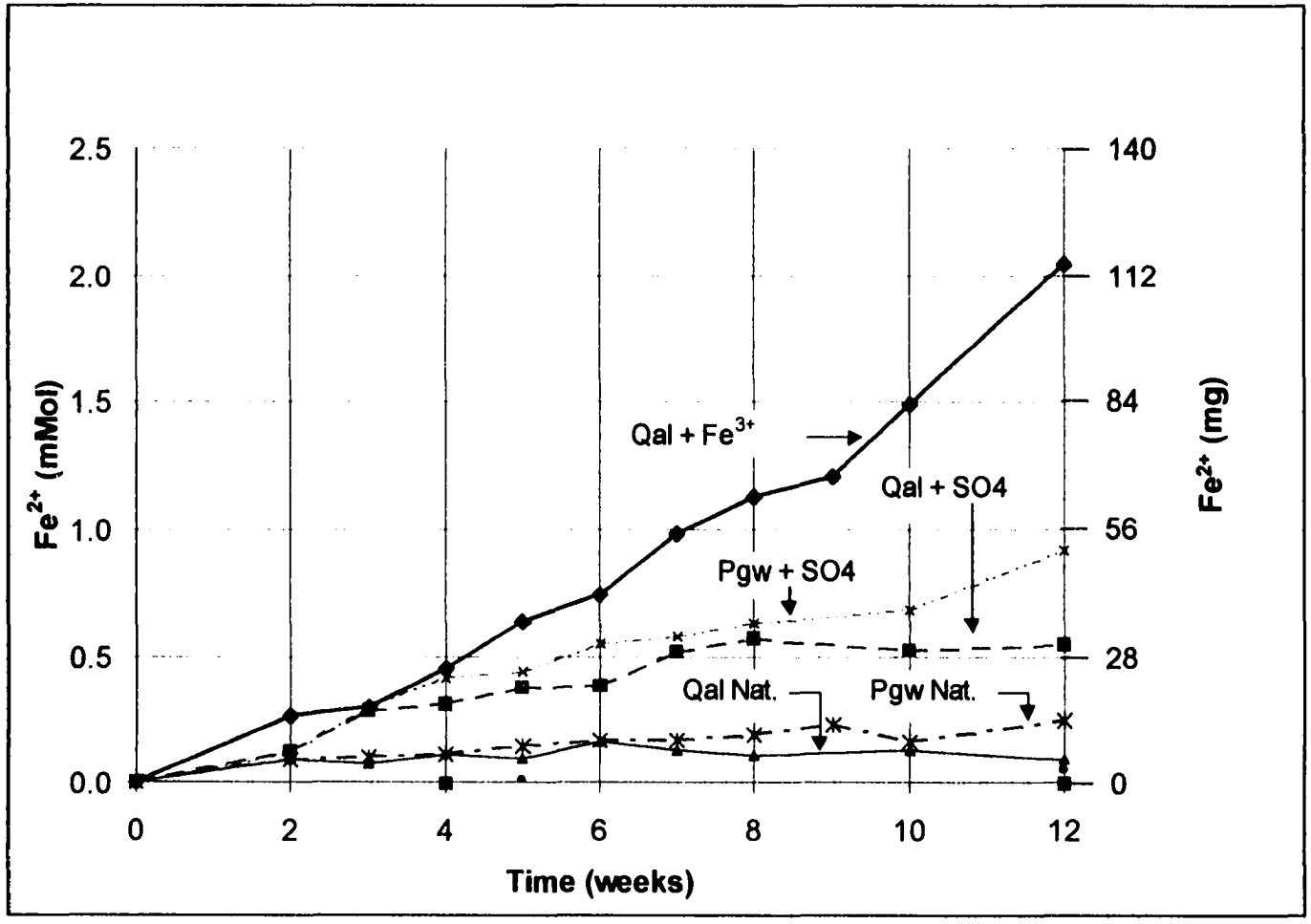

Figure 54. Produced solid Fe^{2+} by microcosm system.

(45) $CH_3COOH + 2H_2O + 8Fe^{3+} \rightarrow 2CO_2 + 8Fe^{2+} + 8H^+$

Note that most of the Fe^{2+} produced in Qal+SO_4^{2-} and Pgw+SO_4^{2-} systems is probably from an abiotic reaction with HS^-.

Compared to solid forms, relatively little aqueous Fe^{2+} was found over the course of the experiment (Figure 55). Note that Figure 55 is reported in terms of mg/L, a common field unit of measurement. The highest concentration of aqueous Fe^{2+} measured was 88 mg/L, occurring in week 9 for the Qal+Fe^{3+} system; a very high value for aqueous iron in any true ground water system. However, that aqueous value represents only 0.03 mMol/microcosm, just 2.5% of the total Fe^{2+} expressed in that system at that time. This poor ratio of aqueous to solid Fe^{2+} worsens with time, becoming only 0.6% at 12 weeks. This suggests that the formation of Fe^{2+} minerals in a natural system is probably equal to or only slightly less than the rate of Fe^{3+} reduction; therefore, measuring dissolved Fe^{2+} is a poor quantitative indicator of Fe^{3+} reduction.

Very little aqueous Fe^{2+} was found in the Qal or Pgw + SO_4^{2-} microcosms. This is consistent with the general tendency for Fe and many other metals, including Co, Ni, Cu, Zn, Cd, Hg, Sn, and Ag, to form solid mineral sulfide complexes at very low aqueous concentrations (Stumm and Morgan, 1996).

In contrast to all other active microcosms, headspace CO_2 was very low in the Qal+Fe^{3+} system, except for the second week (Figure 42). It is probable that

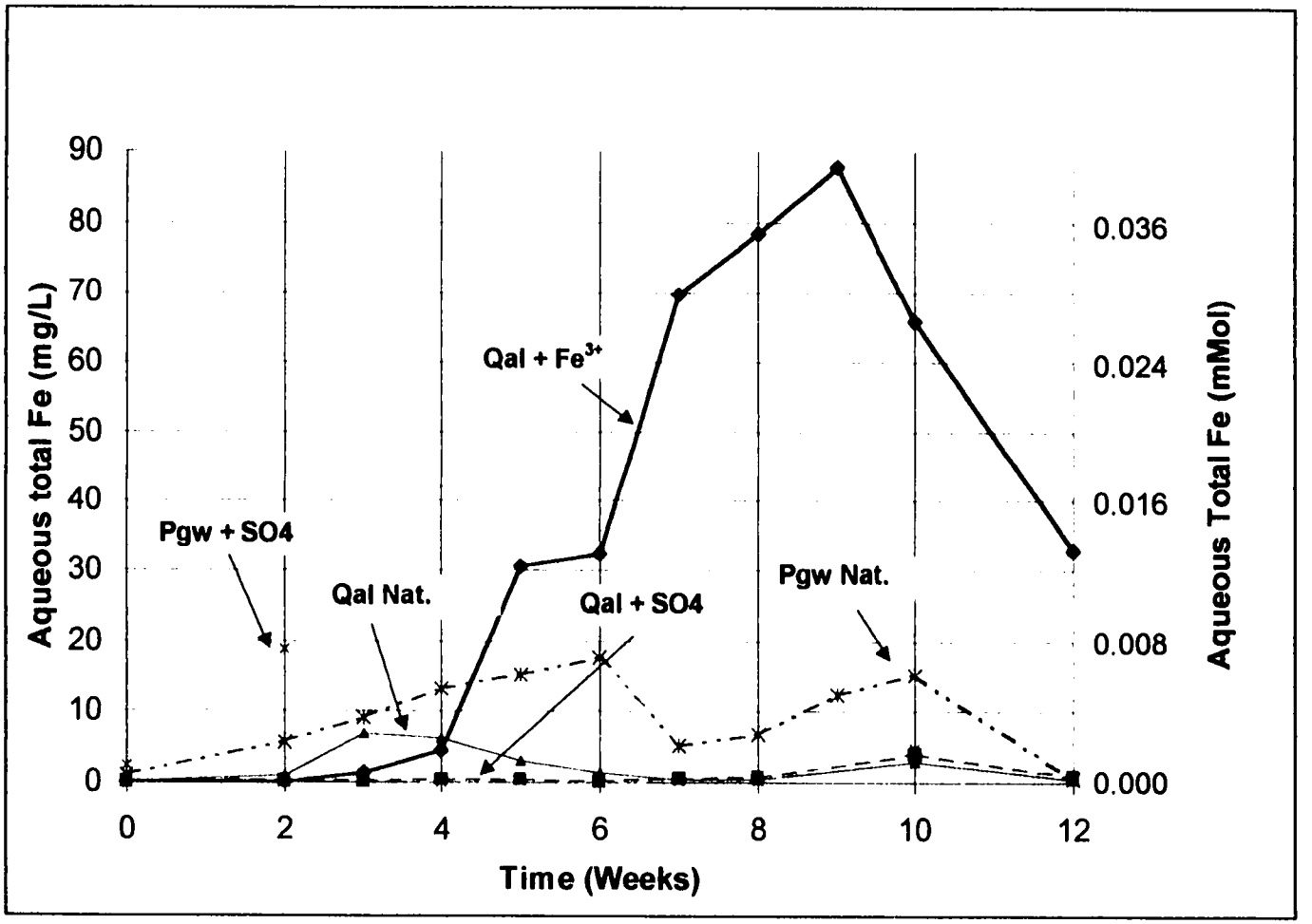

Figure 55. Aqueous Fe^{3+} in mg/L

CO_2 was effectively scavenged by produced Fe^{2+} to form siderite ($FeCO_3$) according to:

(46) $CO_2 + H_2O \rightarrow HCO_3^- + H^+$

(47) $Fe^{2+} + HCO_3^- \rightarrow FeCO_3 + H^+$

According to Equation 45, for enzymatic Fe^{3+} reduction, four times as much Fe^{2+} is produced than CO_2. Therefore, when significant enzymatic Fe^{3+} occurs, excess Fe^{2+} could be produced which can combine and eliminate CO_2 generated from other microbial respiratory processes. Based on the stoichiometry of Equations 33 and 45, the Qal+Fe^{3+} system produced approximately 0.5 mMol CO_2 from enzymatic Fe^{3+} reduction and 0.8 mMol CO_2 from acetoclastic methanogenesis (1.3 mMol CO_2/microcosm total). At the end of 12 weeks, 2.1 mMol mineral Fe^{2+} was produced, which was sufficient to react with all microbially produced CO_2 to form ~1.3 mMol $FeCO_3$. The remaining 0.8 mMol Fe^{2+} apparently precipitated as magnetite or other Fe^{2+} mineral species. This infers that in the absence of another anion pair (such as HS^-), aqueous Fe^{2+} concentrations may be controlled, in part, by CO_2, which can be produced by concurrent acetoclastic methanogenesis.

Fe^{3+} was apparently reduced abiotically to Fe^{2+} in the SO_4^{2-} reduction systems. However, comparing Figure 54 with Figures 44 and 45 shows excess Fe^{2+} formed relative to AVS produced. For the Qal+SO_4^{2-} system, AVS = 0.28 and Fe^{2+} = 0.55 mMol (a ratio of 1:2.0) and for the Pgw+SO_4^{2-} system, AVS =

0.49 and Fe^{2+} = 0.90 mMol (a ratio of 1:1.8). It could be assumed that enzymatic Fe^{3+} reduction occurred concurrent with SO_4^{2-} reduction accounting for the additional Fe^{2+}. Alternatively, it is possible that some reduced S species were cycled to oxidized forms via Fe^{3+} reduction, which could also account for additional Fe^{2+}.

Although methanogenesis was responsible for most NPOC removal in the Qal and Pgw Nat. systems, small amounts of enzymatic Fe^{3+} reduction may have occurred using native iron. Approximately 0.18 and 0.25 mMol Fe^{2+} was formed over the course of the experiment in the Qal Nat. and Pgw Nat. systems respectively. Though small compared to the other microcosm systems, the amount of Fe^{2+} generated in the natural systems is statistically relevant at a 0.05 level of significance.

According to Equation 45, approximately 0.045 and 0.063 mMol NPOC could have been consumed via enzymatic Fe^{3+} reduction for Qal and Pgw Nat. systems. It is concluded that native iron was relatively ineffective as an electron acceptor over the course of the experiment. Fe^{3+} reduction in these microcosms did not generate sufficient Fe^{2+} to deplete headspace CO_2 concentrations significantly.

The Qal and Pgw sediments initially contained 0.28 and 0.35 mMol Fe^{3+} per microcosm each, based on a 48 hour 0.5 HCl extraction. This is only 15% and 4% of the 6N HCl extractable Fe^{3+} present in those sediments, respectively. The residual Fe^{3+} (defined as the original 0.5N HCl extractable Fe^{3+} - measured 0.5N HCl extractable Fe^{2+}) for both systems is shown on Figure 56. Natural Fe^{3+}

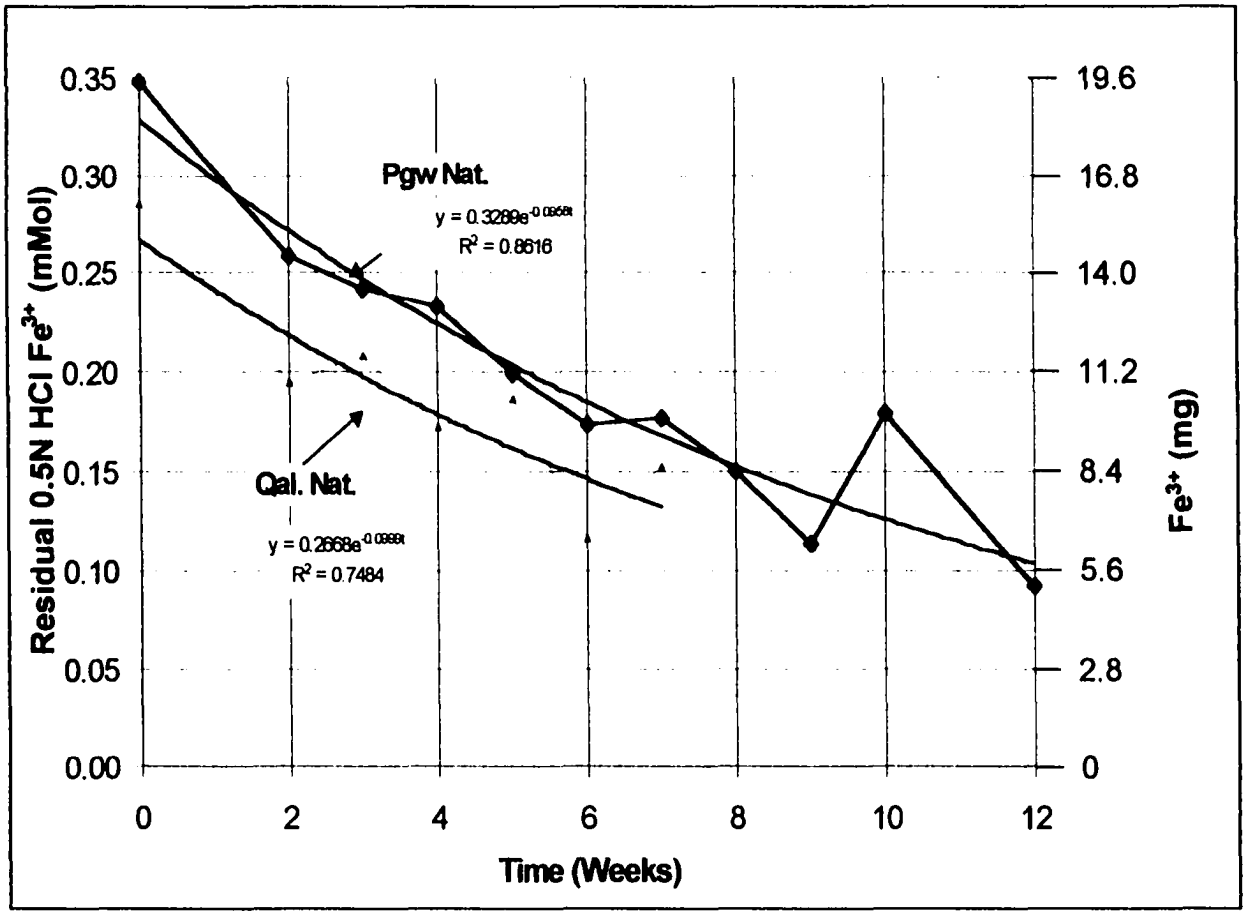

Figure 56. Residual Fe^{3+} in Qal and Pgw Nat. systems. Last three sampling periods for the Qal Nat. system not plotted due to no growth in microcosm. Regression variables refer to graph axes.

reduction for both the Qal and Pgw systems appears to follow a first order model with k = 0.1 week^{-1}. As discussed above, NPOC consumption largely stopped in the Qal Nat. system from week six to twelve, so only weeks zero to six for the Qal system are considered for these calculations. At this rate the easily extractable Fe^{3+} fraction would be reduced to only 0.01 mMol in approximately 32 weeks for the Qal sediment and in 36 weeks for the Pgw sediment assuming labile organic concentrations were continuously present.

As described in Chapter 3, evidence of Fe^{3+} reduction has been observed in aquifers that have been contaminated for many years. Based on the projected time required to utilize the 0.5 N HCl extracted Fe^{3+} for the Qal and Pgw systems it is suggested that the 48 hour extraction time used may yield a conservative estimate of the biologically available Fe^{3+} fraction in native sediments. It is stressed that this conclusion is very tentative and much more research is necessary. These data also suggest that a first order model should be considered for enzymatic solid Fe^{3+} reduction in native sediments.The rate of Fe^{3+} utilization in the Qal+Fe^{3+} system, based on Fe^{2+} production, was k = 0.16 mMol/week, apparently following a zeroth order model. Presumably, decay would become first order if sufficient $Fe(OH)_3$ was consumed, but this was not observed during the experiment. Only 2.1 mMol (14%) of the added $Fe(OH)_3$ was ultimately consumed, sufficient to oxidize approximately 0.53 mMol NPOC or 25% of the total NPOC degraded. It should be noted that some produced Fe^{2+} mineral species may be only partially extracted using 0.5 N HCl, so greater Fe^{3+} reduction may have occurred.

6.5. Microcosm Study Conclusions

As stated, the objectives for this experiment were to examine the potential for using solid Fe^{3+} and SO_4^{2-} in engineered bioremediation systems and to provide insight into natural attenuation processes involving Fe^{3+} and SO_4^{2-} reduction. These two topics are discussed separately below.

6.5.1. Engineered Remediation System Potential

Solid gypsum and Fe^{3+} minerals can be used as terminal electron acceptors by bacteria for degrading simulated landfill leachate. Of interest with respect to engineered systems is that the addition of either solid Fe^{3+} or gypsum did not increase the rate of NPOC degradation over methanogenesis for this experimental system. Although there is no apparent advantage with respect to organic removal rates, adding solid electron acceptors may control biological gases, including the greenhouse gases CH_4 and CO_2. The incorporation of gypsum decreased the production of CH_4 by nearly 70%. For this experiment methanogenesis occurred when the mass transfer (consumption) of SO_4^{2-} fell below 0.09 mMol/week. This rate of SO_4^{2-} utilization is still great (~392 mg/L•week SO_4^{2-}); however, slowing SO_4^{2-} mass transfer from the mineral solid to aqueous phase may have permitted methanogenesis to occur late in the experiment. In an engineered system, this SO_4^{2-} kinetic limitation might be removed by adding gypsum to excess, by mixing, or by the direct addition of dissolved SO_4^{2-} to a reactor cell, which might further inhibit methanogenesis.

With appropriate design, natural sediments containing Fe^{3+} minerals could be used to remove H_2S from SO_4^{2-} respiration by forming various mineral solids. This study shows that the ability of Fe^{3+} minerals to consume H_2S may be limited, but the selection of high Fe^{3+} bearing sediment increases the amount of S_t that can be formed. With experimentation, the mathematical model presented here may be useful in predicting potential S_t for various sediments so that H_2S can be minimized. The addition of mineral SO_4^2, however, does not control the production of CO_2. In contrast, the inclusion of poorly crystalline Fe^{3+}, as $Fe(OH)_3$, reduced CH_4 production by only 25% but virtually eliminated CO_2 production, presumably due to the formation of siderite ($FeCO_3$).

Through engineering design, it may be possible to use Fe^{3+} and/or SO_4^{2-} reduction processes to simultaneously degrade leachate organics while substantially controlling discharge gases. Waste wallboard, predominantly composed of gypsum, could potentially be used as an inexpensive source of SO_4^{2-} and native sediment could be used to scavenge H_2S. A labile source of Fe^{3+}, however, may need to be purchased.

These SO_4^{2-} and Fe^{3+} reduction concepts may be extended to reactive wall or landfill liner designs, where minerals are introduced to the subsurface. However, application to a batch or continuous flow reactor would theoretically optimize the beneficial properties of Fe^{3+} and SO_4^{2-} reduction. For example, a dual system batch reactor using both Fe^{3+} and SO_4^{2-} reduction could be designed as shown on Figure 57. In an SO_4^{2-} reduction chamber, organic constituents could be oxidized to CO_2 and HS^-. Native gypsum or crushed gypsum wallboard

Figure 57. Conceptual batch reactor using sequential SO_4^{2-} and Fe^{3+} reduction processes

from waste could be used as a source of SO_4^{2-}. Inexpensive, Fe^{3+} rich sediment could be used to react with H_2S to form mineral AVS or CrES.

An adjacent Fe^{3+} reduction chamber would use $Fe(OH)_3$ powder as an electron acceptor. There, produced Fe^{2+} would scavenge CO_2 produced from Fe^{3+} and SO_4^{2-} reduction or from any limited acetoclastic methanogenesis to form solid $FeCO_3$. Solid Fe^{3+} reduction is less able to control methanogenesis, however, stoichiometrically, about four times as much Fe^{2+} is produced per unit carbon consumed. Therefore, much less Fe^{3+} reduction is required to control all CO_2. H_2S will readily react with aqueous Fe^{2+} reducing the amount available to react with CO_2. Therefore, the SO_4^{2-} and Fe^{3+} reducing chambers must remain isolated until most of the H_2S in the SO_4^{2-} system is reacted by conversion to AVS or CrES. This may require staggered operation so that the SO_4^{2-} reaction is started before the Fe^{3+} system.

Treatment systems could be developed that used Fe^{3+} or SO_4^{2-} reduction processes singularly. If CO_2 is not of concern, then a very inexpensive and simple SO_4^{2-} reduction system could be used to control CH_4 using gypsum wall board and sand. Alternatively, Fe^{3+} reduction could be used alone. A system using Fe^{3+} reduction could be used to scrub out CO_2 while producing more pure CH_4 that could then be used for electrical cogeneration. Further experiments should also be conducted to determine if Fe^{3+} reduction kinetics can be increased so that methanogenesis is largely inhibited. The operation of an efficient Fe^{3+} reduction system would produce virtually no emissions and would

not require complimentary SO_4^{2-} reduction. Fe^{3+} reduction rates could be increased by:

- Selectively enriching Fe^{3+} reducing bacteria;
- Adding chelating agents to improve Fe^{3+} solubility;
- Obtaining or making more reactive forms of mineral Fe^{3+};

While these systems may not increase the rate at which leachate organics are destroyed, they could potentially convert most organic leachate into solid mineral form, largely eliminating aqueous organics with little gaseous emissions. These system could also eliminate many deleterious dissolved metals, including As or Hg which can be precipitated as sulfide minerals. Mineral solids from the reactor, could be collected and returned to the landfill. Because the landfill environment is largely anaerobic, little mineral oxidation should be expected and the returned sediment sludge should remain relatively stable if containerized. Further research should be conducted to evaluate engineering applications employing Fe^{3+} and SO_4^{2-} reduction processes for the control of problems associated with landfill leachate.

6.5.2. Application to Natural Attenuation Studies

In many native aquifers contaminated with leachate or other labile organic pollutants, SO_4^{2-} and Fe^{3+} reduction occurs naturally. Insight into the behavior of Fe and S under aquifer conditions can be drawn from this study, with implications for natural attenuation or redox zone development field studies. It should be noted that the conditions of an enclosed microcosm system are different from

that of a open, dynamic aquifer and observations from this experiment may not be explicitly correlated to the field. General trends, however, are expected to be comparable between the laboratory and field.

Where Fe^{3+} reduction occurs in an aquifer, the resulting aqueous Fe^{2+} is probably not stable because it is converted rapidly to a mineral form. Therefore, evaluating dissolved Fe^{2+} as part of a natural attenuation field study, is probably a poor indicator of the extent of Fe^{3+} reduction, though such analysis should be conducted for completeness. Aqueous Fe^{2+} can indicate if Fe^{3+} reduction is occurring, but mineral analysis is recommended to examine the expressed contribution of past Fe^{3+} reduction. In the microcosm, the rate of Fe^{2+} mineral formation was virtually instantaneous so that little Fe^{2+} accumulated in the aqueous phase and virtually all of that precipitated by the end of the experiment. Ground water flow velocities are typically slow, on the order of a few feet per day. Therefore, assuming the rate of mineral Fe^{2+} formation found here translates to the field, most produced Fe^{2+} should precipitate in close proximity to the area where Fe^{3+} reduction occurred.

Although relatively large amounts of solid Fe^{3+} minerals may be present in native sediments, only a small portion, here between 4 to 15%, may be available for immediate enzymatic reduction. For the sediments studied, the fraction of native Fe^{3+} minerals extracted using a mild acid (0.5 N HCl) over 48 hours gave a reasonable approximation of the biologically available Fe^{3+}. Solid Fe^{3+} reduction appears to occur over a wide redox range and concurrent with methanogenesis.

In the microcosm, H_2S accumulated in the headspace; a condition that is unlikely in an unconfined aquifer where H_2S would react with oxidized species in the capillary fringe/vadose zone or escape to the atmosphere. The formation of reduced S minerals was found to be rapid compared with typical ground water seepage velocities and very little dissolved HS^- was ever found. Given these considerations, AVS, and CrES minerals will probably precipitate near the point of SO_4^{2-} reduction especially if mineral Fe^{3+} is present.

Increasing amounts of Fe^{3+} in the sediment may shift mineral precipitation somewhat from disulfide (FeS_2) to monosulfies (~FeS). Native sediment varies with its ability to form total mineral sulfides (S_t). It is suggested that increased Fe^{3+} tends to promote the preservation of AVS over time.

Overall, the results of this study imply that the rate of organic landfill leachate degradation may not be greatly different for Fe^{3+} and SO_4^{2-} reduction or for methanogenesis. Consequently, there may not be much variation in organic degradation rates spatially across redox zones or temporally as these redox zones develop in an aquifer impacted with leachate. The primary difference between microbial processes may be with respect to respiratory geochemical products: Fe^{3+} and SO_4^{2-} reduction producing varying amounts of secondary minerals, whereas methanogenesis generates gases.

7. CONCLUSIONS AND RECOMMENDATIONS

In this chapter, the concepts and conclusions developed during this research are summarized. Applications to natural attenuation are discussed followed by potential application to engineered treatment systems. Finally, implications for bioremediation computer modeling are discussed.

7.1. Natural Attenuation

In microcosm, $Fe(OH)_3$ was reduced more readily than the native iron forms that consist mostly of more crystalline Fe_3O_2. In tests, immersion in mild acid extracted much more $Fe(OH)_3$ than Fe_2O_3. It follows that a mild acid extraction might help define the Fe^{3+} fraction that is the most biologically reactive as suggested by Lovley and Phillips (1987). The labile Fe^{3+} fraction may be related to Fe^{3+} mineral type or specific surface area as observed by Roden and Zachara (1996). These Fe^{3+} extraction techniques are strictly chemical processes that attempt to identify a Fe^{3+} mineral fraction that is biologically reactive. Though some correlation exists, comparisons between a chemical extraction of Fe^{3+} and the enzymatic biological utilization of Fe^{3+} are not inherently related processes. As such, these extractions may not be very quantitative, especially with respect to determining the long-term amount of recalcitrant crystalline Fe^{3+} that could be used.

Implementation of a slightly aggressive extraction, such as the 48 hour 0.5 N HCl used here, can provide a reasonable estimate of available Fe^{3+} but is

probably still conservative because portions of the nonextracted, bulk Fe^{3+} might be used in the long term. When this extraction was applied to sediment from old contaminated sites, it showed that 80 to 100% of the extractable Fe^{3+} fraction had been reduced to Fe^{2+}, as would generally be expected. However, for the sediments used in the microcosms, this method identified an Fe^{3+} fraction that appeared to be reducible by microbes in only 32 to 36 weeks, though the overall rate of biological activity in this test was admittedly quite high.

Although extraction testing to determine bioavailable Fe^{3+} is imperfect, such analyses are needed for assimilative capacity estimates. Very little aqueous Fe^{3+} is found at normal pH, so solid sources of Fe^{3+} must be considered. Estimates of available mineral Fe^{3+} are needed for natural attenuation predictive modeling involving Fe^{3+} reduction.

The 0.5 N HCl extraction technique served a second purpose by also isolating the comparatively small fraction of HCl extractable Fe^{2+} minerals deposited as a result of microbial processes. Long extraction time is less critical for Fe^{2+} analysis because extracting the maximum amount of biogenic mineral Fe^{2+} mass is desirable and to a point, over-extraction does not contribute significant Fe^{2+} in sediment where naturally occurring Fe^{2+} concentrations are small. For the systems studied, 80 to 100% of the total Fe was of an Fe^{2+} form where Fe^{3+} reduction occurred although background concentrations of bulk Fe^{3+} were quite high. This implies that the 48-hour extraction time used here isolated biogenically produced Fe^{2+} but did not over extract background Fe^{3+}. Using this

technique permitted the documentation of Fe^{3+} reduction and complimentary Fe^{2+} deposition in the field and laboratory.

An indication of the bulk Fe^{3+} and Fe^{2+} mineral content for a sediment can be determined by analyzing the 6 N HCl extract from AVS analysis. Based on mineral extraction data from both 0.5 N and 6 N HCl extractions, it appears that much of the bulk Fe^{3+} was not used for the time observed. Both field and microcosm data shows that perhaps 5 to 15% of the total Fe^{3+} present is consumed by enzymatic processes. The assimilative capacity of this fraction, however, is still very great. Examining the ratio of Fe^{2+} to Fe total from the 6 N HCl extraction can provide a statistical benchmark to gage the significance of the 0.5 N HCl extracted Fe^{2+}. It is suggested here that significant Fe^{3+} reduction can be inferred when the percent Fe^{2+} from the 0.5 N HCl extraction exceeds the 99% probability limit for the percent Fe^{2+} found from the 6 N HCl extraction.

Aqueous Fe^{2+} is found in association with CH_4 both in the microcosm experiments conducted here and at many intrinsic bioremediation study sites. Thus, it appears that mineral Fe^{3+} reduction does not compete effectively with methanogenic bacteria in aquifer systems. This observation is consistent with thermodynamic analysis wherein the free energy of reaction for many Fe^{3+} minerals is comparable or less than that of methanogenesis. Likewise, no evidence was found in microcosm or natural attenuation studies that natural mineral Fe^{3+} inhibited SO_4^{2-} reduction. This suggests that the competitive exclusion of SO_4^{2-} bacteria by Fe^{3+} is very limited. These observations do not preclude the possibility of SO_4^{2-} inhibition by very reactive Fe^{3+} (e.g. aqueous

Fe^{3+}) early in redox zone development; however, such iron is normally rare and may be discounted overall. In the microcosm tests, excess Fe^{2+} relative to sulfide from AVS, suggests that some Fe^{3+} reduction could have occurred concurrent with SO_4^{2-} reduction. Therefore, the redox sequence for aquifers should be considered $O_2 > NO_3^- > Mn^{4+} > SO_4^{2-} >$ methanogenesis, with Fe^{3+} reduction occurring in a range between SO_4^{2-} reduction and methanogenesis.

As mentioned, in microcosm, $Fe(OH)_3$ was reduced more readily than the native iron forms, which consisted mostly of more crystalline Fe_3O_2. Slower, first order utilization kinetics were found for enzymatic reduction of native minerals. Decreased microbial Fe^{3+} utilization associated with increased Fe^{3+} mineral crystallinity was found in several prior studies (Munch and Ottow, 1980 and 1983; and Roden and Zachara, 1996). Assuming a mixture of Fe^{3+} mineral species occur together in an aquifer, the more biologically reactive fraction may be initially consumed but the more crystalline Fe^{3+} fraction may be reduced slowly, possibly over many years. Data from intrinsic bioremediation studies commonly find some aqueous Fe^{2+}, indicating ongoing Fe^{3+} reduction at sites that have been contaminated for years or decades. Collectively, this evidence supports the concept that recalcitrant Fe^{3+} minerals, which comprise the bulk of Fe^{3+} in an aquifer, are probably being reduced. The presence of large quantities of mineral Fe^{3+}, coupled with slow reduction kinetics, permits Fe^{3+} reduction to occur for long periods. A mixture of reactive and recalcitrant Fe^{3+} mineral forms probably facilitates enzymatic reduction across a wide redox range.

As seen in microcosm and in natural attenuation studies, significant aqueous Fe^{2+} only occurs in the absence of SO_4^{2-} reduction. This is probably because any produced Fe^{2+} from enzymatic Fe^{3+} reduction is scavenged by reaction with HS^- to form FeS and can therefore, only be seen where SO_4^{2-} is depleted in methanogenic areas.

The reaction of aqueous Fe^{2+} with HS^- to form FeS is likely very fast, depressing aqueous Fe^{2+} should concurrent Fe^{3+} and SO_4^{2-} reduction occur. As described, Fe^{3+} reduction occurs with methanogenesis. Therefore, aqueous Fe^{2+} concentrations may more often be controlled by complexation reactions with HCO_3^- formed from acetoclastic methanogenesis. In microcosm, nonassociated aqueous Fe^{2+} demonstrated a remarkable ability to scavenge HCO_3^- (CO_2), presumably to form $FeCO_3$. It is inferred that aqueous Fe^{2+} concentrations increased only when supplies of HCO_3^- are exhausted. Acetoclastic methanogenesis produces HCO_3^-, probably limiting aqueous Fe^{2+} and encouraging $FeCO_3$ precipitation. In microcosm, the rate of $FeCO_3$ formation was at least as fast as HCO_3^- generation. In the absence of HCO_3^-, it is inferred that Fe^{2+} precipitation (presumably Fe_3O_4) is slower than the rate of Fe^{2+} generation, permitting some aqueous Fe^{2+} accumulation.

Based on field and microcosm observations it is concluded that most Fe^{2+} is ultimately expressed in mineral form. The kinetics of Fe^{2+} mineral formation appear to be rapid and nearly concurrent with Fe^{3+} reduction. Typical ground water flow rates are slow, on the order of cm or ft/day. Thus, in a dynamic aquifer system, Fe^{2+} minerals probably form at or near the point of Fe^{3+}

reduction. Occurrences of aqueous Fe^{2+} probably represent areas where Fe^{3+} reduction is active, though much larger quantities of Fe^{2+} minerals are being deposited at the same time. Elevated aqueous Fe^{2+} is possible in the presence of chelating agents though this was not observed here.

Due to the reasons described above, mineral Fe^{2+} analysis is the best method of determining Fe^{3+} expressed capacity. Fe^{2+} mineral analysis should be included as part of a natural attenuation study because expressed capacity calculations based on aqueous Fe^{2+} analysis alone may be very conservative. For the natural attenuation cases examined, aqueous Fe^{2+} did not extend beyond the contaminant plume. Therefore, a second reason for examining Fe^{2+} minerals is that they may be used as a fingerprint denoting the historical position of a retreating hydrocarbon plume.

Fe^{3+} expressed capacity can be overestimated. Fe^{3+} reduction can occur from abiotic processes including reactions with inorganic reductants (principally HS^-). During analysis, the effects of abiotic Fe^{3+} reduction by HS^- can be corrected by subtracting the stoichiometric quantities of Fe^{2+} associated with AVS. Nonenzymatic Fe^{3+} reduction can also occur by organic reductants; however, these compounds are generally microbial fermentation products, such as formic acid (Ghiorse, 1988). Therefore, reactions involving these organic reductants may still be classified as oxidation/reduction and correctly counted towards expressed capacity although they are not truly enzymatically controlled.

It is more likely for expressed capacity to be underestimated for Fe^{2+} due to the formation HCl resistant mineral forms, including crystalline $FeCO_3$, Fe_2O_3,

or FeS_2. Experimental extraction tests on fresh, poorly crystalline, microbiologically produced, $FeCO_3$ and Fe_2O_3 have not been done so their susceptibility to HCl extraction has not been observed. However, much Fe^{2+} was recovered from Fe^{3+} reducing microcosm sediments where $FeCO_3$ and Fe_2O_3 precipitation was suspected.

The experimental techniques developed for reduced S minerals were simple and effective in measuring AVS and CrES. SO_4^{2-} reducing zones could be identified readily in the field based on mineral analysis. Analyzing for only AVS and CrES is a simplified, extended sulfide extraction procedure; however, this level of discrimination is adequate for natural attenuation studies. AVS mostly formed in SO_4^{2-} reducing microcosms. Therefore, it is suggested that the presence of AVS is a general indicator of recent SO_4^{2-} reduction, which could be an important observation in a natural attenuation study. This technique may permit reduced mineral S analysis to become a routine part of natural attenuation assessment.

Total reduced sulfur (S_t) mineral formation was initially rapid in microcosm but decreased with time, possibly in response to limited Fe^{3+} surface reaction sites. CrES formation was zero order and initially slower than S_t. It is suggested that the rate of CrES formation increases when Fe^{3+} is limited. Assuming the models for S_t and CrES formation given in Chapter 6 are correct, AVS would attain a maximum value then decrease over time as CrES is formed. Systems high in Fe^{3+} appear to favor AVS preservation. Though these observations were

made from closed microcosm environments, data from field studies are supportive.

Dissolved HS^- was very low in the SO_4^{2-} reducing microcosms and is found to be small at natural attenuation study sites even where SO_4^{2-} reduction is active. HS^- is scavenged by reaction with Fe^{3+} minerals (or other oxidized species) or by degassing, keeping aqueous concentrations low. Therefore, there is limited opportunity for HS^- migration in an unconfined aquifer system. Comparing the rate of reduced S mineral formation to typical ground water seepage velocities it is concluded that AVS and CrES usually form near the point of SO_4^{2-} reduction. Therefore, the presence of these minerals may act as a fingerprint indicating past SO_4^{2-} reduction and possibly marking the historical extent of a retreating contaminant plume.

AVS and CrES mineral analyses provide a better estimate of SO_4^{2-} expressed capacity than water analysis alone and should be included in natural attenuation studies. Expressed capacity based on reduced S mineral analysis may be conservative due to:

- S cycling,
- HS^- loss as gaseous H_2S, and
- The generation of S species not detected (e.g. organo sulfides) by the techniques described here.

Relative to Fe and S processes, three reaction zones are postulated to occur as viewed in cross-section longitudinally through the centroid of a contaminated aquifer (Figure 58). Zone 1 contains organic contaminants,

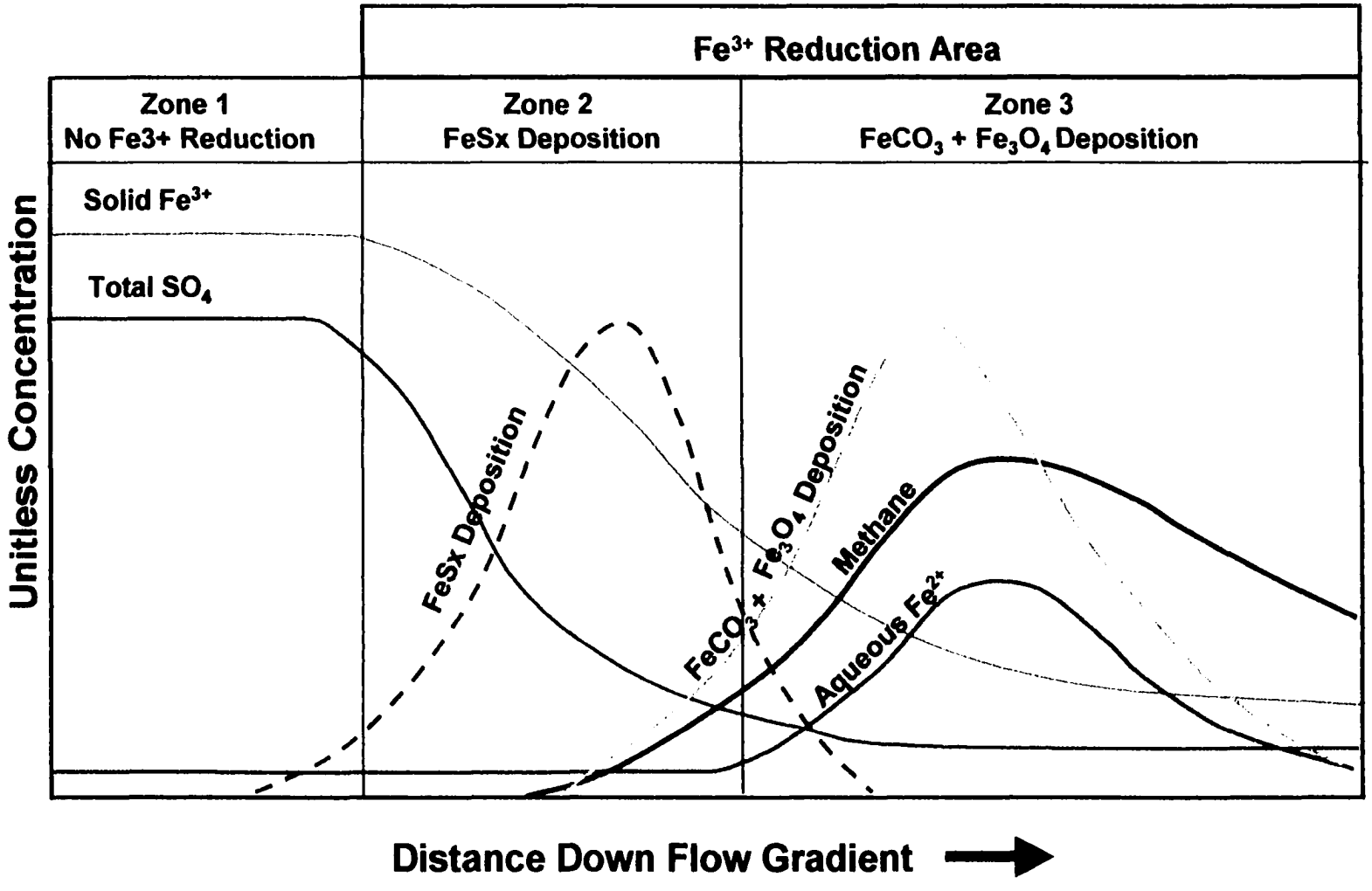

Figure 58. Conceptual Fe and S system through the centerline transect of a contamination plume.

however, neither Fe^{3+} or SO_4^{2-} undergo reduction due to competitive inhibition by O_2 and/or NO_3^- reducing bacteria. Zone 1 contains background concentrations of Fe^{3+} and SO_4^{2-}.

In Zone 2, O_2 and NO_3^- have been depleted and SO_4^{2-} reduction occurs. Fe^{3+} reduction is attributed mostly to abiotic reactions with HS^-; however, limited enzymatic Fe^{3+} reduction may also occur with a small amount of labile minerals or dissolved Fe^{3+}. Enzymatically produced Fe^{2+} can be bound as AVS making discernment of enzymatic Fe^{3+} reduction difficult. Loss of Fe^{3+} occurs as AVS is initially formed. AVS and HCl extractable Fe^{2+} is lost over time as AVS is converted to CrES (FeS_2). HS^- reacts with Fe^{3+} minerals rapidly permitting little migration and causing AVS formation near the point where SO_4^{2-} reduction occurs. Where Fe^{3+} is abundant, the rate of CrES formation is reduced. The presence of SO_4^{2-} in Zone 2 inhibits CH_4 production.

In Zone 3, levels of SO_4^{2-} have been depleted permitting methanogenesis. Redox conditions are sufficiently low as to allow enzymatic Fe^{3+} mineral reduction. Although labile Fe^{3+} mineral species, such as $Fe(OH)_3$, may initially be reduced, recalcitrant forms, like Fe_2O_3, are also utilized over time. In this zone, aqueous Fe^{2+} combines with HCO_3^- to form mineral $FeCO_3$ precipitates. Enzymatic Fe^{3+} reduction produces more Fe^{2+} than HCO_3^-. Therefore, most Fe^{2+} reacts with HCO_3^- generated from concurrent acetoclastic methanogenesis. Kinetically, $FeCO_3$ formation is rapid and limits both aqueous Fe^{2+} and HCO_3^- concentrations. When Fe^{3+} reduction is vigorous and HCO_3^- is depleted, other mineral forms (presumably Fe_3O_4) precipitate. In this case, the rate of mineral

Fe^{2+} deposition may be less than the rate of Fe^{2+} production allowing an increase in aqueous Fe^{2+}. Most Fe^{2+}, however, is deposited in this zone as a mineral a short distance from the point of formation. Fe ion exchange processes may also occur.

7.2. Application to Engineered Systems

For treatment design, this research may best be applied to a batch or continuous flow reactor system. There was no difference in the degradation rates of synthetic leachate for systems amended with Fe^{3+} and SO_4^{2-} minerals compared to systems with no mineral amendments; however, the rate of organic consumption was high for all systems at ~0.34 mMol/week (~ 190 mg/(L•week)). The importance of adding Fe^{3+} and SO_4^{2-} minerals is that the leachate could largely be mineralized while controlling greenhouse gas emissions. The addition of gypsum SO_4^{2-} inhibited CH_4 production. Waste wallboard, which consists largely of gypsum, could conceivably be used as a source for SO_4^{2-}. Through proper selection of native Fe^{3+} bearing sediments, produced H_2S could be controlled by precipitation as reduced sulfur minerals. SO_4^{2-} reduction, however, results in the generation of CO_2. Conversely, the addition of reactive $Fe(OH)_3$ poorly inhibited CH_4 production but was extremely effective in eliminating CO_2. It is not likely that native sediments can serve as a significant source for labile Fe^{3+} and a synthetic source would be needed for commercial application.

If CO_2 is not a concern, then a SO_4^{2-} reducing treatment system could be used alone. Alternatively, a system using Fe^{3+} reduction could be used to scrub

out CO_2 while producing more pure CH_4 that could then be used for electrical cogeneration. A duel system could also be developed where CO_2 from SO_4^{2-} reduction could be scavenged by a secondary Fe^{3+} reduction reactor run in sequence. Finally, with additional research, it might be possible to increase the efficiency of the Fe^{3+} reduction system so that CH_4 is inhibited in addition to CO_2. These systems have the advantage of mineralizing not only the organics but also converting typical microbial respiratory gases into various minerals as well.

7.3. Implications for Bioremediation Modeling

The logical extension to intrinsic bioremediation theory is its application to computer ground water/mass transport modeling. Fundamentally, the approach for such models is to simulate the mass transport of a labile organic that is simultaneously undergoing biological degradation. Such models could be used to:

- Predict the maximum size and ultimate down-gradient limit of organic movement for compliance purposes;
- Predict contaminant concentrations both spatially and temporally for RBCA analysis;
- Estimate the time for complete aquifer restoration via intrinsic bioremediation;
- Evaluate assimilative capacity in a dynamic system; and
- Examine various engineered remediation treatment scenarios in combination with intrinsic processes.

In this section, research results and conclusions are discussed in relationship to existing mass transport/bioreactive computer models. These models are reviewed in terms of their applicability relative to the intrinsic bioremediation concepts presented above. The adaptation of research conclusions into reactive mass transport models is then conceptualized.

7.3.1. Review of Existing Bioremediation Models

Three reactive mass transport models have been developed for public distribution and are reviewed here. These include, Bioplume II (Rafai et al., 1987), Bioscreen (Newell et al., 1996), and Bioplume III (Rafai et al., 1997). These models are selected for review here because they are public domain and they effectively demonstrate the state-of-the-art with respect to biochemical reactive mass transport.

Bioscreen is a one-dimensional model solving the mass transport equation through the use of the Domenico Equation (Domenico, 1987). As developed this analytical solution has the ability to approximate advection, dispersion, adsorption, and simple first order decay. The model has been adapted by Newell et al. (1996) to include intrinsic bioremediation from O_2, NO_3^-, Fe^{3+}, and SO_4^{2-} reduction and methanogenesis. Assimilative capacity is calculated for each soluble electron acceptor or respiratory product by determining the difference between their respective concentrations in the hydrocarbon plume and their background values multiplied by the appropriate stoichiometric mass ratio, similar

to methods described in Chapter 5. For simplicity, a total assimilative capacity value is calculated by effectively adding up the assimilative capacity for each electron acceptor. Only mass transport of the hydrocarbon plume is simulated. The model assumes instantaneous reaction kinetics, simultaneously eliminating both hydrocarbon and assimilative capacity by superposition along the plume length. Bioscreen is intended to be a simple screening tool and has several inherent limitations including the assumption that all redox reactions occur simultaneously and instantaneously, effectively negating the possibility of redox zone development as commonly observed in the field.

Bioplume II and III are two-dimensional models that solve for mass transport using the Method of Characteristics (MOC) as per Konikow and Bredehoeft (1978). Bioplume II simulates aerobic organic decay, but anaerobic processes can be addressed by specifying global first-order decay after oxygen is consumed. Bioplume III is an advancement of Bioplume II. It is designed to simulate all major redox processes independently, including O_2, NO_3^-, Fe^{3+}, and SO_4^{2-} reduction and methanogenesis. As a convention, methanogenesis is still assumed to occur as a redox reaction involving the reduction of CO_2. Bioplume III still has the option of simulating bulk organic decay by specifying first order decay.

For Bioplume III, mass transport is calculated for all electron acceptors as well as for the organic contaminant. Organic decay is simulated using the principle of superposition. Here, the computed mass of electron acceptor is reacted stoichiometrically with an amount of organic predicted to be present in a

model cell causing the mutual destruction of both according to a defined kinetic rate. The kinetic models available include zero-order, first order, instantaneous reaction (a subset of zero order); and Monod. For example, such a model can be specified so that 3.1 mg/L O_2 in a cell would mutually destroy 1 mg/L Benzene according to any of the kinetic models.

For Bioplume III the electron acceptor sequence is O_2 before NO_3^- followed by Fe^{3+} and SO_4^{2-} reduction followed by methanogenesis and the order of this reaction sequence is fixed. Uniquely, this model does assume that the Fe^{3+} source is in the form of a non-migrating solid. However, the resulting reduced Fe^{2+} is modeled as being completely aqueous.

7.3.2. Recommended Model Improvements

Multidimensional models like Bioplume III can approximate natural attenuation. Several improvements in these models are possible based on the conclusions reached in this research. These conceptual modifications could allow the models to better conform to actual conditions observed in the field.

Recommendation 1: Electron Acceptor Sequence

The electron acceptor sequence commonly implemented assumes the classical electron acceptor consumption order of $O_2 > NO_3^- > Fe^{3+} > SO_4^{2-}$ then methanogenesis. With respect to this sequence, one should consider Fe^{3+} reduction across a broad redox range concurrent with SO_4^{2-} reduction and

methanogenesis. Currently, Bioplume III does not include the simultaneous operation of two or more redox processes, which should be included in subsequent code. Conversely, for Bioscreen all redox processes are assumed to operate instantaneously and at once, which can also be an erroneous assumption.

Recommendation 2: Inclusion of Reduced Fe and S Minerals

Current reactive mass transport models do not include reduced Fe and S mineral precipitation. Bioplume III assumes solid Fe^{3+} but predicts that Fe^{2+} is aqueous. Future reactive mass transport models should consider modules that include Fe and S precipitation. Such precipitation may even have effects on aquifer permeability as minerals are dissolved or precipitated. Including such reactions can be important in model calibration, especially if Fe and S mineral analyses are included in a complimentary natural attenuation study. For example, as generally employed in a reaction model, aqueous electron acceptor reaction rates are determined empirically by first estimating a value then refining kinetic rates through successive model iterations until the predicted consumption of an electron acceptor matches observed field conditions. This procedure is impossible for mineral Fe^{3+} because there is no aqueous phase. Iterative kinetic rate determination is possible for SO_4^{2-} reduction, however, calibration against measured mineral sulfides would add significant validity to the model. Fe and S mineral modules should address the following theoretical considerations:

- For sites with moderate SO_4^{2-} and high Fe^{3+} mineral content, iron sulfide deposition could be modeled as an instantaneous precipitation reaction stoichiometrically reducing mineral Fe^{3+} to mineral Fe^{2+} using superposition;
- For sites with high SO_4^{2-} relative to Fe^{3+}, the deposition of iron sulfide could follow an equation similar to Equation 37. HS^- not captured by mineral precipitation should be lost from the system as H_2S gas; and
- Fe^{2+} deposition could be generally modeled as instantaneous without introducing much error.

Reduced Fe and S mineral deposition can be modeled as instantaneous, considering most ground water seepage velocities are slow. This opens the possibility of combining bioreactive mass transport models with equilibrium geochemical models such as PHREEQE (Parkhurst et al., 1980) with the added consideration that unsaturated aquifer conditions are not truly closed with respect to gas phases.

Recommendation 3: Methanogenic Reactions

Organic contaminant degradation via methanogenesis is approached as if CO_2 was an electron acceptor and is consumed during methane formation. This approach treats all microbial degradation as a redox reaction with an external electron acceptor. In fact, during acetoclastic methanogenesis CO_2 is generated

and is not limiting. Future models should assume methanogenesis is independent of CO_2 concentrations and organic decay should proceed according to a specified kinetic model.

7.3.3. Simplified Natural Attenuation Approach

In the microcosm study, it was observed that the rate of organic consumption for Fe^{3+} and SO_4^{2-} reduction and methanogenesis were all approximately equal. As discussed above, methanogenesis is not limited by external electron acceptor stoichiometry. Therefore, the overall organic degradation rate may ultimately be independent of electron acceptor mass at least with respect to Fe^{3+} and SO_4^{2-} reduction and methanogenesis. This provides an opportunity to greatly simplify bioreactive mass transport modeling. Conceptually, contaminant mass transport could be modeled with a single kinetic model and rate variable without tracking electron acceptor mass balance. This single rate idea is supported by field derived organic rate constants. For example, Wiedemeier et al. (1997) develop a technique that estimates a single, first order rate constant for hydrocarbon degradation through the entire length of a plume irrespective of redox zones. Similarly, Bekins et al. (1998) develop a single equation to describe organic decay across all redox zones based on a simplification of Monod (1949). This simplified rate constant approach could be especially useful when there is some doubt as to redox processes or electron acceptor mass. It should be noted that simulations that track electron acceptor

reactions have the advantage of demonstrating redox zone development, which will aid in model calibration and verification.

7.3.4. Summary of Conceptual Model Development

As defined, *natural attenuation* is the reduction of contaminant concentrations by inherent aquifer processes. The most important of these processes include intrinsic bioremediation, advection/dispersion and, adsorption all of which can be simulated with reactive mass transport computer models. Intrinsic bioremediation by Fe^{3+} and SO_4^{2-} reduction can be a significant mechanism for organic destruction. Fe^{3+} and SO_4^{2-} reductive processes are not adequately addressed in existing reaction/mass transport models. New models should be developed that allow Fe^{3+} reduction to occur concurrent with other redox processes including SO_4^{2-} reduction and methanogenesis. These models should also simulate the precipitation of reduced Fe and S minerals. Models need to be developed for organic decay by methanogenesis that are independent of any electron acceptor concentration. These improvements will 1) add to the understanding of the natural system, 2) permit better model calibration and 3) facilitate more accurate modeling of intrinsic bioremediation processes.

8. REFERENCES

Aggarwal, P., J. Means, D. Downey, and R. Hinchee, 1991. Use of Hydrogen Peroxide as an Oxygen Source for In-Situ Biodegradation: Part II, Laboratory Studies; Journal of Hazardous Materials. 27:301-314.

Albrechtsen, H. H. Gorm, and T. Christensen, 1994. Limiting factors for microbial Fe(III) reduction in a landfill leachate polluted aquifer (Vejen, Denmark); Federation European Microbiological Society, Microbiology Ecology, 604:1-15.

Appelo, C., and D. Postma, 1994. Geochemistry, groundwater and pollution; A.A. Balkema, Rotterdam, p. 536.

ASTM, 1995. Standard guide for risk-based corrective action applied at petroleum release sites; Designation: E 1739-95, West Conshohocken, PA., p. 51-68.

ASTM, 1996. Standard guide for remediation by natural attenuation at petroleum release sites (DRAFT).

Atlas, R. and R. Bartha, 1993. Microbial ecology, fundamentals and applications; Benjamin/Cummings, N.Y., NY.

Augenstein D., 1992. The greenhouse effect and US landfill methane; Global Environmental Change, EMCON Association 2(4), 311-328.

Barbaro, J., J. Barker, L. Lemon, and C. Mayfield, 1992. Biotransformation of BTEX under anaerobic denitrifying conditions: Field and laboratory observations, Journal of Contaminant Hydrology, 11:245-272.

Baedecker, M., I. Cozzarelli, J. Evans, and P. Hearn, 1992. Authigenic mineral formation in aquifers rich in organic material; In: Water-Rock Interaction, Proc. 7th International Symp. on Water Rock Interaction, Yousif K. Kharaka and Ann S. Maest eds., A.A. Balkema Pub., p. 257-261.

Baedecker, M. and W. Back. 1979. Hydrogeological processes and chemical reactions at a landfill; Ground Water, 17(5):429-437.

Beeman, R. and J. Suflita, 1990. Environmental factors influencing methaogenesis in a shallow anoxic aquifer: a field and laboratory study; Journal Industrial Microbiology, 5:45-58.

Bekins, B., E. Warren, and E. Godsy, 1997. A comparison of zero-order, first-order, and Monod biotransformation models; Ground Water, 36(2):261-268.

Belevi, H. and P. Baccini, 1992. Long-term leachate emissions from municipal solid waste landfills; in: Landfilling of Wastes: Leachate, T.H. Christensen, R. Cossu, and R. Stegmann eds., Elsevier Applied Science; London, pp. 431-440.

Beller, H., D. Grbic-Galic, and M. Reinhard, 1992. Microbial degradation of toluene under sulfate-reducing conditions and the influence of iron on the process; Applied & Environmental Microbiology, 58:786-793.

Bennett, P., 1991. Quartz dissolution in organic-rich aqueous systems. Geochimica Cosmochimica Acta, 49:1781-1797.

Bennet, P., D. Siegel, M. Baedecker, and M. Hult, 1992. Crude oil in a shallow sand and gravel aquifer: I. Hydrogeology and inorganic geochemistry; Applied Geochemistry, 8:529-549.

Berner, R., 1980. Early digenesis, Princeton University Press, Prenceton, NJ., p. 241.

Bianchi-Mosquera, G., R. Allen-King and D. Mackay. 1994. Enhanced Degradation of Dissolved Benzene and Toluene Using a Solid Oxygen Releasing Compound; Ground Water Monitoring & Remediation (Winter). pp 120-128.

Bjerg, P., D. Rugge, H. Pedersen, and T. Christensen, 1995. Distribution of redox-sensitive groundwater quality parameters down gradient of a landfill (Grindsted, Denmark); Environmental Science Technology, 29:1387-1394.

Brady, C., 1990. The nature and properties of soils, Macmillian Pub. Co., N.Y.

Brown, K and K. Donnelly, 1988. An estimation of the risk associated with the organic constituents of hazardous and municipal waste landfill leachates; Hazardous Wastes and Hazardous Materials, 5(1):1-30.

Canfield D., 1988. Reactive iron in marine sediments; Geochimica et Cosmochimica Acta, 53:619-632.

Canfield, D., B. Jorgensen, H. Fossing, R. Glud, J. Gundersen, N. Ramsing, B. Thamdrup, J. Hansen, L. Nielsen, and P. Hall, 1993. Pathways of organic carbon oxidation in three continental margin sediments; Marine Geology, 113:27-40.

Canfield D., R. Raiswell, J. Westrich, C. Reaves, and R. Berner, 1986. The use of chromium reduction in the analysis of reduced inorganic sulfur in sediments and shales; Chemical Geology, 54:149-155.

Chapelle, F., 1992. Ground-water microbiology; John Wiley and Sons, Inc., N.Y., N.Y.

Chesterman, C., and K. Lowe, 1987. Field guide to north American rocks and minerals; Audobon Society Press, N.Y., NY.

Cline, P., J. Delfino, P. Rao, 1991. Partitioning of aromatic constituents into water from gasoline and other complex solvent mixtures: Environmental Science and Technology, 17(4)227-223.

CFR, Code of Federal Regulations, Part 40, subpart 257.

Crouzet, C., R. Altmann, and A. Bourg, 1994. Sulfur speciation in aquifer sediments contaminated by landfill leachate: Methodology and application of the Vejen landfill, Denmark;Dept. of Geochem. and Phys. Chem., BRGM, 45060 Orleans Cedex 2, France (unpublished), pp. 27.

DOE, 1997. Monthly energy review; Department of Energy, June Report, DOE/EIA-0035(97/06).

DOE, 1994. Annual Energy Review; Department of Energy, DOE/EIA-0384(94).

Domenico, P.A., 1987. Analytical model for multidimensional transport of a decaying contaminant species; Journal of Hydrology, 91:49-58.

Drobner, E., H. Huber, G. Wachtershauser, D. Rose, and K. Stetter, 1990. Pyrite formation linked with hydrogen evolution under anaerobic conditions; Nature, 346:742-744.

Eaton, A., L. Clesceri, and A. Greenberg, eds, 1995. Standard methods for the examination of water and wastewater, American Water Works Association, Denver, CO.

Ehrig, H.J., 1989. Water and element balances of landfills, in: Lecture notes in earth sciences, the landfill; P. Baccini, ed., Springer-Verlag Press, New York, NY, p 83-115.

EPA, 1989. Evaluation of ground-water extraction remedies: Volumes 1 and 2. Washington, D.C., EPA, Office of Emergency and Remedial Response.

EPA, 1992. Evaluation of ground-water extraction remedies: Phase II, Volume 1 – Sumary Report; EPA, Office of Emergency and Remedial Response, Washington, D.C., EPA-9355.4-05.

EPA, 1977. Procedures manual for ground water monitoring at solid waste disposal facilities; EPA, Office of Emergency and Remedial Response, Washington, D.C., EPA/530/ SW-6 11.

EPA, 1984. The hydrologic evaluation of landfill performance (HELP) model: Volume 1 User's guide for version 1; EPA, Office of Emergency and Remedial Response. EPA/530/SW-84-009.

EPA, 1993. Cleaning up the nation's waste sites: Markets and technology trends; Office of Solid Waste and Emergency Response, EPA 542-R-92-012

Ehrlich, H., 1996. Geomicrobiology, Marcel Dekker, N.Y, pp. 719.

Evangelou, V., and Y. Zhang 1995. A review: pyrite oxidation mechanisms and acid mine drainage prevention; Critical Reviews in Environmental Science and Technology; 25(2):141-199.

Farina, M., D. Motta, S. Esquivel, and H. Lins de Barros, 1990. Magnetic iron-sulphur crystals from a magnetotactic microorganism; Nature, 343:256-258.

Federal Register, 1996. Rules and Regulations; June, p. 9905-9944.

Federal Register, 1982. Rules and Regulations; July, pp. 32284.

Federal Register, 1981. Rules and Regulations; Feb., pp. 11128.

Fetter, C., 1994. Applied hydrogeology, Third Edition; Prentice Hall, N.J.,

Fortin, D., B. Davis, G. Southam, and T. Beveridge 1994 Biogeochemical phenomena induced by bacteria within sulfidic mine tailings; Journal Industrial Microbiology.; 14:178-185.

Fortin, D., B. Davis, and T. Beveridge, 1996. Role of thiobacillus and sulfate-reducing bacteria in iron biocycling in oxic and acidic mine tailings; FEMS Microbiology Ecology; in press.

Fossing, H. and B. Jorgensen, 1989. Measurement of bacterial sulfate reduction in sediments: Evaluation of a single-step chromium reduction method; Biogeochemistry, 8:205-222.

Furrer, G., Urs von Gunten, J. Zobrist, 1996. Steady-state modelling of biogeochemical processes in columns with aquifer material: Speciation and mass balances; Chemical Geology, 133:15-28.

Gaudy, A. and E. Gaudy, 1988. Elements of bioenvironmental engineering; Engineering Press, Inc., San Jose, CA.

Ghiorse, W., 1988. Microbial reduction of manganese and iron. In: A.J.B. Zehnder, ed. Biology of Anaerobic Microorganisms. Wiley, New York, N.Y.

Gilbert, R., 1987. Statistical methods for environmental pollution monitoring; Van Nostrand Reinhold Co., N.Y., N.Y.

Goldberg, M., N. Homsi, L. Goulet, and H. Riberdy, 1995. Incidence of cancer among persons living near a municipal solid waste landfill site in Montreal, Québec; Archives of Environmental Health, 50(6):416-424.

Goldstein, N., 1997. The state of garbage in America; Biocycle, 38(4): 60-67.

Ground Water Quality Standards, 1988. Wisconsin Department of Natural Resources.

Gurljala, R. and J. Suflita, 1993. Environmental factors enfluencing methanogenesis from refuse in landfill samples; Environmental Science Technology, 27:1178-1181.

Hardie, L., 1991. On the significance of evaporites. Annual Review fo Earth Planet Science, 19:131-168.

Hach, 1992. Water quality handbook; Hach Company, Loveland CO.

Ham, Robert, 1979. Recovery Processing and Utilization of Gas from Sanitary Landfills; EPA 600/2-79-001.

Hamilton, B., 1995. Automotive gasoline; World wide web data resource, B.Hamilton@irl.cri.nz.

Hiebert F. and P. Bennett, 1992. Microbial control of silicate weathering in organic-rich ground water. Science, 259:278-281.

Hertzman, C., M. Hayes, J. Singer, and J. Highland, 1987. Upper Ottawa street landfill site health study; Environmental Health Perspectives, 75: 173-195.

Herlihy, A., 1987. Sulfur dynamics in an impoundment receiving acid mine drainage; Ph.D. Dissertation, Univ. Virginia.

Heron, G., 1994. Redox buffering in landfill leachate contaminated aquifers; M.S. Thesis, Institute of Environmental Science and Engineering, Technical University of Denmark.

Heron, G. and T. Christensen, 1995. Impact of sediment-bound iron on redox buffering in a landfill leachate polluted aquifer (Vejen, Denmark); Environmental Science and Technology, 29:187-192.

Heron, G., C. Catherine, A. Bourg, and T.H. Christensen, 1994[a]. Speciation of Fe II and Fe III in contaminated aquifer sediments using chemical extraction techniques; Environmental Science and Technology, 28:1698-1705.

Heron, G., T. Christensen, and J. Tjell, 1994[b]. Oxidation capacity of aquifer sediments; Environmental Science Technology, 28:153-158.

Hem, J., 1985. Study and interpretation of the chemical characteristics of natural water; 3ed ed., U.S. Geological Survey, Water Supply Paper No. 2254., Alexandria, VA.

Hinchee, R., D. Downey, and P. Aggarwal, 1991. Use of Hydrogen Peroxide as an Oxygen Source for In-Situ Biodegradation: Part I, Field Studies.. Journal of Hazardous Materials. 27:315-325.

Hoeks, J. and R. Borst, 1982. Anaerobic digestion of free volatile fatty acids in soils below waste tips; Water Air Soil Pollution, 17:165-173.

Horan, N.J., 1990. Biological wastewater treatment systems; John Wiley and Sons, N.Y., N.Y. 310 p.

Howarth, R., 1979. Pyrite: its rapid formation in a salt marsh and its importance in ecosystem metabolism; Science, 203:49-51.

Howarth, R., B. Jorgensen, 1984. Formation of ^{35}S-Labelled elemental sulfur and pyrite in coastal marine sediments (Limfjorden and Kysing Fjord, Denmark) during short-term $^{35}SO_4^{2-}$ reduction measurements; Geochimica et Cosmochimica Acta, 48:1807-1818.

Huang, P. and M. Schnitzer, 1986. Interactions of soil minerals with natural organics and microbes; Soil Science Society of America No 17., Madison, WA.

Huling, S. and B. Bledsoe, 1990. Enhanced Bioremediation Utilizing Hydrogen Peroxide as a Supplemental Source of Oxygen; EPA/600/2-90/006; NTIS: PB90-183435.

Hutchins, S., D. Miller, F. Beck, A. Thomas, S. Williams, and G. Willis, 1996. Nitrate-based bioremediation of JP-4 jet fuel: pilot-scale demonstration; in: Applied bioremediation of petroleum hydrocarbons, R.E. Hincheee and J.A. Kittel eds., Battelle Press, Columbus, OH, pp.123-131.

Hutchins, S., W. Downs, G. Smith, J. Wilson, D. Hendrix, D. Fine, D. Kovacs, R. Douglass, 1991a. Effect of nitrate addition on biorestoration of fuel-contaminated aquifer: field demonstration, Ground Water, 29(4):571-580.

Hutchins, S., S. Moolenaar, and D. Rhodes, 1992. Column studies on BTEX biodegradation under microaerophilic and denitrifying conditions, Journal Hazardous Materials., 32:195-214.

International Technologies, 1996. George Air Force Base draft natural attenuation monitoring treatability study report operational unit 2; Air Force Center for Environmental Excellence, San Antonio, TX.

Jenne, E., 1977. Trace element sorption by sediments and soils – sites and processes; in: W.R. Chappell and K.K. Peterson (Editors), Molybdenum in the Environment, Vol. 2. Marcel Dekker, New York, NY. pp. 425-553.

Johnson, P., C. Stanley, M. Kemblowski, D. Byers, and J. Colthart, 1990. A practical approach to the design, operation, and monitoring of in-situ soil-venting systems; Ground Water Monitoring Review, Spring, pp. 159-178.

Jorgensen, B., 1990. A thiosulfate shunt in the sulfur cycle of marine sediments; Science 249: 152-154.

Kennedy, L., 1998. Application of mineral iron and sulfide analysis to evaluate natural attenuation at a fuel contaminated site; American Society of Civil Engineers, Journal of Environmental Engineering, In Press.

Kennedy, L., and J. Everett, 1996. Augmented in-situ bioremediation of landfill leachate by electron acceptor supplementation using naturally occurring earth minerals; Twelfth International Conference on Solid Waste Management and Secondary Materials, Philadelphia, PA.

Kennedy, L. and S. Hutchins, 1993. Applied geologic, microbiological, and engineering constraints of in-situ BTEX bioremediation; Remediation, Winter: pp. 83 -107.

Kjeldsen, P. and T. Christensen,1994. Soil attenuation of acid phase landfill leachate; Waste Managment Research, 2:247-263.

Kmet, P. and P. McGinley, 1982. Chemical characteristics of leachate from municipal solid waste landfills in Wisconsin; 5th Annual Madison Conference of Applied Research and Practice on Municipal & Industrial Waste, Madison, Wisconsin.

Knox, K and P. Jones, 1979. Complexation characteristics of sanitary landfill leachates; Ground Water Res., 13:839-846.

Komadel, P. and J. Stucki, 1988. Quantitative assay of m3inerals for Fe^{2+} and Fe^{3+} using 1,10-Phenalthroline: III. A rapid photochemical method; Clays and clay minerals, 36(4):379-81.

Konikow, L. and Bredehoeft, J., 1978. Computer model of two-dimensional solute transport and dispersion in ground water; Automated data processing and computations techniques of water resources investigations of the U.S. Geological Society, Washington. D.C.

LaGrega, M., P. Buckingham, and J. Evans, 1994. Hazardous waste management; McGraw-Hill, Inc., New York, NY.

Leach, L., F. Beck, J. Wilson, and D. Kampbell, 1988. Asceptic subsurface sampling techniques for hollow-stem auger drilling; Proceedings of the 2ed National Outdoor Action Conference on Aquifer Restoration, Ground Water Monitoring and Geophysical Methods; Association of Ground Water Scientists and Engineers, Las Vegas, NV, 1:2-24.

Litchfield, J., and L. Clark, 1973. Bacterial activities in ground waters containing petroleum products, Pub. 4211, Am. Petrol. Inst., Washington, D.C., p. 43

Lovley, D., and E. Phillips, 1986. Organic matter mineralization with reduction of ferric iron in anaeroic sediments, Applied and Environmental Microbiology, 51(4):683-689.

Lovley, D., 1991. Dissimilatory Fe(III) and Mn(IV) reduction; Microbiology Review; 55:259-287.

Lovley, D., and E. Phillips, 1987. Rapid assay for microbially reducible ferric iron in aquatic sediments; Applied and Environmental Microbiology.; 53(7):1536-1540.

Lovley, D., 1987. Organic matter mineralization with the reduction of ferric iron: a review, Geomicrobiology Journal, 5(3/4):375-399.

Lovley, D. 1990. Dissimilatory Fe(III) and Mn (IV) reduction. Microbiology Review, 55:259-287.

Lovley, D., Phillips, E. and Lonergan, D. J., 1991. Enzymatic versus nonenzymatic mechanisms for Fe (III) reduction in aquatic sediments. Environmental Science Technology, 25:1062-1067.

Lovley, D., E. Roden, E. Phillips and J. Woodward, 1993. Enzymatic iron and uranium reduction by sulfate-reducing bacteria; Marine Geology, 113:41-53.

Lyngkilde, J., and T. Christensen, 1992. Redox zones of a landfill leachate pollution plume (Vejen, Denmark); Journal Contaminant Hydrology, 10:273-289.

Lyon, W., 1995. Assessment of redox categories in soils and sediments monitoring iron minerals and hydrogen; Internal report, Robert S. Kerr Laboratory, National Environmental Risk Management Laboratory, Ada, OK. pp. 7.

Lyon W., and R. Glass, 1997[a]. Anaerobic HCl extraction of soils or sediments: Rapid sample preparation prior to a screening test for microbially available iron, U.S.E.P.A,. Robert S. Kerr Lab, Ada, OK, p. 13.

Lyon W., and R. Glass, 1997[b]. Development of a rapid iron extraction method using 0.5 M HCl, 3. Drying and extraction experiments with synthetic ferric gels: An interim Internal Report, U.S.E.P.A,. Robert S. Kerr Lab, Ada, OK, p. 28.

Lyon, W., R. Glass, M. Ye, and N. Vela, 1997. Development of a rapid iron extraction method using 0.5 M HCl; 1. Application to samples from George AFB; An interim Internal Report, U.S.E.P.A,. Robert S. Kerr Lab, Ada, OK, p. 25.

Mann, S., N. Sparks, R. Frankel, D. Bazylinski, and H. Jannasch, 1990. Biomineralization of ferrimagnetic gregite (Fe3S3) and iron pyrite (FeS2) in a magnetotactic bacterium; Nature, 343:258-261.

McBean, E., F. Rovers, G. Farquhar, 1995. Solid waste landfill engineering and design; Prentice-Hall, Inc., Englewood Cliffs, NJ

McCarty, P. 1990. Scientific limits to remediation of contaminated soils and ground water; In: Ground water and soil contamination remediation: Toward compatible science, policy, and public perception. Washington, D.C.: National Academy Press, p. 38-53.

McCarty, P. 1971. Energetics and bacterial growth, In: Organic Compounds and Aquatic Environments, Samuel J. Faust and Joseph V. Hunter eds., Marcell Dekker, Inc. Pub., N.Y., Ch 10, 495 - 531

Weast, R., M. Astle, W. Beyer, 1987. CRC handbook of chemistry and physics; 67th ed., CRC Press, Inc., Boca Raton, FL.

Mehlman, M. 1992. Dangerous and cancer-causing properties of products and chemicals in the oil refining and petrochemical industry; Environmental Research, 59: 238-249.

Mehlman, M. 1995. Dangerous and cancer-causing properties of products and chemicals in the oil refining and petrochemical industry: part xv. health hazards and health risks from oxygenated auomobile fuels (MTBE): lessons not heeded; International Journal of Occupational Medicine and Toxicology, 4(2):1-17

Metcalfe, D., 1982. Modeling Gas Transport from Waste Disposal Sites; M.A.Sc. Thesis, Department of Civil Engineering, University of Waterloo, Waterloo, Ontario.

Monod, J., 1949. The growth of bacterial cultures; Annual Review of Microbiology, 3:371-394.

Morse, J., F. Millero, J. Cornwell, and D. Rickard, 1987. The chemistry of the hydrogen sulfide and iron sulfide systems in natural waters; Earth Science Review, 24:1-42.

Moses, C., A. Herlihy, J. Herman, and A. Mills, 1988. Ion-chromatographic analysis of mixtures of ferrous and ferric iron; Talanta, 35(1):15-22.

Moses, C., and J. Herman, 1989. Pyrite oxidation at circumneutral pH; Geochimica et Cosmochimica Acta, 55:471-482.

Murray, J., J. Rouse, , A. Carpenter, 1981. Groundwater contamination by sanitary landfill leachate and domestic wastewater in carbonate terrain: Implications; Water Research, 15:745-757.

Munch, J. and J. Ottow, 1980. Preferential reduction of amorphous to crystalline iron oxides by bacterial activity; Soil Science, 129(1):15-21.

Munch, J. and J. Ottow, 1983. Reductive transformation mechanism of ferric oxides in hydromorphic soils; Environmental Biogeochemistry, 35:383-394.

National Research Council, 1994. Alternatives for ground water cleanup; National Academy Press, Washington D.C., pp. 315.

Newell, C., R. McLeod, and J. Gonzales, 1996. Bioscreen: Natural attenuation decision suport system users manual, version 1.3; Center for Subsurface Modeling Support, Robert S. Kerr Environmental Risk Management Research Laboratory, Ada, OK.

Nicholson, R., J. Cherry, E. Reardon, 1983. Migration of contaminants in groundwater at a landfill: a case study. 6. Hydrogeochemistry; Journal Hydrology, 63, 131-176.

Norris, R., R. Hinchee, R. Brown, P. McCarty, J. T. Wilson, M. Reinhard, E. J. Bouwer, R. Borden, T. M. Vogel, J. M. Thomas, and C. H. Ward, 1994. Handbook of bioremediation; Lewis Publishers, Boca Raton, FL.

Odencrantz, J., J. Johnson, and S. Koenigsberg. 1996. Enhanced Intrinsic Bioremediation Hydrocarbons Using an Oxygen Releasing Compound. Remediation/Fall Vol 6:4. John T. Wiley and Sons, New York pp 95-109.

OTA, 1989. Coming clean: Superfund problems can be solved; Office of Technology Assessment, National Technical Information Service, Springfield, Va., PB90-142209.

Parkhurst, D., S. Christenson, and G. Breit, 1993. Ground-water-quality assessment of the central Oklahoma aquifer, Oklahoma: geochemical and geohydrologic investigations; U.S. Geol. Surv., Open-File Rept, 92-642.

Parkhurst, D., D. Thorstenson, and L. Plummer, 1980. PHREEQE- A computer program for geochemical calculations. U.S. Geol. Surv. Water Resc. Invest. Report 80-96.

Parsons, R., 1998. In-situ bioremediation of methane plumes in unsaturated sediments; MS Thesis, University of Oklahoma, Norman, OK.

Parsons Engineering Science, Inc. 1994. Intrinsic remediation engineering evaluation/cost analysis for ST-29, Air Force Center for Environmental Excellence, San Antonio, TX.

Parsons Engineering Science, Inc.,1995. Treatability study in support of intrinsic remediation for site ST-41, Elmendorf Air Force Base, Anchorage, Alaska, Air Force Center for Environmental Excellence, San Antonio, TX.

Parsons Engineering Science, Inc., 1995. Treatability study in support of intrinsic remediation for the Hangar 10 Site, Elmendorf Air Force Base, Anchorage, Alaska, Air Force Center for Environmental Excellence, San Antonio, TX.

Pedersen, T. and J. Curtis, 1991. Soil vapor extraction technology reference handbook; Office of Research and Development, U.S. Environmental Protection Agency, Risk Reduction Engineering Laboratory, Cincinnati, OH, EPA/540/2-91/003.

Pettijohn, F., 1975. Sedimentary rocks; 3ed ed., Harper and Row, New York, NY.

Plummer, L. 1977. Defining reactions and mass transfer in part of the Floridan aquifer; Water Rescources Research 13:801-812.

Plummer, L., J. Busby, R. Lee, and B. Hanshaw, 1990. Geochemical modeling of the Madison aquifer in parts of Montana, Wyoming, and South Dakota; Water Resources Research 26(9):1981-2014.

Pierzynski, G., J. Sims, and G. Vance, 1994. Soils and environmental quality; CRC Press, Boca Raton, FL.

Postma, D., C. Boesen, H. Kristiansen, and F. Larsen, 1991. Nitrate reduction in an unconfined sandy aquifer: Water chemistry, reduction processes, and geochemical modeling; Water Resources Research, 27:2027-2045.

Postma, D., 1981. Formation of siderite and vivianite and the pore-water composition of a recent bog sediment in Denmark; Chemical Geology, 31:225-224.

Postma, D., 1982. Pyrite and siderite formation in brackish and freshwater swamp sediments; American Journal Science, 282:1151-1183.

Pyzik, A., and S. Sommer, 1981. Sedimentary iron monosulfides: kinetics and mechanism of formation; Geochimica et Cosmochimica Acta, 45:687-698.

Puls, R., 1997. Permeable reactive subsurface barriers for the interception and remediation of chlorinated hydrocarbon and chromium (VI) plumes in ground water; EPA, National Risk Management Research Laboratory, Ada, OK, EPA/600/F-97/008, p. 4.

Rifai, H., P. Bedient, R. Borden, J. Haasbeek, 1987. Bioplume II, computer model of two-dimensional contaminant transport under the influence of oxygen limited biodegredation in ground water; Rice Univ. Houst. Tx.

Rafai, H., S., C. Newell, J. Gonzales, S. Dendrou, L. Kennedy, and J. Wilson. 1997. Bioplume III: Natural attenuation decision support system, ver 1.0; Air Force Center for Environmental Excellence, San Antonio, TX.

Rettenberger, G., 1987. Trace composition of landfill gas, In: Proceedings of International Symposium on Process Technology and Environmental Impact of Sanitary Landfill, Cagliari, Sardinia, Italy, pp. 387-393EE.

Rice, C., M. Tuttle, and R. Reynolds, 1993. The analysis of forms of sulfur in ancient sediments and sedimentary rocks: Comments and cautions; Chemical Geology, 107:83-95.

Ridgeway, H., J. Safarik, D. Phipps, P. Carl, and D. Clark, 1990. Identification and catabolic activity of well-derived gasoline degrading bacteria from a contaminated aquifer; Applied Environmental Microbiology. 56(11):3565-3575.

Robertson, J., C. Toussaint, and M. Jorque, 1974. Organic compounds entering ground water from a landfill; U.S. Environmental Protection Agency Environmental Protection Technology series, EPA 660/2-74-077, pp. 47.

Roden, E. and J. Zachara, 1996. The reduction of Fe Iron (III) Oxides: Measure of oxide surface area and potential for cell growth; Environmental Science and Technology, 30(5):1618-1628.

Robinson, G., 1984. Sequential chemical extractions and metal partitioning in hydrous Mn-Fe-oxide coatings: Reagent choice and substrate composition affect results, Chemical Geology, 47:97-112.

Russell, M., E. Colglazier, and M. English, 1991. Hazardous waste remediation: The task ahead; University of Tennessee, Waste Management Research and Education Institute, Knoxville, TN, pp. 247.

Sidhu, P., R. Gilkes, R. Cornell, A. Posner, and J. Quirk, 1981. Dissolution of iron oxides and oxyhydroxides in hydrochloric and perchloric acids; Clays Clay Miner. 29(4)269-276.

SigmaPlot, 1997. SigmaPlot for Windows 95 Users Manual; SPSS Inc., Chicago, Ill.

Sims, R., D. Sorensen, J. Sims, J. McLean, R. Mahmood, R. Dupont, J. Jurinak, and K. Wagner, 1986. Contaminated surface soils in-place treatment techniques; Noyes Publications, Park Ridge, NJ.

Starr, R. and J. Cherry, 1994. In-situ remediation of contaminated ground water: the funnel-and-gate system; Ground Water, 32(3):465-476.

Stumm, W., and J. Morgan, 1996. Aquatic chemistry an introduction emphasizing chemical equilibrium in natural waters, John Wiley & Sons, N.Y., p. 1022.

Stookey, L., 1970. Analytical Chemistry, 42(7):779.

Suflita, J., C. Gerba, R. Ham, A. Palmisano, W. Rathje, and J. Robinson, 1992. The worlds largest landfill: a multidisciplinary investigation; Environmental Science and Technology, 26(8)1486-1495.

SW-846, 1990. Test methods for evaluating solid waste, physical/chemical methods; 3ed ed.

Tchobanoglous, G., and F. Burton, 1991. Wastewater engineering treatment, disposal, and reuse; Metcalf and Eddy, Inc., McGraw-Hill, New York, NY.

Tchobanoglous, G., H. Theisen, and S. Vigil, 1993. Integrated solid waste management; McGraw-Hill, N.Y, N.Y.

Testa, S. and D. Winegardner, 1991. Restoration of petroleum contaminated aquifers, Lewis Publishers, CRC Press, Boca Raton, FL.

Thorstenson, D., D. Fisher, and M. Croft, 1979. The geochemistry of the Fox Hills-Basal Hell Creek aquifer in southwestern North Dakota and northwestern South Dakota; Water Resources Research 15:1479-1498.

Tohme, C., 1994. Proposed rehabilitation of the old Norman landfill; Masters Thesis, College of Architecture, University of Oklahoma.

Tuttle, J., P. Dugan, C. Macmillan, and C. Rand, 1969. Microbial dissimilatory sulfur cycle in acid mine water; Journal of Bacteriology; 97:594-602.

Ulrich, G. A., L. Krumholdz, and J. Suflita, 1997. A rapid and simple method for estimating sulfate reduction activity and quantifying inorganic sulfides; Applied Environmental Microbiology, 63(4):1627-1629.

U.S. Census Bureau, 1998. On-line internet database resource: http://www.census.gov/population/estimates/state/stts/st8090ts.txt.

U.S. EPA, 1990. Characterization of municipal solid waste in the U.S.:1990 update; EPA 530SW 90-042A Washington, DC.

Weast, R., A. Melvin, and B. William eds., 1987. CRC handbook of chemistry and physics; 67th ed., CRC Press, Inc., Boca Raton, FL.

Weis, M., G. Abbt-Braun, and F. Frimmel, 1989. Humic-like substances from landfill leachates – characterization and comparison with terrestrial and aquatic humic substances; The Science of the Total Environment, 81(82):343-352.

Wicks, C. M., 1989. Early diagenesis of iron and sulfur in sediments of lakes that receive acid mine drainage; Masters Thesis, University of Virginia.

Williams, R., 1990. Iron and the origin of life; Nature, 343:213-2243.

Wesolowski, L. and L. Le Grand, 1996. Arizona Supreme Court, Underground storage tanks; Arizona Supreme Court Arizona/Sonora Judicial Relations Project, National Law Center for Inter-America Free Trade, Flagstaff, AZ.

Wiedemeier, T. H., R. Miller, J. Wilson, and D. Kampbell, 1995. Significance of anaerobic processes for the intrinsic bioremediation of fuel hydrocarbons; In: Proceedings of the Petroleum Hydrocarbons and Organic Chemicals in Ground Water Conference, National Ground Water Association, Houston , TX.

Wiedemeier, T., D. Downey, J. Wilson, D. Kampbell, R. Miller, and J. Hansen, 1997. Technical protocol for implementing the intrinsic remediation with long-term monitoring option for natural attenuation of dissolved-phase fuel contamination in ground water; Air Force Center for Environmental Excellence, Brooks Air Force Base, San Antonio, TX (Draft).

Whittemore, D. and Langmuir, D., 1975. The solubility of ferric oxhydroxides in natural waters; Ground Water, 13:360-365.

9. APPENDIX I: GRAPHS WITH STANDARD DEVIATION BARS

Figure A1: Non-Purgable Organic Carbon Qal + Fe

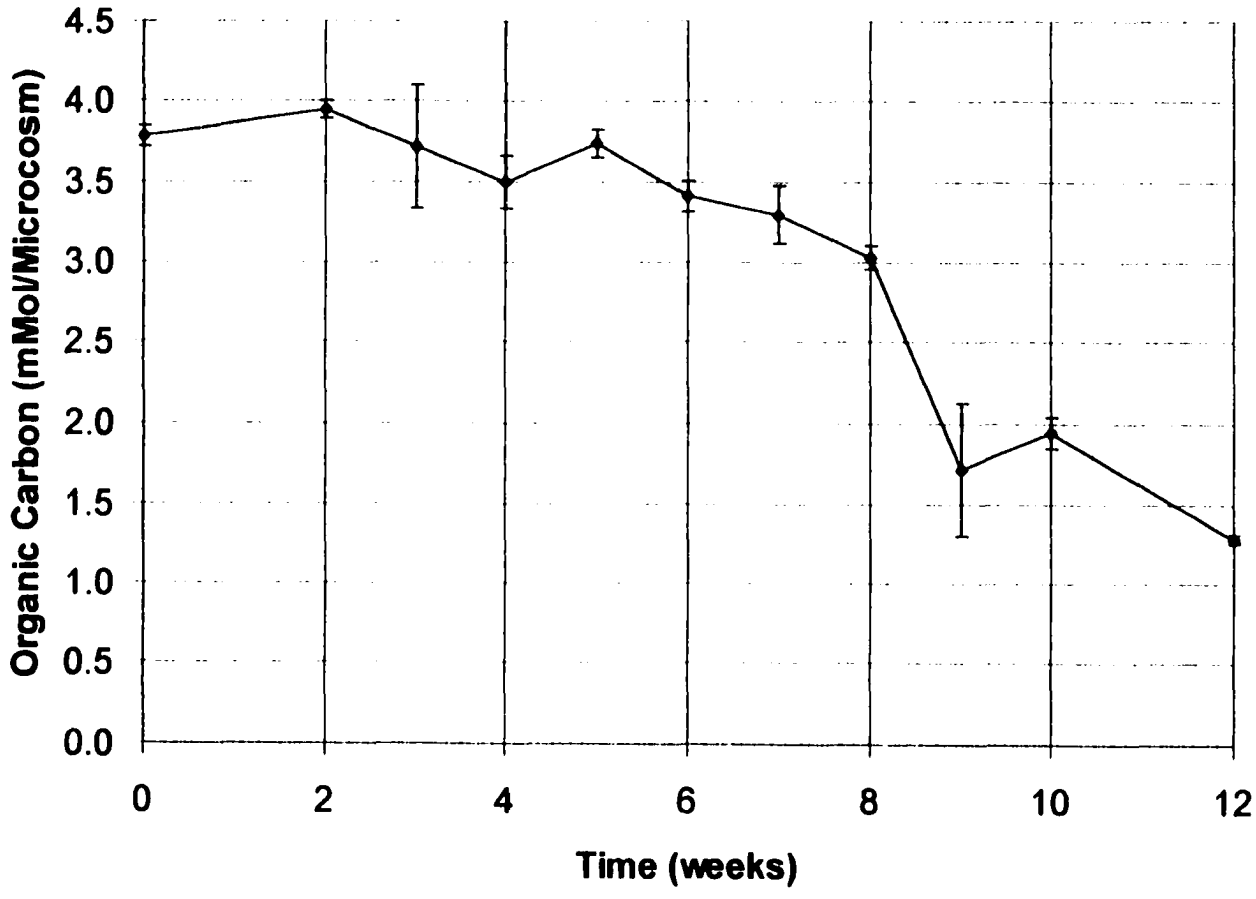

Figure A2: Non-Purgable Organic Carbon Qal + SO4

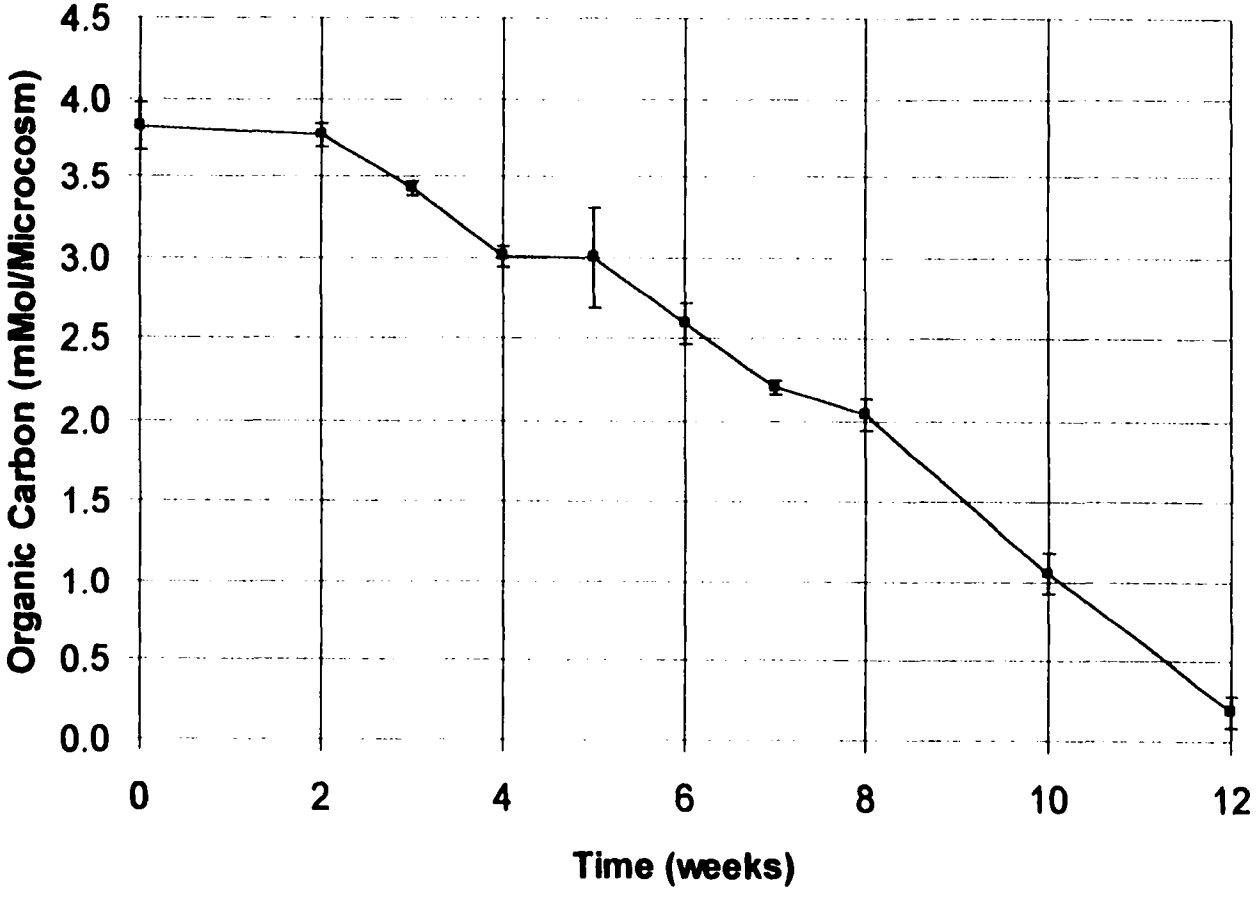

Figure A3: Non-Purgable Organic Carbon Qal Nat.

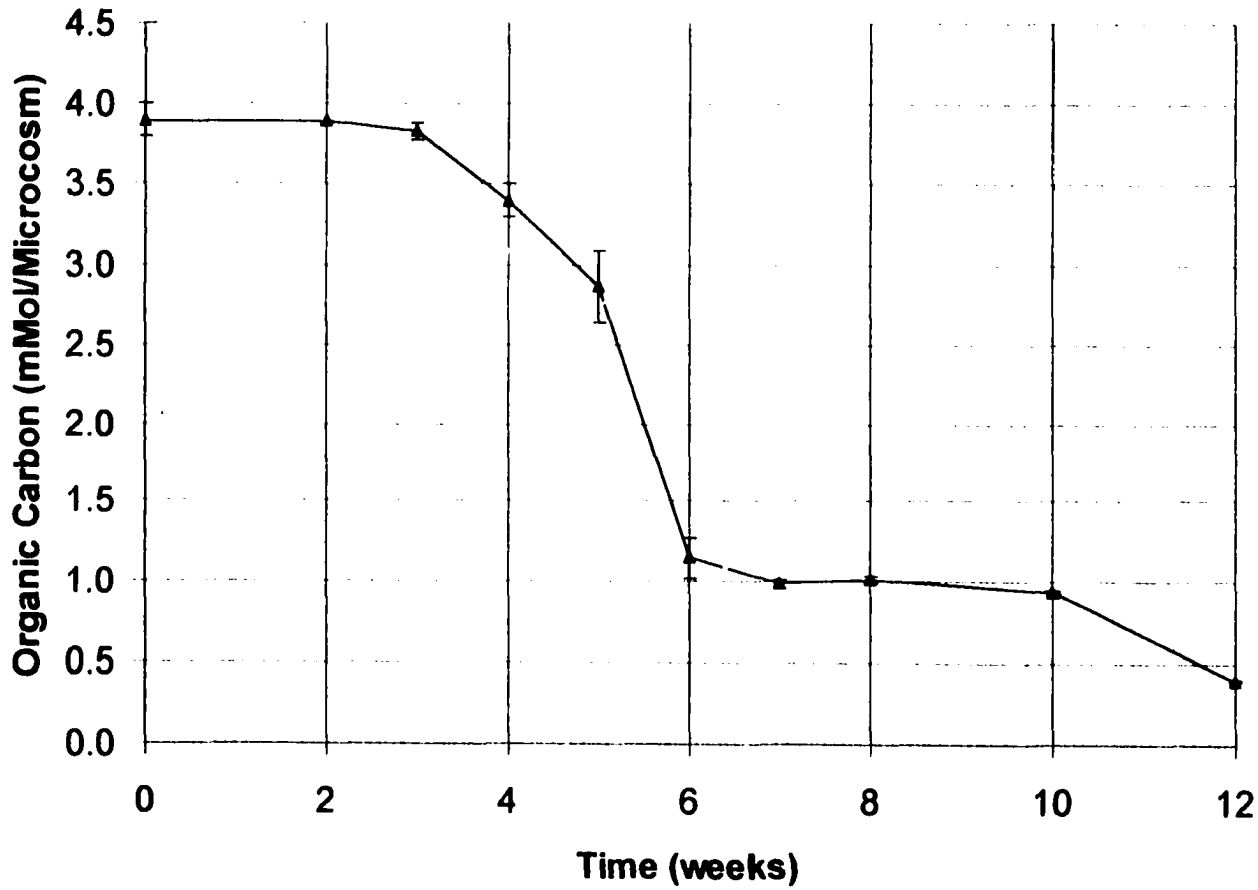

Figure A4: Non-Purgable Organic Carbon Pgw + SO4

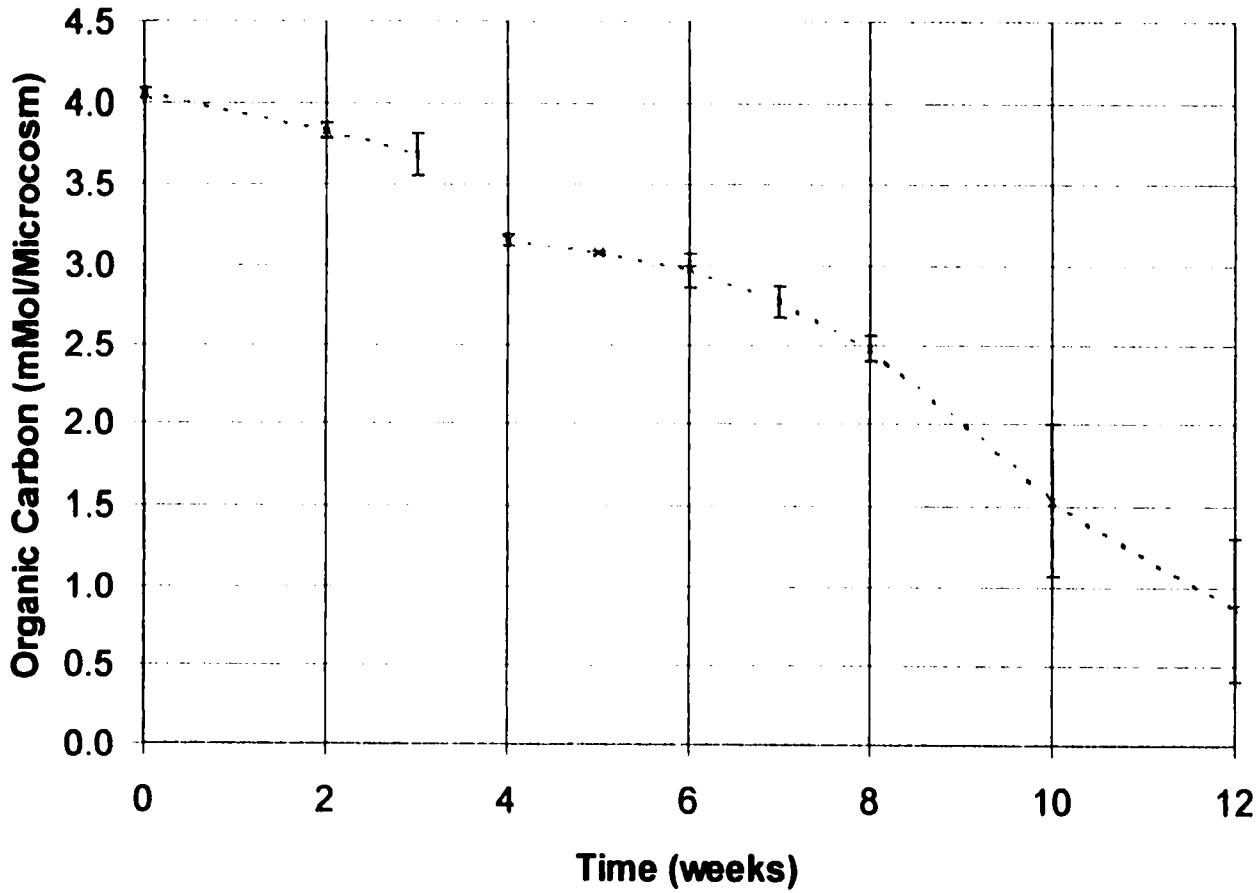

Figure A5: Non-Purgable Organic Carbon Pgw Nat.

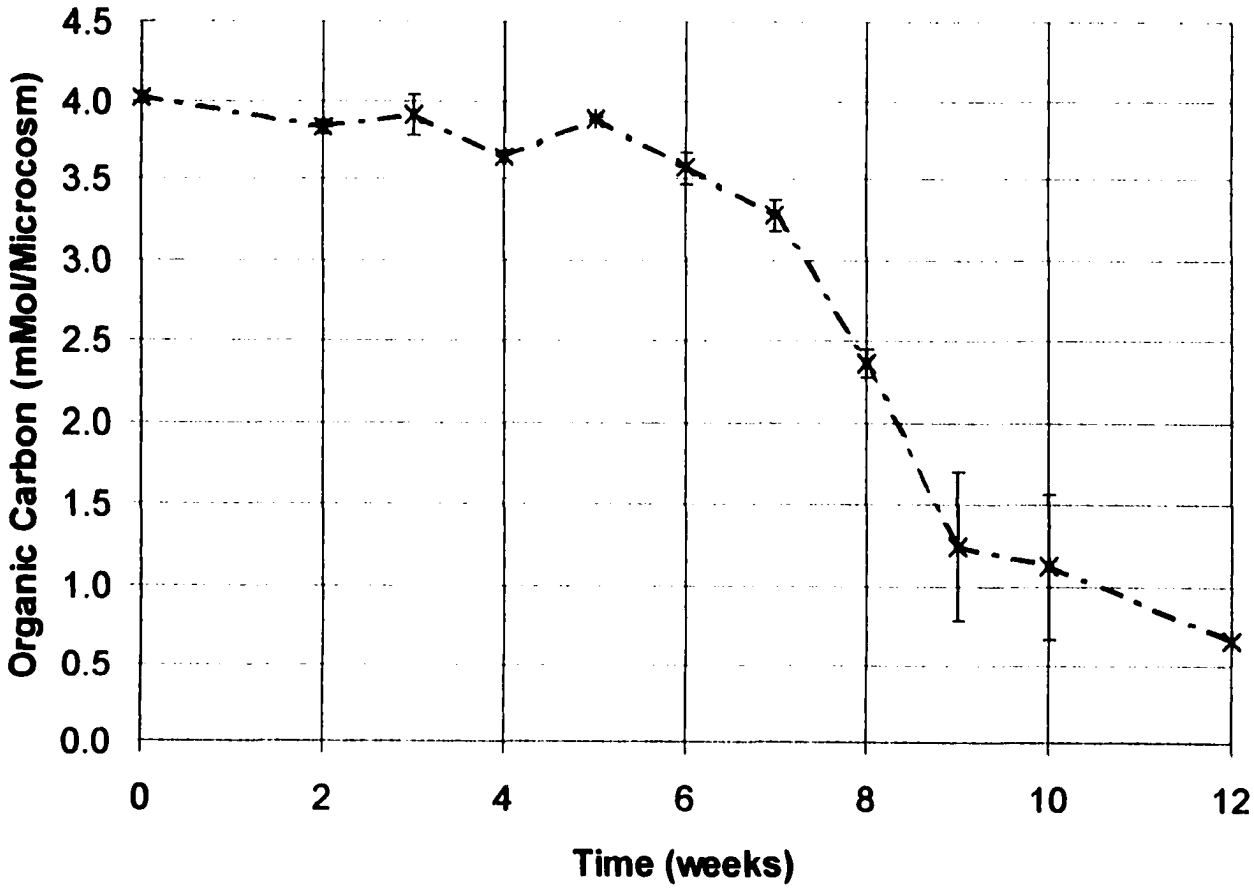

Figure A6: Headspace Methane Qal+Fe

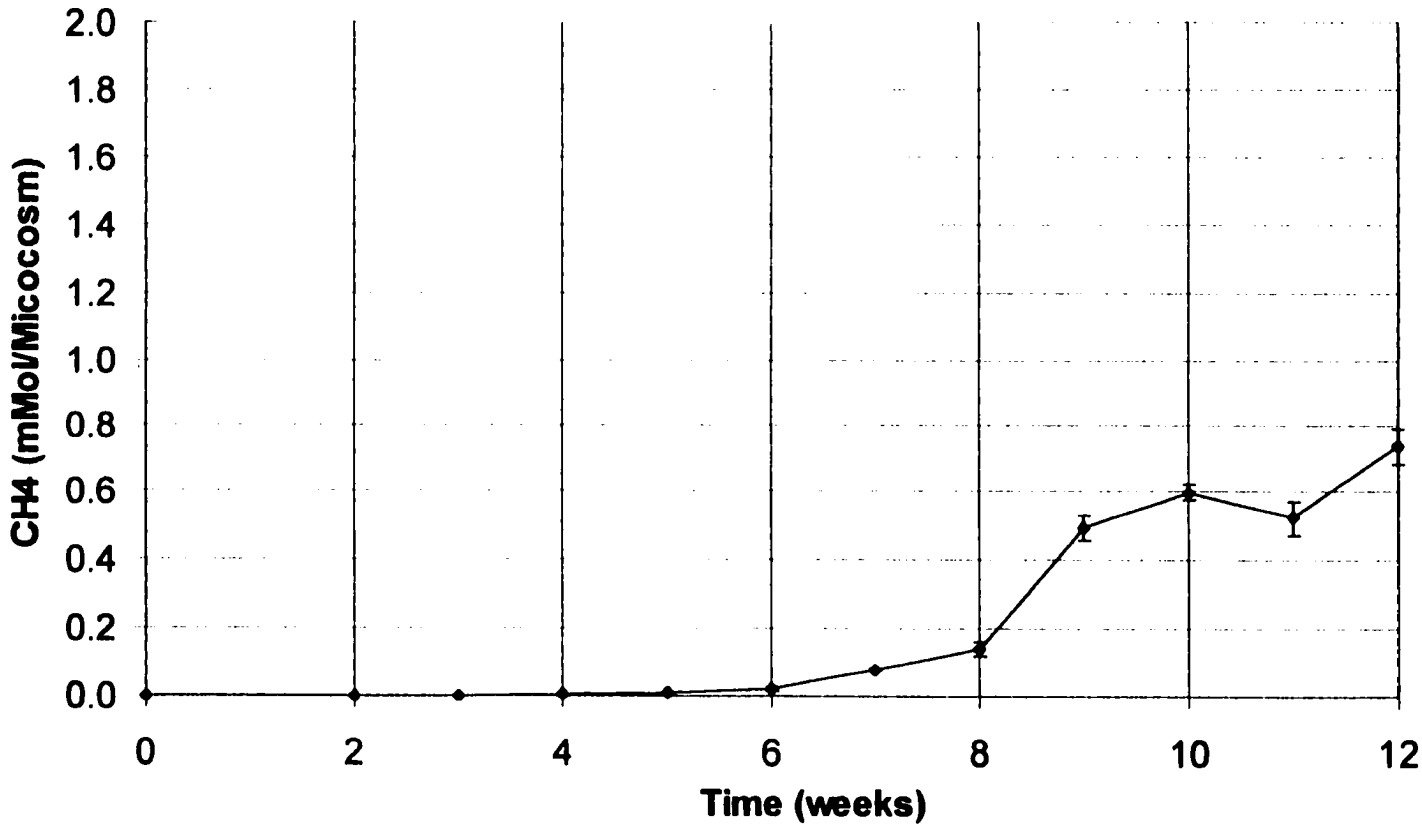

Figure A7: Headspace Methane Qal+SO4

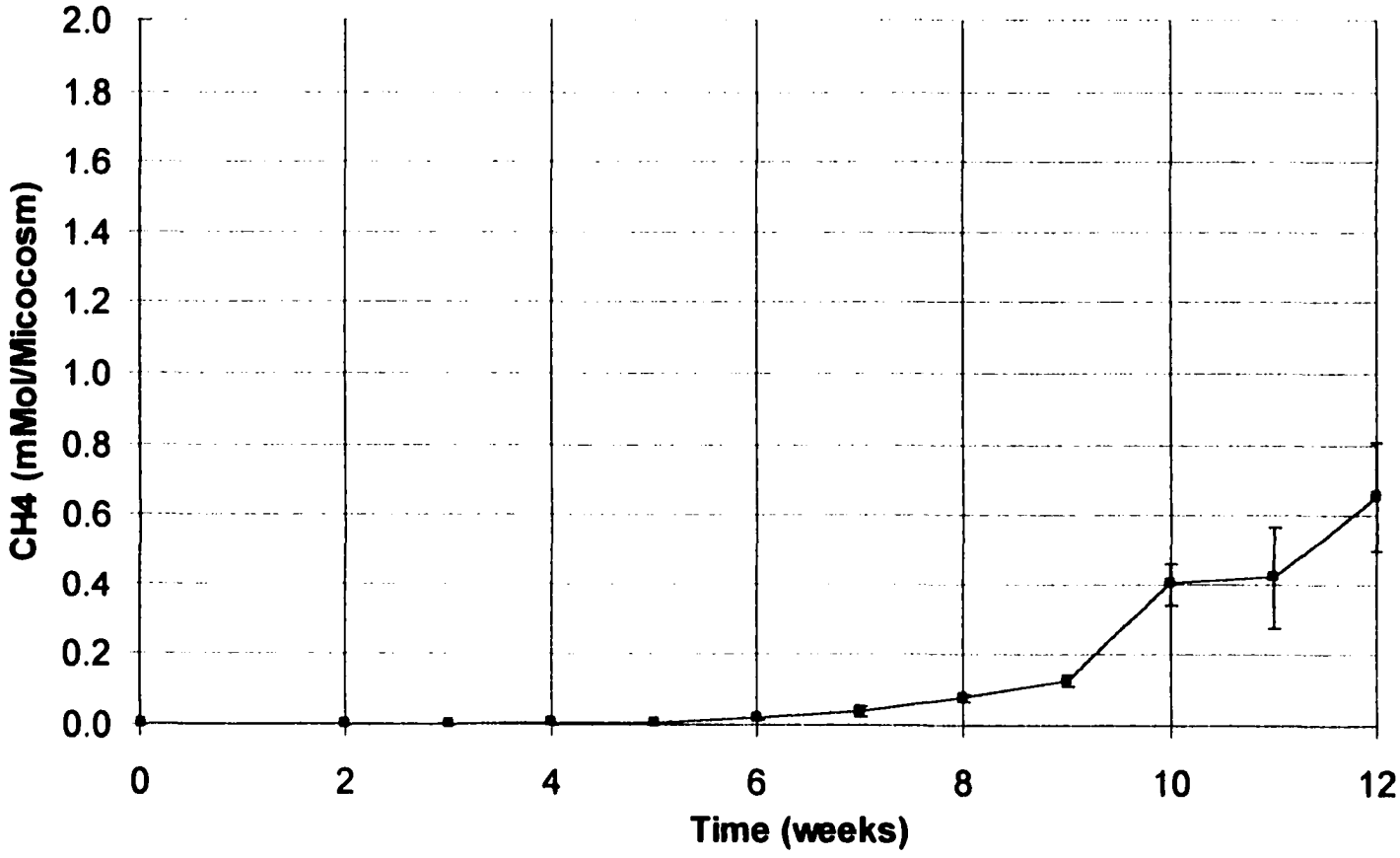

Figure A8: Headspace Methane Qal Nat.

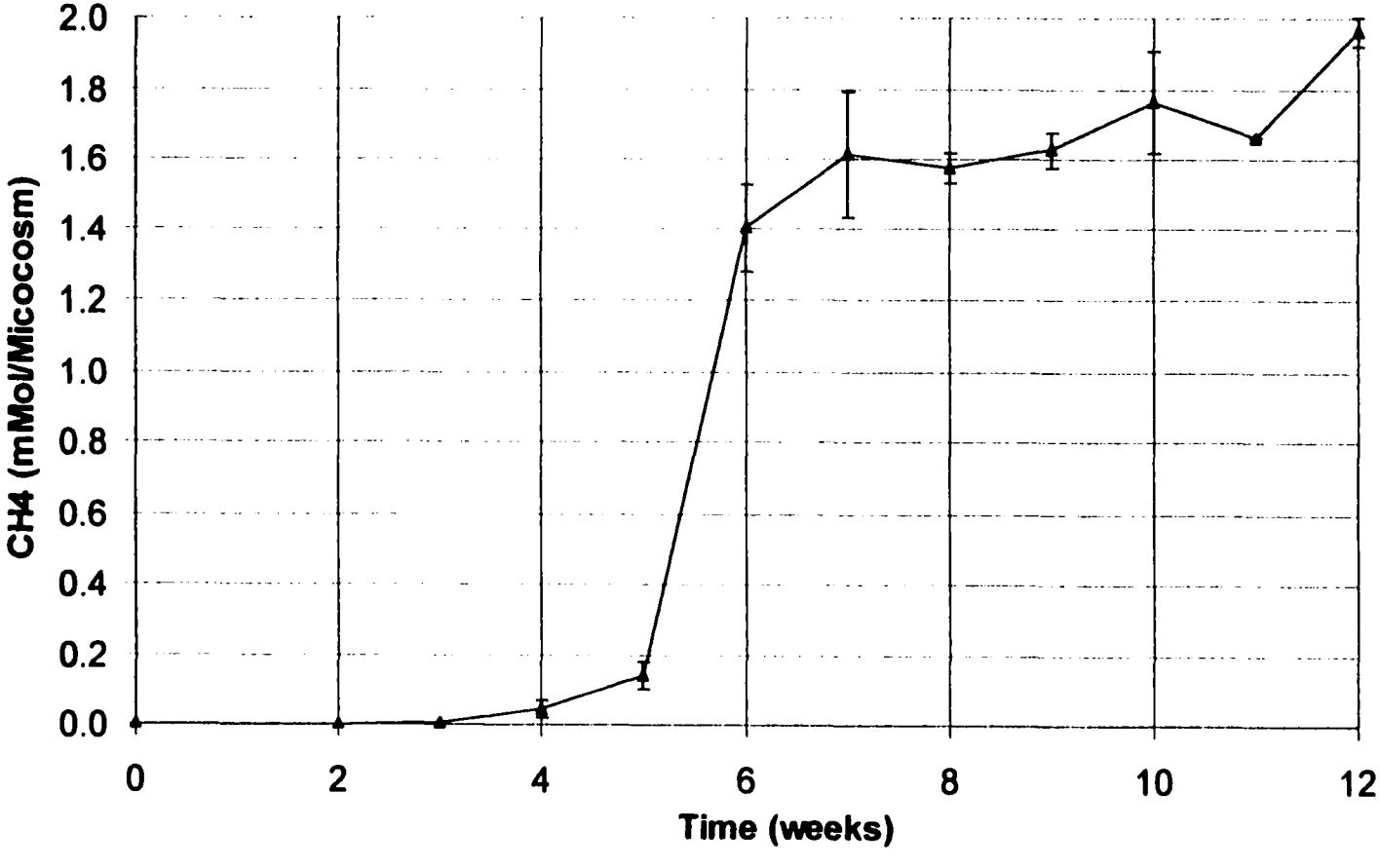

Figure A9: Headspace Methane Pgw + SO4

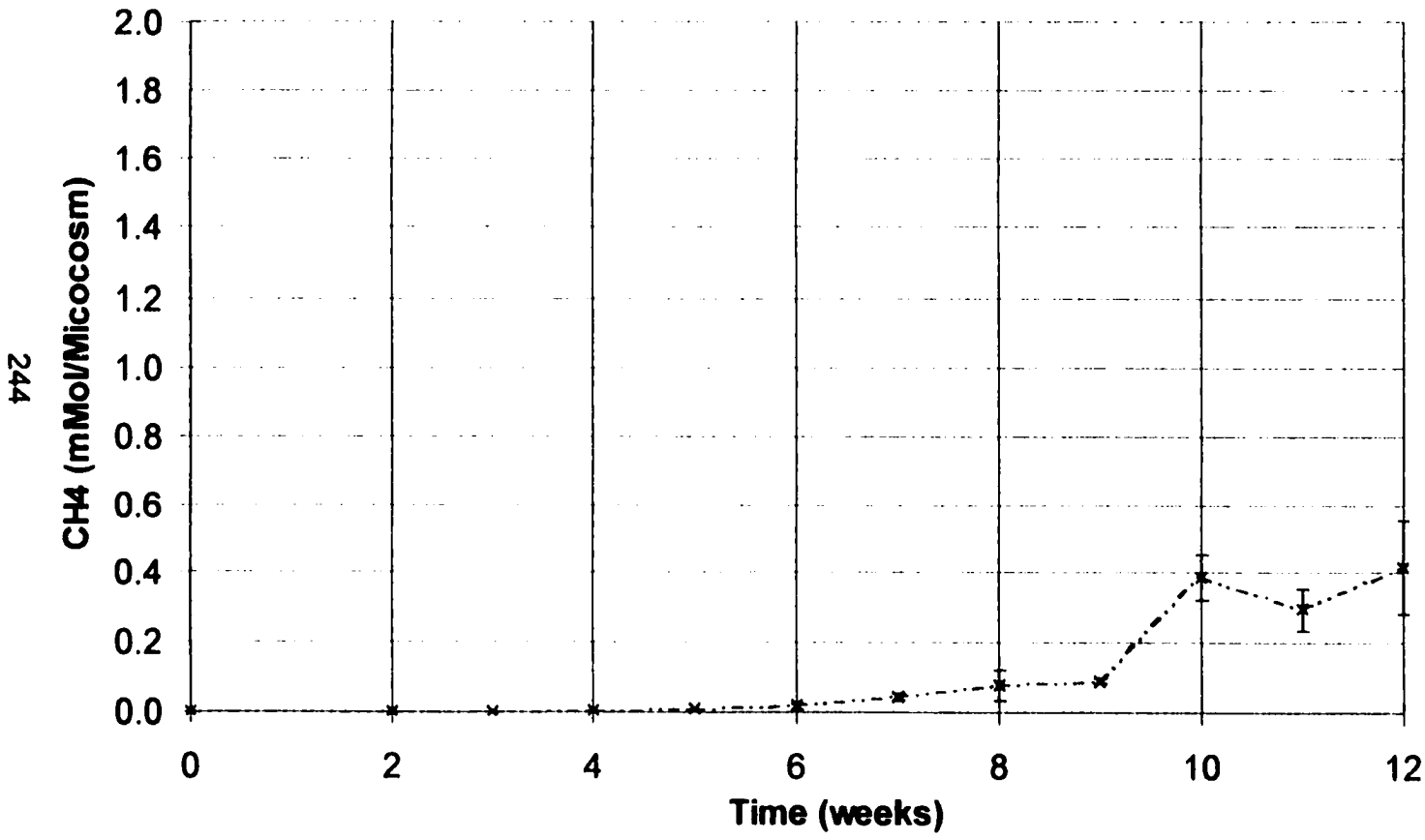

Figure A10: Headspace Methane Pgw Nat.

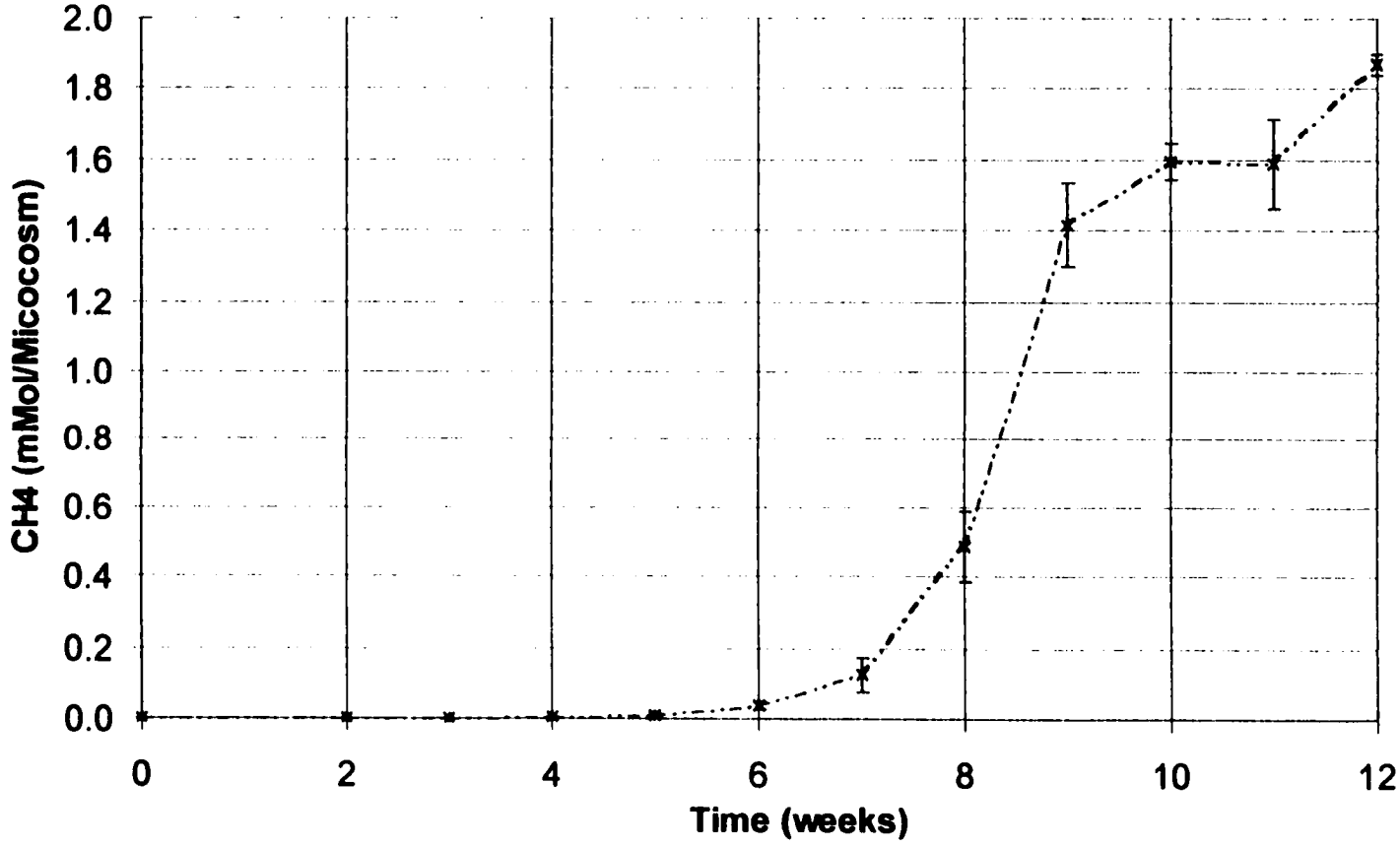

Figure A11: Headspace CO2 Qal + Fe

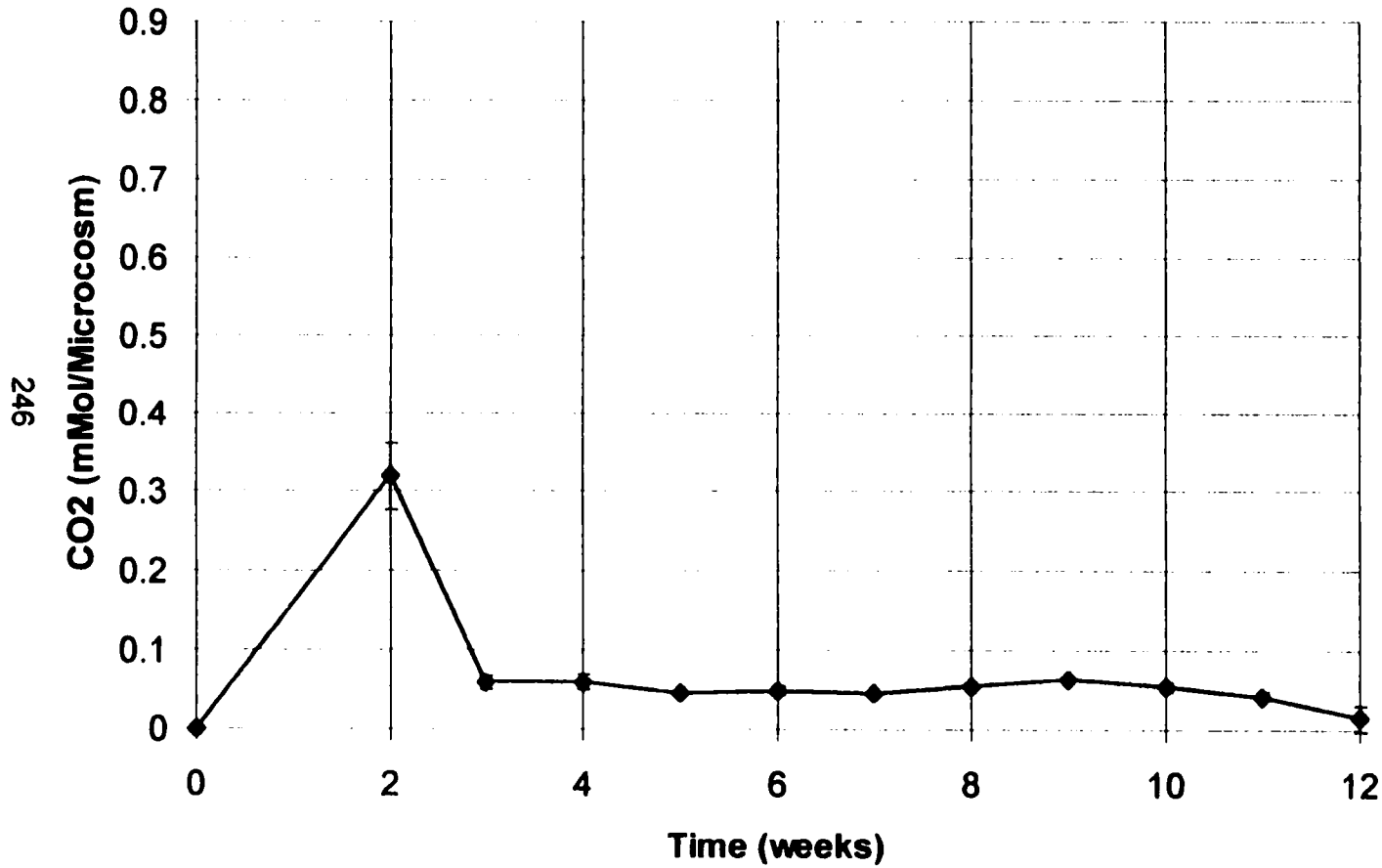

Figure A12: Headspace CO2 Qal + SO4

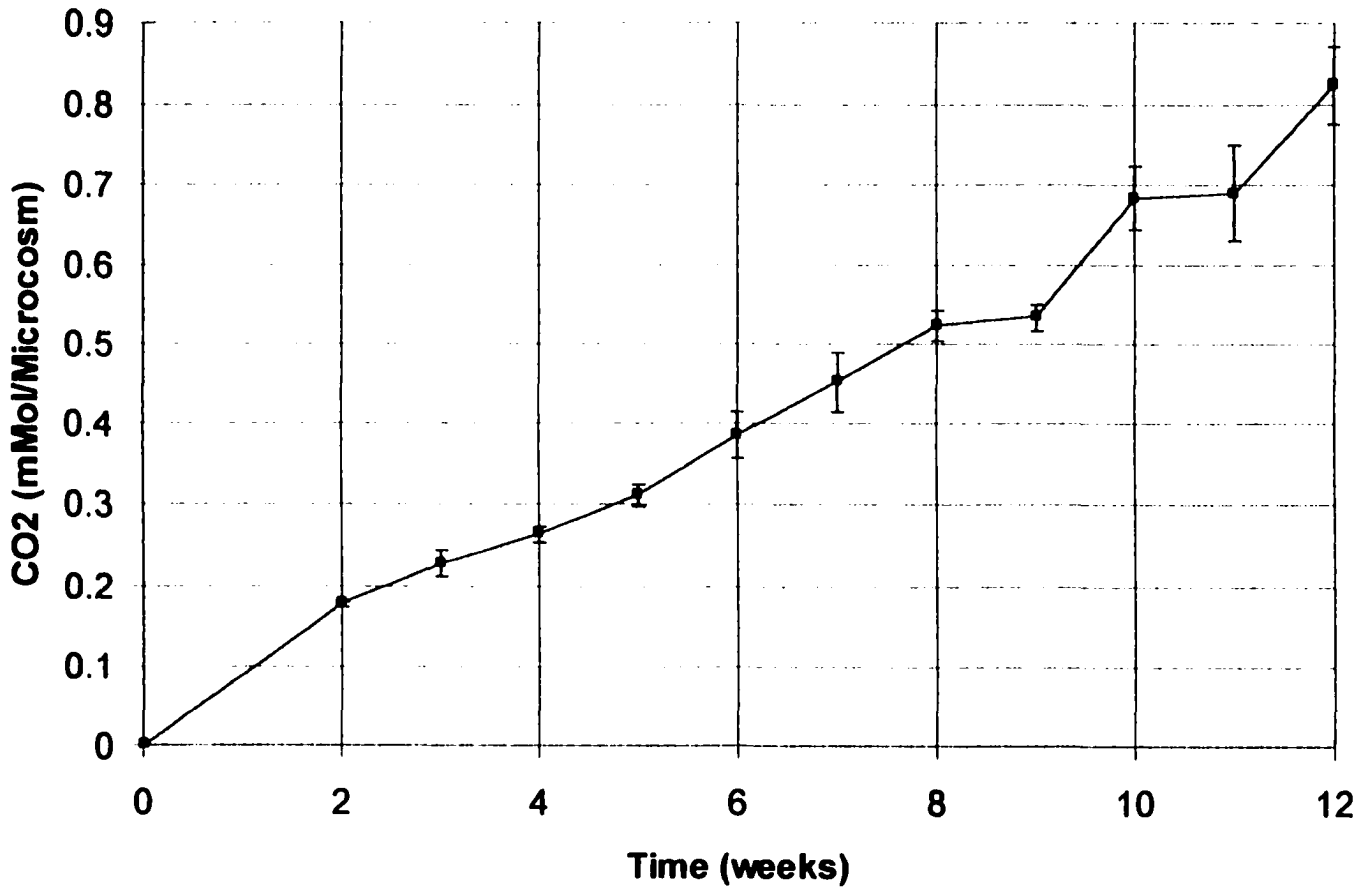

Figure A13: Headspace CO2 Qal Nat.

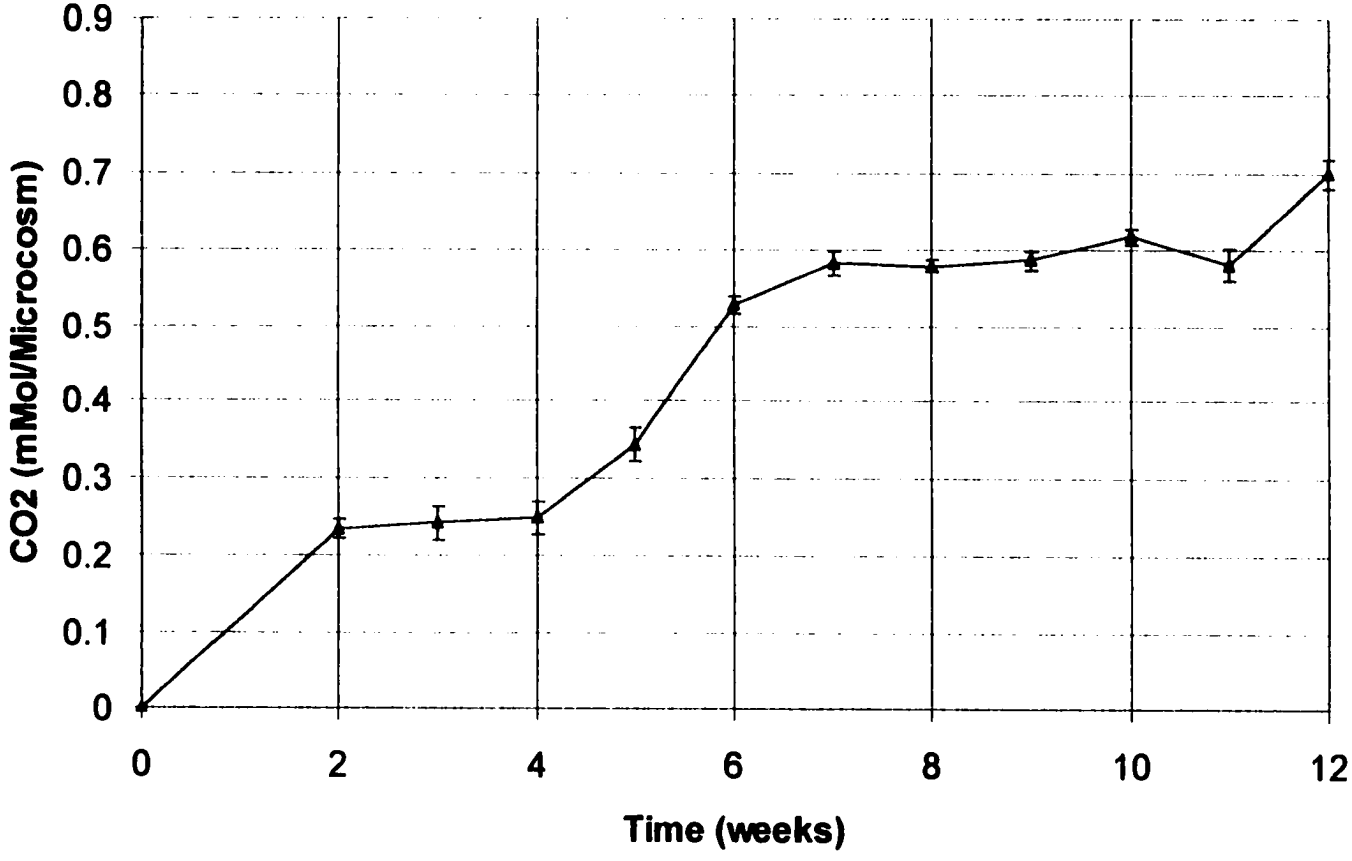

Figure A14: Headspace CO2 Pgw + SO4

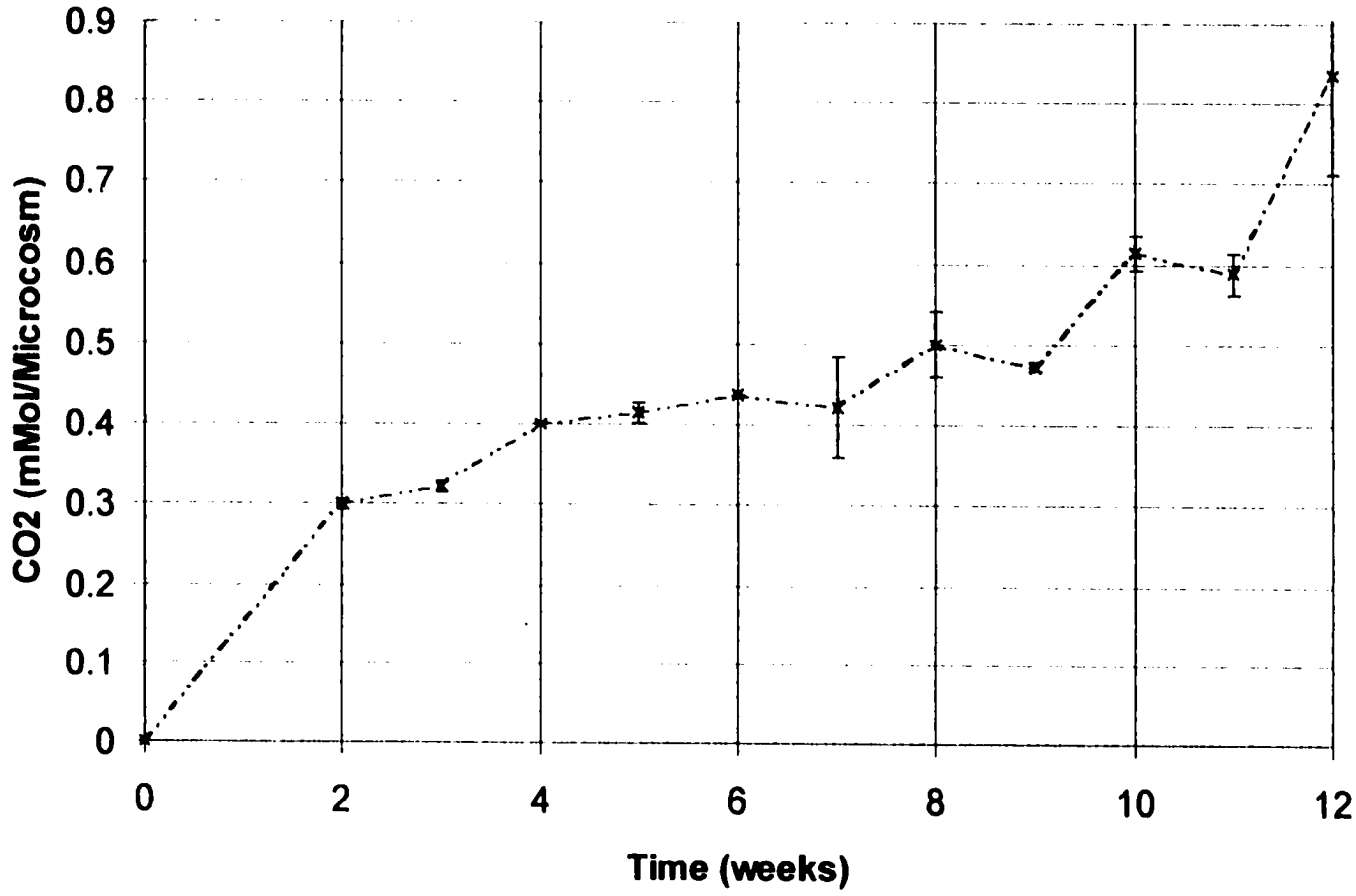

Figure A15: Headspace CO2 Pgw Nat.

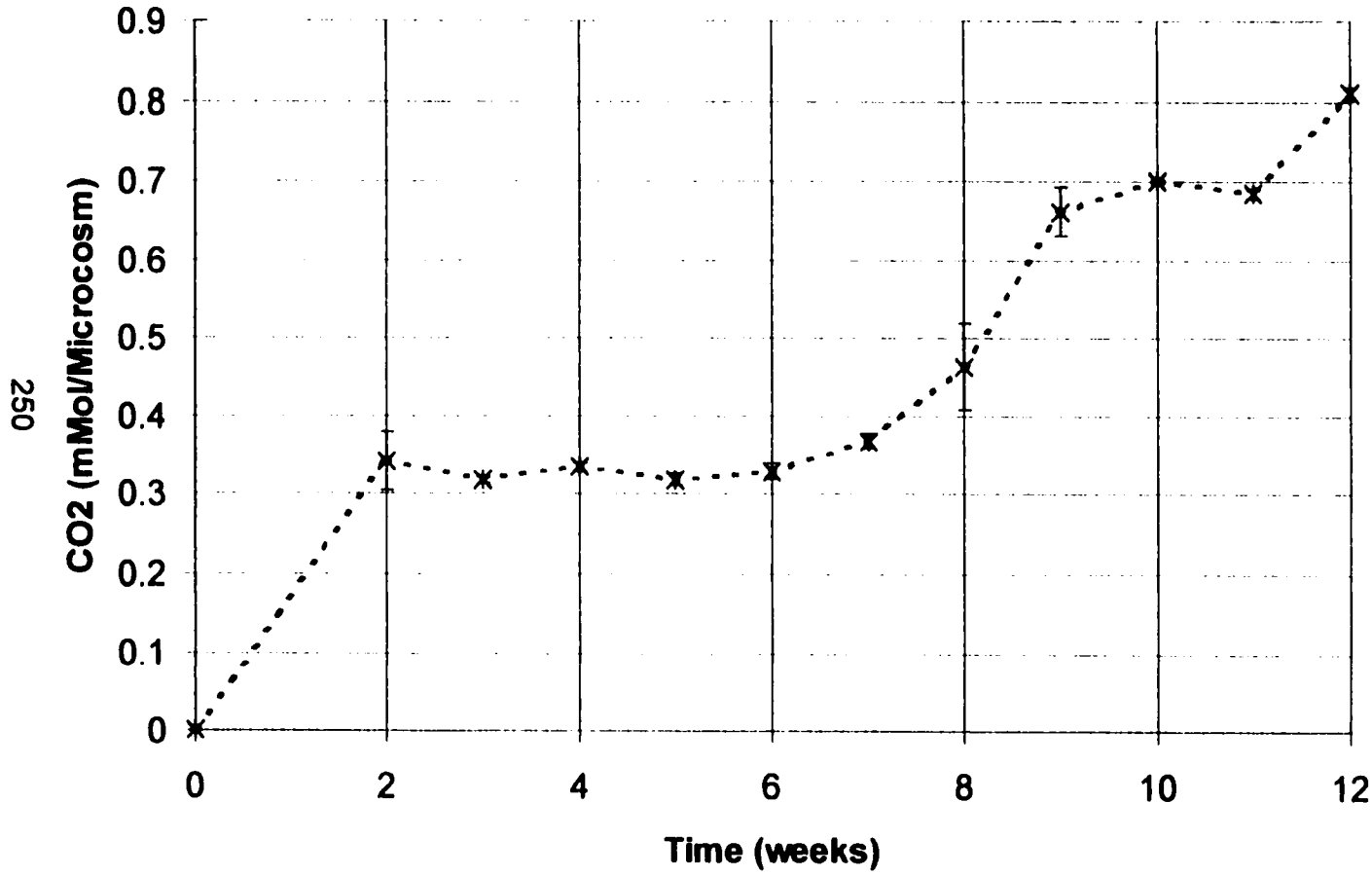

Figure A16: Gypsum Sulfate for Qal + SO4

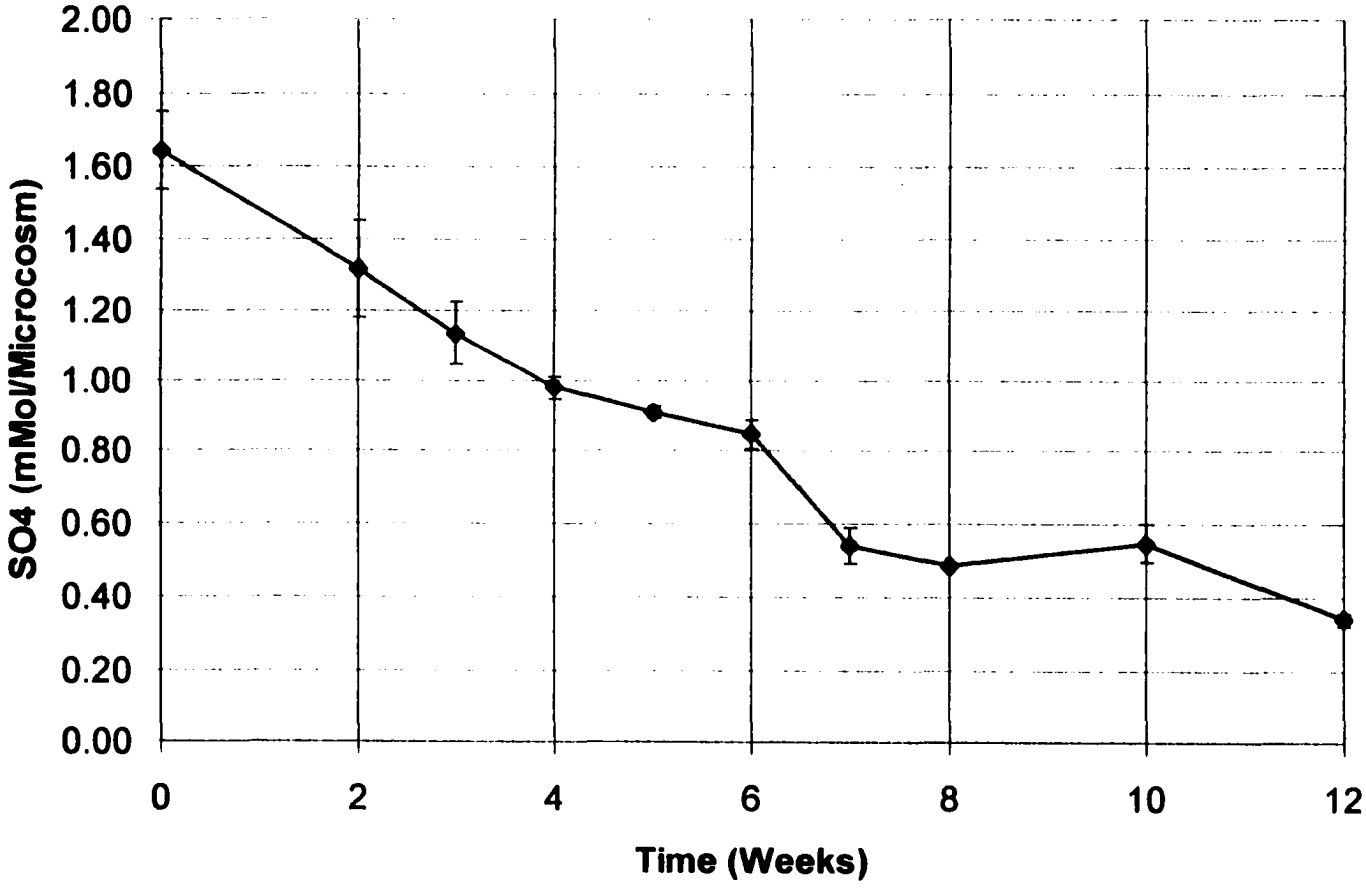

Figure A17: Gpysum Sulfate Pgw + SO4

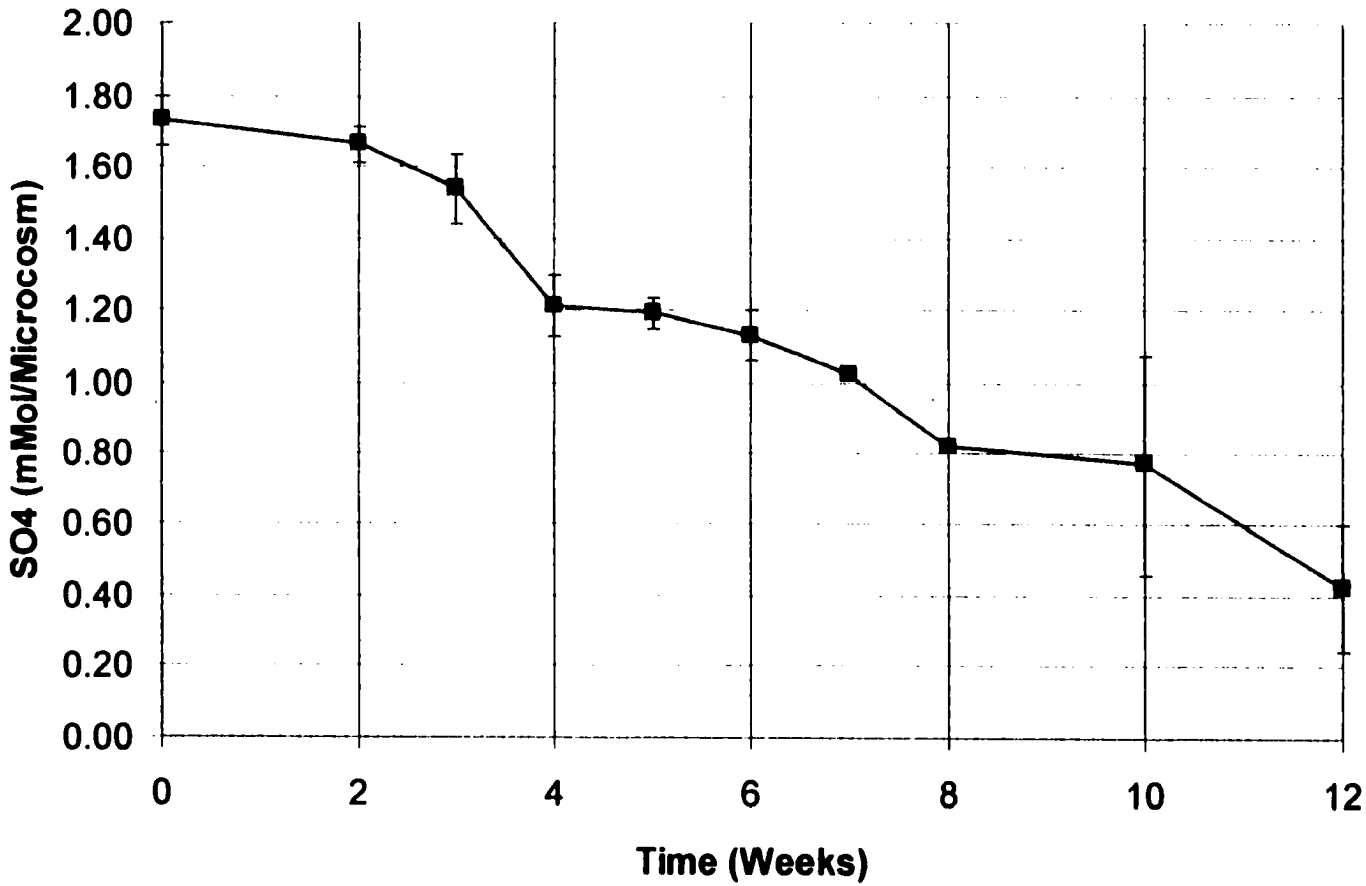

Figure A18: Dissolved Fe Total for Qal + Fe

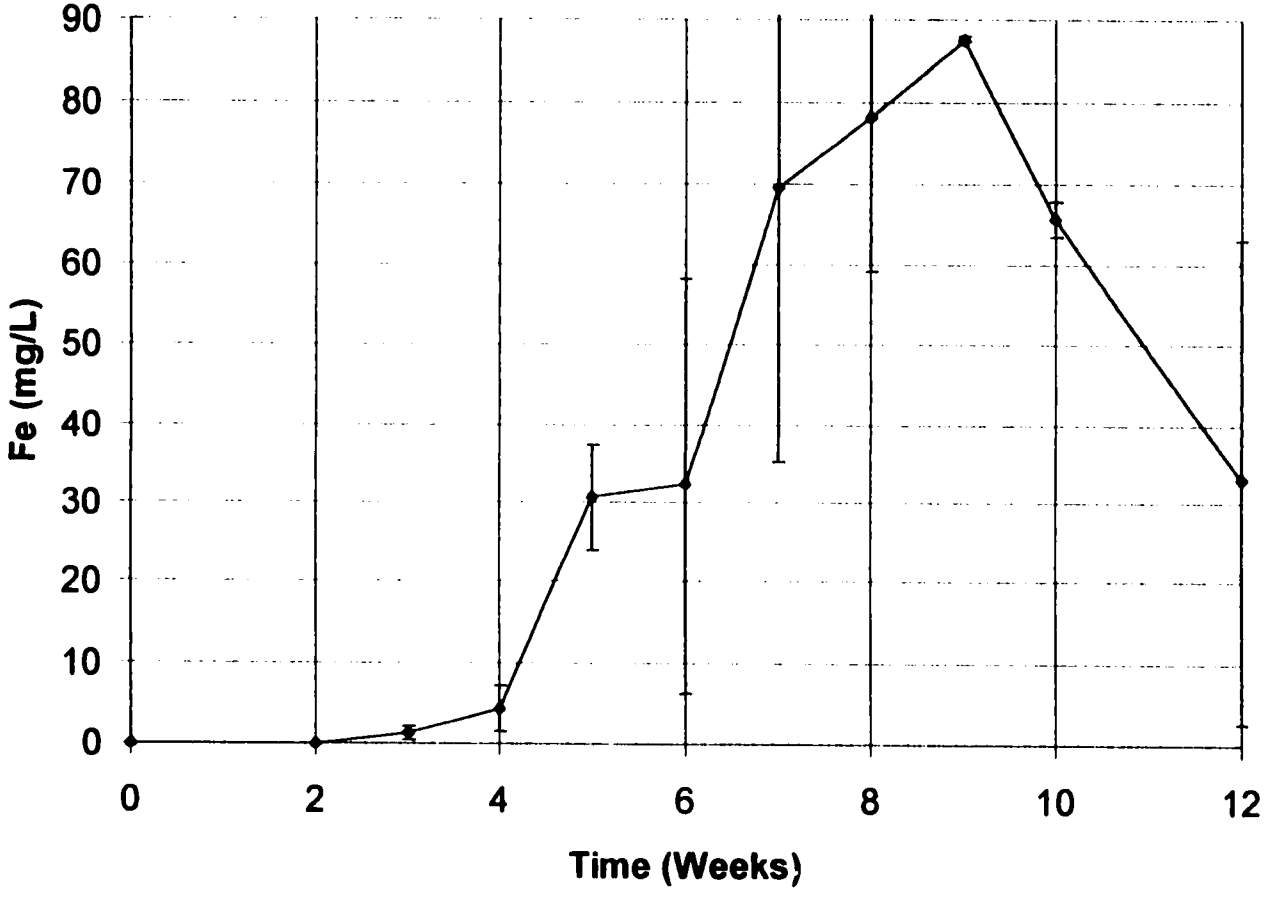

Figure A19: Dissolved Fe Total Qal + SO4

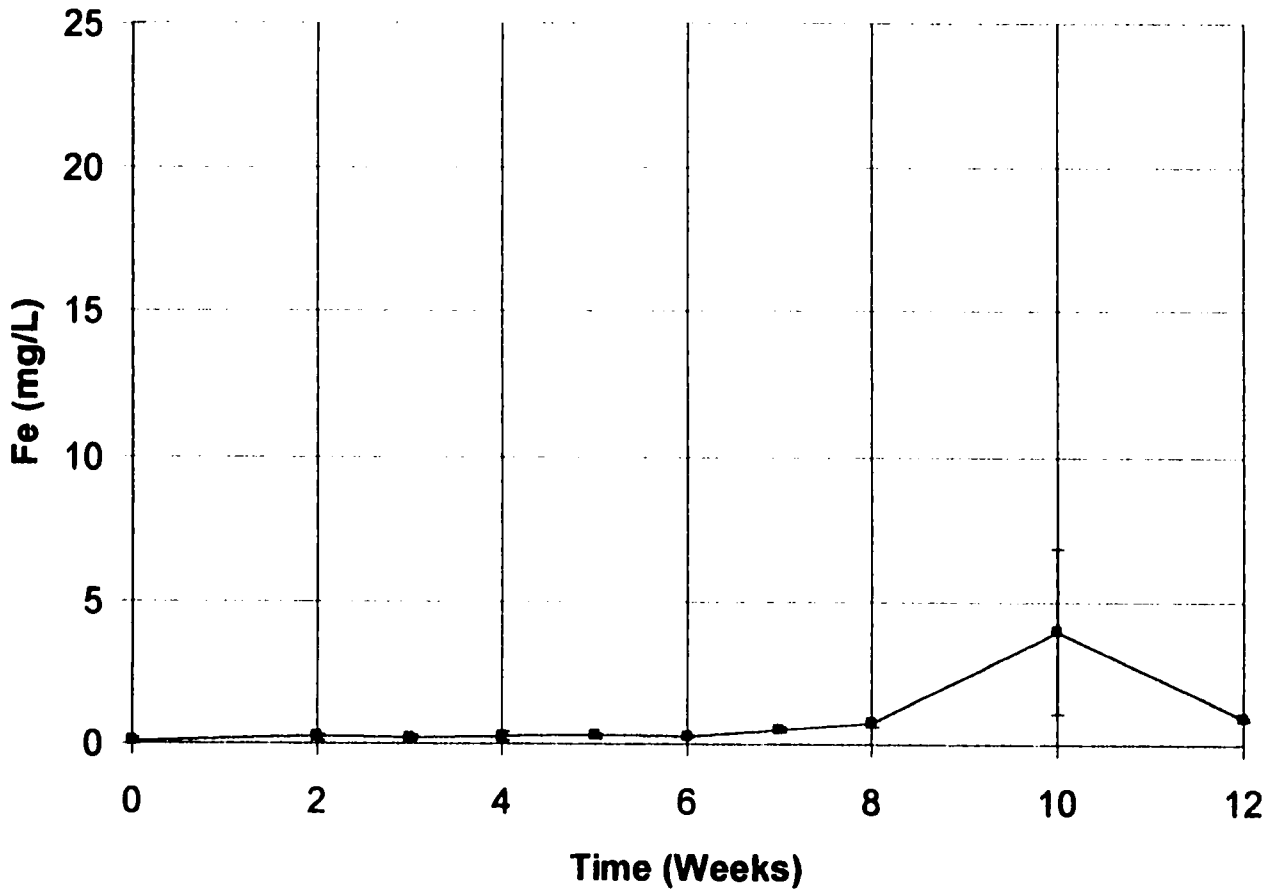

Figure A20: Dissolved Fe Total Qal Nat.

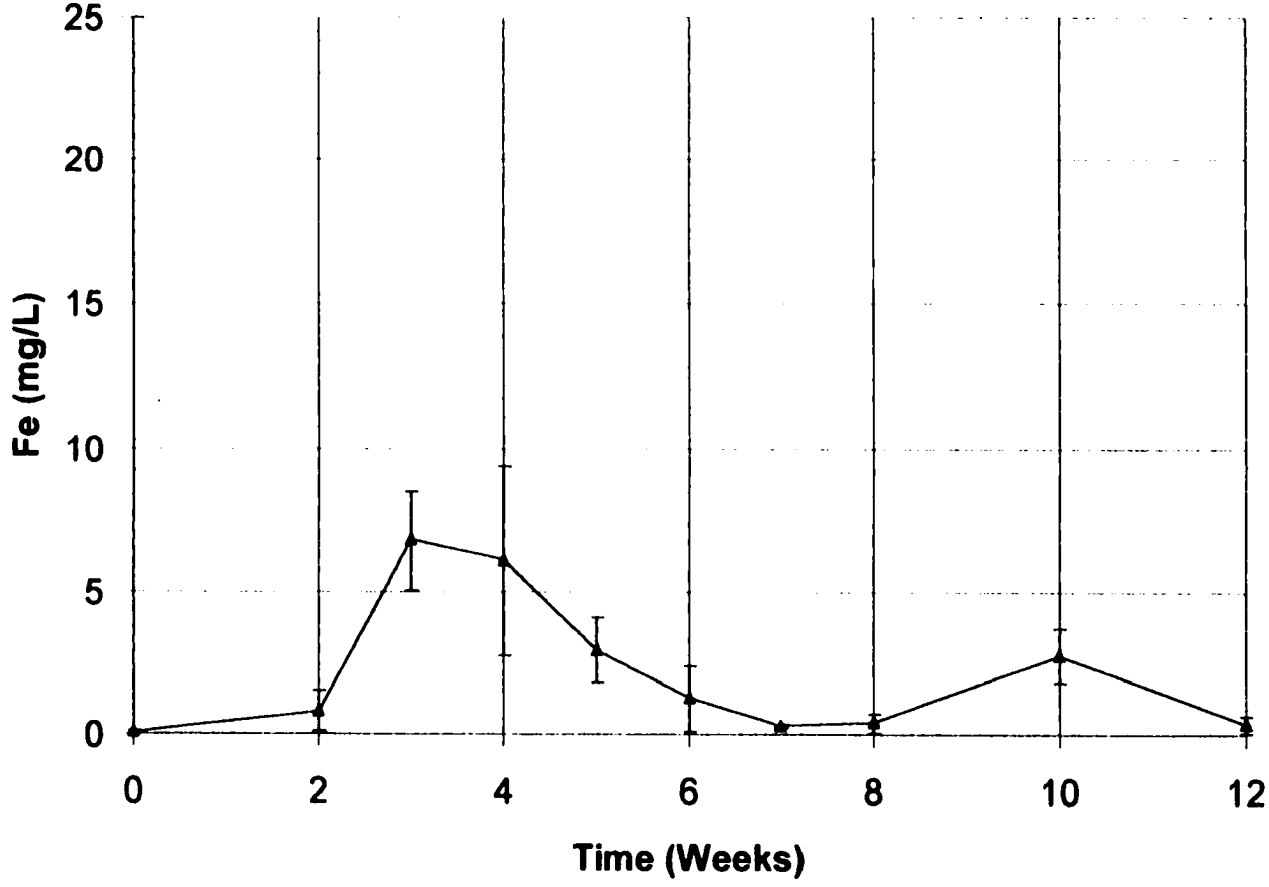

Figure A21: Dissolved Fe Total Pgw + SO4

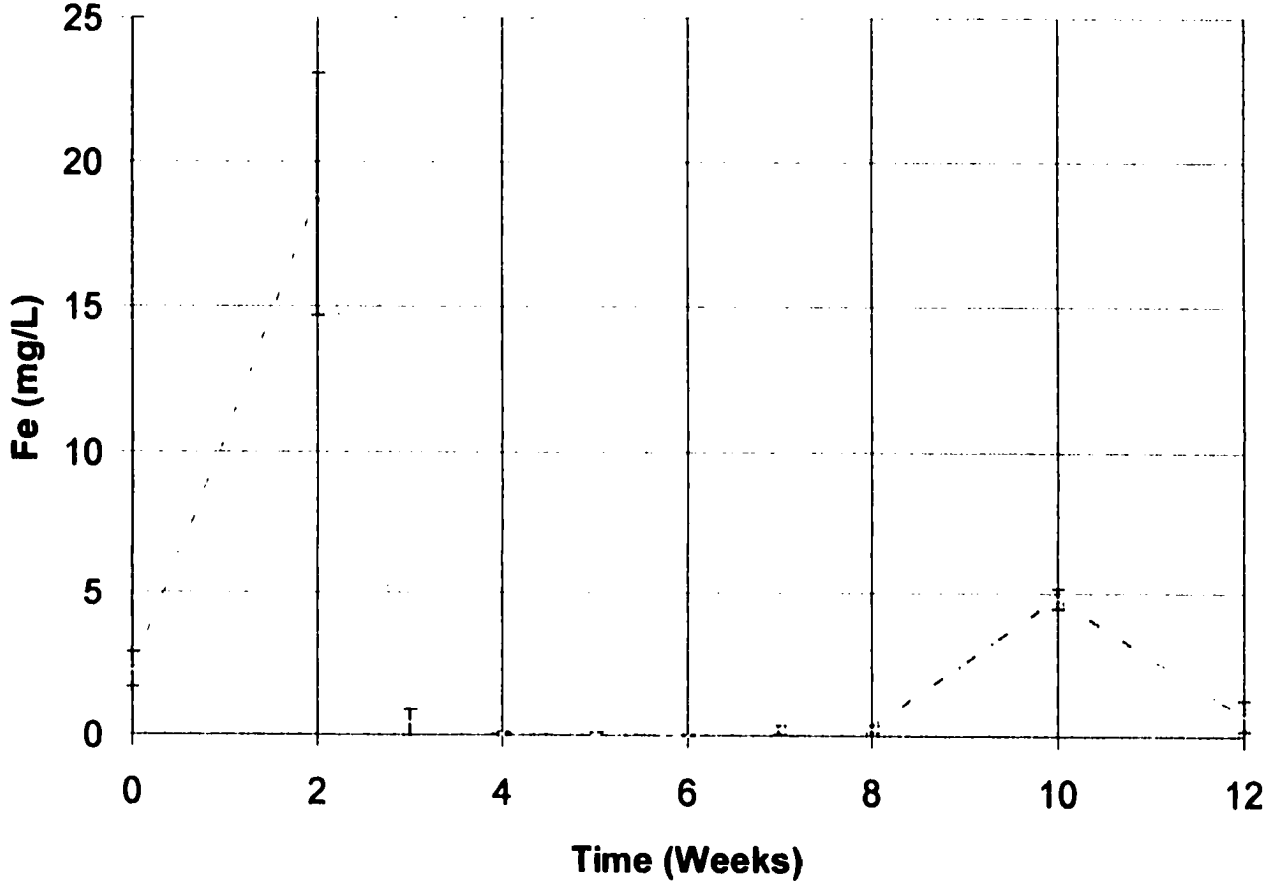

Figure A22: Dissolved Fe Total Pgw + Nat

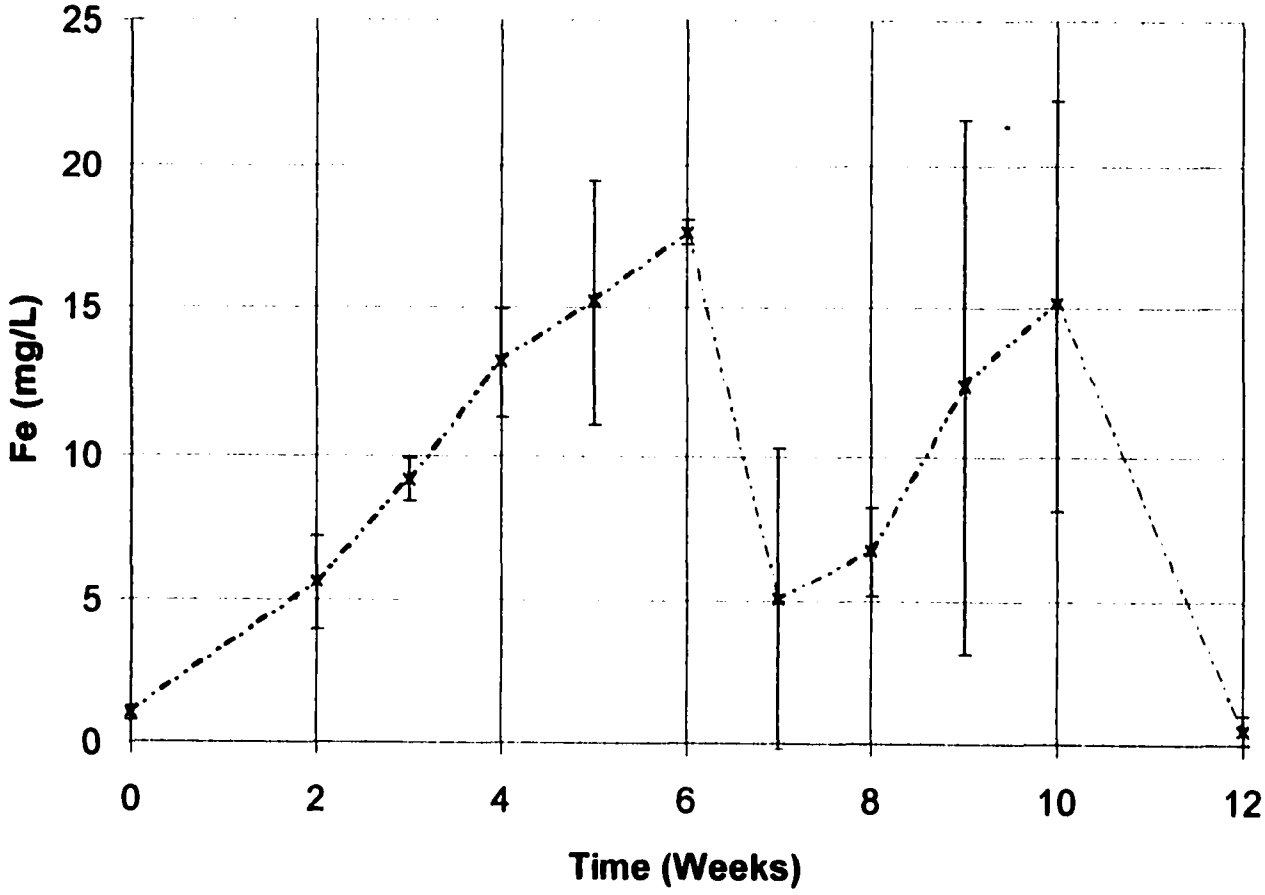

Figure A23: Fe2+ Extracted in 0.5N HCL for Qal + Fe

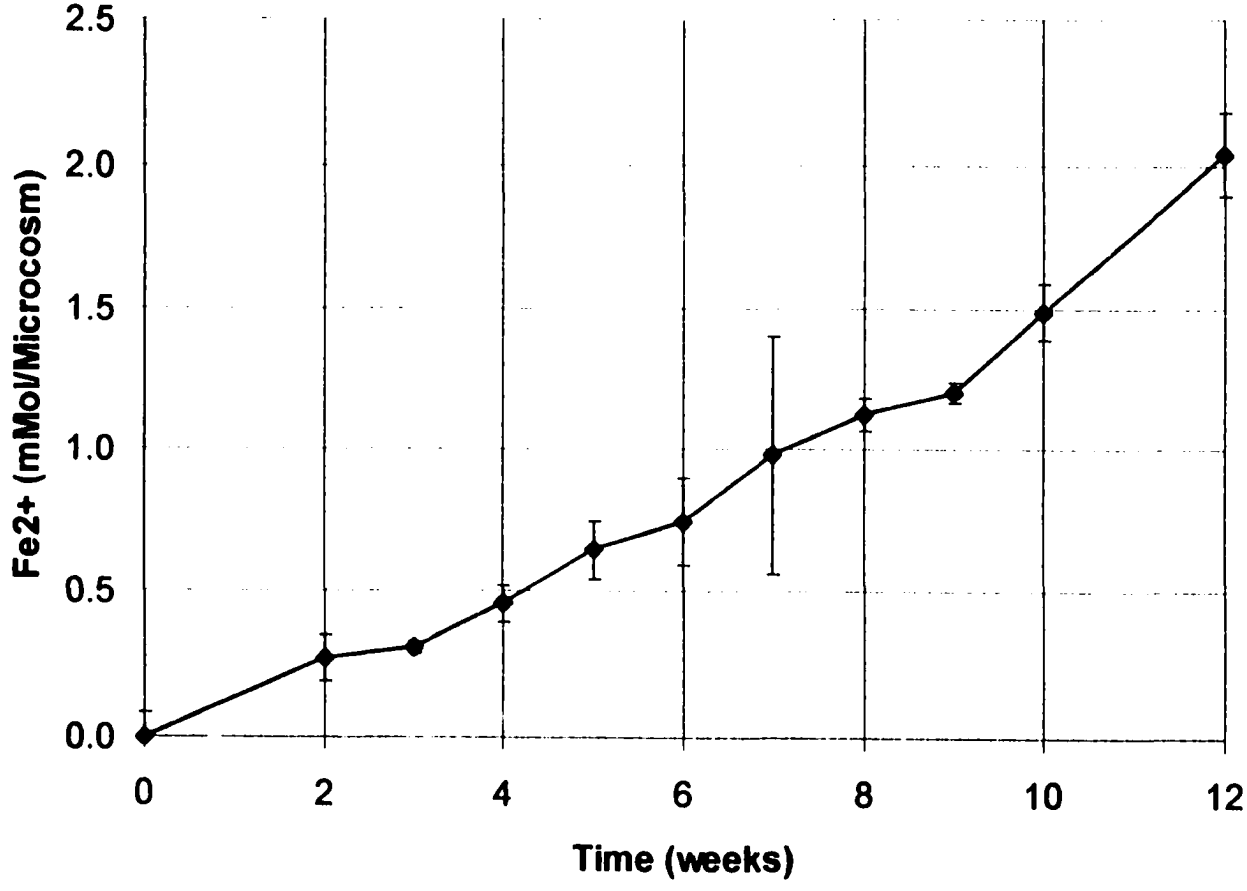

Figure A24: Fe2+ Extracted in 0.5N HCL for Qal + SO4

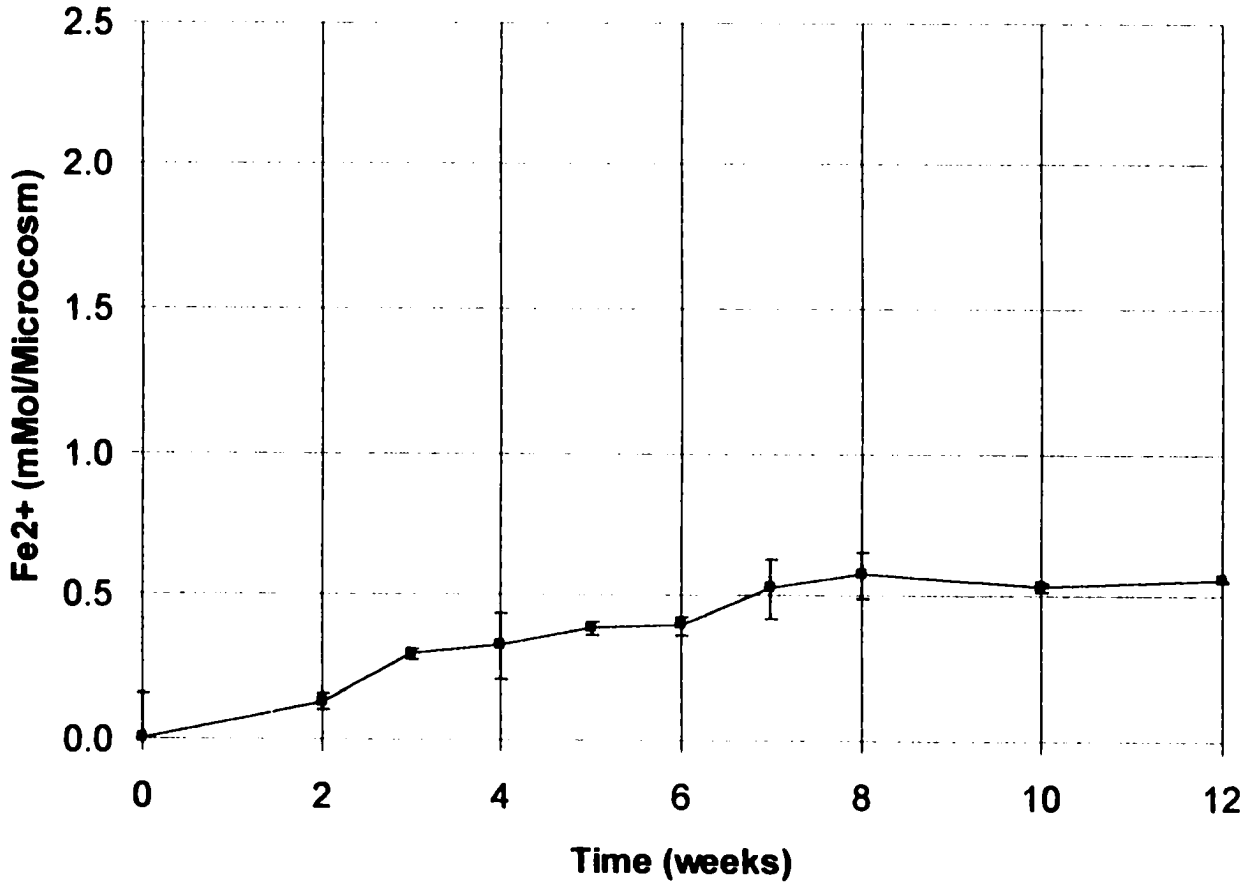

Figure A25: Delta Fe2+ Extracted in 0.5N HCL for Qal Nat.

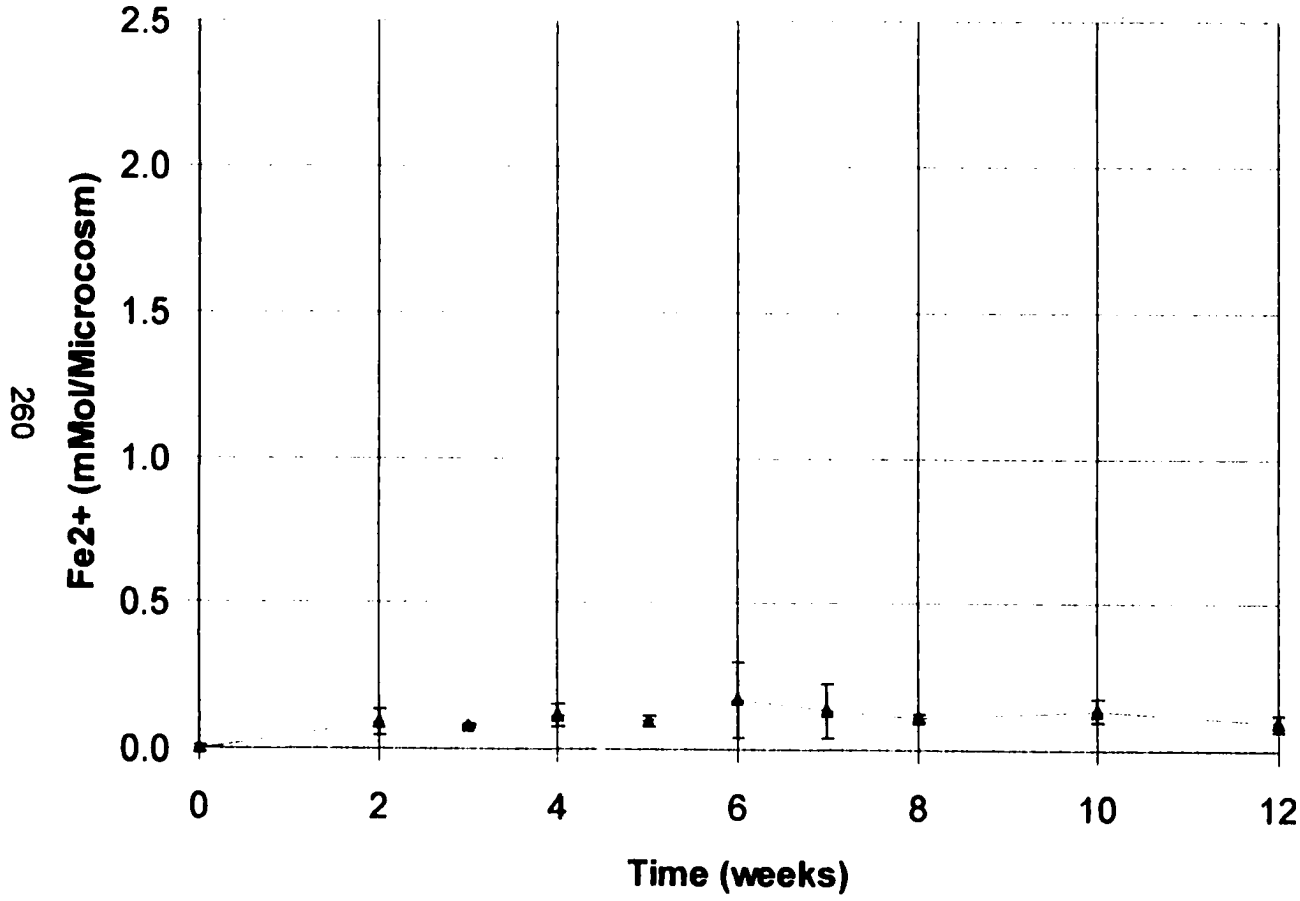

Figure A26: Delta Fe2+ Extracted in 0.5N HCL for Pgw + SO4

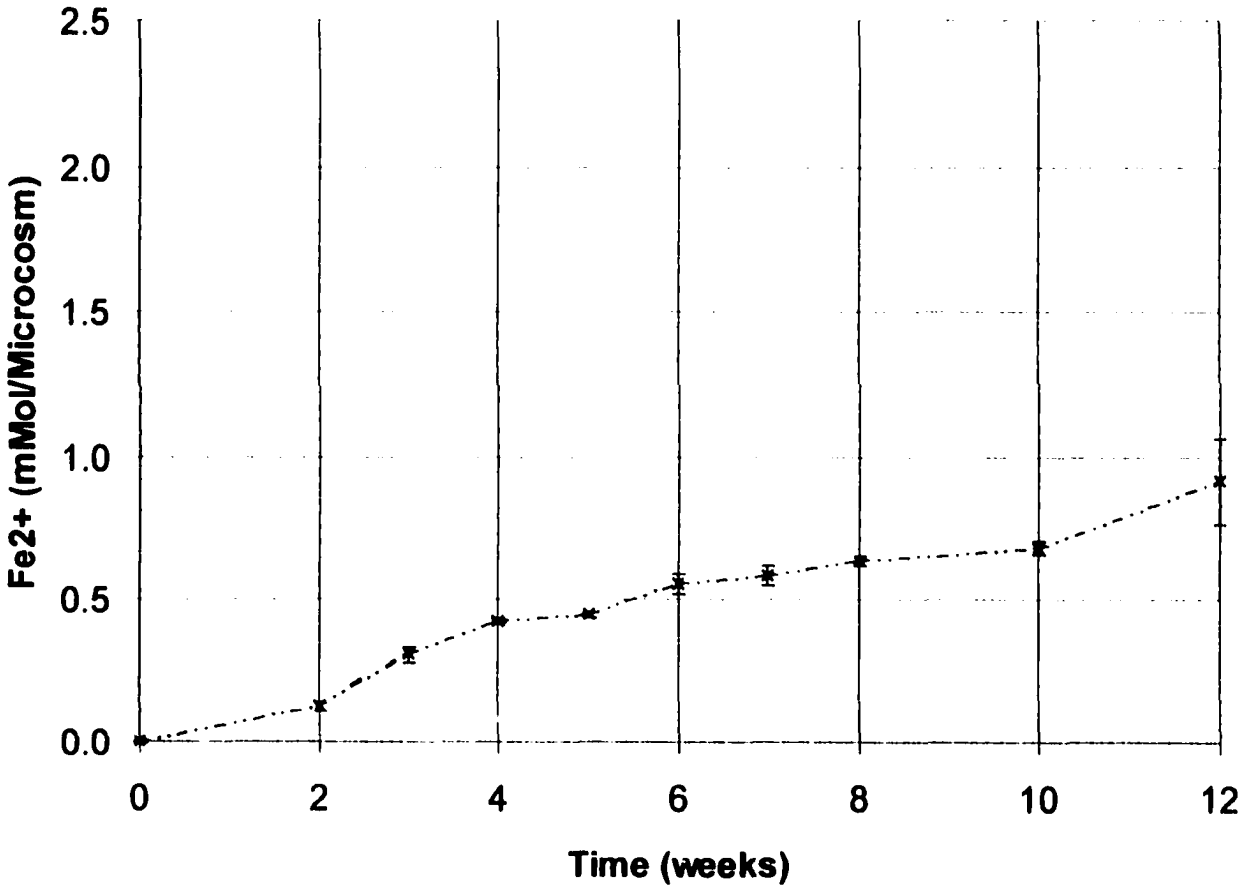

Figure A27: Delta Fe2+ Extracted in 0.5N HCL Pgw Nat.

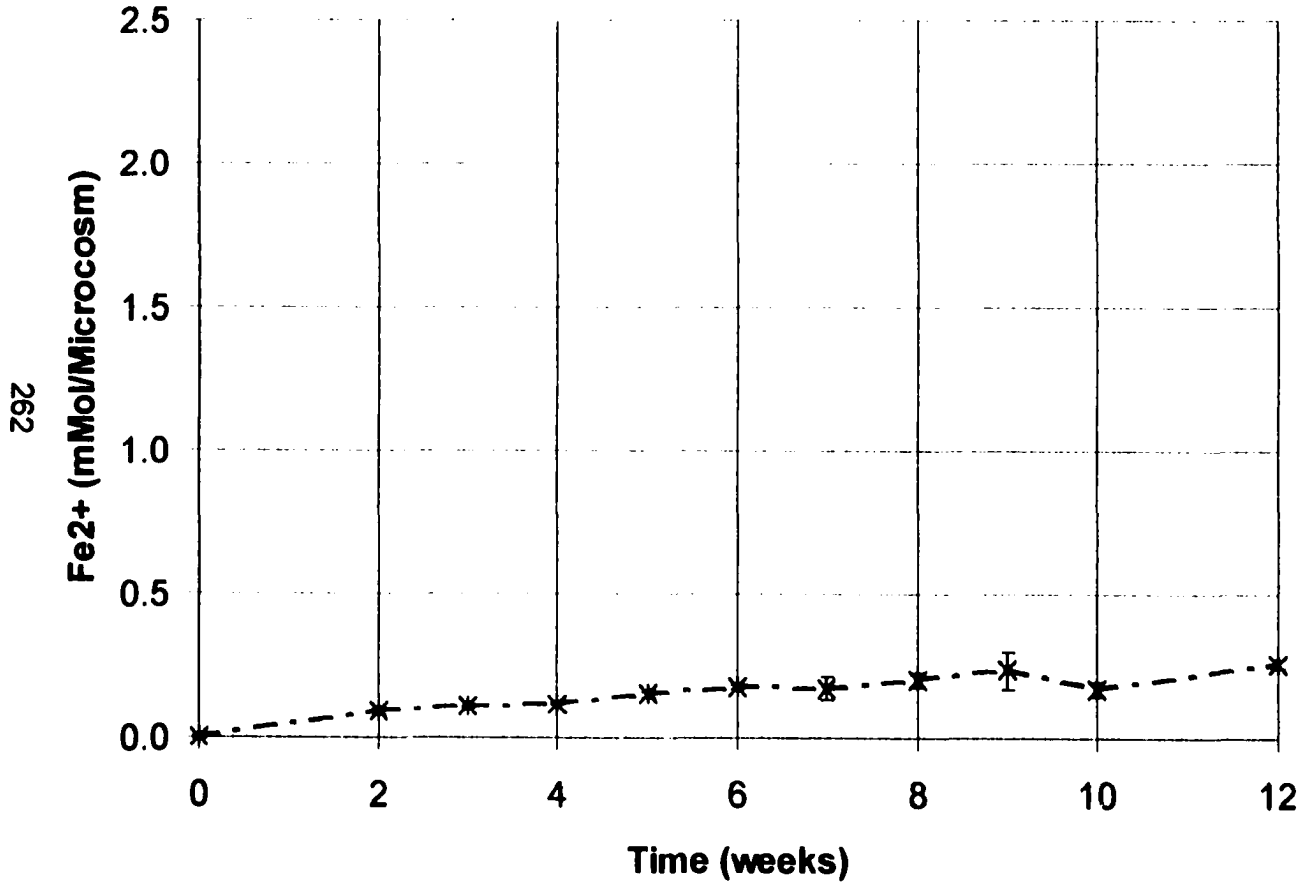

Figure A28: Measured H2S for River+SO4 System

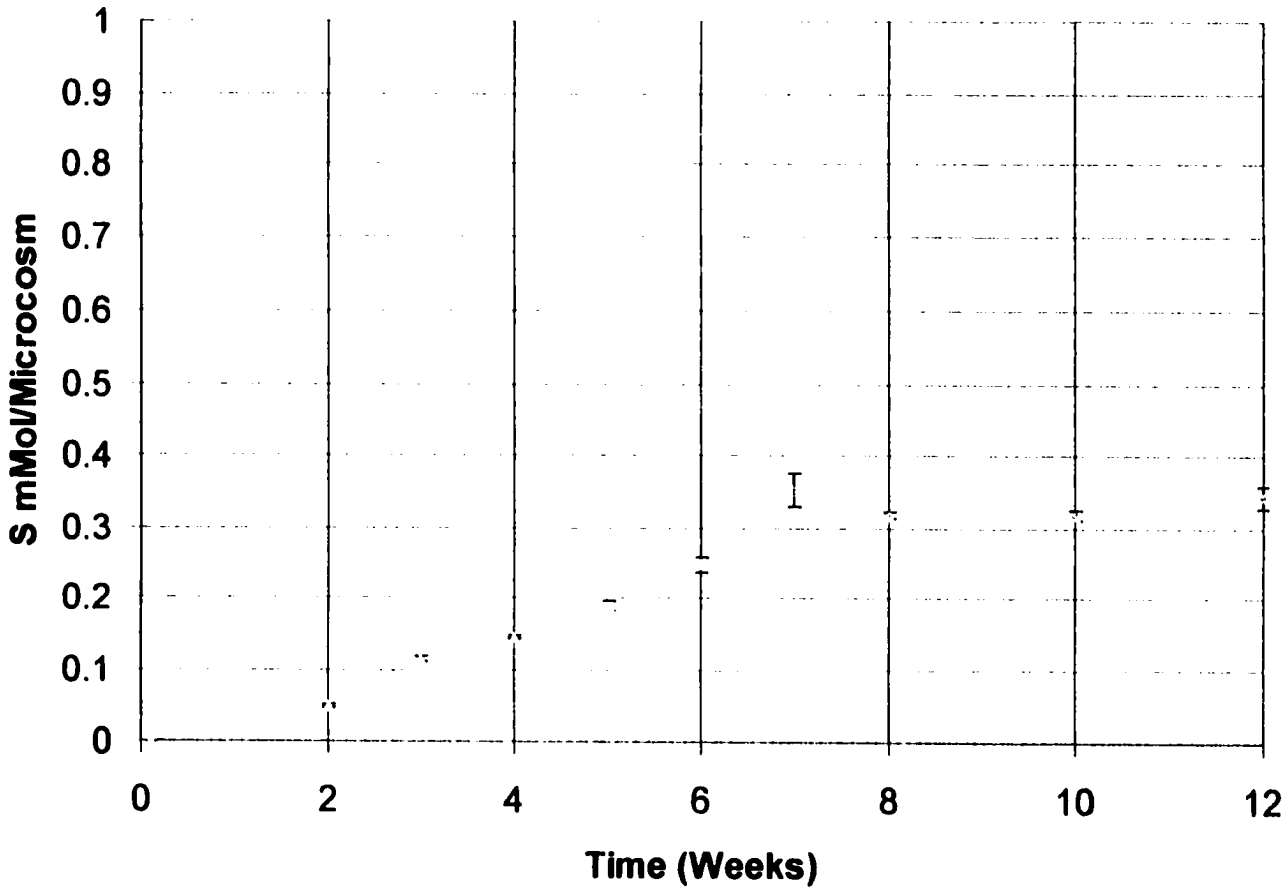

Figure A29: Measured AVS for River+SO4 System

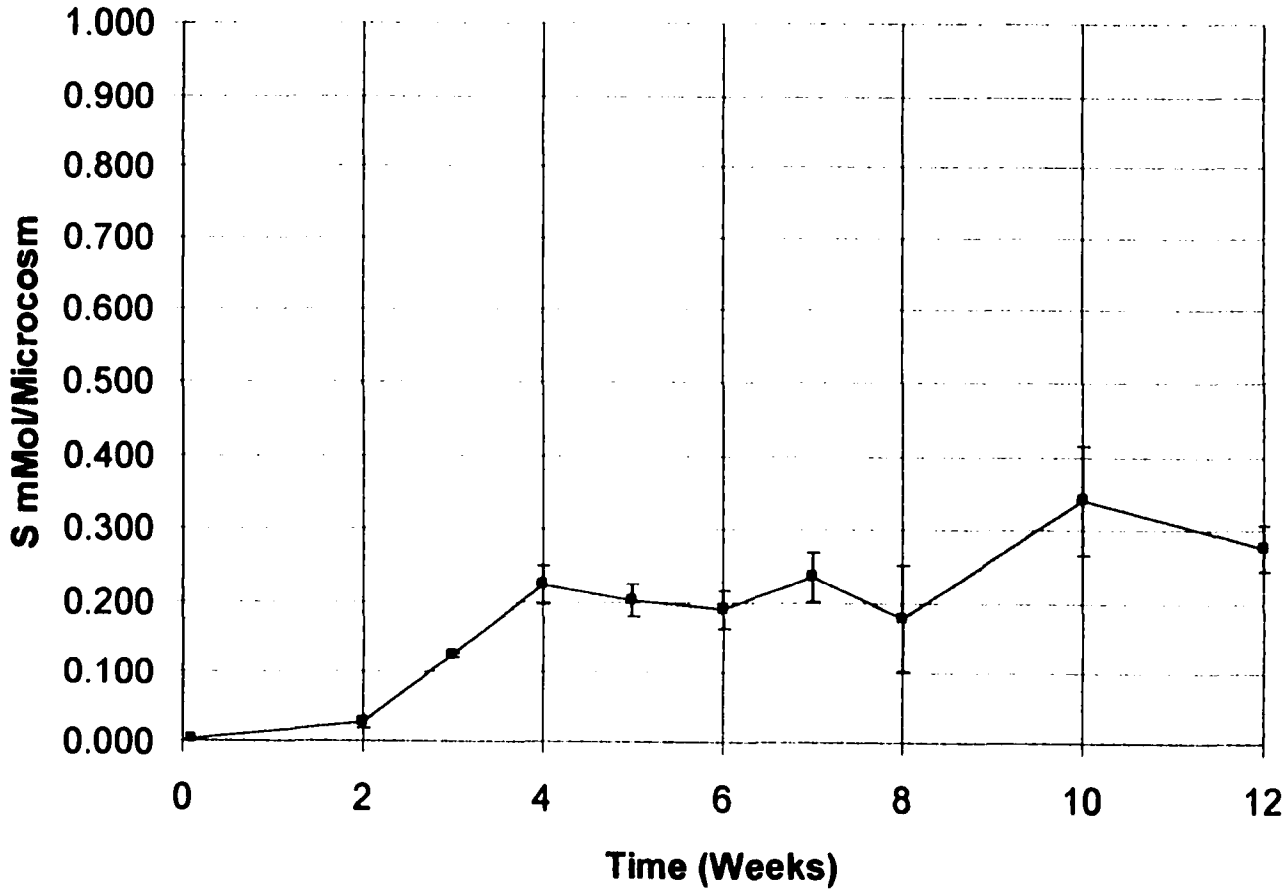

Figure A30: Measured CrES for River+SO4 System

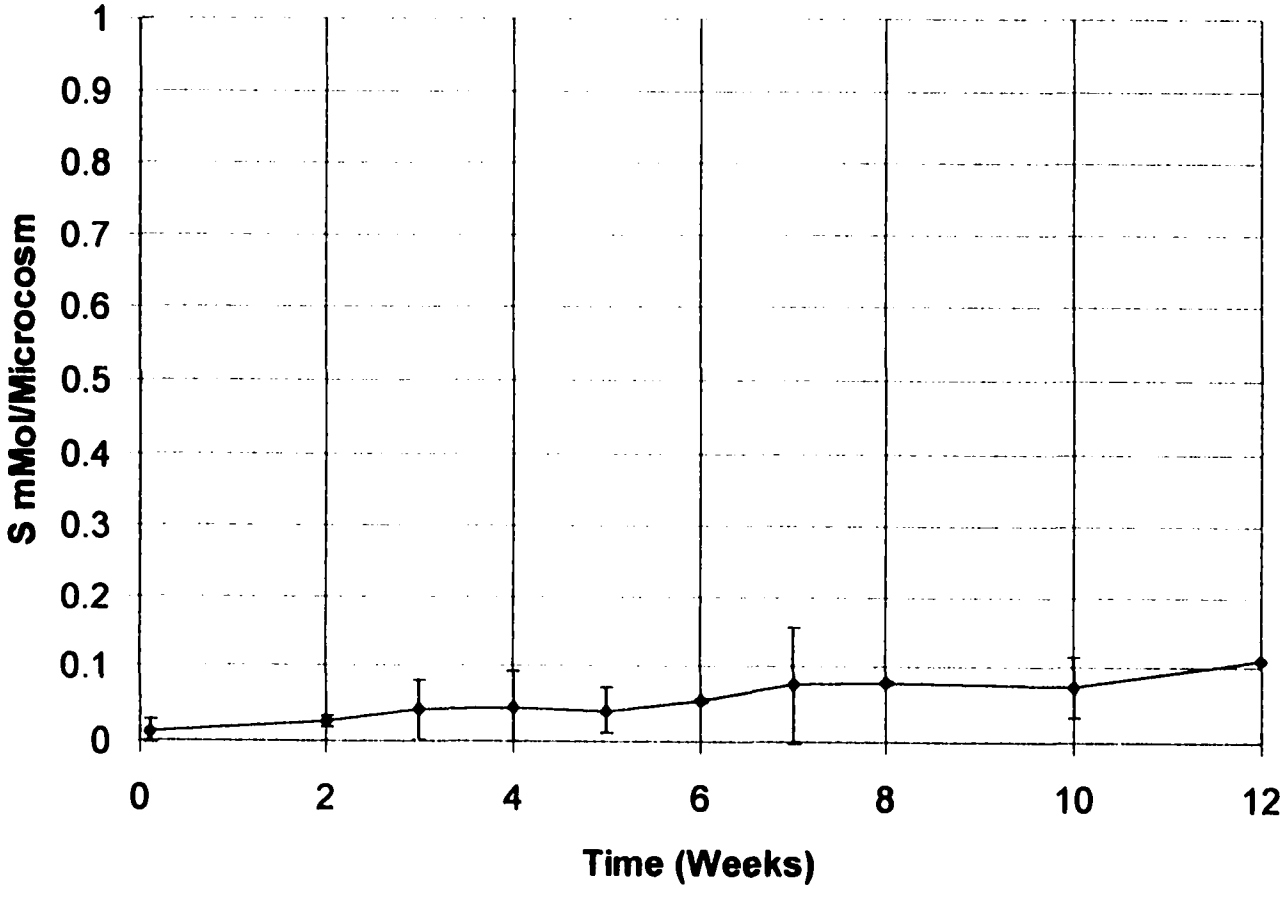

Figure A31: Measured H2S Permian+SO4 System

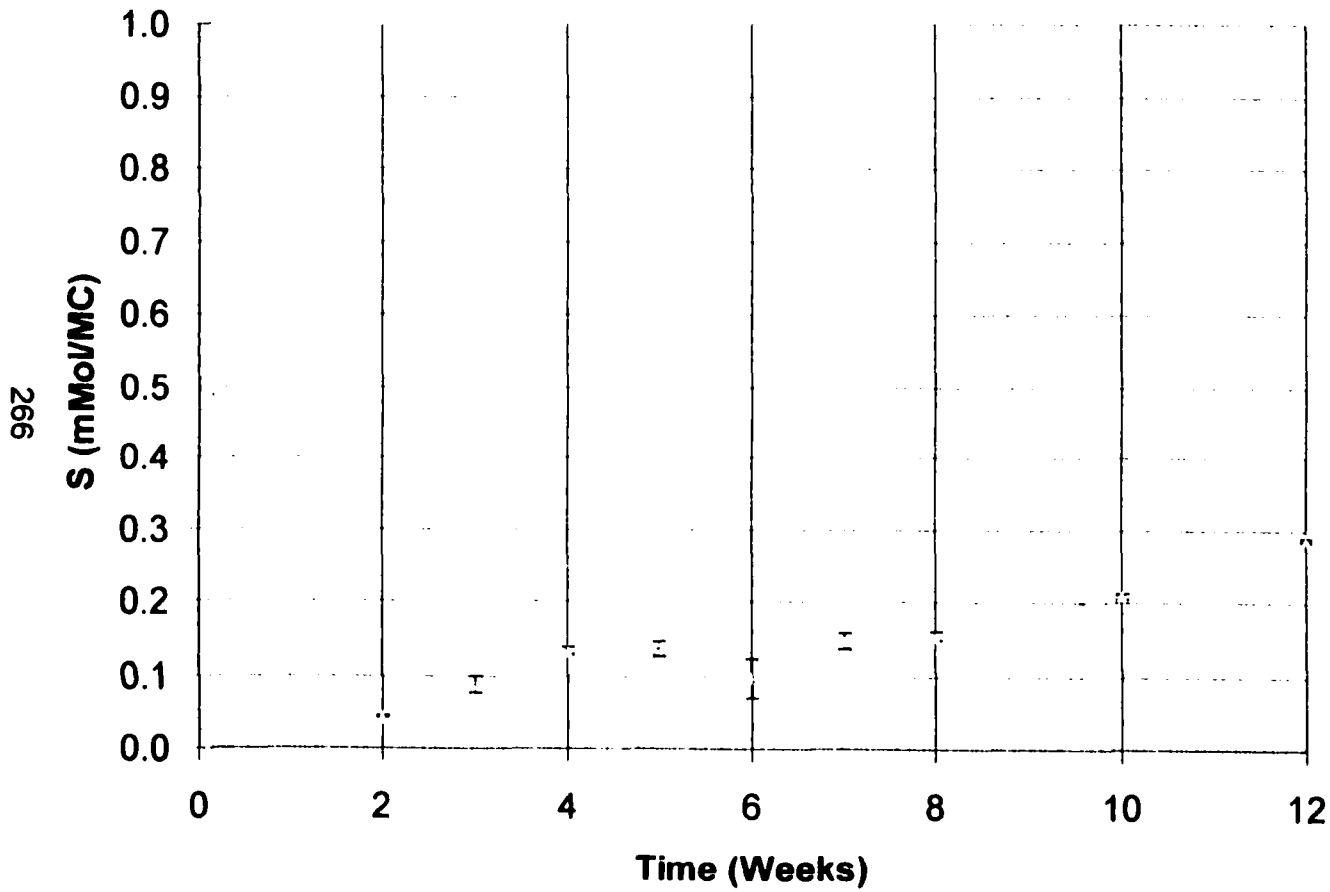

Figure A32: Measured AVS Permian+SO4 System

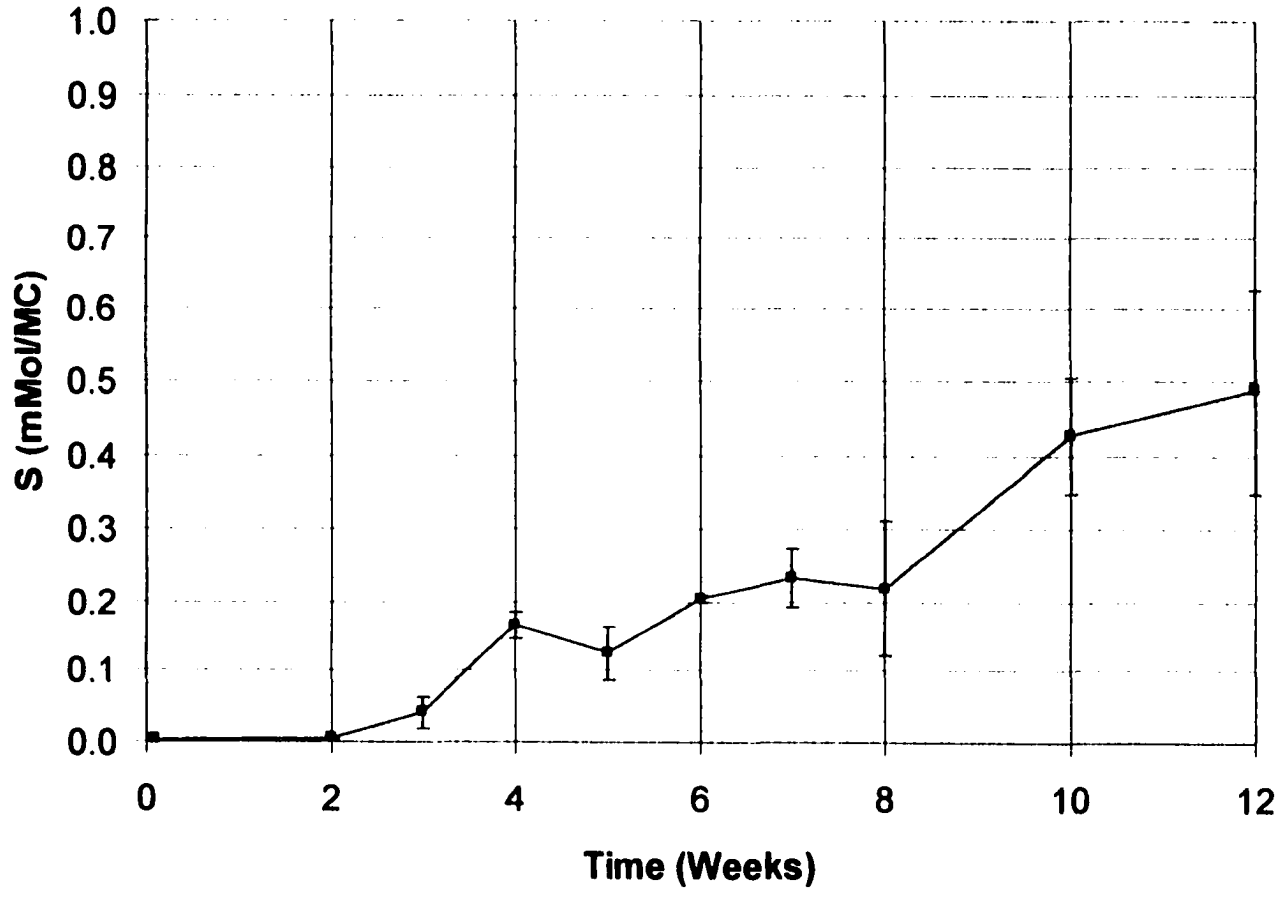

Figure A33: Measured CrES Permian+SO4 System

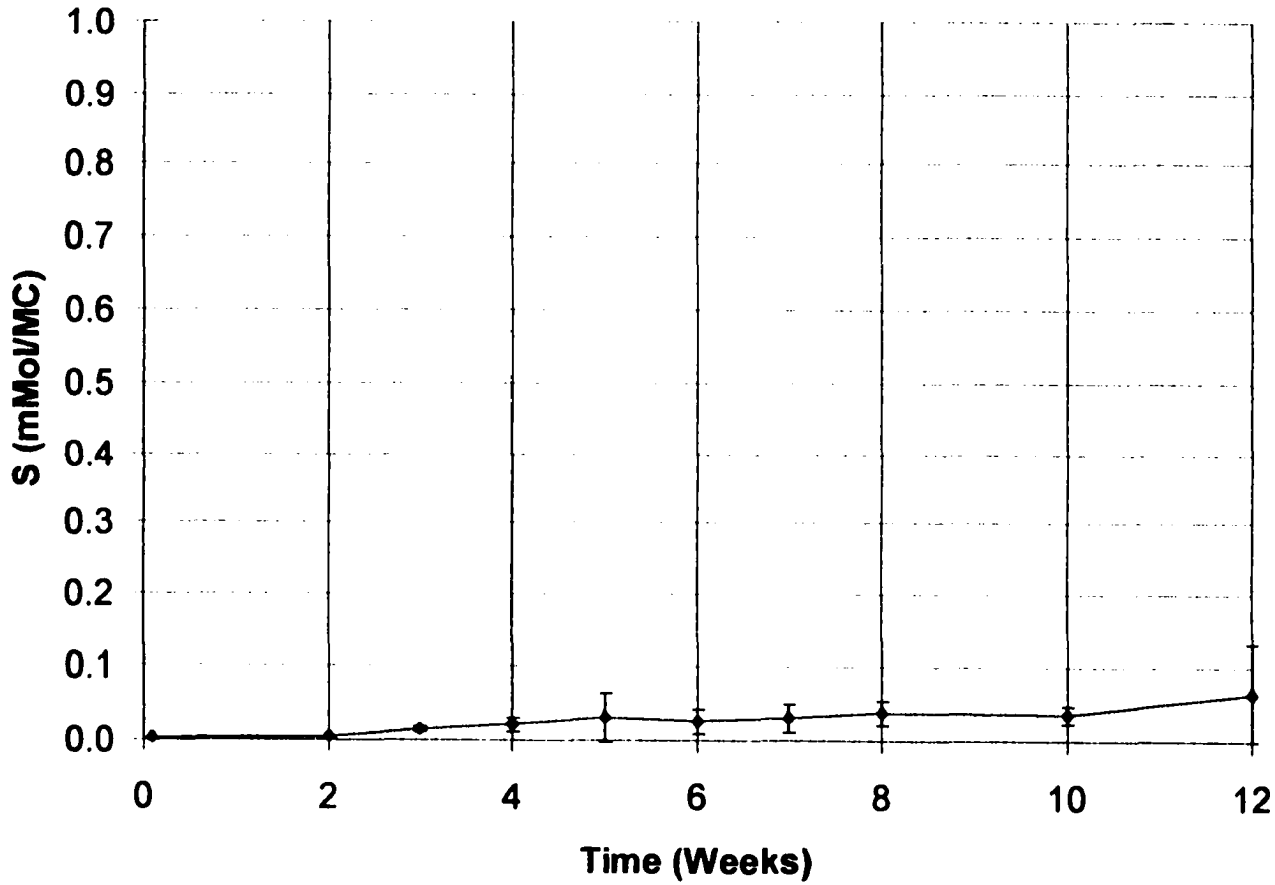

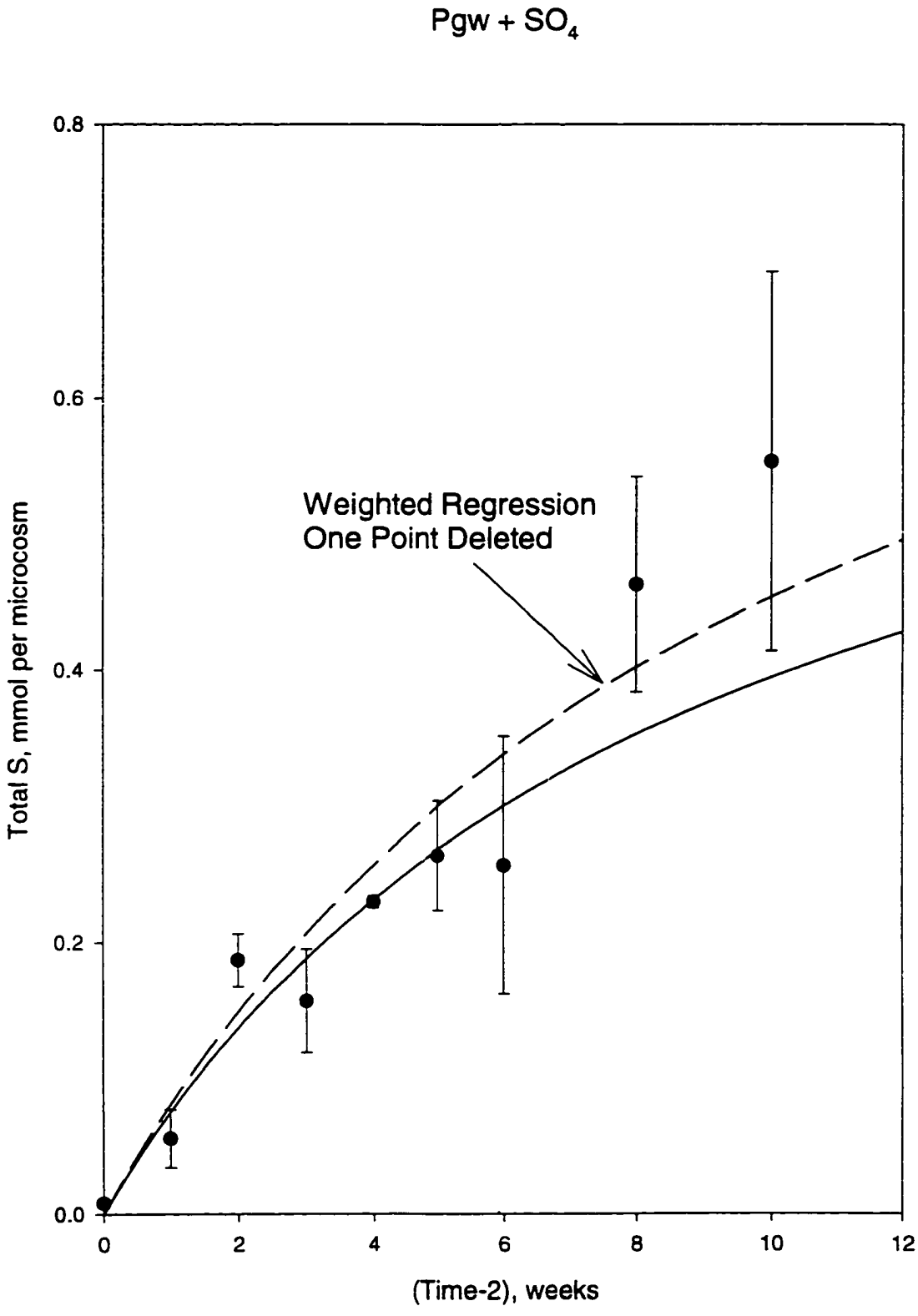
Pgw + SO_4
0.8
0.6
0.4
0.2
0.0
Total S, mmol per microcosm
Weighted Regression
One Point Deleted
0
2
4
6
8
10
12
(Time-2), weeks

Pgw + SCy

Nonlinear Regression

One point deleted

[Variables]
t = col(1)
y = col(2)
w=col(4)
[Parameters]
m=1
k=15
[Equations]
f=m*t/(k+t)
fit f to y with weight w
[Constraints]
m>0
k>0
[Options]
tolerance=0.000100
stepsize=100
iterations=100

R = 0.99944534 Rsqr = 0.99889098 Adj Rsqr = 0.99870615

Standard Error of Estimate = 0.0033

	Coefficient	Std. Error	t	P
m	0.9284	3.3018	0.2812	0.7880
k	10.4604	50.4257	0.2074	0.8425

Analysis of Variance:

	DF	SS	MS	F	P
Regression	1	0.0585	0.0585	5404.2006	<0.0001
Residual	6	0.0001	0.0000		
Total	7	0.0586	0.0084		

PRESS = 0.0001

Durbin-Watson Statistic = 564.5122

Normality Test: Passed (P = 0.6167)

Constant Variance Test: Failed (P = <0.0001)

Power of performed test with alpha = 0.0500: 1.0000

Regression Diagnostics:

Row	Predicted	Residual	Std. Res.	Stud. Res.	Stud. Del. Res.
1	0.0000	0.0080	2.4308	2.4308	18.0100
2	0.0810	-0.0250	-7.5995	-0.2946	-0.2709
3	0.1490	0.0380	11.5409	0.3307	0.3047
4	0.2069	-0.0499	-15.1687	-0.4013	-0.3714
6	0.3003	-0.0363	-11.0163	-0.1991	-0.1823
7	0.3384	-0.0814	-24.7389	-0.3381	-0.3116
8	0.4023	0.0607	18.4324	0.1577	0.1442
9	0.4538	0.0992	30.1539	0.1847	0.1690

Influence Diagnostics:

Row	Cook's Dist.	Leverage	DFFITS

1	0.0000	0.0000	0.0000
2	-0.0435	666.3211	>1e20
3	-0.0547	1218.8372	>1e20
4	-0.0806	1429.5249	>1e20
6	-0.0198	3063.5510	>1e20
7	-0.0572	5354.1421	>1e20
8	-0.0124	13665.2296	>1e20
9	-0.0170	26667.2591	>1e20

95% Confidence

Row	**Predicted**	**Regression 5%**	**Regression 95%**	**Population 5%**	**Population 95%**
1	0.0000	0.0000	0.0000	-0.0081	0.0081
2	0.0810	-0.1269	0.2889	-0.1270	0.2890
3	0.1490	-0.1321	0.4302	-0.1322	0.4303
4	0.2069	-0.0976	0.5114	-0.0977	0.5115
6	0.3003	-0.1455	0.7460	-0.1455	0.7461
7	0.3384	-0.2508	0.9277	-0.2509	0.9277
8	0.4023	-0.5390	1.3437	-0.5391	1.3437
9	0.4538	-0.8613	1.7688	-0.8613	1.7688

Nonlinear Regression

[Variables]
t = col(1)
y = col(2)
[Parameters]
m=1
k=15
[Equations]
f=m*t/(k+t)
fit f to y
[Constraints]
m>0
k>0
[Options]
tolerance=0.000100
stepsize=100
iterations=100

R = 0.97719167 Rsqr = 0.95490356 Adj Rsqr = 0.94846121

Standard Error of Estimate = 0.0416

	Coefficient	**Std. Error**	**t**	**P**
m	685.3760	30201.6684	0.0227	0.9825
k	12552.2263	553517.4793	0.0227	0.9825

Analysis of Variance:

	DF	**SS**	**MS**	**F**	**P**
Regression	1	0.2562	0.2562	148.2229	<0.0001
Residual	7	0.0121	0.0017		
Total	8	0.2683	0.0335		

PRESS = 0.0184

Durbin-Watson Statistic = 2.2596

Normality Test: Passed (P = 0.1191)

Constant Variance Test: Passed (P = 0.4905)

Power of performed test with alpha = 0.0500: 0.9998

Regression Diagnostics:

Row	**Predicted**	**Residual**	**Std. Res.**	**Stud. Res.**	**Stud. Del. Res.**
1	0.0000	0.0080	0.1924	0.1924	0.1786
2	0.0546	0.0014	0.0337	0.0343	0.0318
3	0.1092	0.0778	1.8715	1.9799	2.7636
4	0.1638	-0.0068	-0.1627	-0.1790	-0.1661
5	0.2183	0.0117	0.2805	0.3164	0.2951
6	0.2729	-0.0089	-0.2141	-0.2429	-0.2258
7	0.3275	-0.0705	-1.6945	-1.9078	-2.5494
8	0.4365	0.0265	0.6365	0.7380	0.7115
9	0.5456	0.0074	0.1783	0.3798	0.3553

Influence Diagnostics:

Row	**Cook's Dist.**	**Leverage**	**DFFITS**

1	0.0000	0.0000	0.0000
2	0.0000	0.0354	0.0061
3	0.2337	0.1065	0.9543
4	0.0034	0.1737	-0.0762
5	0.0137	0.2144	0.1541
6	0.0085	0.2230	-0.1210
7	0.4870	0.2111	-1.3187
8	0.0939	0.2563	0.4177
9	0.2551	0.7795	0.6682

95% Confidence

Row	**Predicted**	**Regression 5%**	**Regression 95%**	**Population 5%**	**Population 95%**
1	0.0000	0.0000	0.0000	-0.0983	0.0983
2	0.0546	0.0361	0.0731	-0.0454	0.1546
3	0.1092	0.0771	0.1413	0.0058	0.2126
4	0.1638	0.1228	0.2047	0.0573	0.2703
5	0.2183	0.1728	0.2639	0.1100	0.3267
6	0.2729	0.2265	0.3193	0.1642	0.3816
7	0.3275	0.2823	0.3726	0.2193	0.4357
8	0.4365	0.3868	0.4863	0.3263	0.5467
9	0.5456	0.4588	0.6324	0.4144	0.6767

Pgw + SO_4

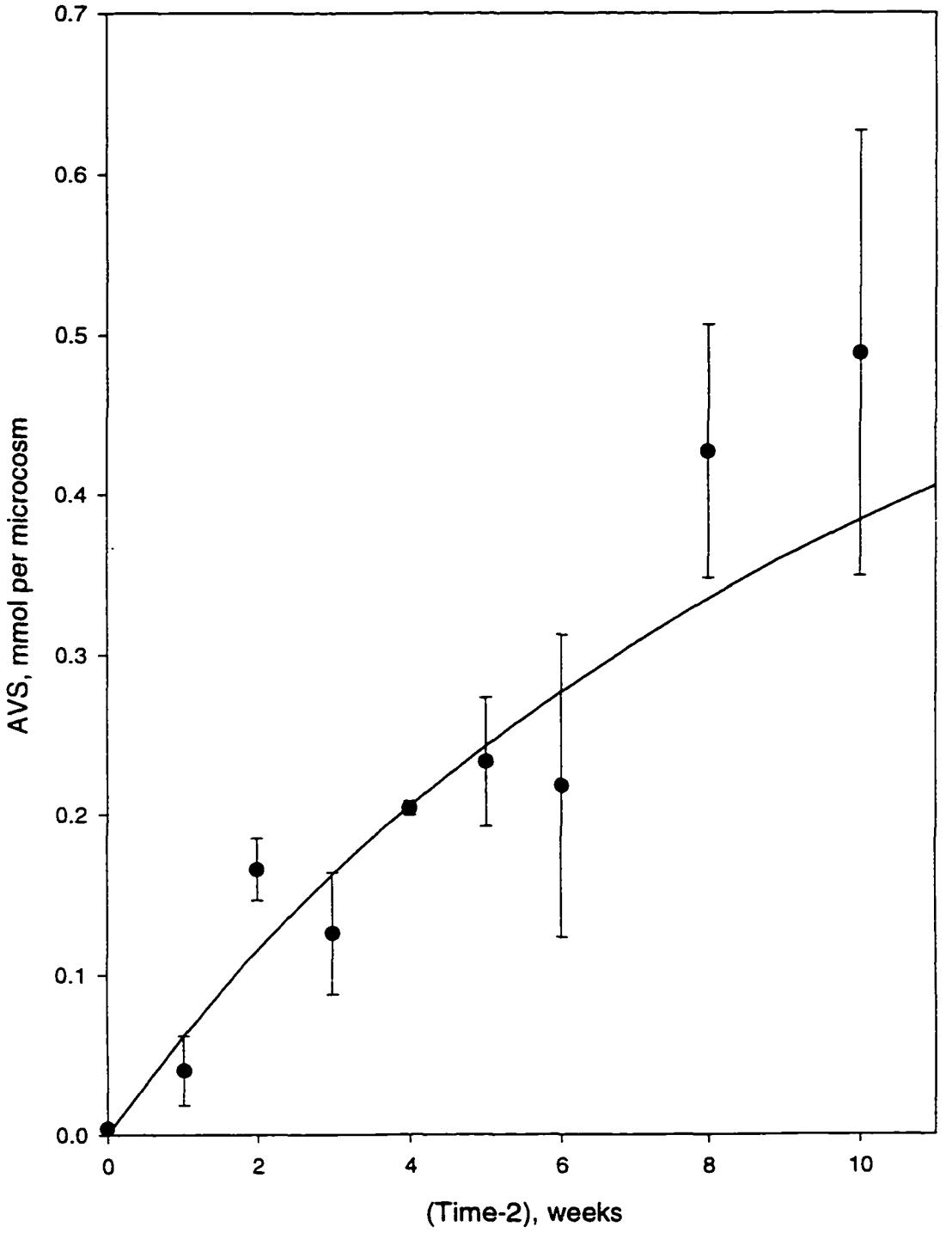
0.7
0.6
0.5
0.4
0.3
0.2
0.1
0.0
AVS, mmol per microcosm
0
2
4
6
8
10
(Time-2), weeks

Nonlinear Regression

[Variables]
t = col(1)
y = col(2)
w=col(4)
[Parameters]
m=0.56
k=6
[Equations]
f=m*t/(k+t)
fit f to y with weight w
[Constraints]
m>0
k>0
[Options]
tolerance=0.000100
stepsize=100
iterations=100

R = 0.99980036 Rsqr = 0.99960075 Adj Rsqr = 0.99954372

Standard Error of Estimate = 0.0016

	Coefficient	Std. Error	t	P
m	0.9165	2.1638	0.4236	0.6846
k	13.8710	42.1828	0.3288	0.7519

Analysis of Variance:

	DF	SS	MS	F	P
Regression	1	0.0444	0.0444	17526.0617	<0.0001
Residual	7	0.0000	0.0000		
Total	8	0.0444	0.0056		

PRESS = 0.0000

Durbin-Watson Statistic = 2258.5081

Normality Test: Passed (P = 0.1660)

Constant Variance Test: Failed (P = 0.0428)

Power of performed test with alpha = 0.0500: 1.0000

Regression Diagnostics:

Row	Predicted	Residual	Std. Res.	Stud. Res.	Stud. Del. Res.
1	0.0000	0.0040	2.5127	2.5127	7.4289
2	0.0616	-0.0216	-13.5870	-0.6524	-0.6232
3	0.1155	0.0505	31.7274	1.2869	1.3636
4	0.1630	-0.0370	-23.2237	-1.3038	-1.3873
5	0.2051	-0.0011	-0.7128	-0.0696	-0.0645
6	0.2428	-0.0098	-6.1752	-0.2573	-0.2394
7	0.2767	-0.0587	-36.8938	-0.7881	-0.7644
8	0.3352	0.0918	57.6442	0.5809	0.5513
9	0.3839	0.1041	65.3709	0.4239	0.3976

Influence Diagnostics:

Pgw AVS

Row	Cook's Dist.	Leverage	DFFITS
1	0.0000	0.0000	0.0000
2	-0.2133	434.7536	>1e20
3	-0.8294	608.8372	>1e20
4	-0.8527	318.2573	>1e20
5	-0.0024	105.8146	>1e20
6	-0.0332	576.8233	>1e20
7	-0.3107	2192.2776	>1e20
8	-0.1687	9847.9379	>1e20
9	-0.0898	23786.9991	>1e20

95% Confidence

Row	Predicted	Regression 5%	Regression 95%	Population 5%	Population 95%
1	0.0000	0.0000	0.0000	-0.0038	0.0038
2	0.0616	-0.0169	0.1401	-0.0169	0.1402
3	0.1155	0.0226	0.2084	0.0225	0.2085
4	0.1630	0.0958	0.2301	0.0957	0.2302
5	0.2051	0.1664	0.2439	0.1662	0.2440
6	0.2428	0.1524	0.3332	0.1523	0.3333
7	0.2767	0.1005	0.4530	0.1004	0.4530
8	0.3352	-0.0383	0.7088	-0.0383	0.7088
9	0.3839	-0.1966	0.9645	-0.1966	0.9645

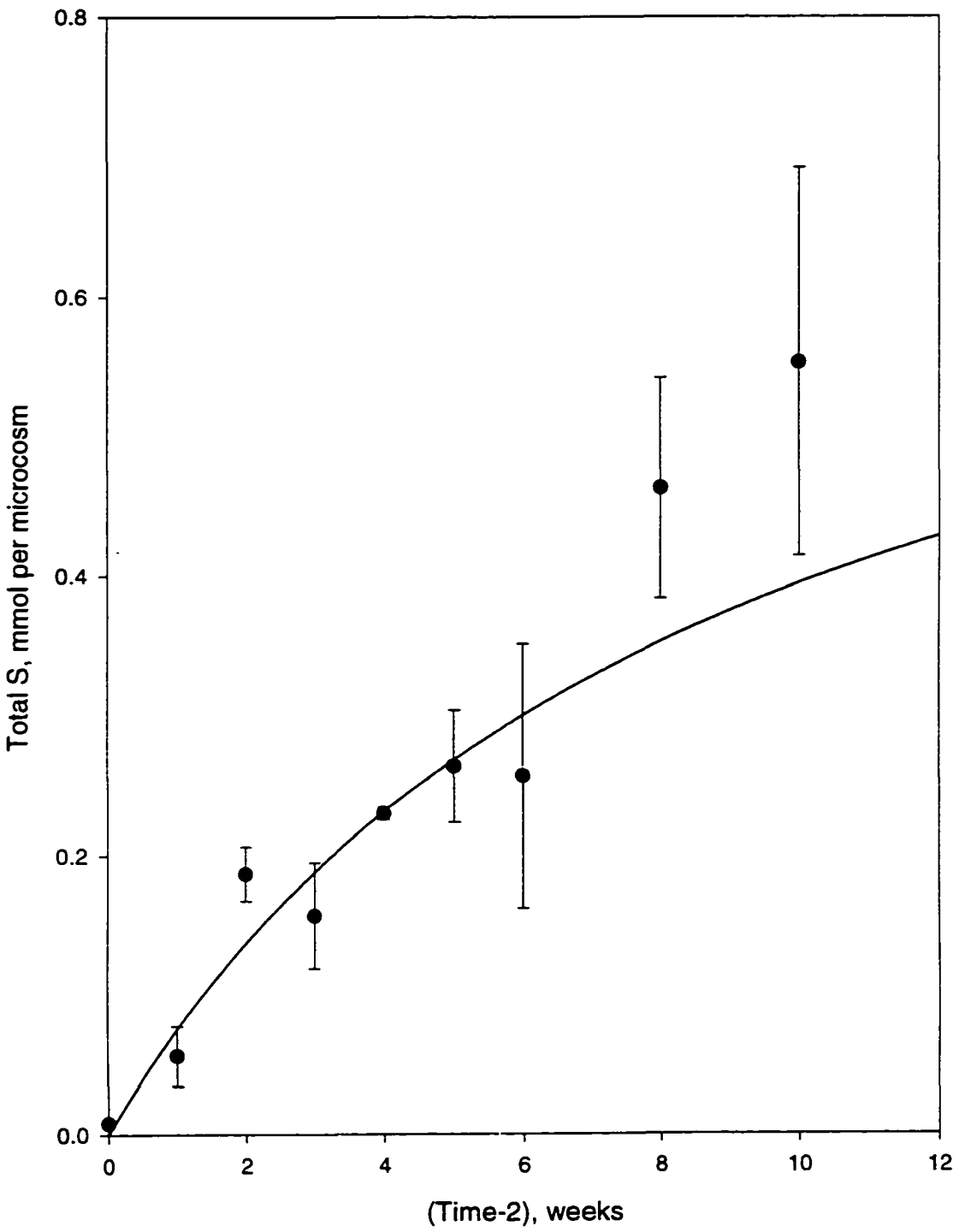
Pgw + SO4
0.8
0.6
0.4
0.2
0.0
Total S, mmol per microcosm
0
2
4
6
8
10
12
(Time-2), weeks

Nonlinear Regression

[Variables]
t = col(1)
y = col(2)
w=col(4)
[Parameters]
m=0.56
k=6
[Equations]
f=m*t/(k+t)
fit f to y with weight w
[Constraints]
m>0
k>0
[Options]
tolerance=0.000100
stepsize=100
iterations=100

R = 0.99943549 Rsqr = 0.99887130 Adj Rsqr = 0.99871005

Standard Error of Estimate = 0.0031

	Coefficient	Std. Error	t	P
m	0.7455	2.1062	0.3540	0.7338
k	8.8817	36.3101	0.2446	0.8138

Analysis of Variance:

	DF	SS	MS	F	P
Regression	1	0.0578	0.0578	6194.8137	<0.0001
Residual	7	0.0001	0.0000		
Total	8	0.0579	0.0072		

PRESS = 0.0001

Durbin-Watson Statistic = 618.6667

Normality Test: Passed (P = 0.0672)

Constant Variance Test: Passed (P = 0.1384)

Power of performed test with alpha = 0.0500: 1.0000

Regression Diagnostics:

Row	Predicted	Residual	Std. Res.	Stud. Res.	Stud. Del. Res.
1	0.0000	0.0080	2.6182	2.6182	16.8506
2	0.0754	-0.0194	-6.3641	-0.2548	-0.2370
3	0.1370	0.0500	16.3560	0.5967	0.5671
4	0.1882	-0.0312	-10.2235	-0.5542	-0.5247
5	0.2315	-0.0015	-0.4909	-0.0479	-0.0444
6	0.2685	-0.0045	-1.4823	-0.0629	-0.0582
7	0.3006	-0.0436	-14.2634	-0.3248	-0.3030
8	0.3533	0.1097	35.9041	0.4142	0.3882
9	0.3948	0.1582	51.7620	0.4058	0.3802

Influence Diagnostics:

Total 5 PGW

Row	Cook's Dist.	Leverage	DFFITS
1	0.0000	0.0000	0.0000
2	-0.0325	624.8191	>1e20
3	-0.1783	752.2738	>1e20
4	-0.1540	341.3528	>1e20
5	-0.0012	105.8828	>1e20
6	-0.0020	556.8516	>1e20
7	-0.0528	1929.6424	>1e20
8	-0.0858	7516.1851	>1e20
9	-0.0824	16268.1930	>1e20

95% Confidence

Row	Predicted	Regression 5%	Regression 95%	Population 5%	Population 95%
1	0.0000	0.0000	0.0000	-0.0072	0.0072
2	0.0754	-0.1052	0.2560	-0.1053	0.2562
3	0.1370	-0.0611	0.3352	-0.0613	0.3353
4	0.1882	0.0547	0.3217	0.0546	0.3219
5	0.2315	0.1572	0.3058	0.1568	0.3062
6	0.2685	0.0980	0.4390	0.0979	0.4392
7	0.3006	-0.0168	0.6180	-0.0169	0.6180
8	0.3533	-0.2731	0.9797	-0.2731	0.9797
9	0.3948	-0.5267	1.3164	-0.5267	1.3164

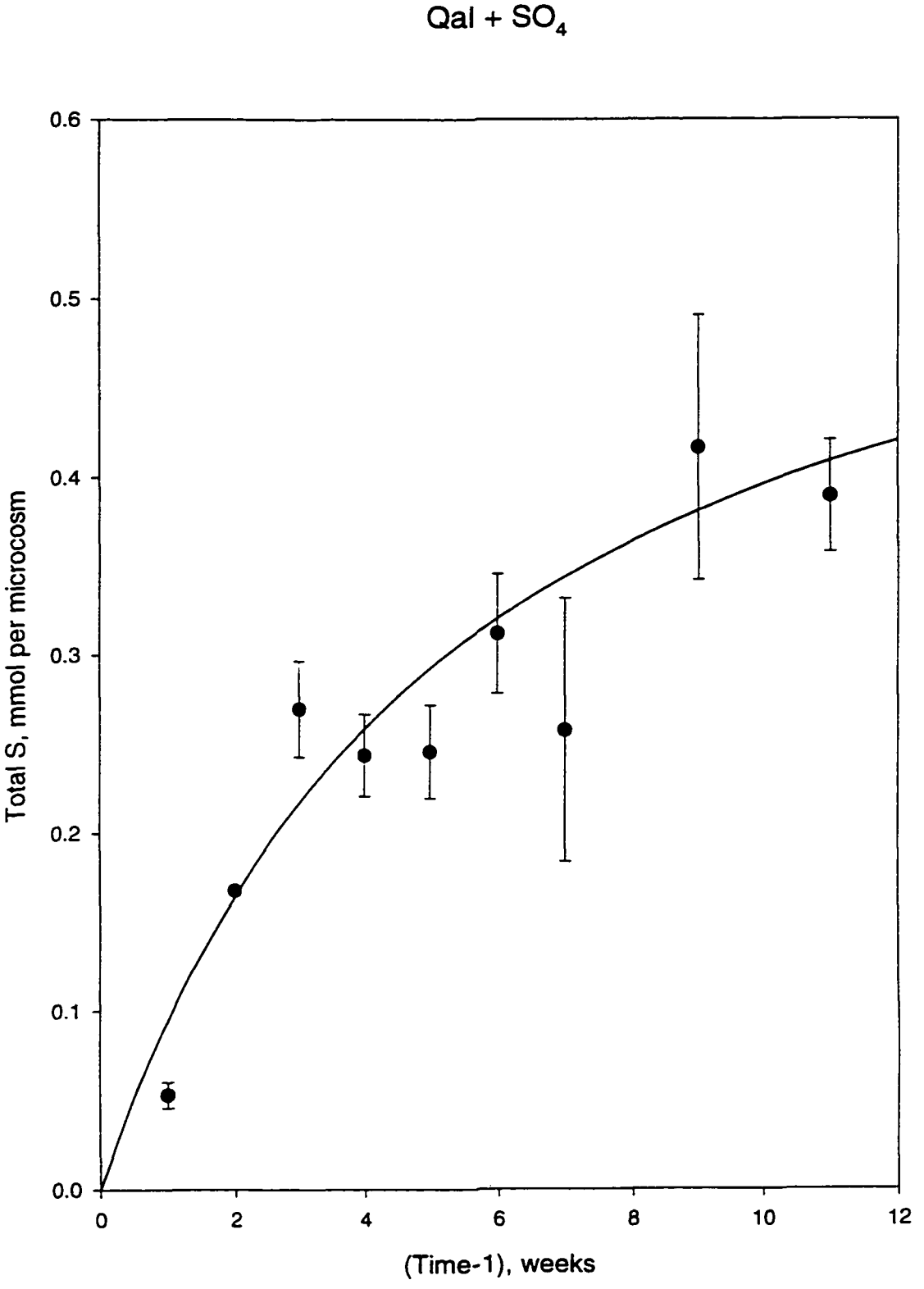
Qal + SO4
Total S, mmol per microcosm
0.0
0.1
0.2
0.3
0.4
0.5
0.6
0
2
4
6
8
10
12
(Time-1), weeks

Nonlinear Regression

[Variables]
t = col(1)
y = col(2)
w=col(4)
[Parameters]
m=0.56
k=6
[Equations]
f=m*t/(k+t)
fit f to y with weight w
[Constraints]
m>0
k>0
[Options]
tolerance=0.000100
stepsize=100
iterations=100

R = 0.98976695 Rsqr = 0.97963863 Adj Rsqr = 0.97672986

Standard Error of Estimate = 0.0057

	Coefficient	Std. Error	t	P
m	0.6099	0.1617	3.7717	0.0070
k	5.4202	2.0218	2.6808	0.0315

Analysis of Variance:

	DF	SS	MS	F	P
Regression	1	0.0111	0.0111	336.7882	<0.0001
Residual	7	0.0002	0.0000		
Total	8	0.0113	0.0014		

PRESS = 0.3214

Durbin-Watson Statistic = 152.7905

Normality Test: Passed (P = 0.8112)

Constant Variance Test: Passed (P = 0.8094)

Power of performed test with alpha = 0.0500: 1.0000

Regression Diagnostics:

Row	Predicted	Residual	Std. Res.	Stud. Res.	Stud. Del. Res.
1	0.0950	-0.0420	-7.3231	-26.7961	>1e20
2	0.1644	0.0036	0.6273	2.5846	11.1943
3	0.2173	0.0527	9.1851	7.6167	>1e20
4	0.2590	-0.0150	-2.6143	-1.0523	-1.0618
5	0.2927	-0.0467	-8.1375	-2.1417	-3.3769
6	0.3205	-0.0085	-1.4744	-0.2908	-0.2709
7	0.3438	-0.0858	-14.9524	-2.3864	-5.1172
8	0.3807	0.0353	6.1571	0.7332	0.7064
9	0.4086	-0.0196	-3.4185	-0.3350	-0.3126

Influence Diagnostics:

Qa | total 5

Row	Cook's Dist.	Leverage	DFFITS
1	-5165.9254	1.0747	>1e20
2	-60.0356	1.0589	>1e20
3	-48.9533	2.4542	>1e20
4	-0.6434	7.1723	>1e20
5	-2.4522	15.4370	>1e20
6	-0.0439	26.7101	>1e20
7	-2.9201	40.2576	>1e20
8	-0.2726	71.5261	>1e20
9	-0.0566	105.1506	>1e20

95% Confidence

Row	Predicted	Regression 5%	Regression 95%	Population 5%	Population 95%
1	0.0950	0.0809	0.1091	0.0755	0.1145
2	0.1644	0.1504	0.1784	0.1449	0.1839
3	0.2173	0.1961	0.2386	0.1921	0.2425
4	0.2590	0.2227	0.2953	0.2202	0.2978
5	0.2927	0.2394	0.3460	0.2377	0.3477
6	0.3205	0.2504	0.3906	0.2491	0.3919
7	0.3438	0.2577	0.4298	0.2566	0.4309
8	0.3807	0.2660	0.4954	0.2652	0.4962
9	0.4086	0.2695	0.5477	0.2689	0.5483

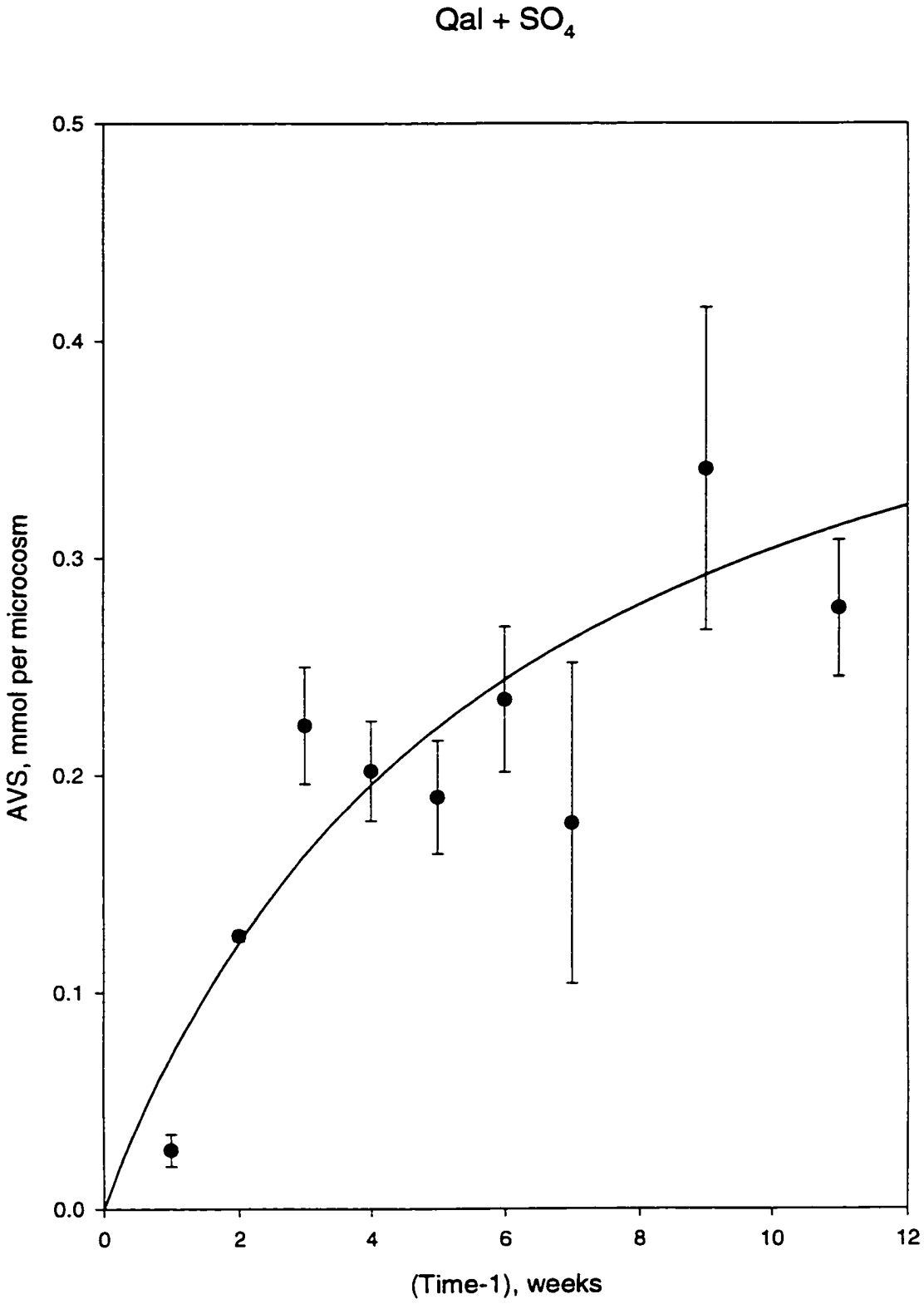
Qal + SO4
0.5
0.4
0.3
0.2
0.1
0.0
AVS, mmol per microcosm
0
2
4
6
8
10
12
(Time-1), weeks

Nonlinear Regression

[Variables]
t = col(1)
y = col(2)
w=col(4)
[Parameters]
m=0.56
k=6
[Equations]
f=m*t/(k+t)
fit f to y with weight w
[Constraints]
m>0
k>0
[Options]
tolerance=0.000100
stepsize=100
iterations=100

R = 0.98297365 Rsqr = 0.96623720 Adj Rsqr = 0.96141394

Standard Error of Estimate = 0.0059

	Coefficient	**Std. Error**	**t**	**P**
m	0.4826	0.1768	2.7300	0.0293
k	5.8640	2.9643	1.9782	0.0884

Analysis of Variance:

	DF	**SS**	**MS**	**F**	**P**
Regression	1	0.0069	0.0069	200.3287	<0.0001
Residual	7	0.0002	0.0000		
Total	8	0.0071	0.0009		

PRESS = 2665.0117

Durbin-Watson Statistic = 171.2327

Normality Test: Passed (P = 0.7447)

Constant Variance Test: Passed (P = 0.4342)

Power of performed test with alpha = 0.0500: 0.9999

Regression Diagnostics:

Row	**Predicted**	**Residual**	**Std. Res.**	**Stud. Res.**	**Stud. Del. Res.**
1	0.0703	-0.0433	-7.3881	-255.0547	>1e20
2	0.1227	0.0033	0.5545	2.2652	4.0585
3	0.1634	0.0596	10.1738	8.6614	>1e20
4	0.1957	0.0063	1.0709	0.4413	0.4144
5	0.2221	-0.0321	-5.4806	-1.4663	-1.6308
6	0.2441	-0.0091	-1.5506	-0.3088	-0.2878
7	0.2626	-0.0846	-14.4357	-2.3124	-4.4055
8	0.2922	0.0488	8.3168	0.9844	0.9819
9	0.3148	-0.0378	-6.4509	-0.6237	-0.5942

Influence Diagnostics:

AUS Q.1

Row	Cook's Dist.	Leverage	DFFITS	
1	-38797238.2818		1.0008	>1e20
2	-45.3811	1.0599	>1e20	
3	-64.6961	2.3797	>1e20	
4	-0.1139	6.8883	>1e20	
5	-1.1519	14.9712	>1e20	
6	-0.0496	26.2212	>1e20	
7	-2.7421	39.9730	>1e20	
8	-0.4913	72.3805	>1e20	
9	-0.1963	107.9824	>1e20	

95% Confidence

Row	Predicted	Regression 5%	Regression 95%	Population 5%	Population 95%
1	0.0703	0.0564	0.0842	0.0507	0.0899
2	0.1227	0.1085	0.1370	0.1029	0.1426
3	0.1634	0.1420	0.1847	0.1379	0.1888
4	0.1957	0.1593	0.2321	0.1568	0.2347
5	0.2221	0.1685	0.2758	0.1667	0.2775
6	0.2441	0.1731	0.3151	0.1718	0.3164
7	0.2626	0.1750	0.3503	0.1739	0.3514
8	0.2922	0.1743	0.4102	0.1735	0.4110
9	0.3148	0.1708	0.4589	0.1701	0.4596

IMAGE EVALUATION
TEST TARGET (QA-3)

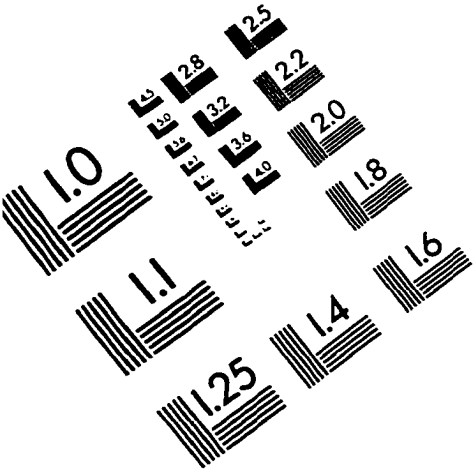

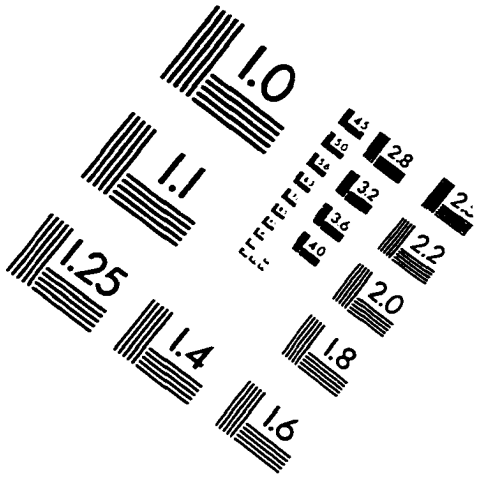

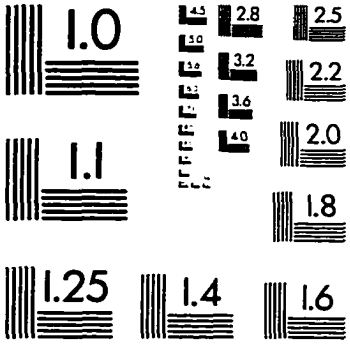

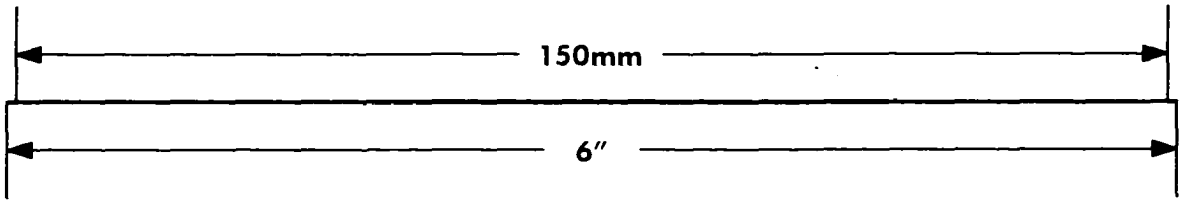

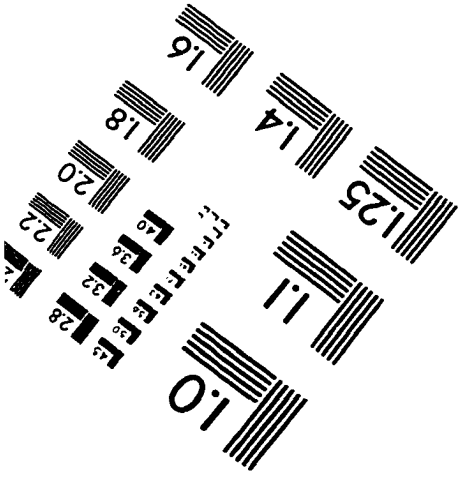

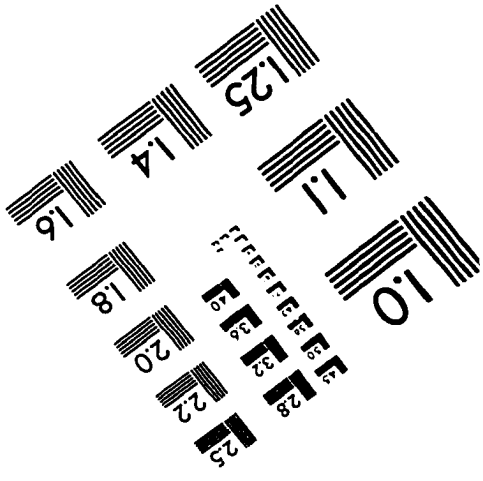

APPLIED IMAGE, Inc
1653 East Main Street
Rochester, NY 14609 USA
Phone: 716/482-0300
Fax: 716/288-5989